



CONTENTS

	Page No.
FOREWORD	0.5
EXECUTIVE SUMMARY	0.8
1. INTRODUCTION	1.1
2. THE 2D DEMONSTRATION STRUCTURE	2.1
3. CONSTRUCTION	3.1
3.1 FABRICATION	3.1
3.1.1 Rig Fabrication	3.2
3.1.2 Frame Fabrication	3.2
3.2 TEST PREPARATIONS	3.7
3.2.1 Support Conditions	3.7
3.2.2 Instrumentation	3.7
3.2.3 Loading System	3.9
3.2.4 Visual Systems	3.11
3.3 SAFETY	3.11
4. TESTING AND REPAIR SCENARIOS	4.1
4.1 PROGRAMME OVERVIEW	4.1
4.2 REPAIR / INTER-TEST SEQUENCES	4.1
4.3 TEST SEQUENCES	4.4
5. CONCLUSIONS	5.1
6. REFERENCES	6.1
APPENDIX A 3D FRAME STRUCTURAL DRAWINGS	
APPENDIX B REACTION RIG DRAWINGS	
APPENDIX C RIG AND FRAME MEMBER AND NODE NUMBERING SCHEMES	

FOREWORD

This report is one of a series describing different aspects of Phase III of the Joint Industry Tubular Frames Project. Each report is self contained providing detailed information in the subject area and summarising relevant data from other documents. The following table lists and briefly describes the focus of each report for cross-referencing purposes.

Report Title	Reference	Circulation
Summary and Conclusions Overview report describing the project and principal findings	C636\04\478R	1
Background, Scope and Development Scene setting report summarising previous work, identified needs and Phase III programme definition and development	C636\04\435R	1
3D Test Set Up Brief description of the 3D test set up and structural configuration	C636\06\313R	1
Material Testing Report Description of material testing procedures, test results and disposition of specific materials within test structure	C636\23\004R	1
Assessment of Locked-In Fabrication Stress Explanation for the build up of locked-in fabrication stresses, description of their measurement and summary of the locked-in force values in key components at the start of each test	C636\21\050R	1
Test Frame Instrumentation Detailed description of all instrumentation systems used in the 3D frame, accuracy, sign conventions etc. Data on CD in final report	C636\25\071R	1
Loadcase 1 Test Report - Multiplanar K Joint Action Detailed description of the Loadcase 1 static test response and interpretation of the results and their significance	C636\37\014R	1
Loadcase 2 Test Report - Interaction Between X-Braced Planes Detailed description of the Loadcase 2 static test response and interpretation of the results and their significance	C636\39\011R	1
Loadcase 3 Test Report - Multiple Member Failures and 3D System Action Detailed description of the Loadcase 3 static test response and interpretation of the results and their significance	C636\40\021R	1



Report Title	Reference	Circulation
<p>Philosophy of Cyclic Testing Discussion of the background to cyclic response issues in the context of ultimate system strength and basis for specific loading scenarios</p>	C636\24\021R	1
<p>Loadcase 1 Cyclic Test Report Detailed description of the Loadcase 1 cyclic test response and interpretation of the results and their significance. Comparison with LC1 static results</p>	C636\38\010R	1
<p>Monotonic and Cyclic testing of Isolated K Joints Description and presentation of results from isolated component tests undertaken by SINTEF in Norway</p>	STF22 F98704 (C636\24)	1/2
<p>Loadcases 2 and 3 Cyclic Test Report Detailed description of the Loadcases 2 and 3 cyclic test responses and interpretation of the results and their significance. Comparison with LC2 and LC3 static results</p>	C636\41\011R	2
<p>Loadcases 1 and 3 'Alternative' Cyclic Tests Detailed description of the Loadcases 1 and 3 alternative cyclic test responses and interpretation of the results and their significance. Comparison with LC1 and LC3 static and cyclic tests</p>	C636\45\008R	3
<p>Multiplanar SCFs Joint BG / BOMEL report describing analytical work and experimental measurements of multiplanar SCFs. Includes comparison with 'standard' empirical approaches</p>	C636\18\018R	1
<p>Site Testing Programme results - Report to Benchmark Analysts Comprehensive report describing results for benchmark cases LC1, LC2 and LC3, including all pertinent data and providing response plots 'matching' the contributions from individual analysts</p>	C636\32\066R	4
<p>Benchmark Conclusions Report comparing blind and post test analyses with measured responses and assimilating learnings and recommendations for future practice identified by Benchmark Analysts</p>	C636\32\084R	1

Key to circulation.

Circulation	All participants	Participants in 1st extension	Participants contributing finance/analytical results to 2nd extension	Benchmark Analysts
1	✓	-	-	×
2	-	✓	-	×
3	-	-	✓	×
4	✓	-	-	✓

JOINT INDUSTRY TUBULAR FRAMES PROJECT - PHASE III

3D FRAME TEST SET UP

EXECUTIVE SUMMARY

Phase III of the Joint Industry Tubular Frames Project involved a series of ultimate strength tests of a 3D jacket-type structure. These tests were the largest ever undertaken and this report describes the purpose built test facility and structural configuration.

The test specimen and reaction rig were fabricated by AKD Engineering in Lowestoft. The designs had been developed by BOMEL in consultation with Frames Project Participants and detailed drawings are provided. The concept was to repeatedly test and repair damaged areas of the structure and the report describes the sequence.

Testing relied on a team of specialist sub-contractors and the roles of AKD (site support services), AV Technology (instrumentation), Bodycote Materials Testing (loading) and Eastern Associates (video) are described.

This report concludes by showing the test facility at the start of three of the eight tests. The configuration and systems are clearly evident and provide a reference base for the description of the tests and specific results in companion reports.



1. INTRODUCTION

The principal focus within the Phase III Frames Project was the execution of a large scale demonstration programme of collapse tests on a jacket type structure. The objectives were to quantify the reserve strength within offshore structural systems and to validate industry practices for assessing ultimate capacity. A companion report⁽¹⁾ describes the background to the project and the basis for selecting the specific test structure configuration. The test set up is shown in Figure 1.1.

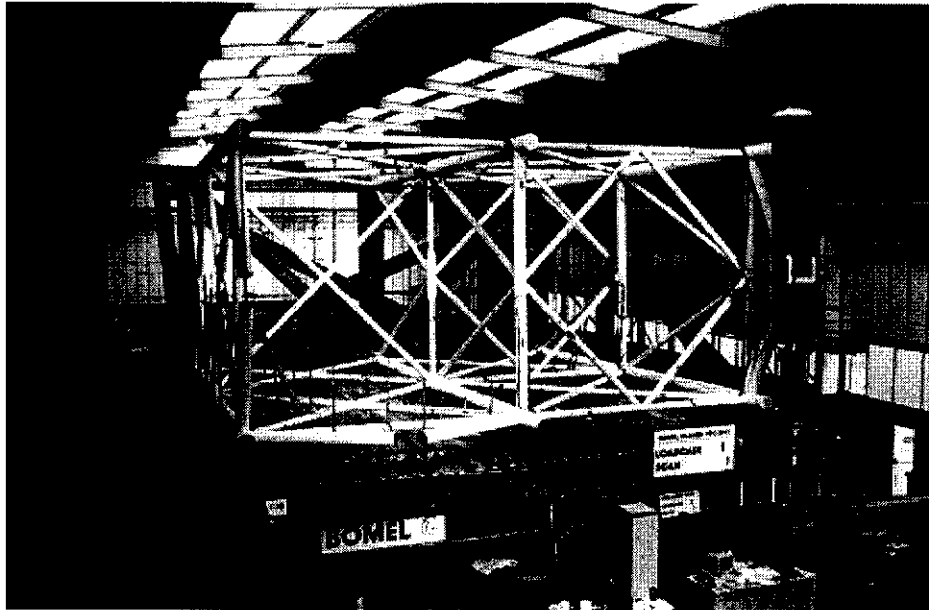


Figure 1.1 3D Frames Project test facility

The present report briefly describes how the facility was established and outlines the role of the various parties. Specific aspects of the construction which are relevant to the interpretation of the tests, such as the survey of material properties, are covered in more detail in associated reports. These are referenced out from this document. Similarly the test results themselves are presented and interpreted separately.

However these structural frame tests were the largest collapse tests ever to have been undertaken and the setting up of the facility is in itself a significant achievement. Section 2 of the report references the structural drawings and numbering schemes defining the test specimen and reaction rig, as-built. Section 3 then relates these to the test site in Lowestoft and describes the sequence of construction. Completion of the facility required the installation of extensive loading and monitoring equipment and these stages are also outlined. The test programme encompassed a series of static and cyclic tests with loads applied to different parts of the structure. Between each test major repairs were carried out and Section 4 describes the extent and sequence. The conclusion, in the form of a functioning 3D structural frame test facility, is illustrated in Section 5.

2. THE 3D DEMONSTRATION STRUCTURE

Structural drawings for the test specimen are presented in Appendix A. The structure comprises a six-leg space frame, two-bays high. Longitudinally the structure is X-braced and transverse planes introduce K and X bracing. At the plan levels there is a combination of X and diamond bracing. Horizontal bracing at plan intermediate levels within the face frames is also considered. The configuration therefore combines typical features of past and present offshore jacket structures. The size of the specimen is comparable to a Southern North Sea structure at 1/3 scale, with 350 - 450mm diameter legs and 170 - 280mm diameter bracing. Non-dimensional geometry ratios were selected to be representative of offshore practice. Similarly material selection criteria required characteristics to be similar to those exhibited by offshore grade steels.

Where the frame weight was some 10 tonnes the purpose built reaction rig weighed over 110 tonnes in order to provide the necessary stiffness for a clear demonstration of the frame nonlinear collapse behaviour. Structural drawings for the rig are presented in Appendix B.

The combination of the frame and rig is shown in Figure 2.1. The tubular frame specimen is painted white; the reaction rig is brown. The rig rests on load distributing support stools. The six-leg jacket structure is effectively on its side, with the base of the legs welded to the reaction rig. As shown in the figure, this arrangement enabled alternative loading scenarios to be applied and reacted safely near ground level.

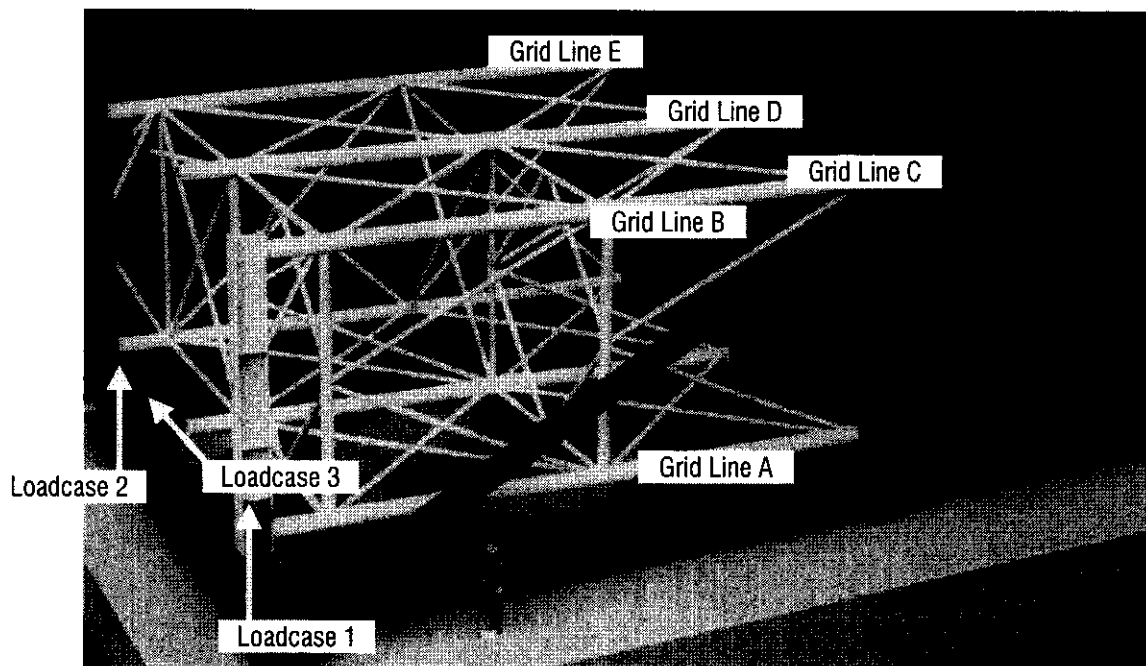


Figure 2.1 Test frame and reaction rig model

It can be seen that the 'vertical' part of the rig actually raked 'backwards' (to the right in Figure 2.1) by some 2°. The purpose of this was to give sufficient clearance at the front of the structure for the specimen to be deflected downwards as well as upwards in cyclic loading scenarios.

In addition to illustrating the general test configuration, Figure 2.1 is annotated to indicate the principal grid lines used in the structural drawings and the points of load application and lines of action for the three loading scenarios. A consistent scheme for node and member numbering was also used throughout all experimental and analytical aspects of the project activity as shown in Appendix C. The only variations between tests relate to the repositioning of the loading beam and installation of additional plan X-bracing in the later tests.

Together Appendices A, B and C give a complete definition of the 3D demonstration structure.

3. CONSTRUCTION

3.1 FABRICATION

The structures were fabricated by AKD Engineering Limited at their works in Lowestoft (Figure 3.1). The base dimensions of the rig were some 22m x 14m with an overall height of 8m occupying one third of the length of the workshop and all but a few metres of the width.

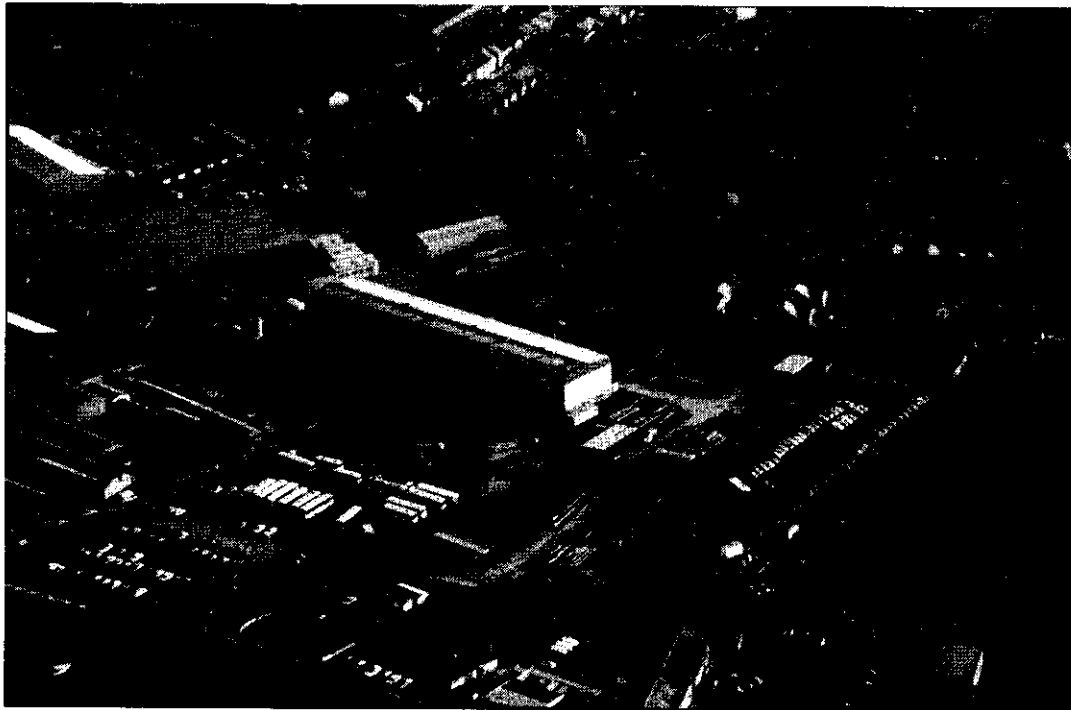


Figure 3.1 Fabrication / test site

Once assembled the main 20 tonne crane could not pass over the structure and the build sequence therefore had to be carefully planned. Specifications for fabrication^(2,3) were developed by BOMEL built around EEMUA offshore publications, with supplements as appropriate reflecting the scale of construction and special requirements of the test programme.

AKD provided a quality plan for BOMEL approval prior to work on site commencing. Thorough supervision and inspections were carried out with complete traceability of materials and welding records. A negative reporting scheme for inspections was agreed. Comprehensive documentation packages were provided by AKD for the rig⁽⁴⁾ and frame⁽⁵⁾ on completion of the work. These are available from BOMEL on request.

3.1.1 Rig Fabrication

The reaction rig comprised some 110 tonnes of heavy steel fabrication. Rolled sections were provided by British Steel and deep (~1m) beams were fabricated by AKD from 45mm TMCP plate supplied by Thyssen. Figure 3.2 shows the elements of the reaction rig as fabricated in plan.

The next operation was to roll up the back frame of the rig within the two base frames. A number of schemes were considered and work was undertaken by a specialist firm operating three computer controlled crane units working in parallel. Once these elements had been positioned and welded out, the back raking members and long diagonal ties to the side of the front of the rig were installed.

Figures 3.3 and 3.4 show views of opposite ends of the completed rig.

3.1.2 Frame Fabrication

Once construction of the rig was complete, fabrication of the tubular frame specimen commenced. A number of tubular sections were provided by Thyssen. Primary bracing tubulars were purchased from stockholders. As discussed in Reference 6, the materials were carefully selected and, where appropriate, heat treated to give response characteristics representative of offshore tubulars. The size, and hence scale, of the structure provided for direct comparison with earlier research and the non-dimensional properties reflected offshore design practice. Further details of the material properties are provided in a companion report⁽⁶⁾.

Similarly results of investigations to monitor the build up of locked-in forces during fabrication are discussed separately in Reference 7. Reference 8 discusses the extent of instrumentation on the test specimen and includes details of the load cells welded in to primary braces during fabrication.

In Figure 3.4 some of the frame tubulars can be seen laid out on the rig base. Prior to fabrication they were surveyed at 1m intervals to give accurate records of diameter and thickness for each pipe length; these marks were traced through to the final location within the 3D structure. Individual planes within the frame were fabricated in 2D on the bed shown in Figure 3.5. These frames were welded in turn into position on the reaction rig and then the infill bracing was welded in situ. Figure 3.6 shows the scaffolded structure as fabrication was being completed.

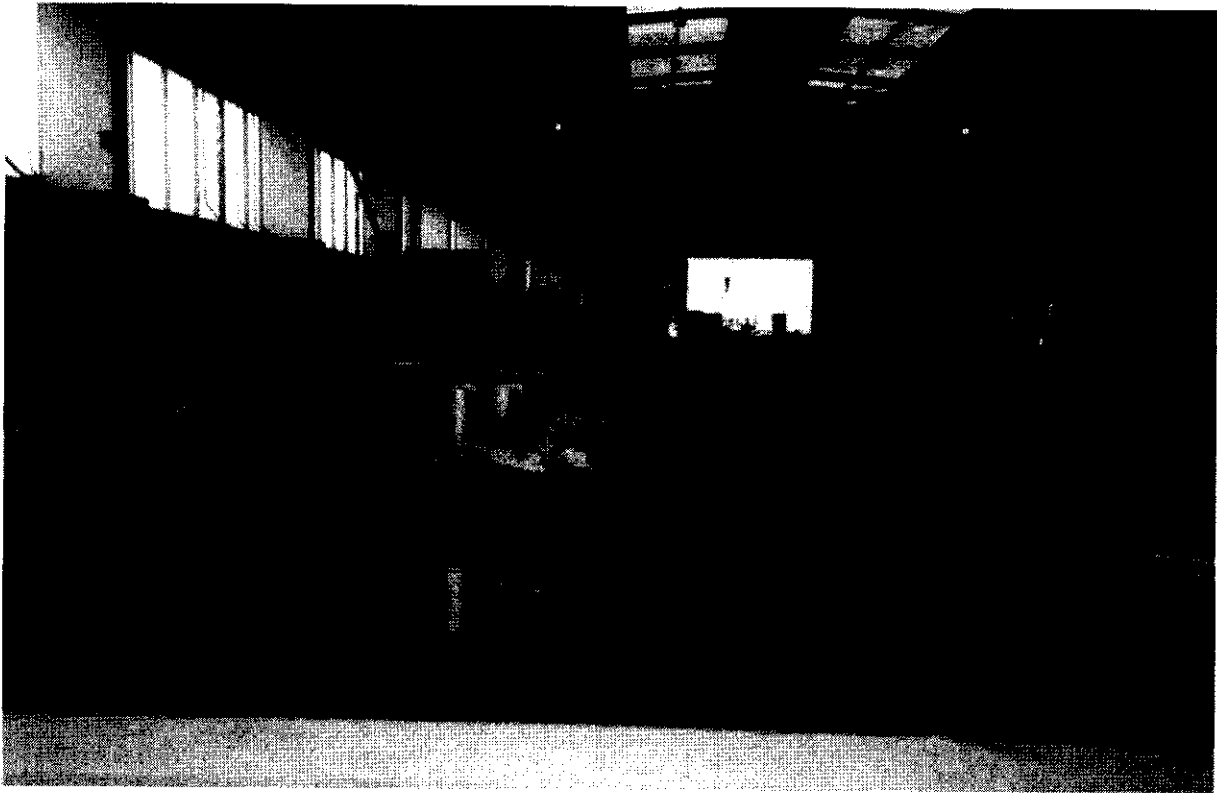
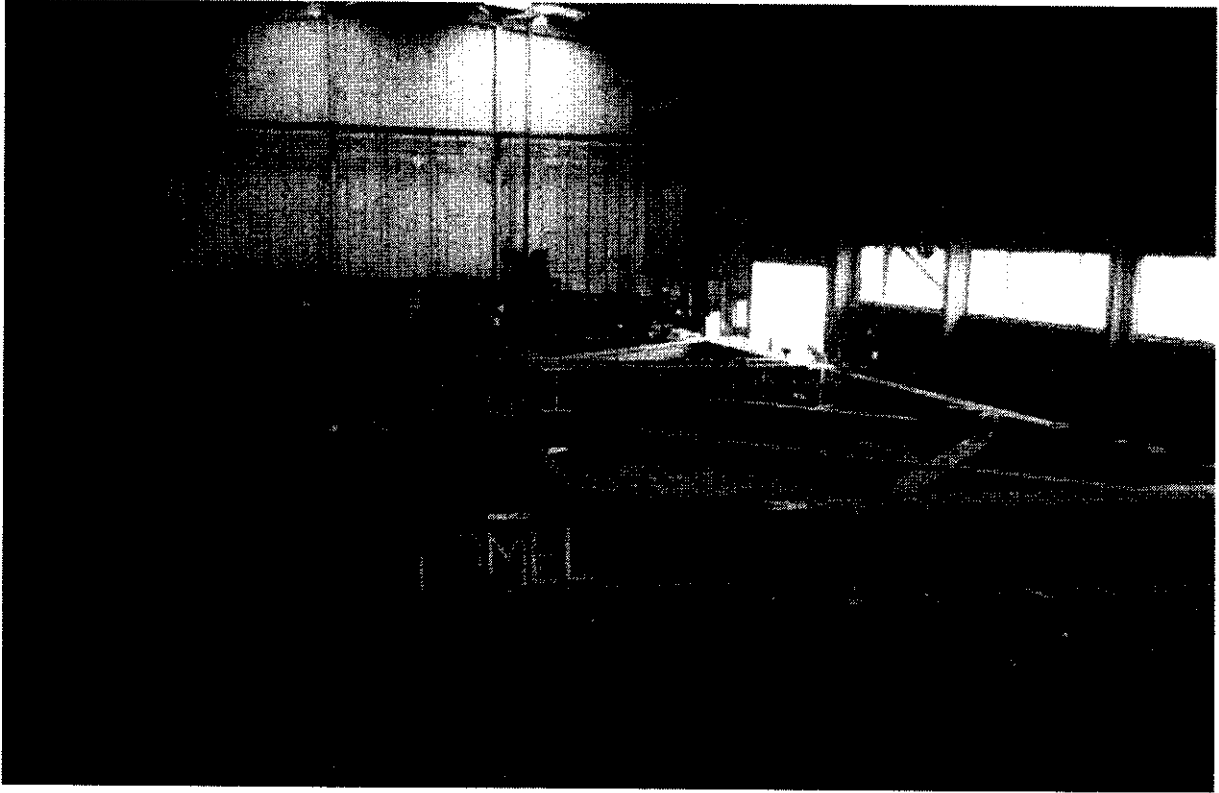


Figure 3.2 Initial fabrication of reaction rig in plan



Figure 3.3 'Rear' view of raking support to completed reaction rig

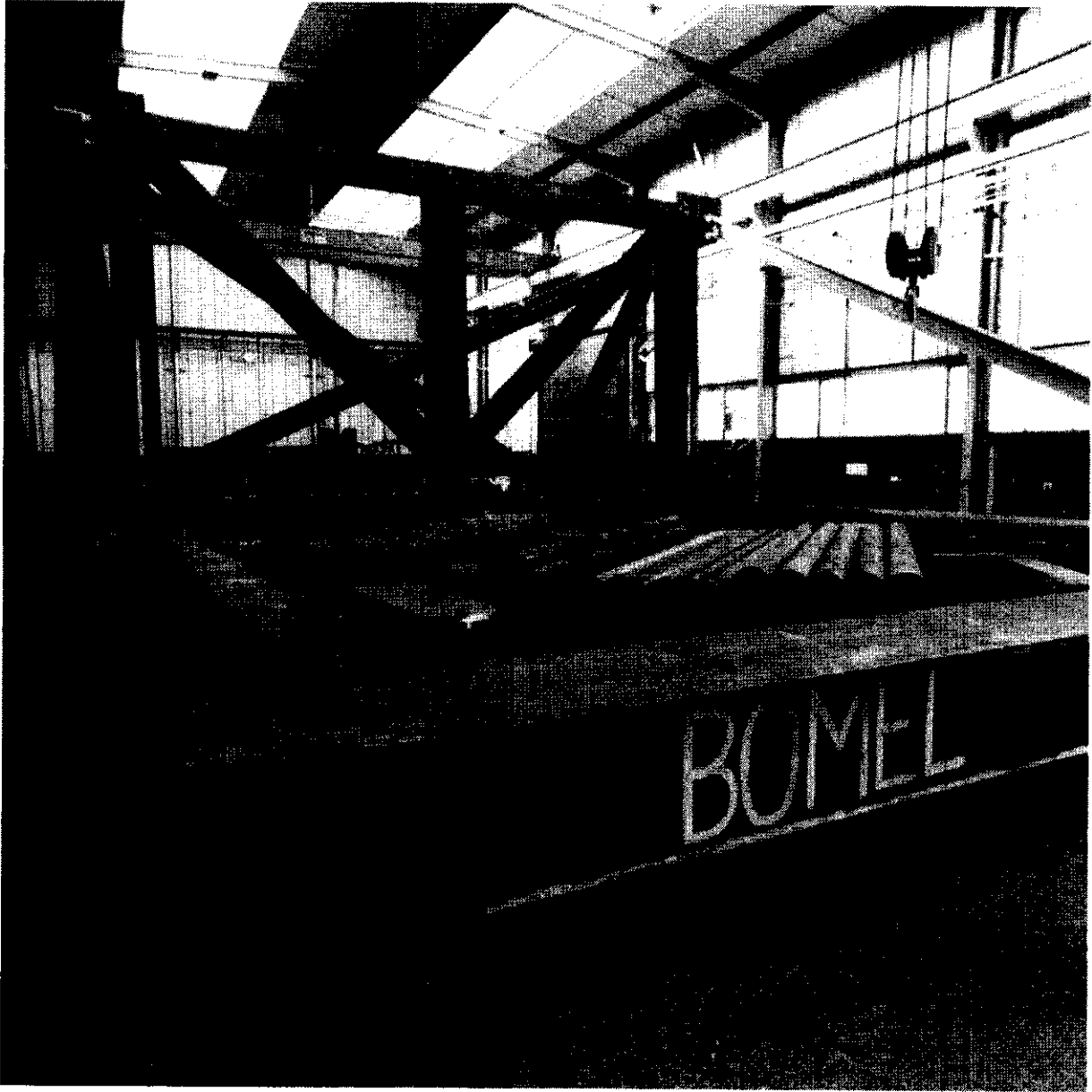


Figure 3.4 'Front' view of completed reaction rig

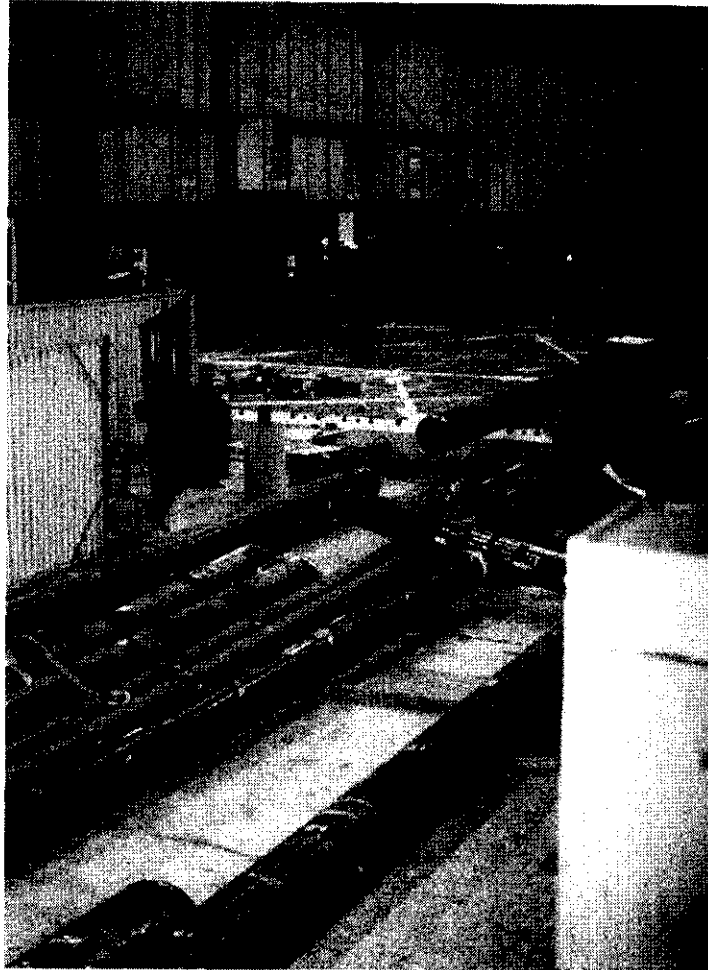


Figure 3.5 Fabrication of transverse frames in plan

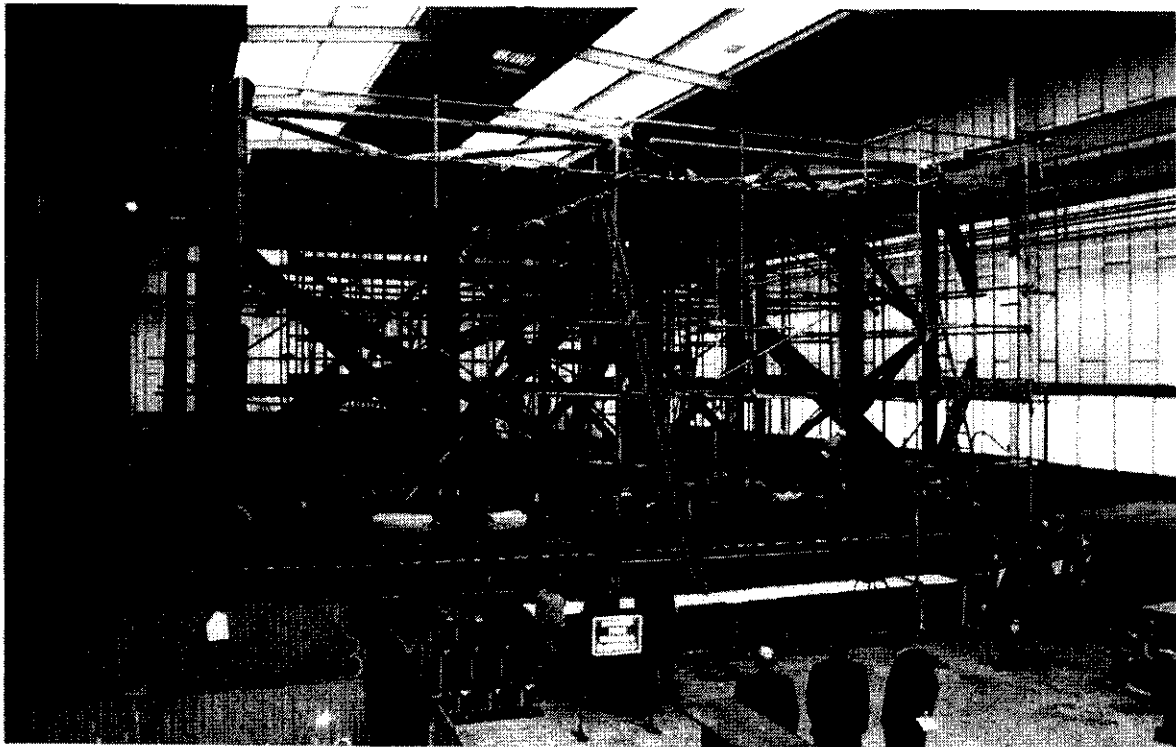


Figure 3.6 3D frame as fabrication of infill bracing is completed



3.2 TEST PREPARATIONS

3.2.1 Support Conditions

Once fabrication of the frame and rig was complete, the final stage was to jack the whole assembly onto the support stools.

The base of the reaction rig rested on support stools at thirteen node points (Nodes 45, 47-48, 51-52 and 54 - 61 shown in Appendix C). Once loads were applied to the test specimen the rig distorted and global reactions were taken out at just three points. The role of the support stools was therefore to dissipate these concentrated forces across a wider area of the workshop floor.

With reference to Figure 2.1, the most distant node at the back of the rig (Node 61), was 'fixed' to prevent rotation and translation of the loading rig in the plane of the base. Four vertical dowel bars were welded to the top of the support stool and each was a sliding fit in a hole drilled in the bottom flange of the loading rig base member, thereby permitting uplift. The support stool was secured to the floor by four vertical anchor bolts, one at each corner.

The interfaces at the other twelve supports were identical. A sliding bearing was tack welded to the underside of the rig base and this rested down on a rubber pad on the surface of the stool. The stool itself was supported off the floor on an epoxy mortar bedding.

Figure 3.7 shows the support at Node 59 taken prior to placing of the epoxy mortar bedding. The bolts, temporarily located at the corners to level the stool prior to placement of the epoxy mortar bedding can be seen, along with the temporary timber formwork for the bedding. The bearings and rubber pads were designed and supplied by Glacier Metals Limited. They provided for lateral translation and rotation in the plane of the base and permitted uplift.

3.2.2 Instrumentation

The frame was instrumented by AV Technology Limited (AVT) whilst the scaffolding remained in place⁽⁸⁾. However, to provide a clear view of the structural behaviour the scaffolding was removed prior to testing. Although comprehensive details of the instrumentation are provided in Reference 8, it should be noted that the 880 channel scheme encompassing strain and displacement monitoring was a massive undertaking requiring several weeks for installation. A bespoke logging system was developed and extensive off-site trials were undertaken by AVT working in conjunction with BOMEL to give accuracy and reliability throughout the programme.

Figure 3.8 shows the logging cabinet and PC station in front of the test structure. As described in Reference 8, this enabled the structural response to be monitored on line and compared with predictions. This facility was extremely important to give a basis for decision making as each test progressed.

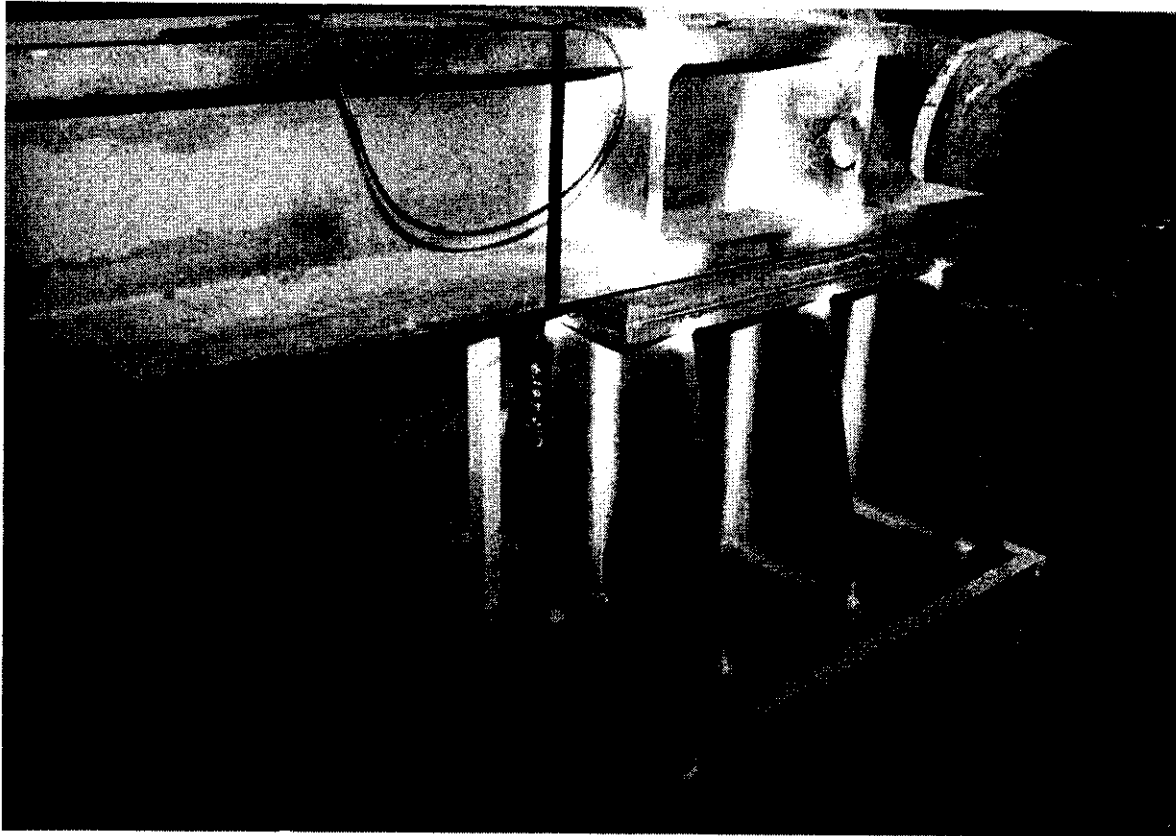


Figure 3.7 Rig support (typical)

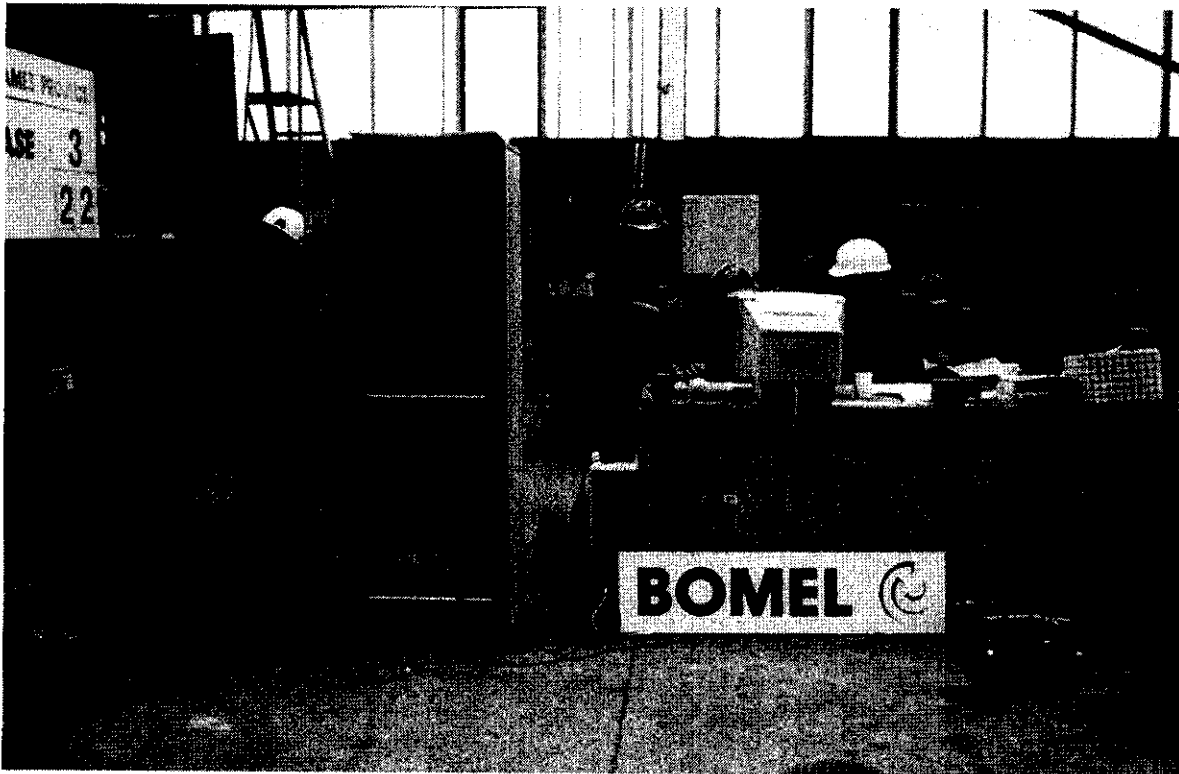


Figure 3.8 Instrumentation logging equipment



3.2.3 Loading System

The actuator loading system was retrieved by BOMEL from an offshore research programme undertaken in the 1980s. The actuator had an exceptionally high capacity / long stroke specification and was refurbished by Bodycote Materials Testing Limited. All internal seals were replaced and the hydraulic system and control unit were subject to extensive trials at Bodycote Laboratories. The system comprised the actuator assembly, which applied load in displacement control, connected to a 15 KW hydraulic power pack controlled by a servo control system using feedback from a displacement transducer incorporated into the actuator assembly. Use of displacement control was imperative to prevent catastrophic collapse when peaks in the system capacity were experienced. Furthermore it enabled data on the unloading response characteristics of components and systems to be gathered in a controlled manner.

The actuator was double acting with a maximum load capacity of 3000 kN in the forward loading direction and approximately 2000 kN in the reverse loading direction. The stroke of the actuator was 1000mm. The system was assembled with an initial 300mm ram extension thereby allowing a 700mm displacement capacity in the forward loading direction and 300mm in the reverse loading direction. The servo control system was capable of providing a resolution on load and displacement of 0.01% of full scale. The displacement transducer was accurate to at least $\pm 2.5\%$ and the load cell to at least $\pm 1\%$.

For test Loadcases 1 and 2 (see Figure 2.1) load was applied within a tubular loading beam to a plate at the centreline of the structure. In the lateral Loadcase 3, the anticipated loads were greater and so were applied to the end of a stiffened I-section beam straddling two frame legs. These scenarios are illustrated in photographs in Section 5. Specific details are given in the loading beam drawing in Appendix A.

To ensure loads would be applied axially without damaging lateral loads being experienced by the ram, bespoke articulation units were provided at both ends of the actuator. Figure 3.9 shows the loading beam into which the top articulation unit, a load cell and the actuator have been positioned. The assembly is being lifted into position on the frame. The lower articulation unit can be seen in the centre of the figure bolted to the reaction rig.

Figure 3.10 shows the loading control equipment positioned in front of the 3D test structure. The computer trace provided a second by second record of the force and displacement applied to the frame by the hydraulic system. The degree of force relaxation once the actuator was locked-in position gave an indication of the degree of plasticity within the structure. Furthermore the constant sampling enabled the maximum load sustained by the structure between scans to be determined. Output from the Bodycote actuator control system was channelled into the AVT logging system to combine the results in a single datafile.



Figure 3.9 Installation of the actuator and loading beam for Loadcase 1

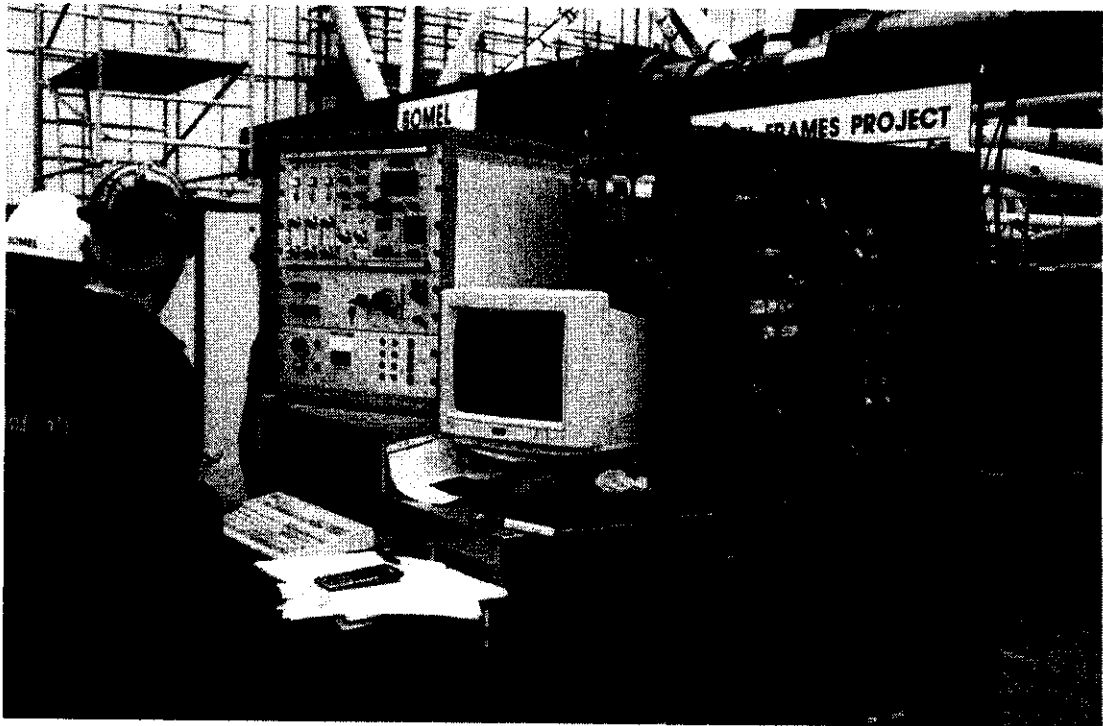


Figure 3.10 Actuator control system



3.2.4 Visual Systems

The final stage in the test preparations was to paint the structure. This served two purposes, firstly to clearly define the frame against the fabric of the building for the video records, and secondly to enable zones of high strain to be identified with flaking of the paint. In addition grid lines were drawn on key components to provide a reference against which distortions become clearly visible. The filming systems were also an important part of the test set. Remote monitors, as shown in Figure 3.11, enabled global and local details of the response to be reviewed safely throughout each test.

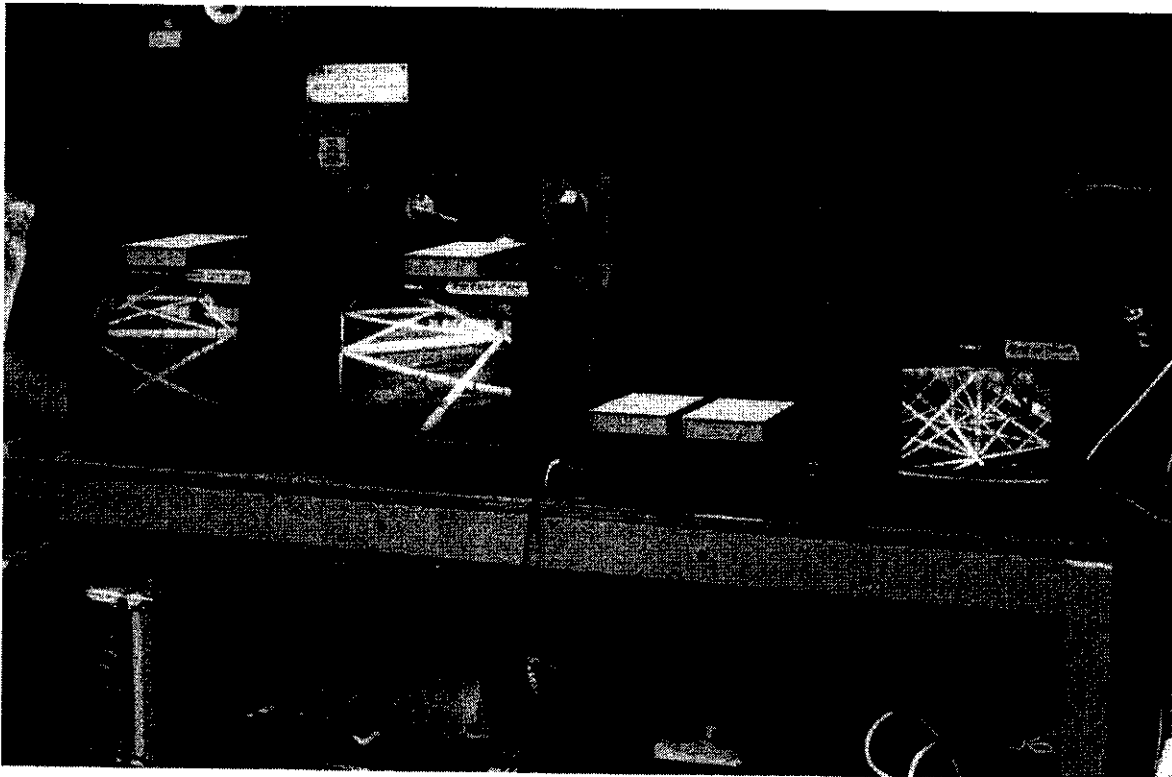


Figure 3.11 Monitors for video recording of tests

3.3 SAFETY

Once AKD had completed fabrication of the structures, AVT commenced the instrumentation. Bodycote personnel then came to site to assist with the installation of the actuator system. Finally Eastern Associates brought in camera equipment and lighting to video the tests. All sub-contractor activities were overseen by BOMEL and support was provided by AKD personnel. On test days the fabricator's workshop essentially became a laboratory. Testing was performed under the direction of BOMEL with all contractors required to work as a team. Figure 3.12 shows the combined team on conclusion of the Loadcase 3 test.



Figure 3.12 Integrated testing team (AKD, AVT, Bodycote, BOMEL and Eastern Associates)

A paramount concern throughout the preparations and testing was safety, particularly recognising the forces involved and the need for close interaction and coordination between the parties. In addition the site was visited by project Sponsors and Benchmark Analysts to witness the tests.

Prior to work commencing a hazard identification exercise was organised by BOMEL involving several representatives from each party. An initial Safety Procedures Manual was circulated and updated following the meeting to reflect discussions⁽⁹⁾. Copies were issued to every individual attending site. The exercise was valuable, not just in terms of the manual, but also for the insight each contractor gained of the potential hazards associated with the equipment and systems being operated by others within the team.

The HAZID was hosted by Shell at its training centre in Lowestoft and an offshore safety representative, an electrical engineer and the Chairman of the Participants' steering committee from Amoco attended.

4. TESTING AND REPAIR SCENARIOS

4.1 PROGRAMME OVERVIEW

The 3D experimental programme involved a series of tests on the 3D frame structure. Figure 2.1 illustrates the three alternative loading scenarios. The baseline tests involved monotonic loading of the structure in stages under displacement control until failure occurred. In subsequent tests the cyclic effects of load reversal that may be experienced in a storm were investigated, with the actuator acting in forward and reverse modes.

In total eight frame collapse tests were undertaken using the unique facility. In each case different components failed and had to be cut-out and replaced prior to the next test. The instrumentation and surface painting of the structure ensured that all highly stressed areas could be identified and removed in order that residual plasticity did not influence the subsequent structural performance. Figure 4.1 shows the sequence of the tests, the dates and times, and the associated data files, and provides an illustrated record of the components that failed and were replaced. The strategy worked extremely well in that eight independent tests were undertaken successfully. The structural drawings in Appendix A document the changes in structural details between tests, for example as chord cans were introduced at joints which has previously been configured to represent past construction practices.

4.2 REPAIR / INTER-TEST SEQUENCES

The approach did however require strong cooperation between the contracted parties and the typical scenario was as follows:

- On conclusion of a test BOMEL examined the instrumentation and inspected the structure for signs of damage and decided on the extent of repairs necessary.
- Instrumentation and loading contractors (AVT and Bodycote) remained on site in order that the equipment could be used and monitored to minimise the loads within individual members within the deformed structure as they were cut.
- A sequence of controlled deformations of the structure were applied and readings of the instrumentation were taken until the member forces (with due account for self-weight and locked in fabrication forces) were sufficiently low for the component to be cut safely without spring back. AKD personnel then cut through the designated

Test	Date	Recording Times (24hr)	AVT Filename	Scan Numbers	BOMEL Working File C3381	Member Failures (Scan No)	Members Cut
LC1 *	T 25/04/98	17:25-23:05	LC1a_infil	1 to 18			
	T 26/04/98	09:30-10:44	LC1a_test	19 to 29	37/011w.xls	K38 (20), 72b (32) & K37 (softening)	61, 62, 63, 64, 66, 67, 68, 69, 71, 98 & 101
	C 30/04/98	09:15-14:40	LC1a_test	1 to 38			
LC1C	T 29/05/98	14:23-17:50	LC1Ca_infil	1 to 26		K38 (159) & K37 (184)	
	T 30/05/98	13:45-21:18	LC1Ca_test	1 to 185	39/009w.xls		61, 62, 63, 64, 66, 67, 68, 69 & 95
	T 31/05/98	08:20-23:28	LC2h_T1	1 to 15		X42 (15), 81/83y (21), 78b (37) & 82b (42)	76, 81, & 82
LC2 *	T 15/06/98	14:30-18:32	LC2a_test	1 to 49			
	T 20/06/98	10:27-20:05	LC2a_test	50 to 59			
	C 20/06/98	20:03-22:34	LC2a_cut	1 to 22			
LC2C	T 19/07/98	17:30-18:44	LC2Ca_infil	1 to 22			
	T 20/07/98	08:47-09:40	LC2Ca_test1	1 to 9			
	T 21/07/98	08:52-20:44	LC2Ca_test2	1 to 143	41/008w.xls 41/009w.xls	X42 (116) & 81/83y (134)	
LC3C	T 04/08/98	19:55-23:47	LC3Ca_infil	1 to 35			
	T 05/08/98	09:40-10:47	LC3Ca_test1	1 to 33	42/013w.xls 42/014w.xls	51b (125), 57b (127), 50/52y (126), 54/56y (125) & 46/48y (126)	
	T 06/08/98	08:25-18:18	LC3Ca_test2	1 to 133			
LC3 *	T 06/08/98	08:25-18:18	LC3Ca_cut	134 to 252			
	T 28/08/98	14:45-17:42	LC3Ca_test	253 to 285			
	T 29/08/98	09:34-20:47	LC3Ca_test	1 to 73	40/016w.xls	49/51y (19), 45/47y (32), 57/59y (33), 53/55y (37), 50b (37), 60b (38), 46b (41), 54b (44), X16 (65), X44 (59), X18 (61) & 61b (62)	49, 51, 52, 57, 59 & 60
LC3CA	T 23/10/98	10:38-11:32	LC3Cab_infil	1 to 41			
	T 23/10/98	12:12-21:07	LC3Cab_test	1 to 25		X36comp (90), X35comp (154), 59/67y (164), X33ten (165), X34ten (165) with possible 50/52y (165) & 46/48y (165)	45, 46, 47, 49, 50, 51, 53, 54, 55, 57, 56, 59 & 61
	T 24/10/98	08:16-15:10	LC3Cab_test	1 to 205	44/010w.xls		
LC3CA	T 09/11/98	09:29-10:33	LC3Cab_infil	1 to 22			
	T 09/11/98	10:46-22:00	LC3Cab_test	1 to 168	45/007w.xls	K37 (69), K38 (125), 72b (140), 70b (146) & K38 severed (162)	57, 60, 54, 55, 46, 51, 47, 50, 61, 63, 69, 71, 98 & 101
	C 10/11/98	08:10-08:56	LC3Cab_cut	169 to 174			

KEY:

- * Benchmark case
 - T: Loadcase trial
 - K: Loadcase cut
 - X: X: Joint number
 - D: Member buckled
 - Y: Member yielded
 - Material has been tested
- eg X42 = X Node 42 failed
81y = Member 81 yielded

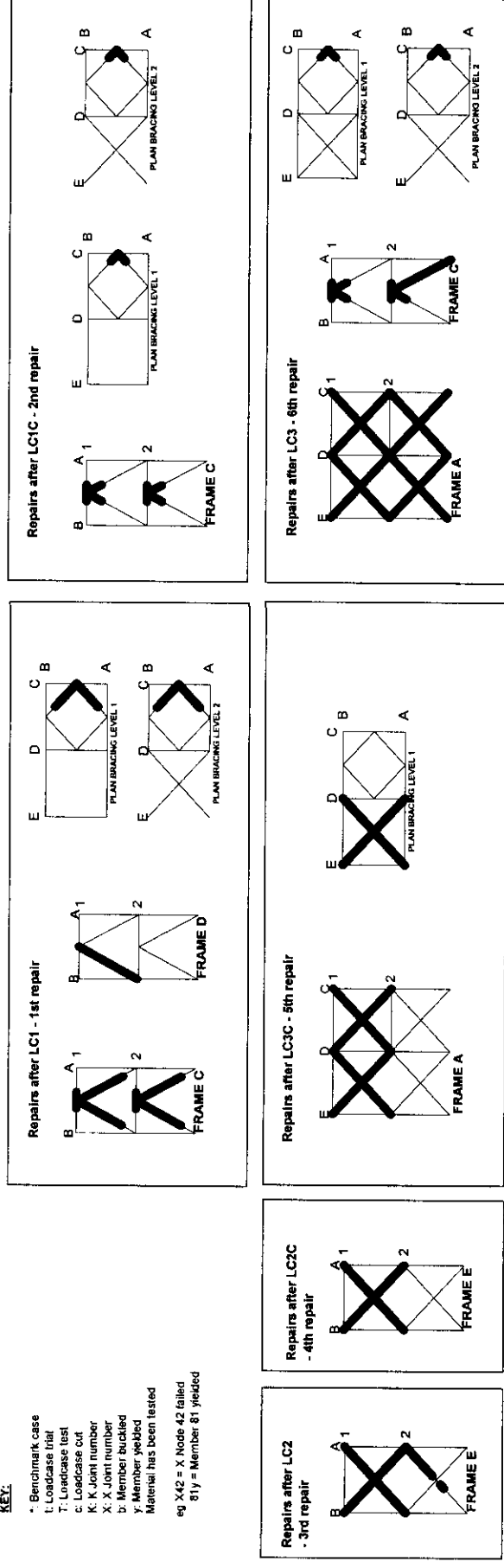


Figure 4.1 Frames Project Phase III summary of member failures, cuts and repairs through test programme





member. This was repeated for every designated member within the frame that could be reached safely from the scaffold decking. Only once this was complete were the sub-contractor teams demobilised.

- BOMEL then worked with AKD engineers to specify the replacement configuration and procure additional material where necessary. Although predictions of the response modes had been made in advance it was not until the tests were complete that the full extent of damage could be confirmed.
- Material had to be cut and prepared as build sequences were identified. The rigour of the initial build fabrication procedures was applied to all aspects of the repair, and comprehensive records are contained in AKD documentation packages⁽⁵⁾.
- A key element in the repairs was the rigging of the scaffolding from which the repairs could be effected. Progress was often tied in to the availability of scaffolders.
- At certain stages within the test programme, it was also necessary to schedule in the removal of the loading beam and repositioning on an alternative axis.
- As the test programme developed an unanticipated constraint was brought in which was to try and coincide testing with weekends. Other activities within the workshop generally ceased at weekends and the lower noise level made communications easier between parties.
- BOMEL therefore worked with AKD to identify the programme for repairs and the next target test date.
- Close coordination through the repairs was necessary in order that AVT could return to site as soon as possible to instrument new components within the structure and recheck elements that might have been damaged in the repair process.
- Bodycote then came to site to reconnect the hydraulic and electrical control systems for the actuator.
- Prior to every test, a series of trials was undertaken under the direction of BOMEL to ensure that all instrumentation channels and loading systems were functioning and that the initial take-up of loads was as anticipated.



- Only once all NDT was complete and the test systems had been shown to be fully functional was the repair scaffolding rased. This was often undertaken through the night in order to provide continuity on site for the sub-contractor teams. The works were supervised by AKD on behalf of BOMEL to minimise damage to the delicate testing systems.
- With a short series of trials to re-confirm functionality the test proceeded the following day.

This cycle of testing and repair repeated throughout the test programme, alongside communications between BOMEL and Participants as the scope was revised and expanded to build on the initial findings and maximise the benefit from the test facility.

4.3 TEST SEQUENCES

The conduct of the tests themselves followed a defined sequence. Some understanding of these is necessary to the interpretation of the results:

- Each test day commenced with a safety briefing from BOMEL to all parties. Each individual was provided with a listing of personnel on site (BOMEL and sub-contractors) confirming individual roles and responsibilities. Information was circulated on the predicted test responses and corresponding sequence of controls.
- The frame was set at the datum position (zero applied load) relative to which all forces and movements are measured*. Watches were synchronised.
- A datum scan of the instrumentation was taken (Scan 1) as the scan number was displayed on the master board. These scan numbers provided a consistent reference base between all contractors and are used extensively in the test descriptions.
- An increment of load was applied under displacement control at the direction of BOMEL. Once complete, the actuator was locked-off in position. The on-screen trace of actuator load with time was monitored; a flat trace indicated a state of static

* In the first four tests (LC1, LC1C, LC2 and LC2C) the actuator datum was incorrectly set with zero load in the actuator. The actuator was not therefore supporting the weight of the load cell and top hinge unit (15kN total measured weight) and these were effectively hanging from the 3D structure. The true reference datum for comparison with the analyses required that measurements of the initial state of stress and applied load effects be adjusted accordingly. This correction has been made for all the results presented in the programme reports and conveyed to Benchmark Analysts.



equilibrium had been achieved. This was almost instantaneous when the structure was elastic but took a couple of minutes to reach once there was extensive plasticity.

- The scan number on the master board was incremented by one.
- The instrumentation system was scanned and backed up⁽⁸⁾. Dial gauges were read manually.
- Throughout, all parties (BOMEL, AVT, Bodycote and Eastern Associates) maintained independent logs with respect to scan number and clock time of key events (eg. physical observations, checks on spurious gauge readings, ramp rate changes, movements in camera position, etc).
- Results within the data acquisition spreadsheet were reviewed by BOMEL. Graphs were generated automatically, plotting incremental measured values against BOMEL predictions. Built-in checks on maximum and minimum strains and functionality were monitored. Based on a review of the data the appropriate value for the next load / displacement increment was determined.

In all cases the tests were undertaken in a quasi static manner. The structure was subject to distinct increments of displacement after each of which the condition was monitored. In the so called 'static' or monotonic collapse tests the above sequence was repeated until the ultimate capacity of the structure for the given loading configuration had been attained and the pattern and level of post-peak loading capacity had been determined. The extent of post-peak deformation was limited to ensure extensive plasticity was not generated in distant parts of the structural frame.

- Once the desired static or cyclic scenarios had been achieved, the applied load was reduced in three or four decrements with scans of the instrumentation and record keeping at each stage as before. In all cases there was a displacement offset due to the plastic deformations within the structure when the applied load was reduced to zero.

The tests and overall programme were therefore conducted in a carefully controlled and structured manner. The success of the programme is attributable to the way in which the contractors embraced these procedures and the constructive and professional manner in which each party discharged their individual responsibilities.



5. CONCLUSIONS

This report has described the setting up of the 3D demonstration test structure and provides drawings completely defining the configuration at each stage of the programme. It also describes how the fabrication workshop was turned into a test laboratory as BOMEL brought specialist sub-contractors to site and established a working team.

The conclusion is therefore the existence and safe and reliable functioning of the facility itself, complete with loading, instrumentation and video monitoring systems. Figure 5.1 shows the structure in its initial-build condition at the start of the first Loadcase 1 static collapse test. In Figure 5.2 the loading beam has been repositioned for the Loadcase 2 test. Finally Figure 5.3 shows the longitudinal loading scenario for the Loadcase 3 test. The loading control, instrumentation and video monitoring systems are all evident in the pictures. Companion reports, as detailed in the Foreword, provide information on precise properties of the structure and present the specific results from each test.

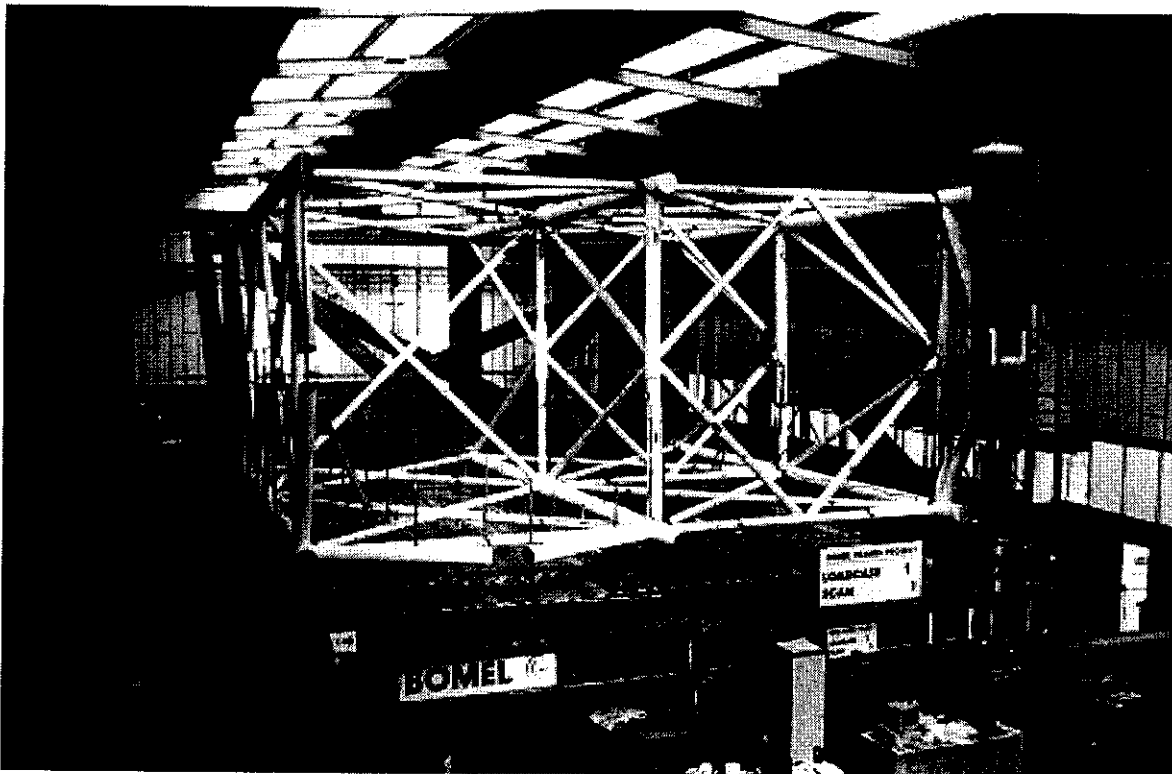


Figure 5.1 Loadcase 1 set up



Figure 5.2 Loadcase 2 test set up

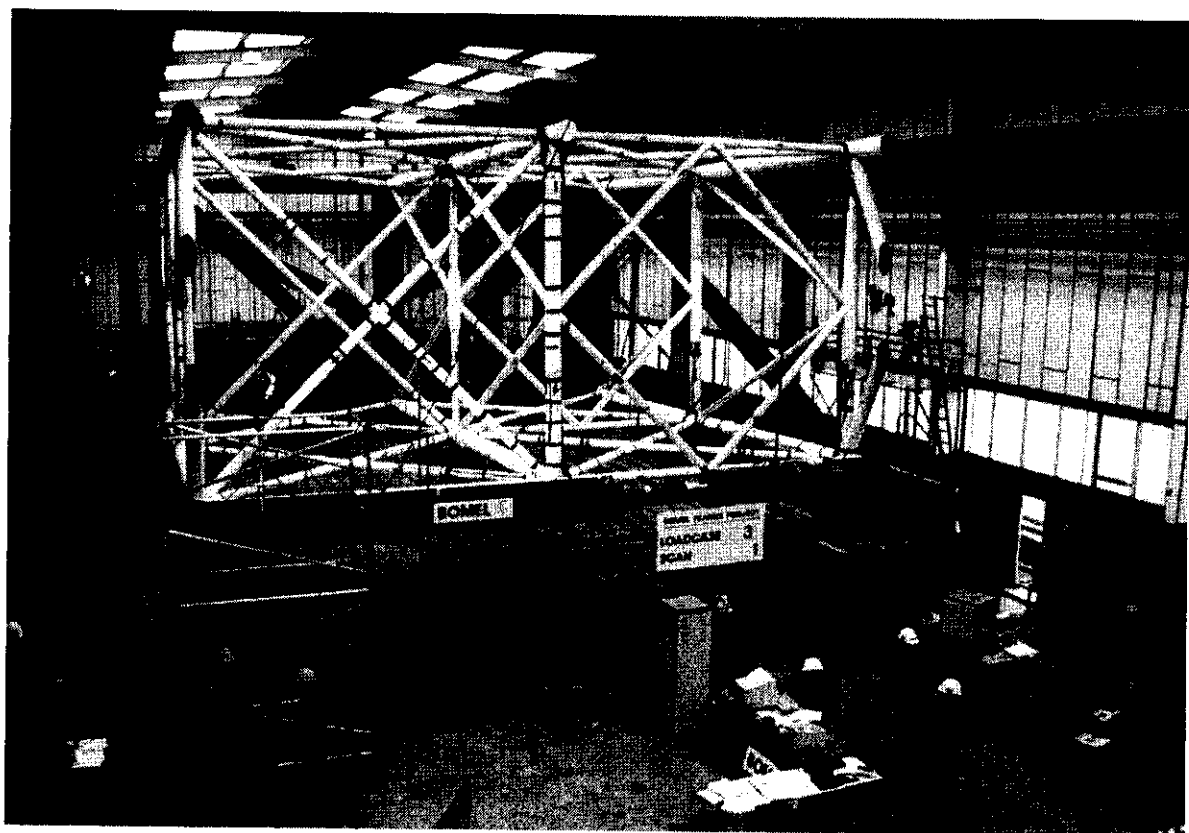


Figure 5.3 Loadcase 3 test set up



6. REFERENCES

1. BOMEL Limited. 'Frames Project - Phase III - background, scope and development', BOMEL Reference C636\04\435R, Revision O, August 1999.
2. BOMEL Limited. 'Specification for fabrication and provision of site services', BOMEL Reference C636\06\031S, Revision A, June 1997.
3. BOMEL Limited. 'Fabrication specification - Supplement to EEMUA publication No 158', BOMEL Reference, C636\06\007S, Revision C, March 1997.
4. AKD Engineering Limited. 'Loading rig - documentation package', AKD Reference 4017, BOMEL Incoming Document 10955 - File C636\31, July 1998.
5. AKD Engineering Limited. 'Test specimen - documentation package', AKD Reference 4065/4413-2/4570, BOMEL Incoming Document 11900 - File C636\31, November 1998.
6. BOMEL Limited. 'Material testing report', BOMEL Reference C636\23\004R, Revision B, April 1999.
7. BOMEL Limited. 'Assessment of locked-in fabrication stress', BOMEL Reference C636\21\050R, Revision O, July 1999.
8. BOMEL Limited. 'Test frame instrumentation', BOMEL Reference C636\25\071R, Revision O, July 1999.
9. BOMEL Limited. 'Safety procedures manual', BOMEL Reference C636\36\004S, Revision B, April 1998.
10. BOMEL Limited. 'Philosophy of cyclic testing', BOMEL Reference C636\24\021R, Revision O, August 1999.

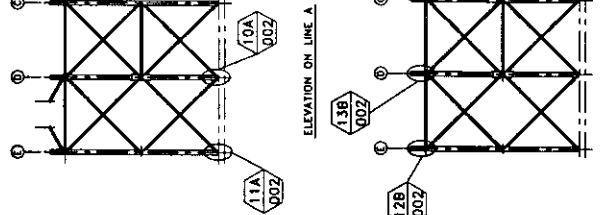


APPENDIX A

3D FRAME STRUCTURAL DRAWINGS

- General arrangement of test specimen - C636\15\002D, Revision G
- General arrangement of test specimen - dimensions - C636\15\003D, Revision G
- Detail drawing of node points 1A, 2A, 3A, and 4A - C636\15\004D, Revision F
- Detail drawing of node points 6A, 7A, 8A and 9A - C636\15\005D, Revision F
- Detail drawing of node points 10A, 11A, 12B and 13B - C636\15\006D, Revision F
- Detail drawing of node points 14B, 15B, 16B and 17B - C636\15\007D, Revision E
- Detail drawing of node points 5B, 18B, 19B, 20B, 22B and 30B - C636\15\008D, Revision E
- Detail drawing of node points 23C, 24D, 25D, 26X, 27E, 28E and 29X - C636\15\009D, Revision G
- Detail drawing of jacking beams for Loadcases 1, 2 and 3 - C636\15\010D, Revision B

Drawing No. C836/15/006D



KEY ELEVATIONS

NOTES
 1. FOR GENERAL NOTES REFER TO DRG:- C836/15/002D

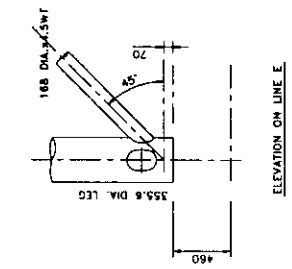
F	7/98	AS BUILT	TKG	JADC	HMB	CJB
E	10/07/02	APPROVED FOR CONSTRUCTION	TKG	JADC	HMB	CJB
D	11/07/02	APPROVED FOR CONSTRUCTION (DETAILS FOR REBAR)	TKG	JADC	HMB	HMB
C	11/07/02	APPROVED FOR CONSTRUCTION (KEY ELEVATION)	TKG	JADC	HMB	JADC
B	10/11/00	MINOR AMENDMENTS	TKG	PC	JADC	
A	11/07/02	CHECKED TO ANALYSIS	P-C	JADC		
O	10/07/02	PRELIMINARY	MMS	PC		
REV	DATE	DESCRIPTION OF REVISION	BY	CHECKED BY	APPROVED BY	SCALE

BOMEL CONTRACT No. C083601
 CLIENT JOINT INDUSTRY PROJECT
 PROJECT FRAMES PHASE III
 DRAWING TITLE
 DETAIL DRAWING OF NODE
 POINTS 10A, 11A, 12B AND 13B.

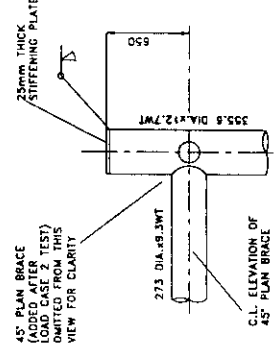
BOMEL ENGINEERING

100/1000, The Arcade, Level 10, 1000, North Sydney, NSW 1585, Australia
 Tel: +61 (0)2 9387 7770
 Fax: +61 (0)2 938 77877

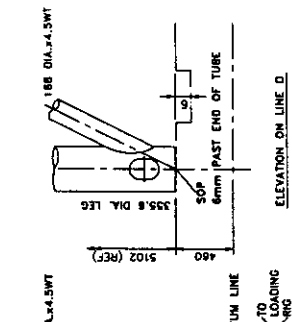
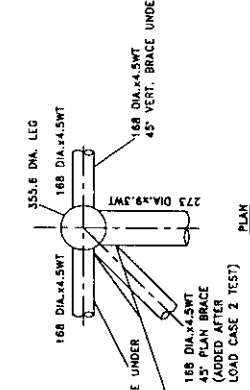
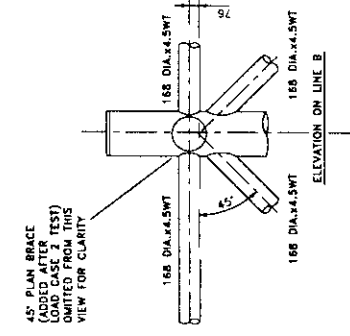
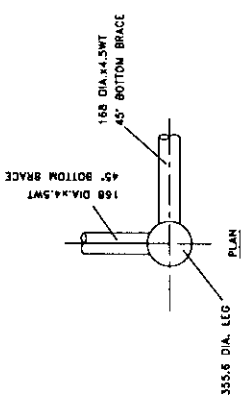
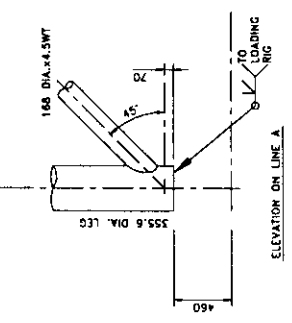
Drawing No. C836/15/006D



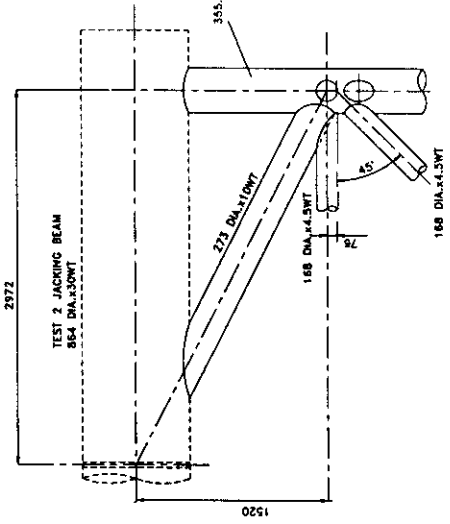
DETAIL 11A/002



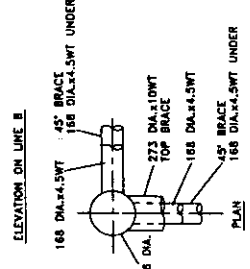
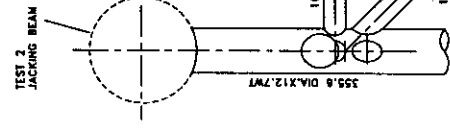
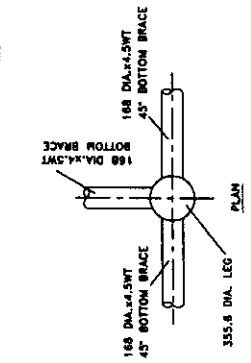
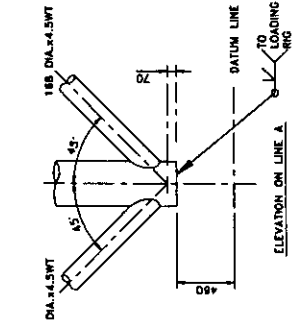
DETAIL 13B/002

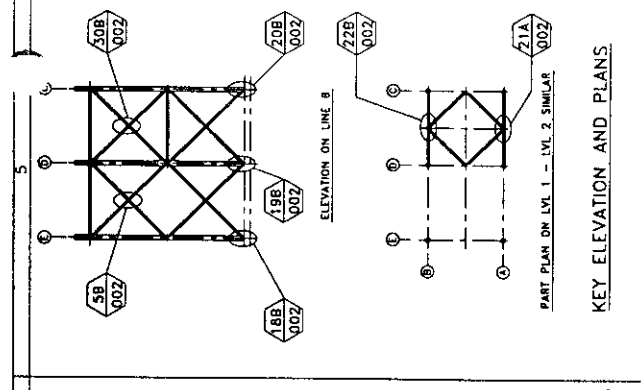
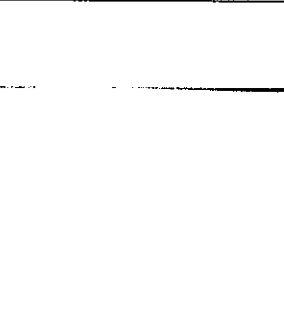
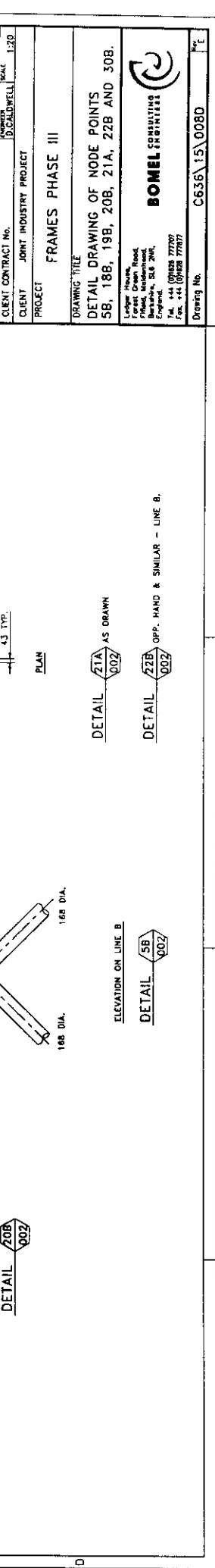
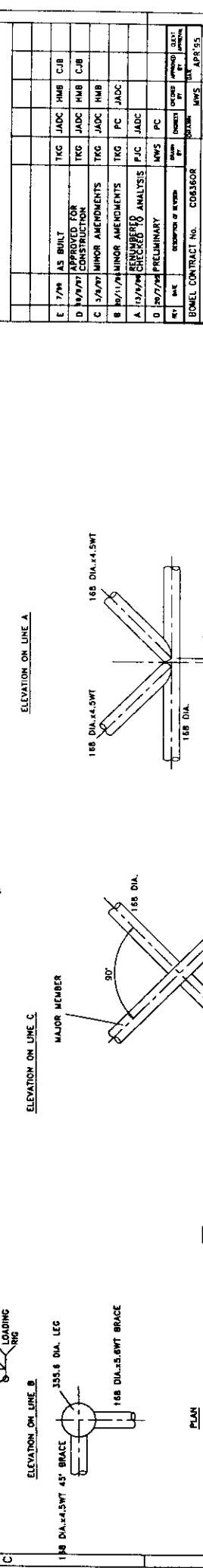
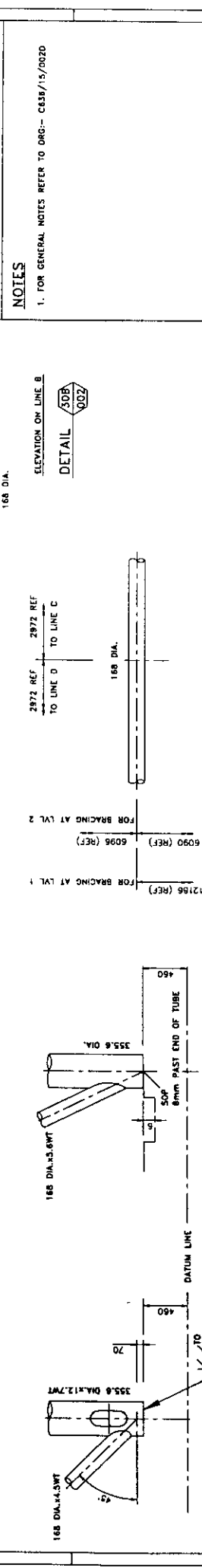
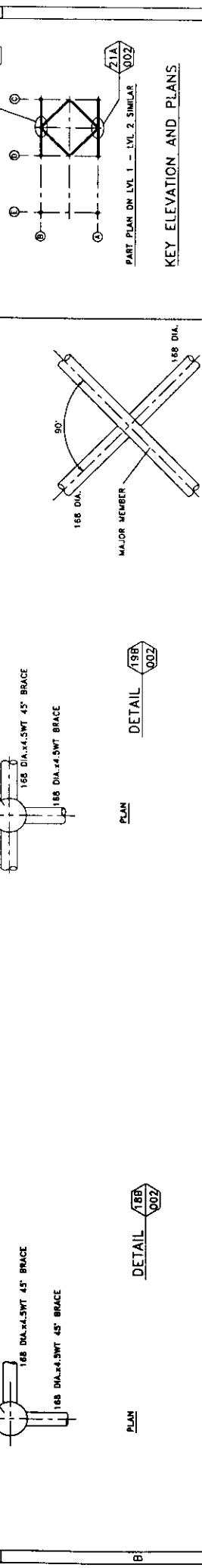
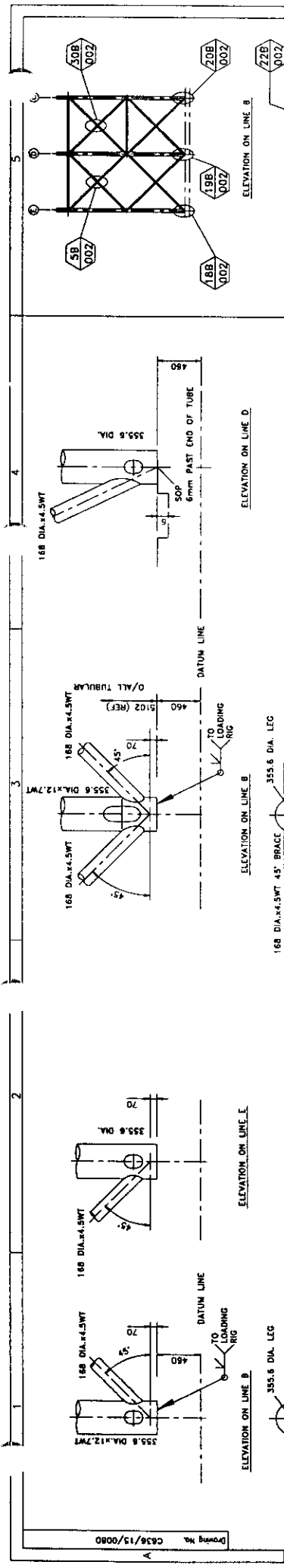


DETAIL 10A/002



DETAIL 12B/002





NOTES

1. FOR GENERAL NOTES REFER TO DRG-- C636/15/0020

REV	DATE	DESCRIPTION OF REVISION	DESIGNED BY	CHECKED BY	APPROVED BY
E	7/79	AS BUILT	TKC	JADC	HMB
D	10/9/77	APPROVED FOR CONSTRUCTION	TKC	JADC	HMB
C	1/2/77	MINOR AMENDMENTS	TKC	JADC	HMB
B	10/11/76	MINOR AMENDMENTS	TKC	PC	JADC
A	10/2/76	CHECKED TO ANALYSIS	PJC	JADC	JADC
D	10/2/76	PRELIMINARY	MWS	PC	PC

BOMEL CONTRACT No. C063608
 CLIENT CONTRACT No. 30 CALDWELL
 PROJECT JOINT INDUSTRY PROJECT
 DRAWING TITLE FRAMES PHASE III
 DETAIL DRAWING OF NODE POINTS SB, 188, 198, 208, 218, 228 AND 308.
 BOMEL CONSULTING
 11000 170th Street, Richmond, B.C. V6V 2M1, Canada
 Tel. +1 (604) 277-7707 Fax. +1 (604) 277-7707
 Drawing No. C636/15/008D

APPENDIX B

REACTION RIG DRAWINGS

General arrangement and setting out of loading rig - C636\16\001D, Revision D

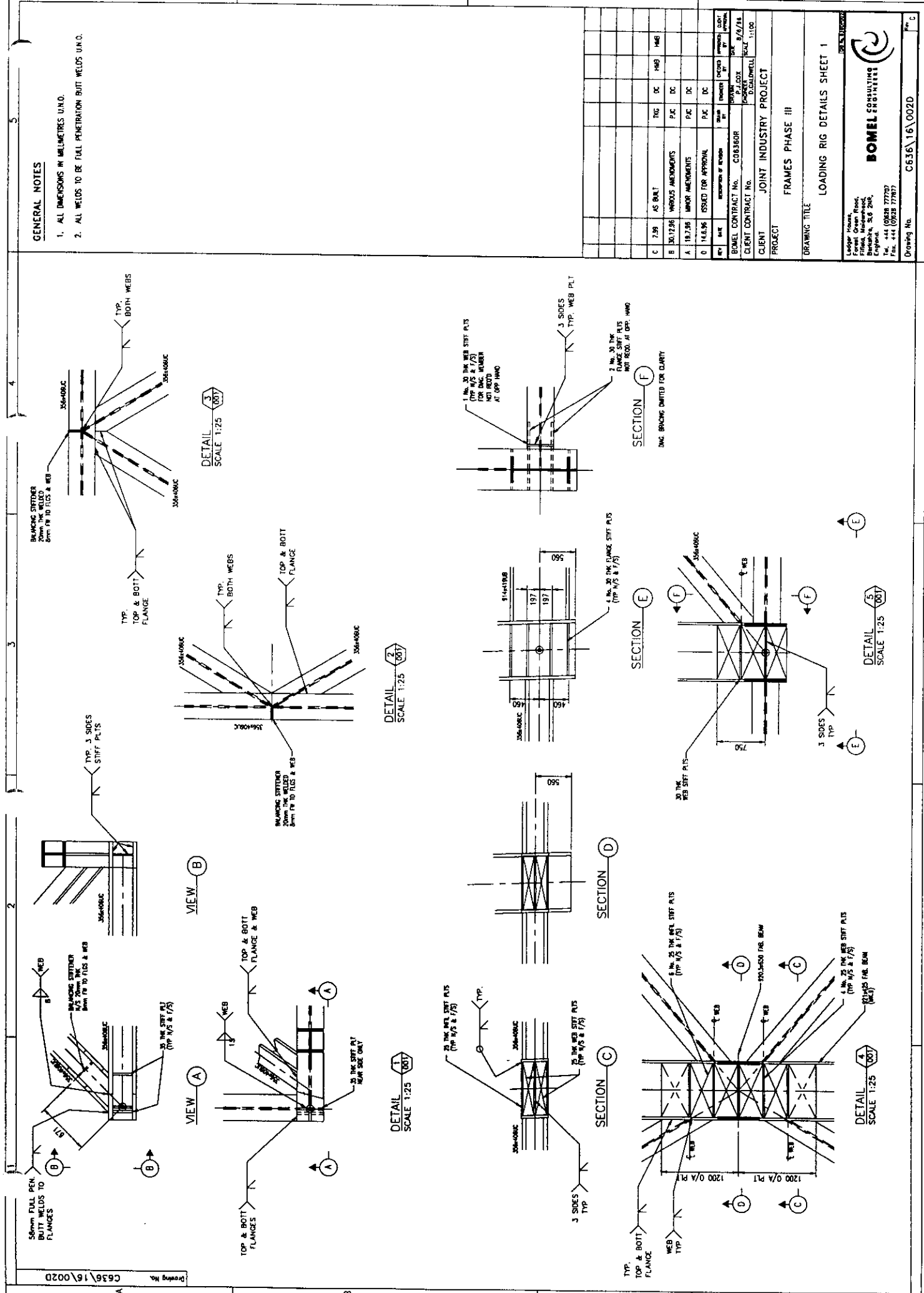
Loading rig details - sheet 1 - C636\16\002D, Revision C

Loading rig details - sheet 2 - C636\16\003D, Revision C

Loading rig details - sheet 3 - C636\16\004D, Revision C

GENERAL NOTES

1. ALL DIMENSIONS IN MILLIMETRES UNO.
2. ALL WELDS TO BE FULL PENETRATION BUTT WELDS UNO.



REV	DATE	DESCRIPTION OF REVISION	DESIGNED BY	CHECKED BY	APPROVED BY
C	7.99	AS BUILT	TNG	DC	HMG
B	10.12.06	MINOR AMENDMENTS	PJC	DC	HMG
A	19.2.96	MINOR AMENDMENTS	PJC	DC	
D	14.6.96	ISSUED FOR APPROVAL	PJC	DC	

BOMEL CONTRACT No.	C063608	DATE	8/9/18
PROJECT	JOINT INDUSTRY PROJECT	PROJECT MANAGER	JOHN MCELWELL
CLIENT	JOINT INDUSTRY PROJECT	SCALE	1:100
PROJECT	FRAMES PHASE III		

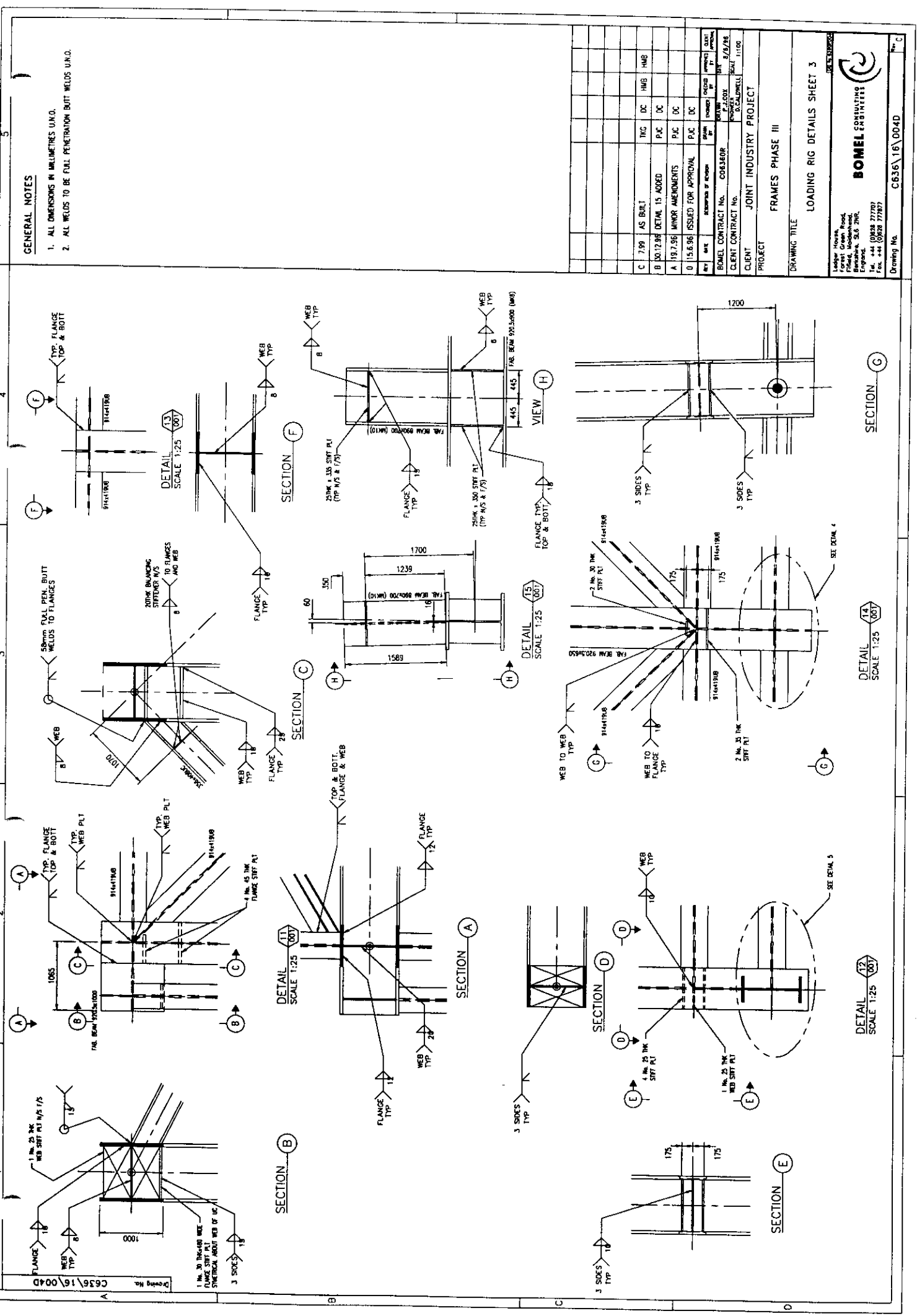
DRAWING TITLE	LOADING RIG DETAILS SHEET 1
DESIGN NUMBER	C636\16\002D

Ledge Hours,	
Forest Owen Reed,	
Structural Engineer,	
Birmingham, S.E. 20th,	
England.	
Tel. +44 (0)228 777707	
Fax. +44 (0)228 777877	

Drawing No.	C636\16\002D
-------------	--------------

GENERAL NOTES

1. ALL DIMENSIONS IN MILLIMETRES UNLESS OTHERWISE STATED.
2. ALL WELDS TO BE FULL PENETRATION BUTT WELDS UNLESS OTHERWISE STATED.



Drawing No. C636/16/004D

1 No. 20 THICK WEB STIFFENER (W/S) SYMMETRICAL ABOUT WEB OF UC

3 SIDES TYP

FLANGE TYP

WEB TYP

3 SIDES TYP

FLANGE TYP

WEB TYP

3 SIDES TYP

SEE DETAIL 4

1 No. 20 THICK WEB STIFFENER (W/S) SYMMETRICAL ABOUT WEB OF UC

3 SIDES TYP

FLANGE TYP

WEB TYP

3 SIDES TYP

FLANGE TYP

WEB TYP

3 SIDES TYP

SEE DETAIL 5

1 No. 20 THICK WEB STIFFENER (W/S) SYMMETRICAL ABOUT WEB OF UC

3 SIDES TYP

FLANGE TYP

WEB TYP

3 SIDES TYP

FLANGE TYP

WEB TYP

3 SIDES TYP

SEE DETAIL 6

1 No. 20 THICK WEB STIFFENER (W/S) SYMMETRICAL ABOUT WEB OF UC

3 SIDES TYP

FLANGE TYP

WEB TYP

3 SIDES TYP

FLANGE TYP

WEB TYP

3 SIDES TYP

SEE DETAIL 7

1 No. 20 THICK WEB STIFFENER (W/S) SYMMETRICAL ABOUT WEB OF UC

3 SIDES TYP

FLANGE TYP

WEB TYP

3 SIDES TYP

FLANGE TYP

WEB TYP

3 SIDES TYP

SEE DETAIL 8

1 No. 20 THICK WEB STIFFENER (W/S) SYMMETRICAL ABOUT WEB OF UC

3 SIDES TYP

FLANGE TYP

WEB TYP

3 SIDES TYP

FLANGE TYP

WEB TYP

3 SIDES TYP

SEE DETAIL 9

1 No. 20 THICK WEB STIFFENER (W/S) SYMMETRICAL ABOUT WEB OF UC

3 SIDES TYP

FLANGE TYP

WEB TYP

3 SIDES TYP

FLANGE TYP

WEB TYP

3 SIDES TYP

SEE DETAIL 10

1 No. 20 THICK WEB STIFFENER (W/S) SYMMETRICAL ABOUT WEB OF UC

3 SIDES TYP

FLANGE TYP

WEB TYP

3 SIDES TYP

FLANGE TYP

WEB TYP

3 SIDES TYP

SEE DETAIL 11

1 No. 20 THICK WEB STIFFENER (W/S) SYMMETRICAL ABOUT WEB OF UC

3 SIDES TYP

FLANGE TYP

WEB TYP

3 SIDES TYP

FLANGE TYP

WEB TYP

3 SIDES TYP

SEE DETAIL 12

1 No. 20 THICK WEB STIFFENER (W/S) SYMMETRICAL ABOUT WEB OF UC

3 SIDES TYP

FLANGE TYP

WEB TYP

3 SIDES TYP

FLANGE TYP

WEB TYP

3 SIDES TYP

SEE DETAIL 13

1 No. 20 THICK WEB STIFFENER (W/S) SYMMETRICAL ABOUT WEB OF UC

3 SIDES TYP

FLANGE TYP

WEB TYP

3 SIDES TYP

FLANGE TYP

WEB TYP

3 SIDES TYP

SEE DETAIL 14

REV	DATE	DESCRIPTION OF REVISION	DESIGNED BY	CHECKED BY	APPROVED BY
C	7.99	AS BUILT	MJC	DC	HMB
B	30.12.98	DETAIL 15 ADDED	PJC	DC	
A	19.7.96	MINOR AMENDMENTS	PJC	DC	
D	15.6.96	ISSUED FOR APPROVAL	PJC	DC	

BOMEL CONTRACT No. C063609
 PROJECT No. 16/004D
 CLIENT CONTRACT No. 001
 PROJECT No. 16/004D
 CLIENT CONTRACT No. 001

PROJECT: JOINT INDUSTRY PROJECT
 PHASE: III
 DRAWING TITLE: LOADING RIG DETAILS SHEET 3

Company Name: BOMEL ENGINEERING
 Address: Ladbroke Grove, London, W8 3NF
 Tel: +44 (0)20 7777 7777
 Fax: +44 (0)20 7777 7777

Drawing No. C636/16/004D

APPENDIX C

RIG AND FRAME MEMBER AND NODE NUMBERING SCHEMES

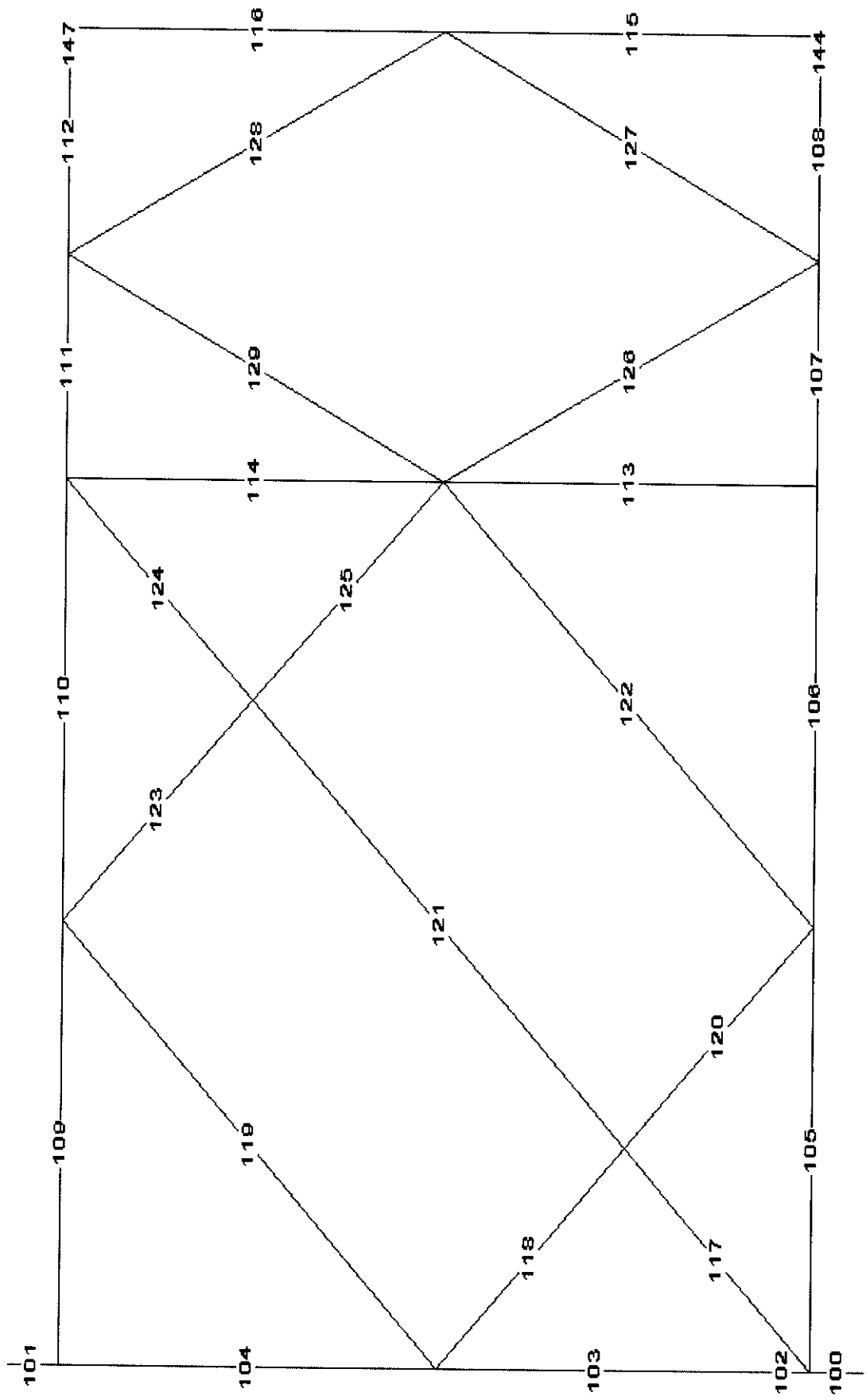


Figure C.1 Member Numbering - Plan on Base

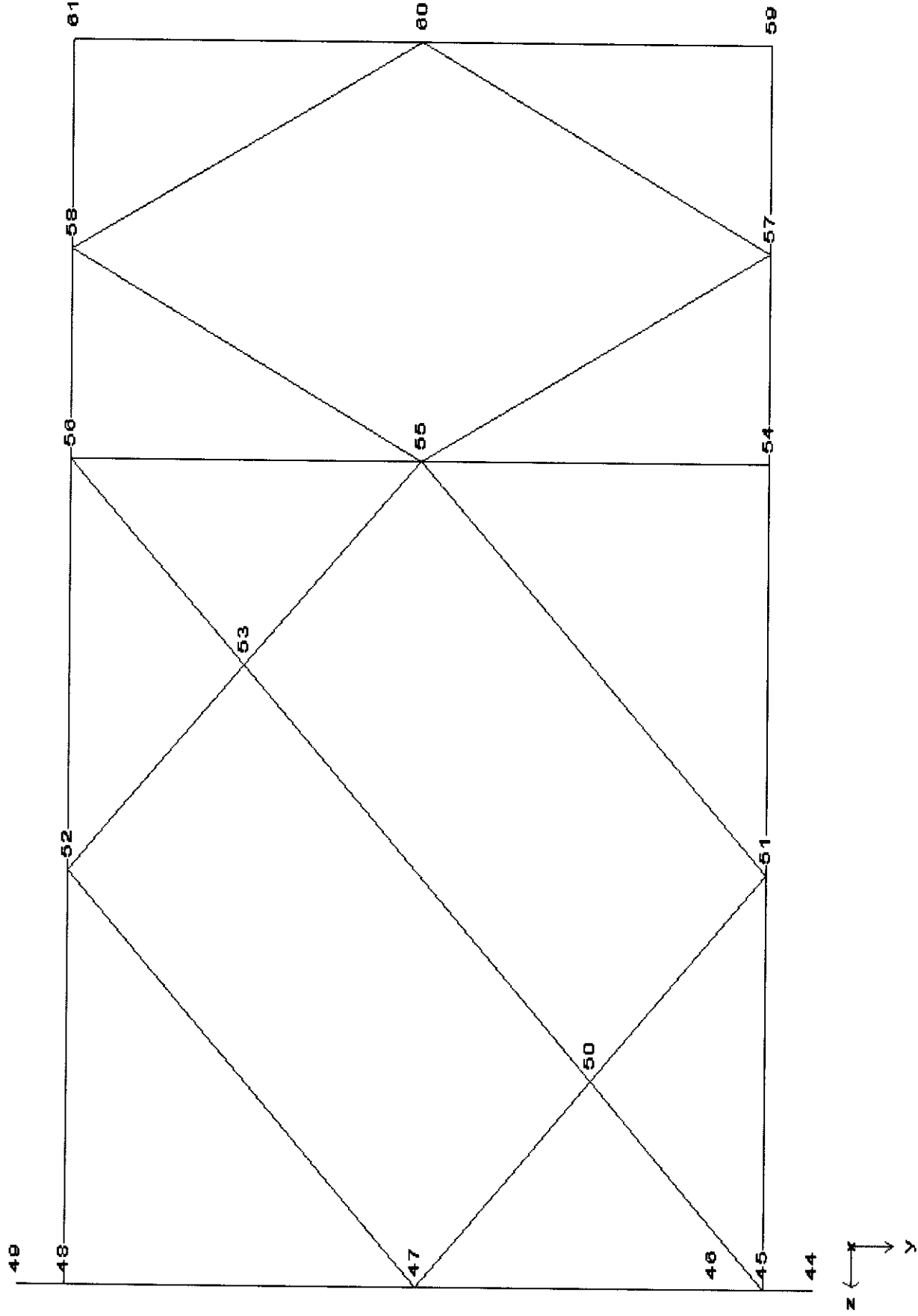
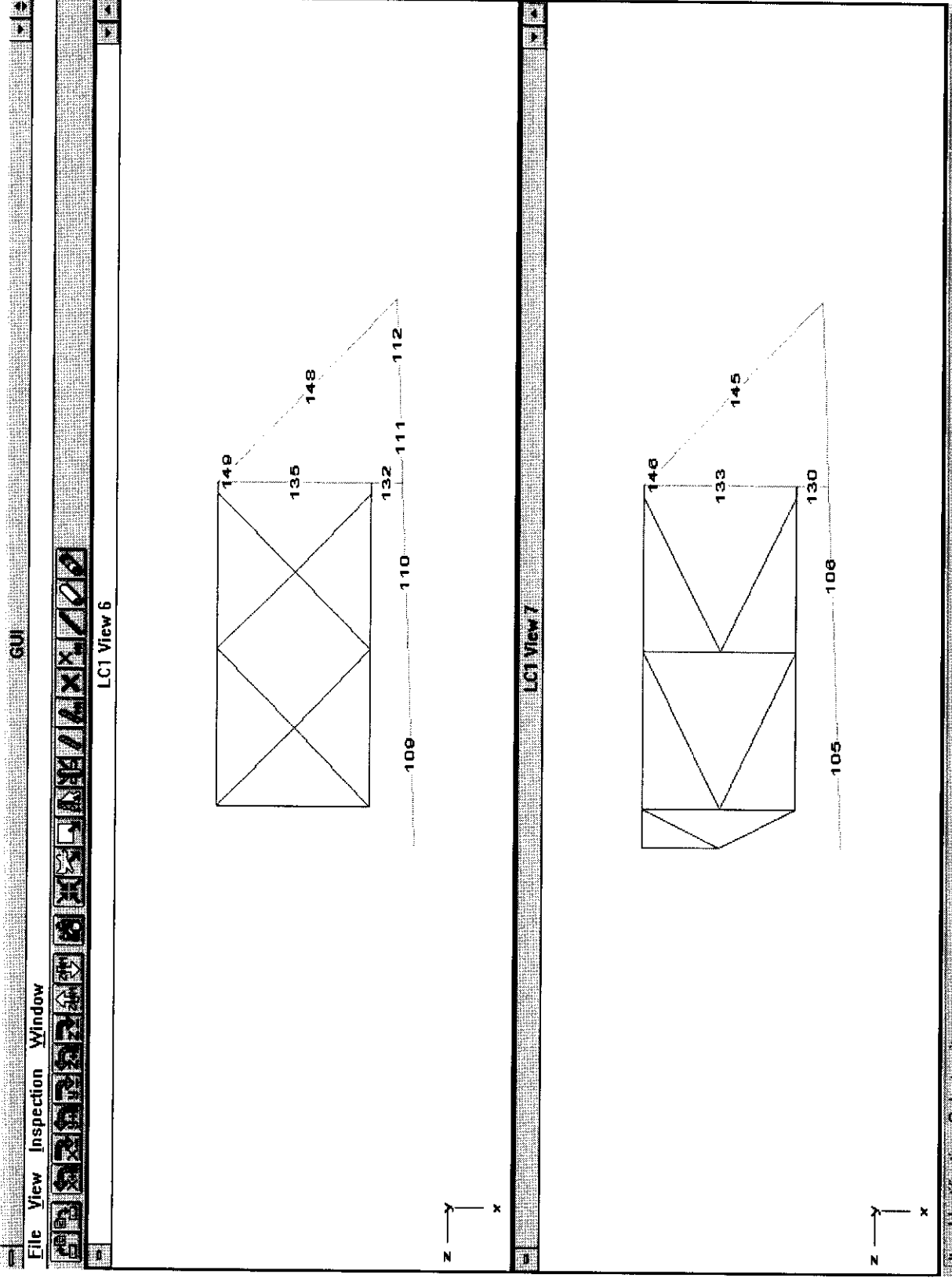


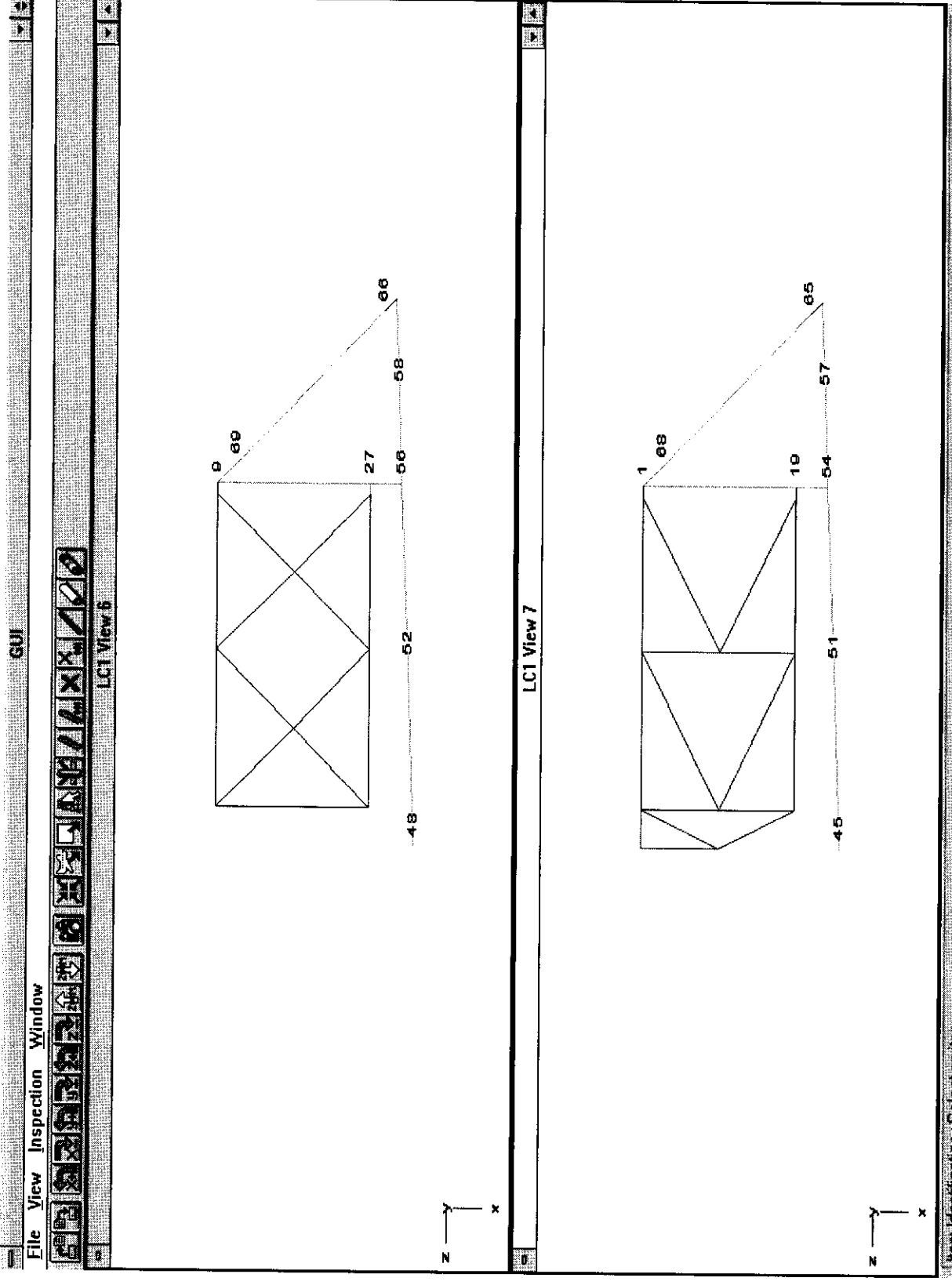
Figure C.2 Node Numbering - Plan on Base



Structural

Figure C.3 Member Numbering - Elevation on Support Rig on Frames E and C





Item Identification: Select an item Structure

Figure C.4 Node Numbering - Elevation on Supporting Rig on Frames E and C

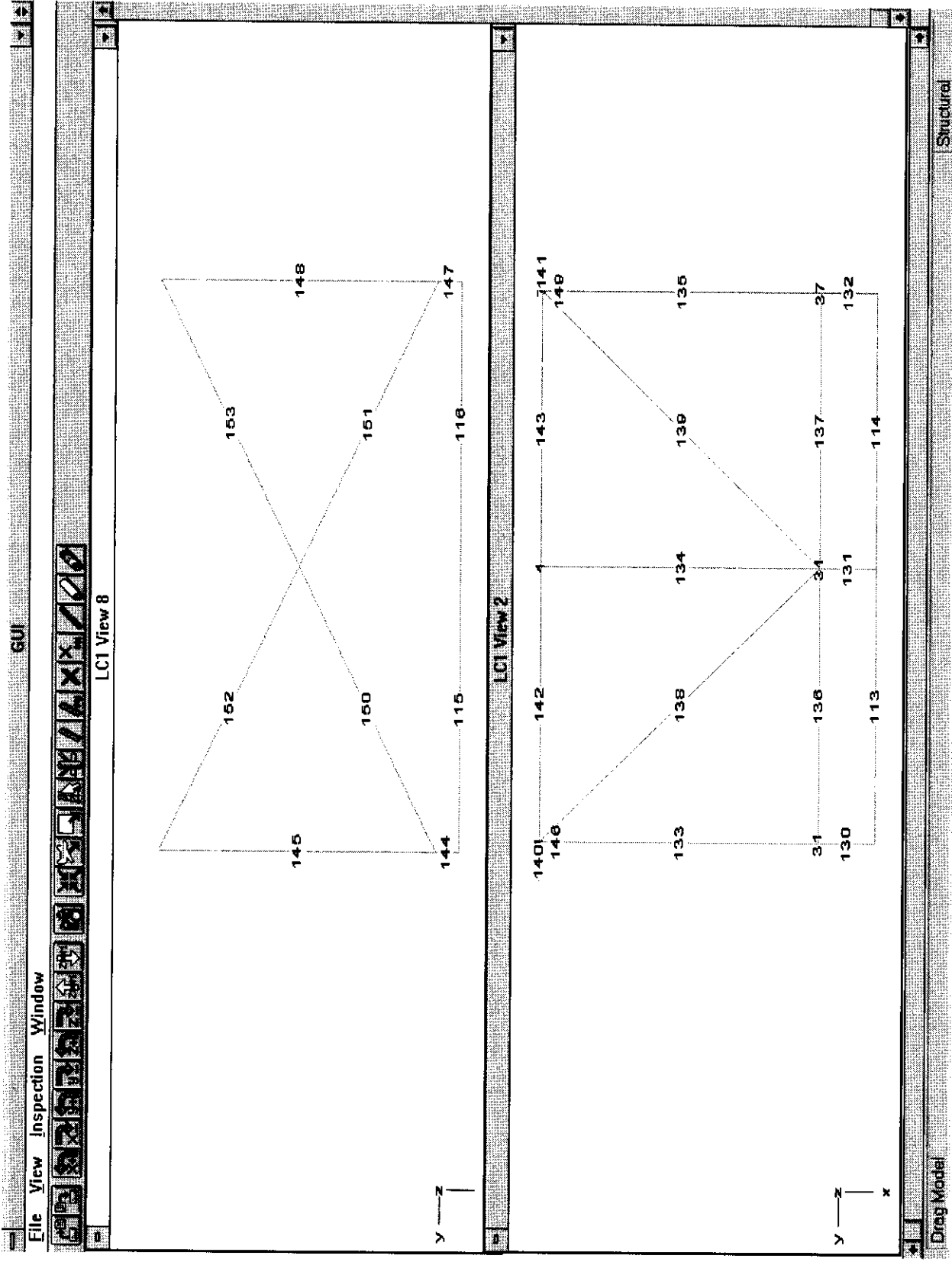


Figure C.5 Member Numbering - Elevation on 'Raking' and 'Vertical' Sections at back of Support Rig



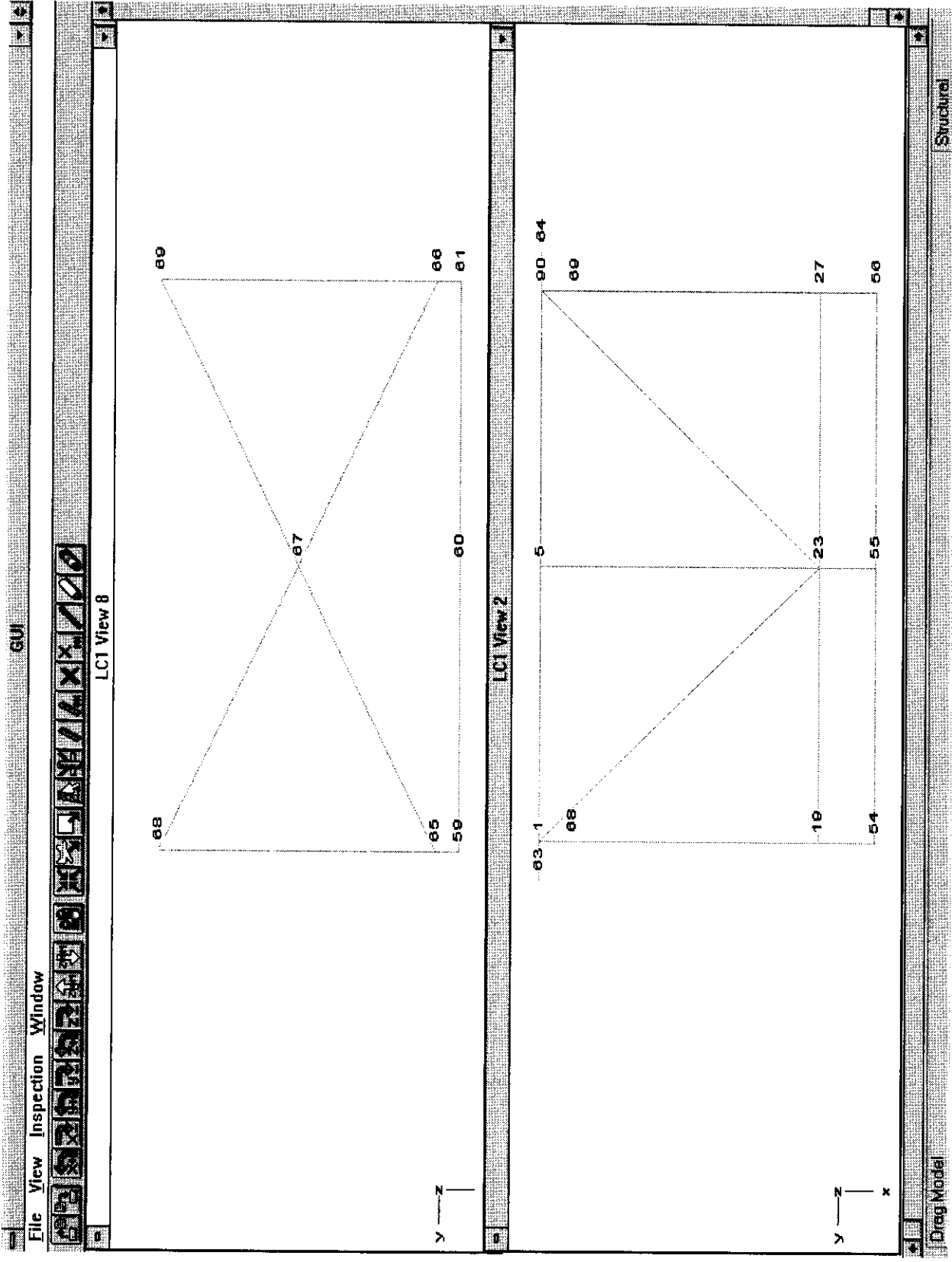


Figure C.6 Node Numbering - Elevation on 'Raking' and 'Vertical' Sections at back of Support Rig



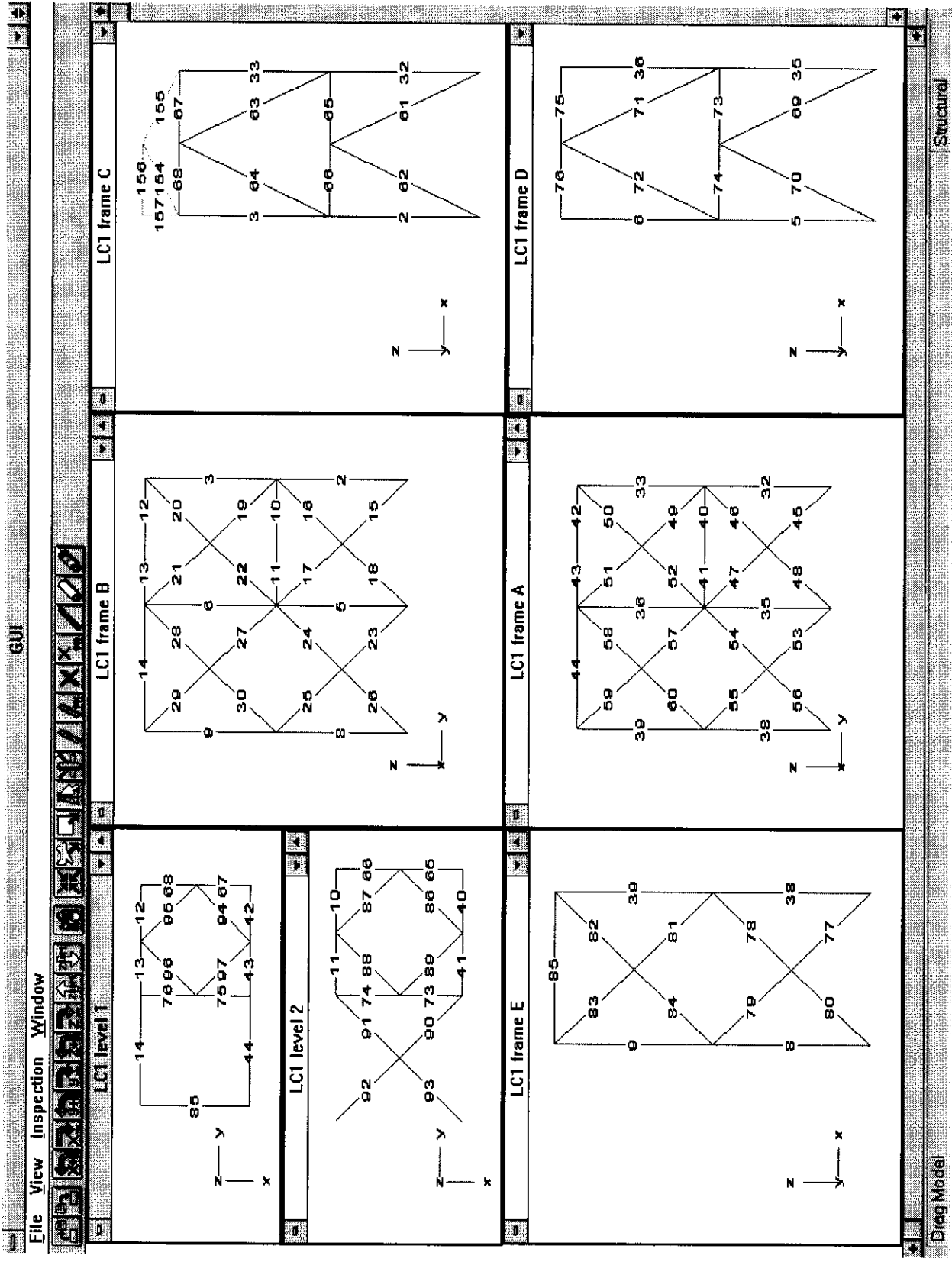


Figure C.7 Member Numbering System Load Case 1



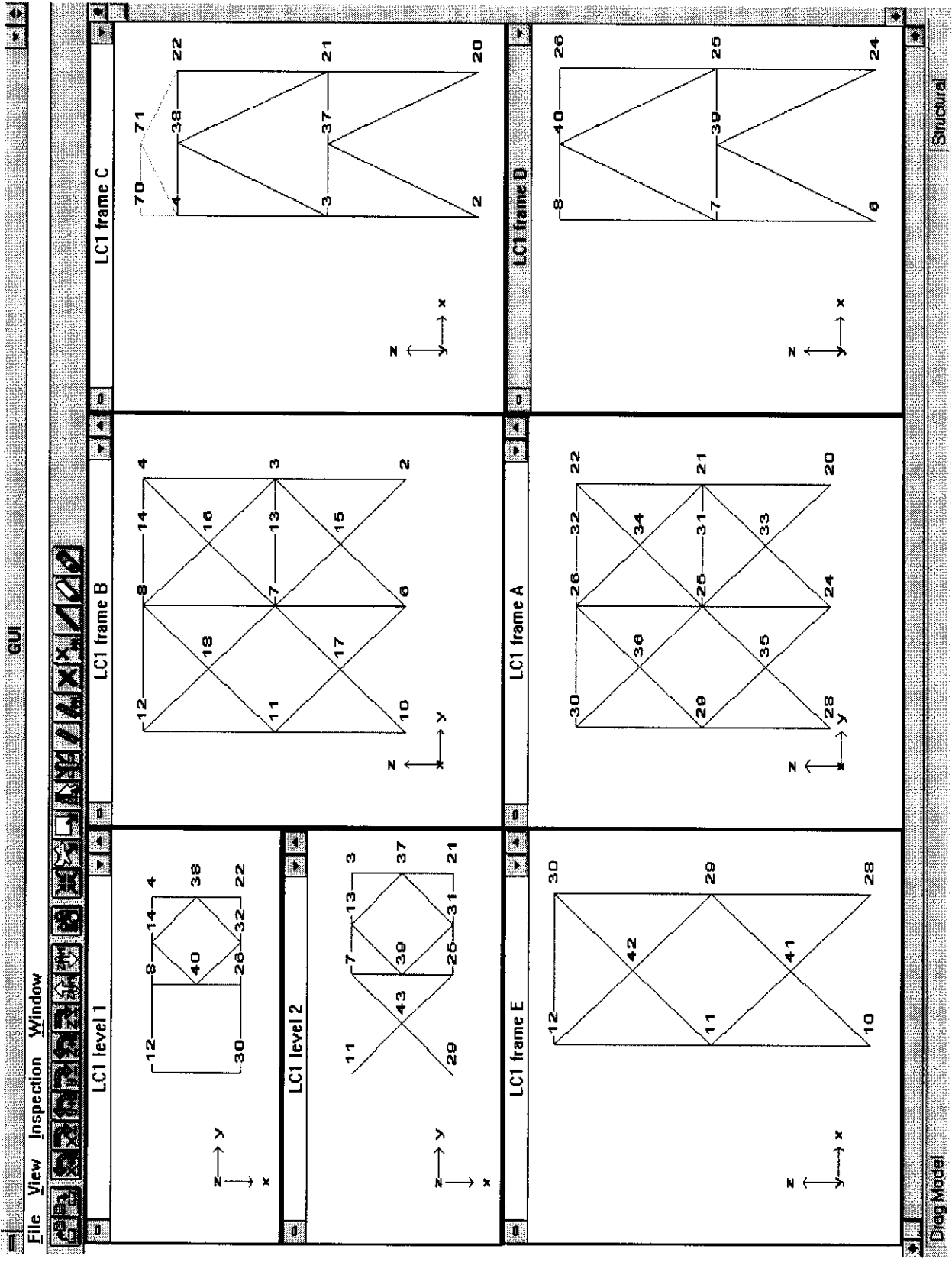


Figure C.8 Node Numbering Load Case 1

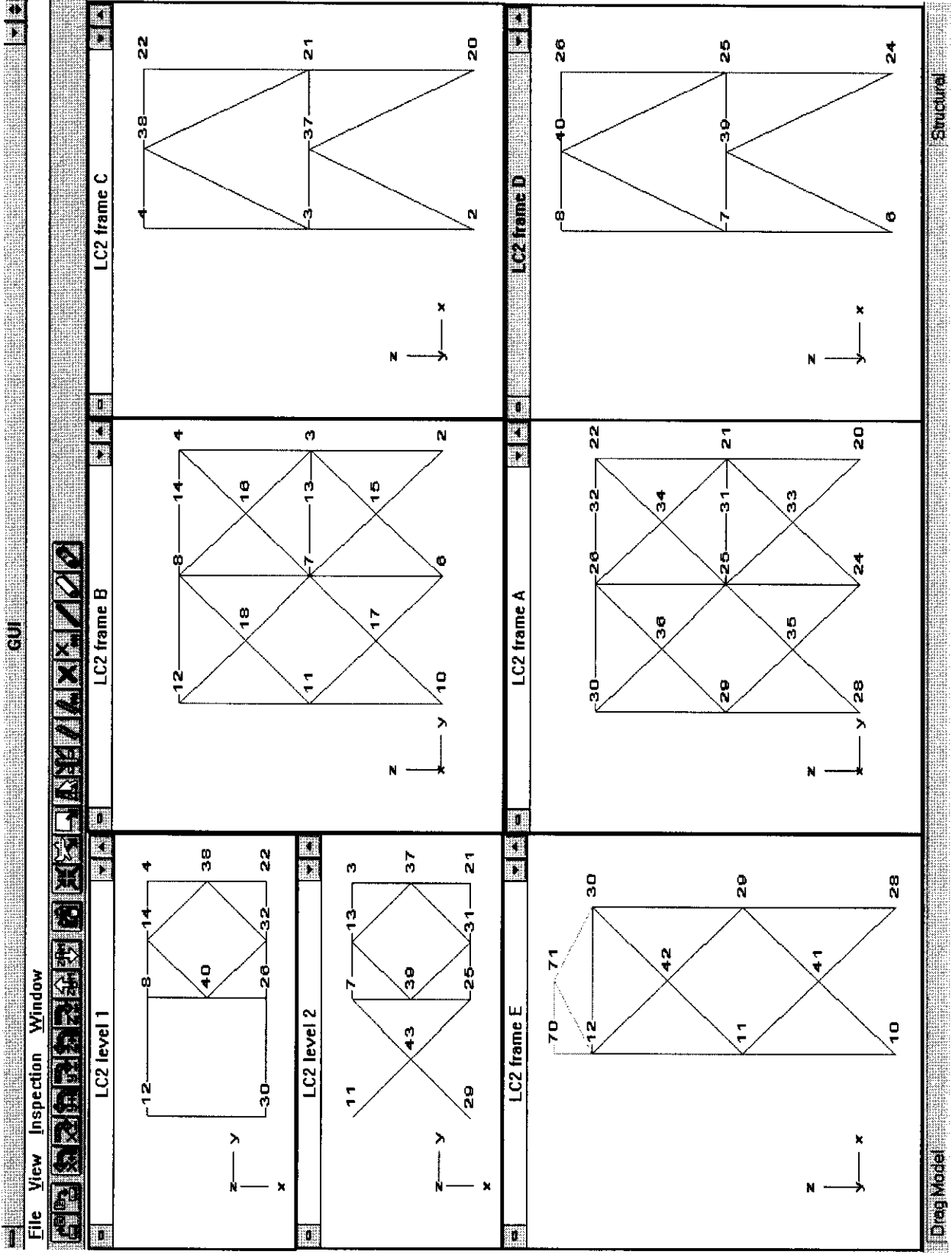


Figure C.10 Node Numbering Load Case 2

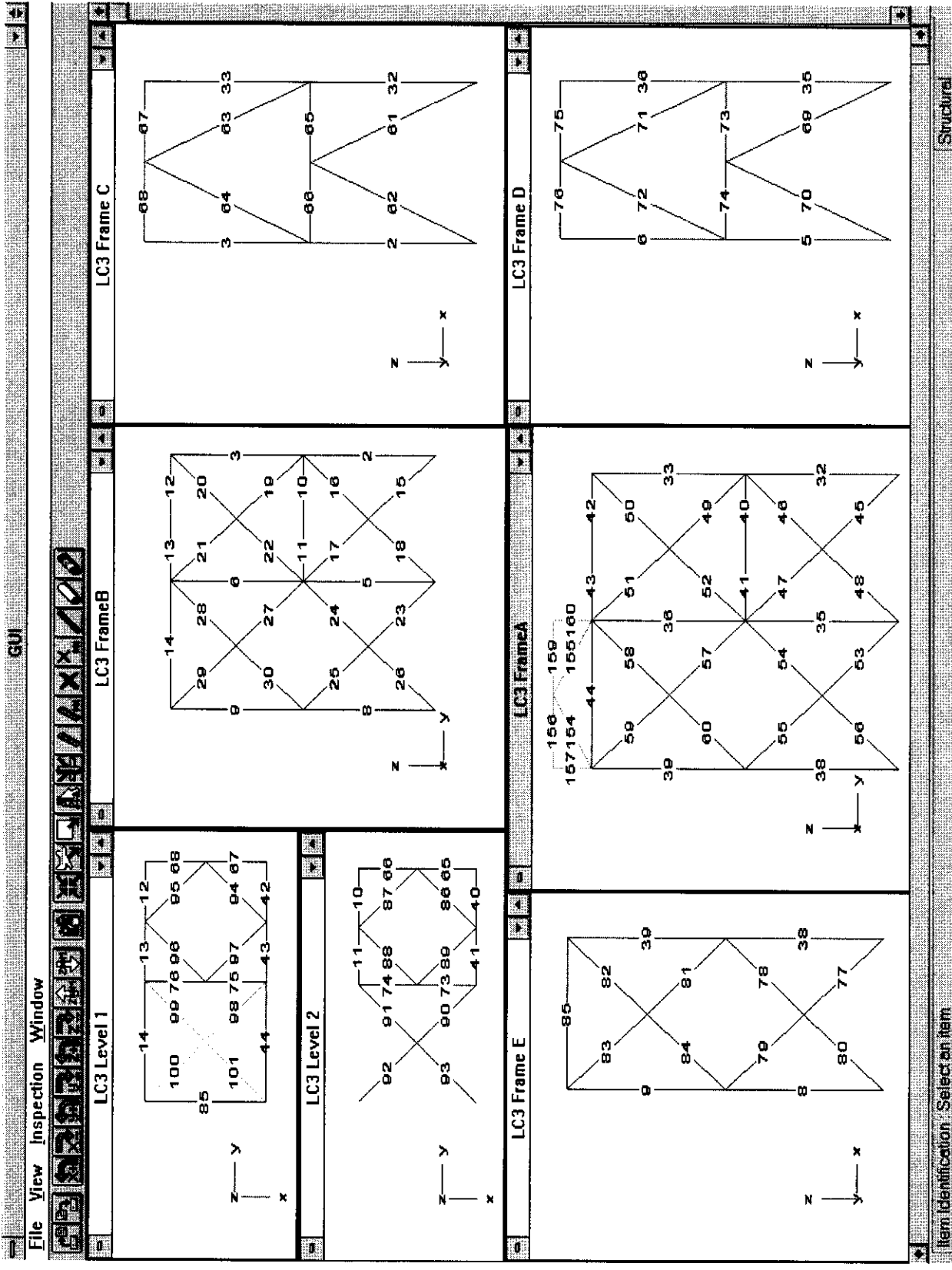


Figure C.11 Member Numbering Load Case 3

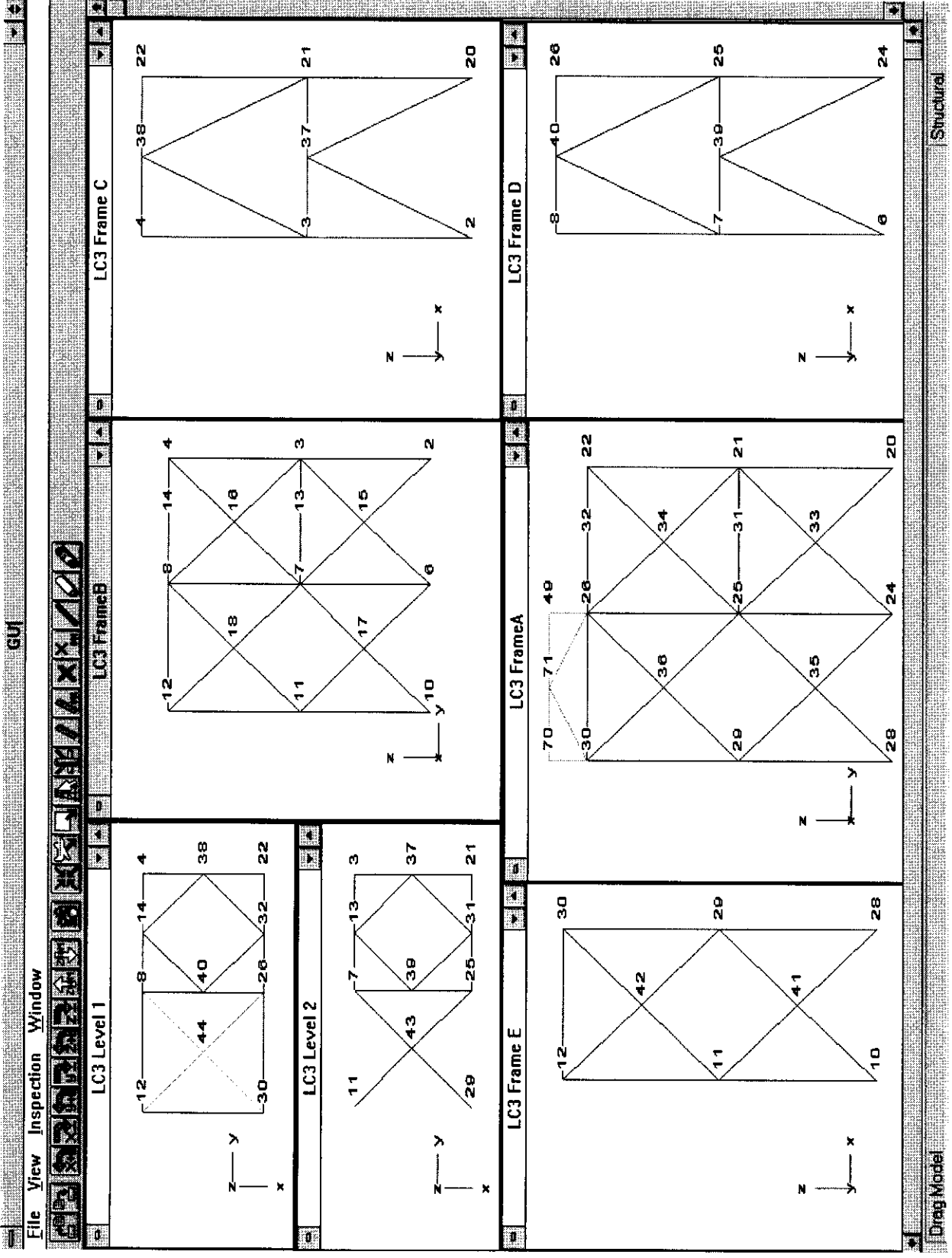


Figure C.12 Node Numbering Load Case 3



The contents of this document are confidential to the Participants of the Frames Project - Phase III, under the terms of their contract for participation in the project

**JOINT INDUSTRY TUBULAR FRAMES PROJECT
PHASE III**

MATERIAL TESTING REPORT

C636\23\004R REV B APRIL 1999

Purpose of Issue	Rev	Date of Issue	Author	Checked	Approved
Initial results for information	0	February 1998	HMB	PJK	CJB
Inclusion of all pre-frame test results	A	March 1998	HMB	PJK	CJB
Inclusion of all post frame test results	B	April 1999	KMM	HMB	CJB

Controlled Copy	10	Uncontrolled Copy	
-----------------	----	-------------------	--

BOMEL LIMITED
Ledger House
Forest Green Road, Fifield
Maidenhead, Berkshire
SL6 2NR, UK

Telephone + 44 (0) 1628 777707
Fax + 44 (0) 1628 777877
Email bomel@compuserve.com

REVISION SHEET

REVISION	DETAILS OF REVISION	DATE
0	Initial results of static tensile coupon tests (Batch 1)	19.2.98
A	Updated report to include all static tensile coupon test results available before frame testing (Batches 1 and 2)	24.3.98
B	Updated report to include all static tensile coupon test results available after completion of the frame testing (Batches 1, 2 and 3)	23.4.99

FILE SHEET

PATH AND FILENAME	DETAILS OF FILE
C636\23\002W.WK4 Rev B	Spreadsheet of test results containing Table 3.1 Figures 3.2, 3.3, 3.4
C636\23\Inc Doc 8523	Test results Batch 1: Table 3.1 and Figure 3.1
C636\23\Inc Doc 9377	Test results Batch 2: Table 3.1
C636\23\Inc Doc 9099	Appendix B: AKD sketches
C636\23\Inc Doc 12632	Test results Batch 3: Table 3.1
C636\06\294W-B.xls	Appendix A: Initial build and repair data
C636\12\images\gui11.pcx	Figure 4.1: Member Numbering
C636\23\022u.pcx	Figure 1.1
C636\23\023u.pcx	Figure 3.1

CONTENTS

	Page No.
FOREWORD	0.4
EXECUTIVE SUMMARY	0.7
1. INTRODUCTION	1.1
1.1 OBJECTIVES	1.1
1.2 EFFECTS OF RATE OF FRAME TESTING	1.1
1.3 STATIC TENSILE COUPON TEST PROCEDURES	1.2
2. TEST FRAME TUBULARS	2.1
2.1 TUBULARS	2.1
2.2 TEST BATCH 1	2.1
2.3 TEST BATCH 2	2.2
2.4 TEST BATCH 3	2.3
3. TENSILE COUPON TEST RESULTS	3.1
3.1 RESPONSE CHARACTERISTICS	3.1
3.2 YIELD STRESS RESULTS	3.1
3.3 TUBULAR GEOMETRY	3.6
3.4 OBSERVATIONS	3.6
4. MATERIALS WITHIN THE TEST STRUCTURE	4.1
5. CONCLUSIONS	5.1
6. REFERENCES	6.1
APPENDIX A FRAME MEMBER PROPERTIES AT START OF EACH TEST	
APPENDIX B STRUCTURE-MATERIAL CROSS REFERENCING	

FOREWORD

This report is one of a series describing different aspects of Phase III of the Joint Industry Tubular Frames Project. Each report is self contained providing detailed information in the subject area and summarising relevant data from other documents. The following table lists and briefly describes the focus of each report for cross-referencing purposes.

Report Title	Reference	Circulation
Summary and Conclusions Overview report describing the project and principal findings	C636\04\478R	1
Background, Scope and Development Scene setting report summarising previous work, identified needs and Phase III programme definition and development	C636\04\435R	1
3D Test Set Up Brief description of the 3D test set up and structural configuration	C636\06\313R	1
Material Testing Report Description of material testing procedures, test results and disposition of specific materials within test structure	C636\23\004R	1
Assessment of Locked-In Fabrication Stress Explanation for the build up of locked-in fabrication stresses, description of their measurement and summary of the locked-in force values in key components at the start of each test	C636\21\050R	1
Test Frame Instrumentation Detailed description of all instrumentation systems used in the 3D frame, accuracy, sign conventions etc. Data on CD in final report	C636\25\071R	1
Loadcase 1 Test Report - Multiplanar K Joint Action Detailed description of the Loadcase 1 static test response and interpretation of the results and their significance	C636\37\014R	1
Loadcase 2 Test Report - Interaction Between X-Braced Planes Detailed description of the Loadcase 2 static test response and interpretation of the results and their significance	C636\39\011R	1
Loadcase 3 Test Report - Multiple Member Failures and 3D System Action Detailed description of the Loadcase 3 static test response and interpretation of the results and their significance	C636\40\021R	1

Report Title	Reference	Circulation
<p>Philosophy of Cyclic Testing Discussion of the background to cyclic response issues in the context of ultimate system strength and basis for specific loading scenarios</p>	C636\24\021R	1
<p>Loadcase 1 Cyclic Test Report Detailed description of the Loadcase 1 cyclic test response and interpretation of the results and their significance. Comparison with LC1 static results</p>	C636\38\010R	1
<p>Monotonic and Cyclic testing of Isolated K Joints Description and presentation of results from isolated component tests undertaken by SINTEF in Norway</p>	STF22 F98704 (C636\24)	1/2
<p>Loadcases 2 and 3 Cyclic Test Report Detailed description of the Loadcases 2 and 3 cyclic test responses and interpretation of the results and their significance. Comparison with LC2 and LC3 static results</p>	C636\41\011R	2
<p>Loadcases 1 and 3 'Alternative' Cyclic Tests Detailed description of the Loadcases 1 and 3 alternative cyclic test responses and interpretation of the results and their significance. Comparison with LC1 and LC3 static and cyclic tests</p>	C636\45\008R	3
<p>Multiplanar SCFs Joint BG / BOMEL report describing analytical work and experimental measurements of multiplanar SCFs. Includes comparison with 'standard' empirical approaches</p>	C636\18\018R	1
<p>Site Testing Programme results - Report to Benchmark Analysts Comprehensive report describing results for benchmark cases LC1, LC2 and LC3, including all pertinent data and providing response plots 'matching' the contributions from individual analysts</p>	C636\32\066R	4
<p>Benchmark Conclusions Report comparing blind and post test analyses with measured responses and assimilating learnings and recommendations for future practice identified by Benchmark Analysts</p>	C636\32\084R	1

Key to circulation.

Circulation	All participants	Participants in 1st extension	Participants contributing finance/analytical results to 2nd extension	Benchmark Analysts
1	✓	-	-	×
2	-	✓	-	×
3	-	-	✓	×
4	✓	-	-	✓



JOINT INDUSTRY TUBULAR FRAMES REPORT PHASE III

MATERIAL TESTING REPORT

EXECUTIVE SUMMARY

This report presents results from static tensile coupon tests for offcuts of the tubulars used to fabricate the three-dimensional test specimen for the Phase III Frames Project tests. The results are related to specific locations within the structure but are also used to indicate the average yield level and potential variability for each material specification.

It is found that the bracing materials on average have yields between 10 and 22% higher than assumed in the baseline benchmark analyses whereas the leg yields are about 9% lower than anticipated. The static yield values, reflecting the rate and manner of structural testing, are typically 12% less than standard tensile coupon test results which is consistent with findings from earlier phases of the work.

The variability between tests from the same sample is found to be a significant contributor to the apparent variability between the yield properties for different tubulars to the same specification. Nevertheless some material variability is discernible.

Although the coefficient of variation is small, it is recognised that the absolute differences in yield may affect the sequence of nonlinear component responses in the test structure.

Tables are presented giving geometric properties and static yield stress values for every segment of each member in the frame for the individual structural collapse tests.

The level of detail adopted in post-test assessments will depend on the nature and purpose of individual investigations.



1. INTRODUCTION

1.1 OBJECTIVES

This report presents results from 75 static tensile coupon tests undertaken by BOMEL Limited for use in the structural frame tests in Phase III Tubular Frames Project investigation into the ultimate response of jacket type structures.

The purpose of the tests was:

- to determine the **actual** yield properties of tubular members within the structure rather than rely on nominal values, and
- to generate material data relevant to the manner of structural testing.

The remainder of this section describes the correlation between the test procedures and details the manner in which the static tensile tests were carried out. Section 2 then describes the material types and identifiers for individual tubulars in the frame. Seventy five material tests were conducted in three batches and Section 3 details the results by tubular and material type and makes comparison with nominal values. In Section 4 the tensile yield and tubular geometry values are allocated to individual members in the structure, allowing for repairs and member replacement, at the start of each frame test. Section 5 summarises the measured yield properties in comparison with values assumed for the structural design and original benchmark analyses.

1.2 EFFECTS OF RATE OF FRAME TESTING

The yield stress level exhibited by steel is influenced by the rate of testing⁽¹⁾. Tests performed by steel manufacturers and carried on the material certificates will generally be undertaken at the maximum rate permitted by the code⁽²⁾. The apparent yield will be higher than tests undertaken at a slower rate and this present investigation identifies the potential significance of this for interpreting the frame test results.

Testing of the structural frame was carried out under quasi static conditions; load was applied under displacement control at a rate of approximately 3 mm per minute. After a suitable increment the ram was locked in position for the instrumentation to be scanned to record the state of strain (stress) throughout the structure. However, once plasticity begins to develop in

a structure, forces redistribute as the structure settles to a state of static equilibrium. With the amount of instrumentation specified, it took a finite time to complete a scan of all channels. To ensure readings were consistent, it was essential that the structure had reached equilibrium at the point data were recorded.

The frame test procedure was therefore:

- apply load under displacement control (at the rate of approximately 3 mm per minute),
- after a suitable increment, lock the ram in position,
- 'hold' the structure for about 2-3 minutes until online monitoring of the instrumentation shows a stable equilibrium to have been achieved,
- scan the instrumentation,
- apply the next displacement increment, etc.

1.3 STATIC TENSILE COUPON TEST PROCEDURES

To ensure that the recorded yield values correspond to the rate of structural testing, 'static' tensile coupon tests were performed consistent also with established test practice^(e.g.3). The test procedure taken from the BOMEL specification⁽⁴⁾ is as follows:

- A The cross-sectional dimensions of the test zone shall be determined with a micrometer.
- B Up to the 'yield' load (from zero load to point Y in Figure 1.1) the speed of cross head separation shall give a constant rate of stressing between 6 and 30 N/mm.s⁻¹ in accordance with BSEN 10002⁽²⁾.
- C In the plastic range of the test, i.e. from point Y onwards, the speed of cross head separation shall maintain a strain rate of 0.00025/s within the parallel length of the specimen in accordance with BSEN 10002.
- D When, in the plastic phase, the strain measured across the gauge length approaches 0.005, the cross heads shall be stopped for 2 minutes (± 5 secs).
- E Some unloading will occur during this stoppage and the lowest nominal stress sustained during this stoppage shall be taken as the static yield stress (SY1).

- F The cross heads shall be separated again as at Step C until the strain reaches 0.008 when the cross heads shall be stopped for 2 minutes (± 5 secs).
- G The lowest nominal stress sustained during this stoppage shall be taken as the static yield stress (SY2).
- H The cross heads shall be separated again as at Step C until the strain reaches 0.012 when the cross heads shall be stopped for 2 minutes (± 5 secs).
- I The lowest nominal stress sustained during this stoppage shall be taken as the static yield stress (SY3).
- J The cross heads shall then be separated to give a strain rate of 0.008/s in accordance with BSEN 10002.
- K The elongation at rupture (%) shall be recorded.

The figure indicates a slight increase in the static yield load at successive hold points and the general procedure enables the static yield value at 0.2% strain to be determined by extrapolation. It will be seen in Section 3 that in these Frames Project tests the static yield values at each hold point were similar, variously increasing, decreasing or fluctuating. The quoted values are therefore based on the average of the static values SY1, SY2 and SY3.

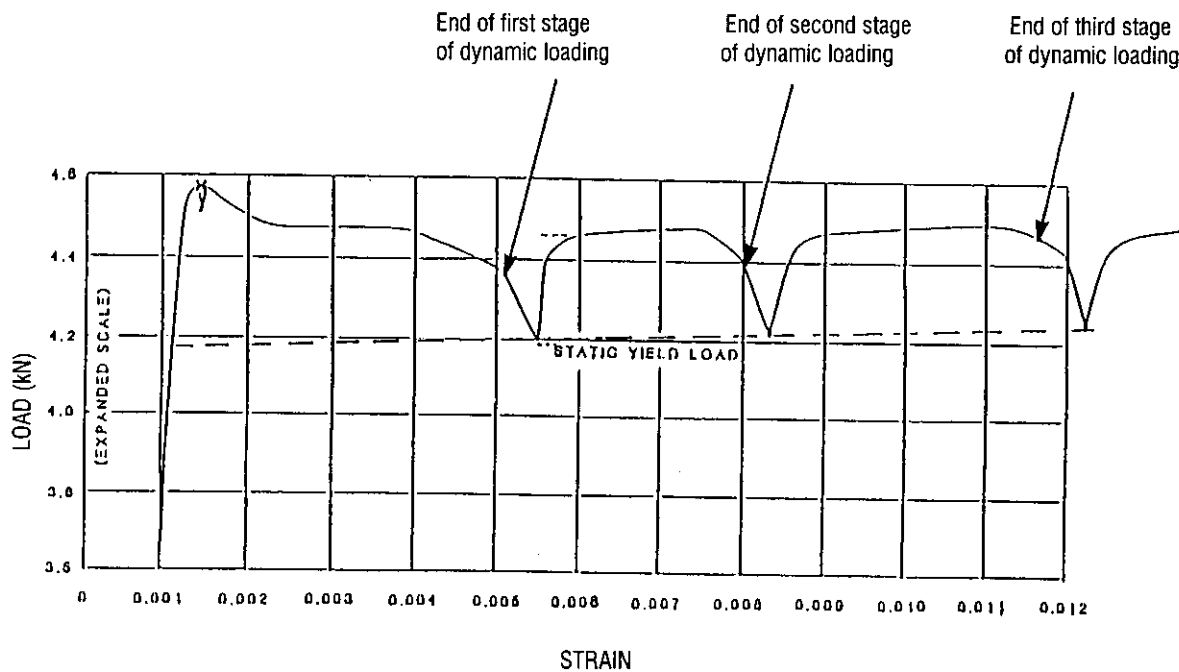


Figure 1.1 Measurement of Static and Dynamic Yield Loads in a Tensile Test



2. TEST FRAME TUBULARS

2.1 TUBULARS

Some 116 tubular lengths were procured for the fabrication and repair of the test frame. These were supplemented with remaining material from the Phase II Frames Project test programme. In order to provide a comprehensive basis for interpreting the structural response, complete information on material and geometric properties was gathered with complete traceability from each component in the structure to the surveys⁽⁸⁾.

Individual tubulars were identified (P1 to P116) and measurements of diameter and thickness and overall straightness were taken at metre intervals⁽⁸⁾. The static tensile coupon tests reported here provide the data on tensile yield properties. Tubulars retained from the Phase II programme are designated accordingly (e.g. P30II). Directly comparable data were gathered⁽¹⁰⁾ during the earlier work and relevant values are reproduced in this document.

Table 2.1 summarises the materials and nominal dimensions for all tubulars. Where it has been necessary to source tubulars to the same specification from different heat treatments, the materials have been separated out in the table accordingly.

The basis for the material tests in the Phase III test programme is described below.

2.2 TEST BATCH 1

At the initial stage of the work, the final allocation of tubulars within the structural frame was not determined. However, a set of representative static tensile coupon tests was commissioned with Materials Engineering Limited in Aberdeen to give an initial indication of the yield properties in the as-delivered materials. This set of tests is subsequently referred to as Batch 1 in this report. The material tests focussed on key tubular categories within the framing anticipated to play a role in the ultimate structural responses. Materials 'over' specified to remain elastic (e.g. load cells) were not tested and reference was made to mill certificates to confirm adequacy.

For Batch 1 representative tubulars were selected at random and individual tests performed. In addition, multiple tests for an individual tubular (P39) were undertaken to assess the apparent variability between tubulars with the inherent variability between tests on the same material.

Table 2.1 Frames Project Tubulars

TUBULAR REFERENCE	MATERIAL/BATCH	SIZE OD X WT (mm)
P1 - 10	API 5L X 52	355.6 x 12.7
P11	API 5L X 52	355.6 x 25.4
P12	API 5L X 52	457.2 x 12.7
P13 - 14	API 5L X 52	168.3 x 18.3
P15 - 18 / P24	API 5LB	273.0 x 5.6
P19	API 5L X 52 / C6104E	168.3 x 9.5
P20	API 5L X 52 / 51669	168.3 x 9.5
P21 - 22	API 5L X 52	273.1 x 10.0
P23	API 5L x 52	273.1 x 9.3
P25 - 37	BS 3602 430 ERW / 5B25816	168.3 x 5.6
P38 / P40 - 45 / P49 - 55	BS 3602 430 ERW / 5B22797	168.3 x 4.5
P39 / P56 - 110	BS 3602 430 ERW / 5B19704	168.3 x 4.5
P113 - 116	BS 3602 430 ERW / 5B43139	163.3 x 4.5
P30II - 31II / P34II - 35II / P45II	BS 3602 430 ERW / 5B31325	163.3 x 4.5
P46	BS 4848 Gr 50C	168.3 x 5.0
P47	BS 4848 GR 50D	168.3 x 5.0
P48	DIN 1629 St 52	168.3 x 5.0

2.3 TEST BATCH 2

Once fabrication was at an advanced stage, each member could be traced to the tubular reference. Appendix A contains the sketches provided by the fabricator, AKD Engineering Limited for the initial build. A second batch of tensile coupon tests (Batch 2) was therefore commissioned to provide comprehensive data for the tubulars used within the structure.

2.4 TEST BATCH 3

Following completion of the Phase III frame testing it was necessary to perform a further set of static coupon tests for the purposes of analysis. These ensured that material properties were available for the specific tubulars used in all components which failed in the frame tests. This set of supplementary tests is referred to as Batch 3 within this report.

The results from Batches 1, 2 and 3 have been combined in this report and are presented in Section 3.



3. TENSILE COUPON TEST RESULTS

3.1 RESPONSE CHARACTERISTICS

Tests were undertaken on three tubular types (steel grade / manufacturing process) of different sizes:

- API 5L X 52
- API 5LB
- BS 3602 430 ERW (annealed).

The electric resistance welding manufacturing process for the BS 3602 tubulars leaves considerable residual stresses. Stub column tests in earlier phases of the Frames Project⁽⁵⁾ showed that as welded, the tubulars exhibit a gradual softening characteristic without the well defined yield point representative of offshore rolled and welded members. However, the tubulars are supplied in appropriate sizes for the geometric properties and proportions of offshore jackets to be retained at the scale of testing. Subsequent to delivery the ERW tubulars were annealed to relieve the residual stresses using procedures proven in earlier phases of the work^(5, 6).

Figure 3.1 shows representative plots of load against cross-head displacement recorded in tensile tests on a sample from each tubular type. It should be noted that these plots do not relate to the gauge area alone and should not be used to infer Young's modulus characteristics. (Previous stub column tests⁽⁵⁾ on ERW tubulars confirmed an average value of 207×10^3 N/mm²).

However, the plots do confirm that all materials exhibit a well defined yield point and sustained yield plateau (subsequent strain hardening at large strains/displacements is not shown). Furthermore, the relaxation at each hold point can be seen, together with the basis for determining SY1 etc.

3.2 YIELD STRESS RESULTS

Table 3.1 presents results for the 75 tests undertaken in the Phase III test programme⁽⁹⁾ together with relevant results from Phase II⁽¹⁰⁾. The static yield loads are averaged for each sample and for each heat treatment of nominally identical tubulars. The coefficient of variation (COV) of the results for each set is presented based on the sample standard deviation.

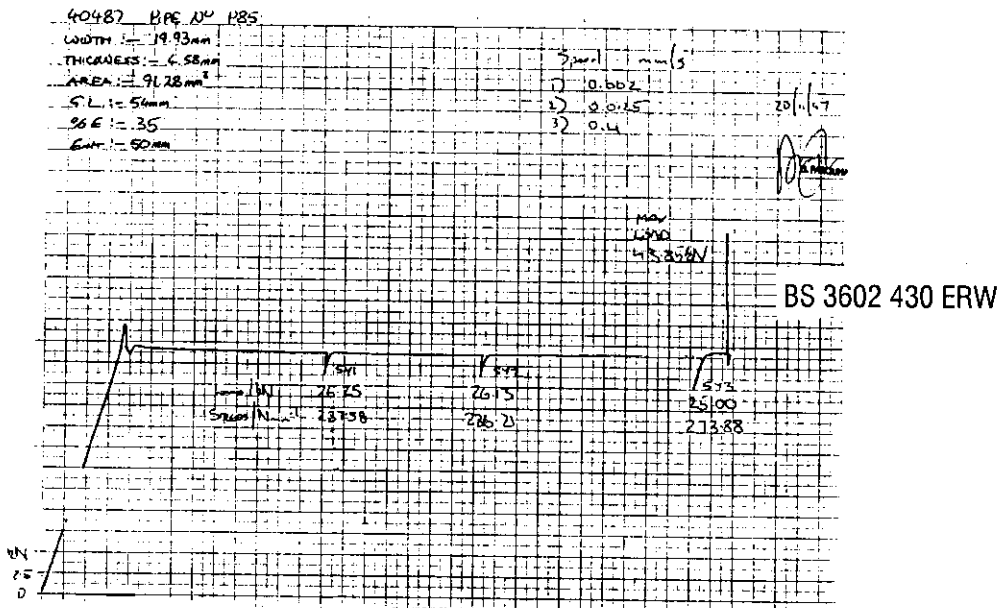
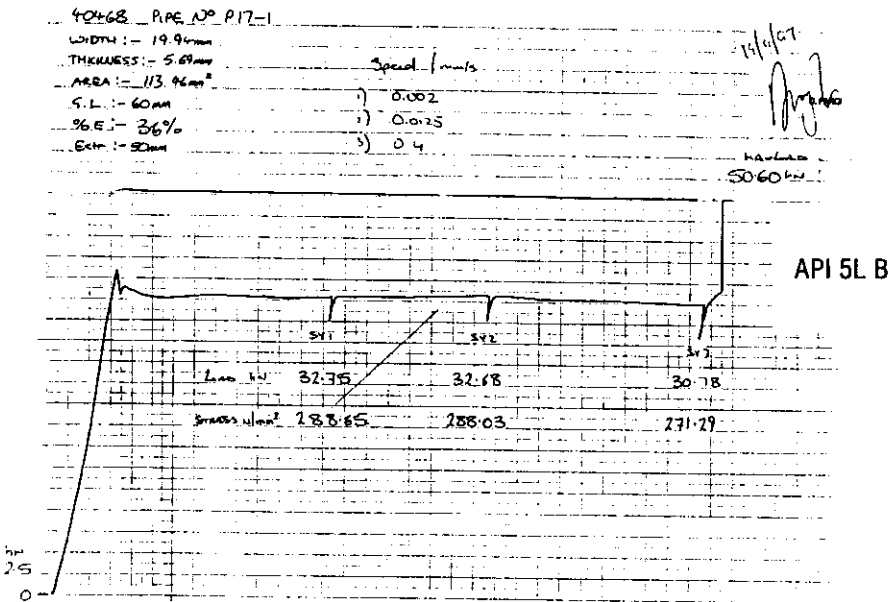
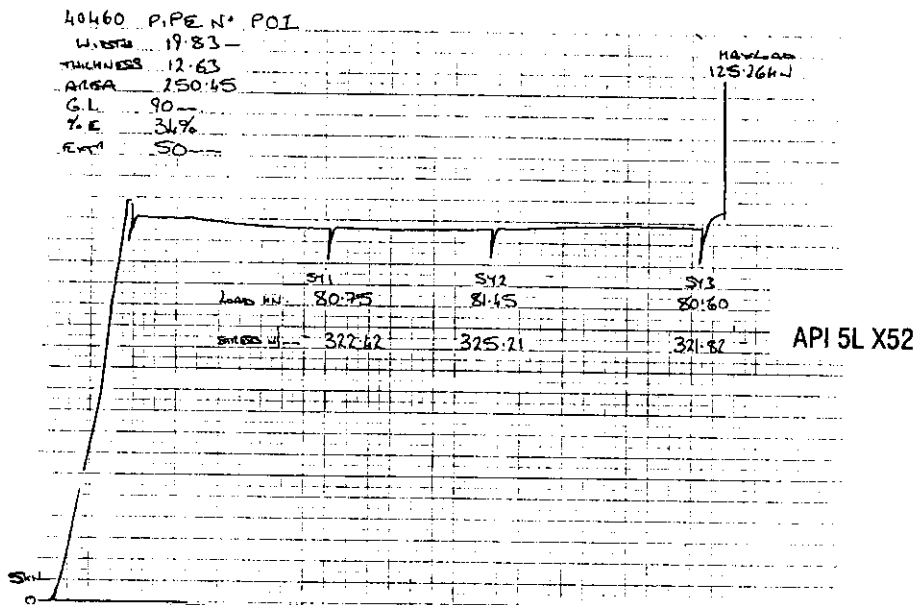


Figure 3.1 Static Tensile Coupon Test Plots



Table 3.1 Static Yield Test Results (Part 1 of 3)

MEL REF.	AKD REF.	TEST BATCH	WIDTH (mm)	THICKNESS (mm)	X AREA (mm ²)	SY1 (N/mm ²)	SY2 (N/mm ²)	SY3 (N/mm ²)	SY1-3 Avg. (N/mm ²)	ELONG. %	
Material API 5L Gr X52			Nominal properties 355.6mm OD x 12.7mm WT			Heat No. 93310					
40460M	P01	1	19.83	12.63	250.45	322.42	325.21	321.82	323.2	34	
40461M	P03	1	20.04	12.72	254.91	323.64	321.68	313.84	319.7	34	
40462M	P05	1	20.03	12.81	256.58	323.68	329.52	329.33	327.5	33	
40463M	P07	1	20.18	12.38	249.83	318.22	325.82	318.22	320.8	34	
40464M	P09	1	20.08	12.74	255.82	330.27	328.36	338.13	332.3	33	
40939M	P10	2	19.88	12.51	248.69	335.36	336.76	337.77	336.6	33	
Test Results			Avg T (mm):	12.63	Avg SY1:	325.60	Avg SY1-3:		326.67	COV SY1-3:	2.2%
Material API 5L Gr X52			Nominal properties 457.2mm OD x 12.7mm WT			Heat No. 197120					
40465M	P012	1	20.05	12.81	256.84	356.25	355.28	354.31	355.3	31	
Test Results			Avg T (mm):	12.81	Avg SY1:	356.25	Avg SY1-3:		355.28	COV SY1-3:	0.3%
Material API 5L Gr B			Nominal properties 273.1mm OD x 5.6mm WT			Heat No. 5B19468					
40466M	P15-1	1	19.94	5.65	112.66	295.14	288.48	281.82	288.5	36	
40467M	P16-1	1	19.91	5.61	111.70	291.67	294.36	279.76	288.6	35	
40468M	P17-1	1	19.94	5.69	113.46	288.65	288.03	271.29	282.7	36	
40469M	P18-1	1	19.88	5.70	113.32	315.04	316.18	303.12	311.4	34	
40470M	P24	1	19.87	5.58	110.87	292.01	290.88	279.61	287.5	36	
Test Results			Avg T (mm):	5.65	Avg SY1:	296.50	Avg SY1-3:		291.74	COV SY1-3:	4.2%
Material BS3602 430 ERW			Nominal properties 168.3mm OD x 5.6mm WT			Heat No. 5B25816					
40471M	P25	1	19.88	5.53	109.94	267.87	270.42	256.78	265.0	37	
40472M	P28	1	19.91	5.47	108.91	274.08	274.99	273.16	274.1	36	
40473M	P31	1	19.85	5.45	108.18	282.68	279.63	269.27	277.2	35	
42029M	P32	3	20.10	5.41	108.74	274.78	277.08	281.68	277.8	35	
40474M	P34	1	19.92	5.48	109.16	274.83	270.52	262.92	269.4	37	
40475M	P37	1	19.9	5.51	109.65	276.33	283.45	275.7	278.5	36	
Test Results			Avg T (mm):	5.48	Avg SY1:	275.10	Avg SY1-3:		273.68	COV SY1-3:	2.5%



Table 3.1 Static Yield Test Results (Part 3 of 3)

MEL REF.	AKD REF.	TEST BATCH	WIDTH (mm)	THICKNESS (mm)	X AREA (mm ²)	SY1 (N/mm ²)	SY2 (N/mm ²)	SY3 (N/mm ²)	SY1-3 Avg. (N/mm ²)	ELONG. %	
Material BS3602 430 ERW			Nominal properties 168.3mm OD x 4.5mm WT			Heat No. 5B43139					
42031M	P114	3	20.10	4.52	90.85	279.03	284.53	291.69	285.1	36	
42034M	P115	3	20.10	4.51	90.65	275.78	275.23	276.66	275.9	36	
42037M	P116	3	20.09	4.60	92.41	298.67	298.67	290.88	296.1	34	
Test Results			Avg T (mm):	4.54	Avg SY1:	284.49	Avg SY1-3:		285.68	COV SY1-3:	3.4%
Material BS3602 430 ERW			Nominal properties 168.3mm OD x 4.5mm WT			Heat No. 5B19704 (same pipe)					
40477M	P39	1	19.94	4.59	89.53	294.59	293.20	277.84	288.5	37	
40477M/2	P39	1	19.91	4.58	91.19	283.80	282.38	281.06	282.4	35	
40477M/3	P39	1	19.92	4.56	90.84	287.59	286.22	280.71	284.8	37	
40477M/4	P39	1	19.92	4.57	91.03	278.75	281.50	274.63	278.3	36	
40477M/5	P39	1	19.89	4.61	91.69	286.29	293.11	275.38	284.9	37	
Test Results			Avg T (mm):	4.58	Avg SY1:	286.20	Avg SY1-3:		283.80	COV SY1-3:	2.2%
Material BS3602 430 ERW			Nominal properties 168.3mm OD x 4.5mm WT			Heat No. 5B22797					
40476M	P38	1	19.83	4.40	87.25	269.34	268.19	271.63	269.7	38	
40940M	P40	2	20.29	4.55	92.32	288.45	293.87	284.34	288.9	36	
40478M	P42	1	19.94	4.57	91.13	282.56	282.56	271.59	278.9	35	
40941M	P43	2	20.04	4.48	89.78	283.80	284.03	282.69	283.5	37	
40479M	P45	1	19.92	4.61	91.83	281.77	279.05	258.63	273.2	35	
40942M	P49	2	19.96	4.41	88.02	267.67	268.46	274.14	270.1	37	
40943M	P50	2	20.24	4.60	93.10	292.70	297.85	294.84	295.1	37	
40480M	P51	1	19.94	4.50	89.73	261.90	266.08	254.93	261.0	37	
40944M	P52	2	20.01	4.36	87.24	283.70	285.19	279.46	282.8	36	
40945M	P53	2	19.77	4.42	87.38	281.87	279.01	277.52	279.5	35	
40946M	P54	2	20.26	4.37	88.54	276.15	276.71	273.89	275.6	36	
40481M	P55	1	19.91	4.41	87.80	254.84	253.42	236.30	248.2	36	
Test Results			Avg T (mm):	4.48	Avg SY1:	279.08	Avg SY1-3:		275.53	COV SY1-3:	4.8%
Material BS3602 430 ERW			Nominal properties 168.3mm OD x 4.5mm WT			Heat No. 5B31325 (Phase II Programme)					
OMT28423	P30 II	Phase II	25.39	4.48	113.75	250.56	258.29	252.75	253.9	40	
OMT28424	P31 II	Phase II	25.42	4.57	116.17	247.48	257.21	254.37	253.0	38	
OMT28427	P34 II	Phase II	25.37	4.58	116.19	243.13	249.58	251.73	248.1	37	
OMT28428	P35 II	Phase II	25.43	4.53	115.20	251.74	251.74	249.57	251.0	37	
OMT28438	P45 II	Phase II	25.40	4.51	114.55	252.02	255.34	257.52	255.0	38	
Test Results			Avg T (mm):	4.53	Avg SY1:	248.99	Avg SY1-3:		252.20	COV SY1-3:	1.6%

The results for the first 37 tests undertaken in Batch 1 are plotted by tubular type and section size in Figure 3.2 so the variability can be further assessed. Figure 3.3 compares the results from multiple tests from the same tubular with other individual samples from tubulars in the same batch.

The 'dynamic' results indicated on the figures come from standard coupon tests commissioned by AKD in the course of material selection/procurement activities. As anticipated, the faster rate of testing gives higher 'yield' values.

Figure 3.4 collates all BS 3602 430 ERW results from all 75 Phase III project coupon test batches and heat treatments for 168.3 mm OD by 4.5 mm WT tubulars. The distribution is evident but it is clear that the average value arrowed is generally representative. Table 3.1 shows the Phase II material to have a significantly lower yield level. However, the quantity of Phase II material used was relatively small and its use is confined to the final repair and in components whose response did not govern the overall frame behaviour. Therefore for interpreting the frame test results, and particularly for the benchmark cases, the Phase III average value of 277.7 N/mm² is deemed to be appropriate

Table 3.2 sets the average static yield test results against the mill certificate data (where appropriate), the results from standard 'dynamic' tensile tests performed by AKD as part of the material selection process, and the baseline assumptions used in the benchmark analyses at the time no data were available. The final columns provide material data comparing the actual static yields with dynamic values and the baseline assumptions used in the initial benchmark predictions.

3.3 TUBULAR GEOMETRY

Table 3.1 also includes the measured tube wall thicknesses sampled within the gauge length of the tensile test samples, providing further basis for comparison of nominal and actual properties.

3.4 OBSERVATIONS

With reference to the Phase III results in Tables 3.1 and 3.2 and Figures 3.2 to 3.4, the following observations can be made:

- The API 5L X 52 is slightly more consistent between samples than the other tubulars but the degree of difference is not great.



- The COV for five tests from the same tubular (2.2%) is less than between 37 tests from different tubulars within the same heat treatment (3.7%). The results might suggest that variability due to testing may be more or at least equally significant as any inherent differences between the materials. However, the COV is affected by the sample size and the range of results from the smaller test set from the same tubular (278.3 to 288.5) is considerably less in absolute terms than for the remainder (257.3 to 304.0 N/mm²).
- There is a small difference between the average static yield values for the three heat treatments to the same BS 3602 430 ERW 168.3 x 4.5 mm specification; namely 275.5 N/mm², 277.8 N/mm² and 285.7 N/mm².
- The apparent increment of dynamic yield over static yield is of the order of 12% which is consistent with previous findings^(5,6). These figures are indicative and it should be recognised that only isolated 'dynamic' results are available for statistical comparison with multiple static results. Nevertheless, the trends are consistent.
- The brace materials have generally delivered yield strengths somewhat higher than assumed in the baseline analysis predictions (on average 10 to 22% higher) whereas the leg steel has a slightly lower yield (on average 1 to 10% lower).
- The average static yield for all BS 3602 430 ERW 168.3 x 4.5mm tubulars, across all heat treatment batches, is 277.7 N/mm².

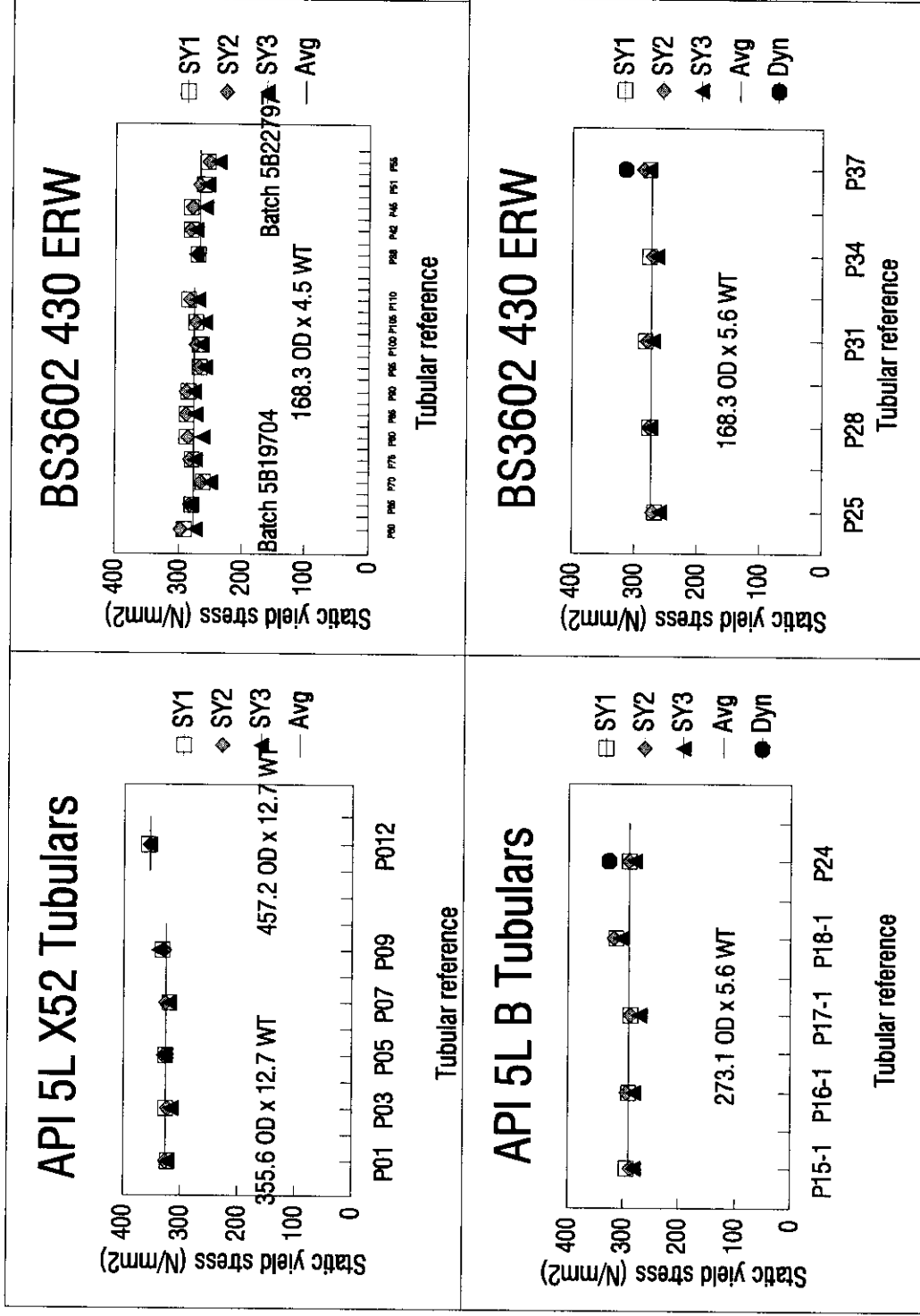


Figure 3.2 Static Yield Test Results for Different Tubular Sizes and Specifications (Batch 1)

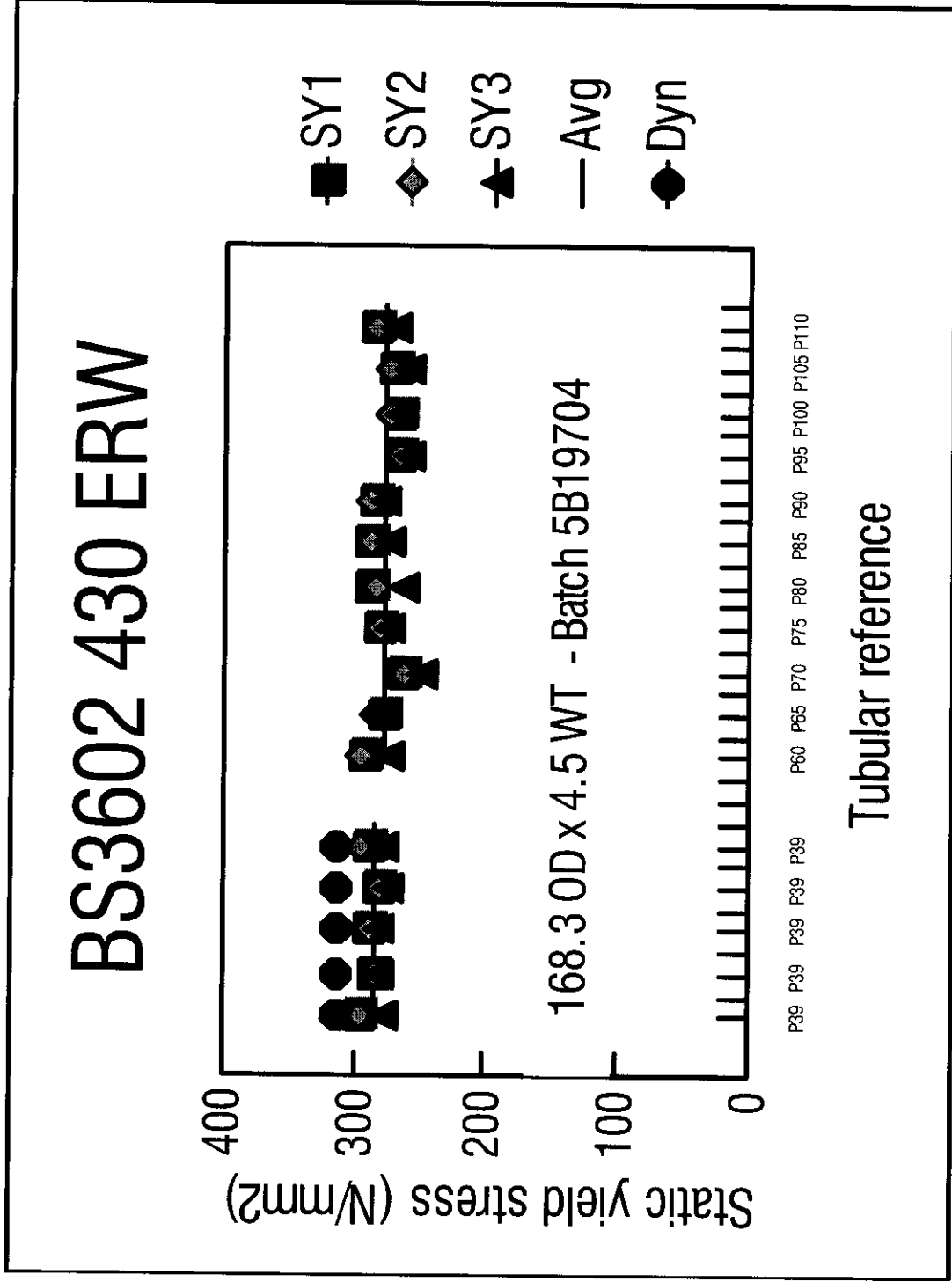


Figure 3.3 Comparison of Testing and Inherent Material Variability in Static Yield Test Results (Batch 1)

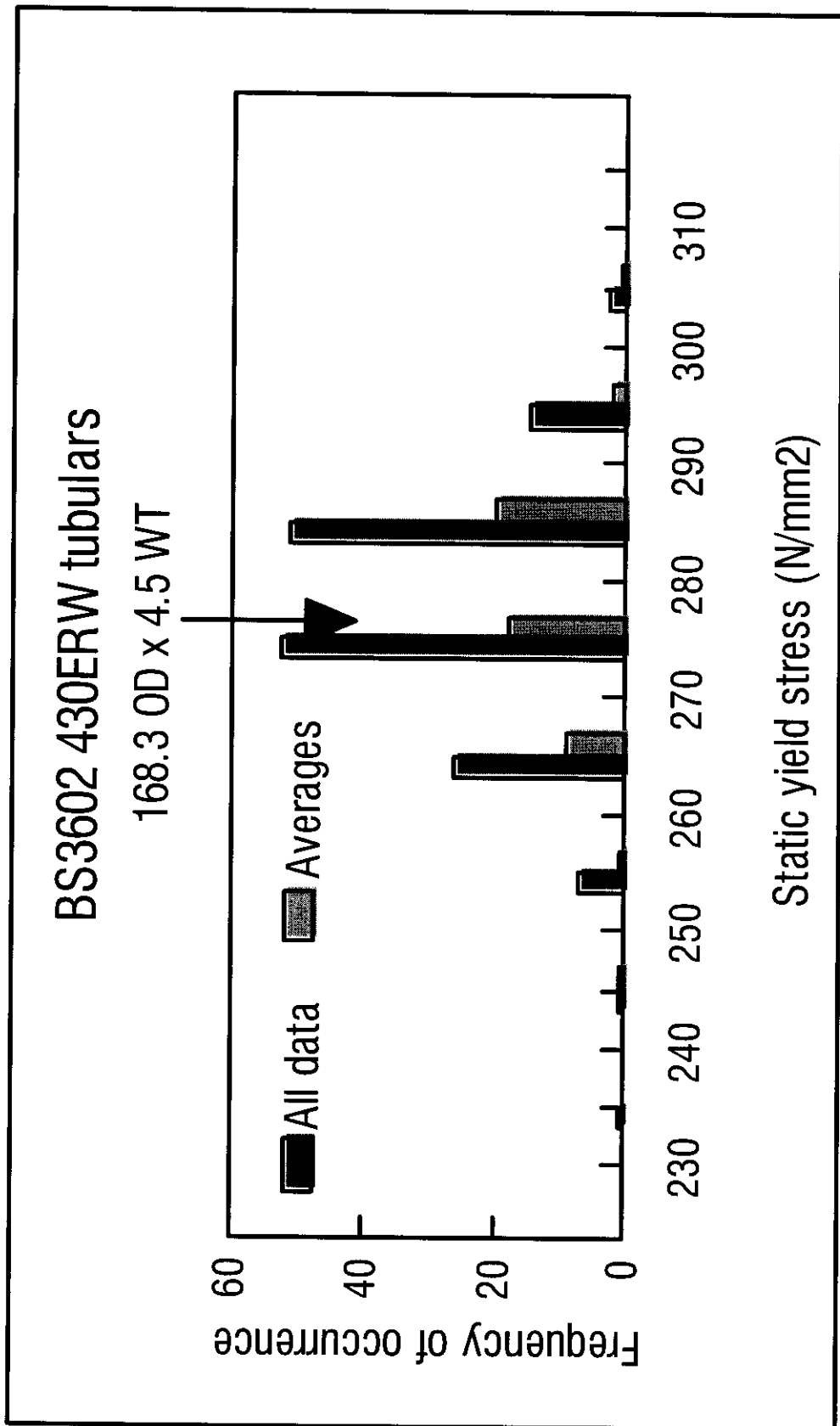


Figure 3.4 Distribution of Individual and Averaged Static Yield Stress Values (Batches 1, 2 and 3)

Table 3.2 Comparison of Measured and Assumed Yield Stress Values (using Batches 1, 2 and 3)

TUBULAR	MATERIAL/ BATCH	SIZE OD x WT (mm)	YIELD STRESS N/mm ²				STATIC YIELD COV	STATIC/ ANALYSIS	MILL CERT OR DYNAMIC/ STATIC
			MILL CERTIFICATE DYNAMIC	AKD DYNAMIC	AVERAGE STATIC Batches 1,2&3	ORIGINAL ANALYSIS ASSUMPTION			
P1 - 10	API 5L X 52	355.6 x 12.7	369	-	326.7	358	2.2%	91%	113%
P11	API 5L X 52	355.6 x 25.4	473	-	-	358	-	-	-
P12	API 5L X 52	457.2 x 12.7	379	-	355.3	358	-	99%	107%
P13 - 14	API 5L X 52	168.3 x 18.3	363	-	-	358	-	-	-
P15 - 18/P24	API 5LB	273.0 x 5.6	330	325.7	291.7	240	4.2%	122%	117%
P19	API 5L X 52/C6104E	168.3 x 9.5	389	-	-	358	-	-	-
P20	API 5L X 52/51669	168.3 x 9.5	375	-	-	358	-	-	-
P21 - 22	API 5L X 52	273.1 x 10.0	416	-	-	358	-	-	-
P23	API 5L x 52	273.1 x 9.3	397	-	-	358 *(8.7wt)	-	-	-
P25 - 37	BS 3602 430 ERW / 5B25816	168.3 x 5.6	N/A	314.9	273.7	250	2.5%	109%	115%
P111 - 112	BS 3602 430 ERW / 5B40729	168.3 x 5.6	N/A	-	-	250	-	-	-
P38/P40 - 45/ P49 - 55	BS 3602 430 ERW / 5B22797	168.3 x 4.5	N/A	299.0	275.5	250	4.8%	110%	109%
P39/P56 - 110	BS 3602 430 ERW / 5B19704	168.3 x 4.5	N/A	314.0	277.8	250	3.7%	111%	113%
P113 - 116	BS 3602 430 ERW / 5B43139	168.3 x 4.5	N/A	-	285.7	250	3.4%	114%	-
52 off	P39 (5 samples)	168.3 x 4.5	N/A	314.0	283.8	250	2.2%	114%	111%
	Combined Phase III batches	168.3 x 4.5	N/A	-	277.7	250	3.8%	111%	-
P30II-31II/ P34II-P35II / P45II	BS 3602 430 ERW / 5B31325	168.3 x 4.5	N/A	-	252.2	250	1.6%	101%	-
P46	BS 4848 Gr 50C	168.3 x 5.0	457	-	-	-	-	-	-
P47	BS 4848 Gr 50D	168.3 x 5.0	395	-	-	-	-	-	-
P48	DIN 1629 St 52	168.3 x 5.0	446	-	-	-	-	-	-



4. MATERIALS WITHIN THE TEST STRUCTURE

Every tubular sourced for use in the frame was given a reference identifier P1 to P116 on receipt (see Section 2).

A sample from each tubular was despatched to the test house to be available for static tensile tests. Tests were undertaken and are reported in Section 3 for tubulars relevant to the collapse response of the frame. For non-critical sections averaged properties for the tubular type are assumed.

Prior to cutting, each tubular was surveyed at 1m intervals to give orthogonal diameter and wall thickness measurements⁽⁸⁾. At critical joints, diameters and thicknesses were recorded at 0.1m intervals. In addition micrometer measurements associated with the materials tests gave accurate wall thickness values. Once fabrication was complete the tubular identifier and survey marks on each member segment were recorded.

Each member within the structure was numbered as shown in Figure 4.1. It is therefore possible to cross-reference every member with the material reference and measured diameter and thickness values.

The first table in Appendix A presents the correlation for the initial build of the structure. It can be seen that in several cases an individual member comprises a number of segments. Appendix B reproduces the fabricator's sketches for the initial build indicating, for example, segments to either side of a load cell within a member. In all cases, properties for the largest segment are assigned to Segment One in the table. In order that the potential variability between segments in a member can be assessed the final columns of the table compare the maximum and minimum axial capacities for the shorter sections with Segment One. Where specific measured values are not available average properties are given and these are shown in italic; roman text signifies measured values.

After each test, damaged areas of the structure were replaced. The material and geometric properties for each repaired member were recorded as for the initial build.

Subsequent tables in Appendix A include updated details for all members following the first to sixth repairs respectively. The changes are shown by asterisks within the first column. Each table therefore presents the properties of the structural members at the start of the subsequent test. Tables are presented in the chronological order of testing as follows:

- Initial build Loadcase 1 (LC1)
- 1st repair Loadcase 1 cyclic (LC1C)

- 2nd repair Loadcase 2 (LC2)
- 3rd repair Loadcase 2 cyclic (LC2C)
- 4th repair Loadcase 3 cyclic (LC3C)
- 5th repair Loadcase 3 (LC3)
- 6th repair Loadcase 3 cyclic A and 1 cyclic A (LC3CA and LC1CA).

Initial build and 3rd and 5th repair tables therefore give data relevant to the benchmark analysis cases.

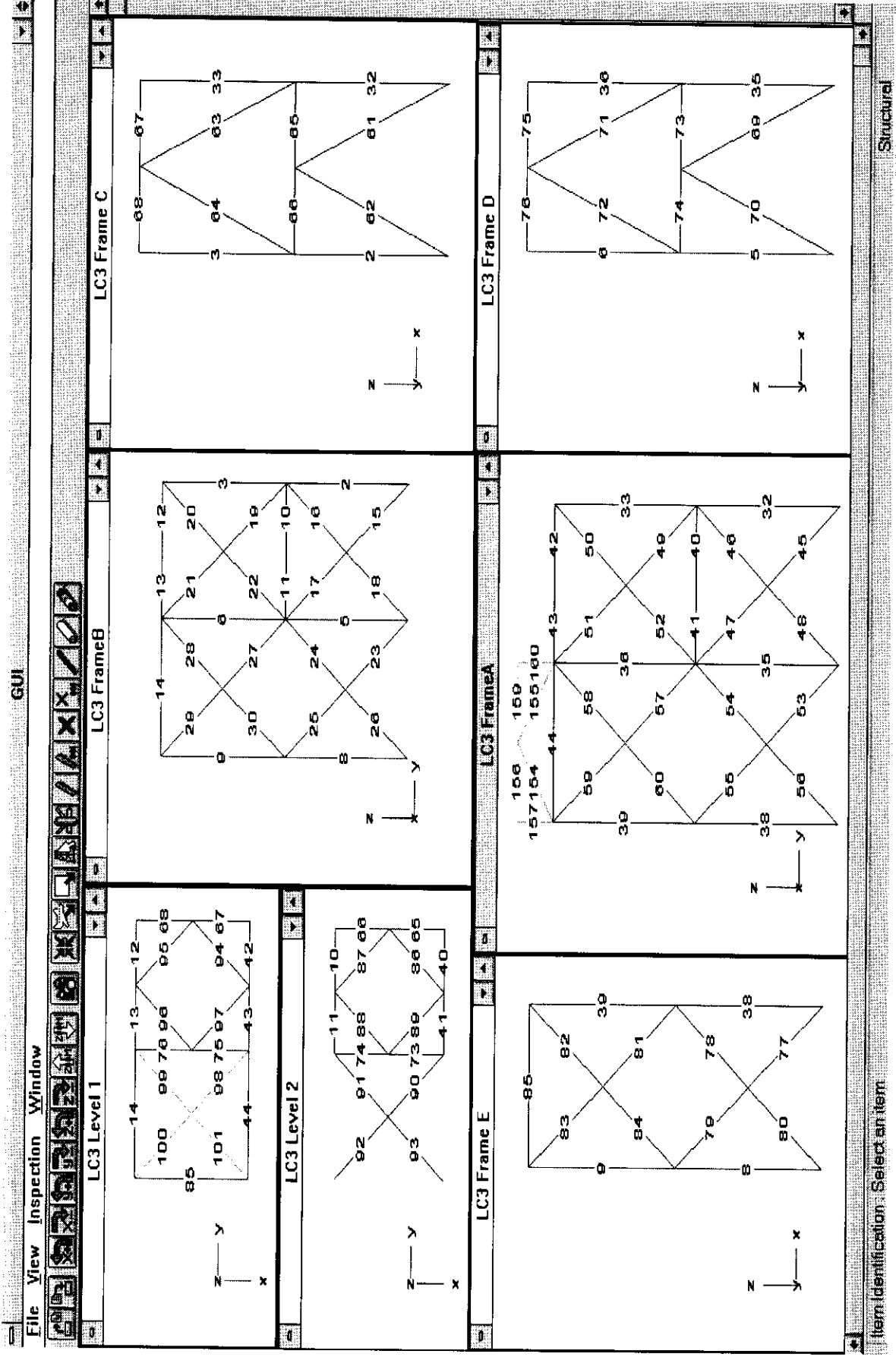


Figure 4.1 Member Numbering (Loadcase 3)





5. CONCLUSIONS

Based on the material test results, the following conclusions are reached:

- Tables in Section 3 provide measured static yield stress values for individual tubulars and values averaged by material batch.
- Tables in Section 4 provide member by member details of actual section properties and material yield values for the structure in each test.
- The difference between the measured steel yield values and the properties assumed prior to testing is sufficiently significant for it to be appropriate to account for the actual properties in updated analyses. Table 5.1 provides an update to the nominal material properties appended to the Benchmark Analysis Specification⁽⁷⁾ using average values.
- The level of detail adopted will depend on the purpose of the investigation and information is provided in Section 3 on the degree of inherent and sampling variability which can be accounted for.

Table 5.1 Material Properties Based on Static Coupon Tests (Averaged)

Product	Minimum Specified Yield (N/mm ²)		
	Original Assumptions	Preliminary Tests	Updated after All Tests
RIG SECTIONS			
TMCP plate - fabricated sections*	420	420	-
Rolled Sections*	355	330	-
SPECIMEN TUBULARS			
168.3 DIA x 4.5 WT BS 3602 ERW	250	273	278
273.0 DIA x 5.6 WT API 5L GRADE B	240	292	-
273.0 DIA x 9.3 WT API 5L X52 *	358	354	-
273.0 DIA x 10.0 WT API 5L X52 *	358	371	-
355.6 DIA x 12.7 WT API 5L X52	358	325	327
457.2 DIA x 12.7 WT API 5L X52	358	355	-
168.3 DIA x 18.3 WT API 5L X52 *	358	324	-
168.3 DIA x 9.5 WT API 5L X52 *	358	335	-
168.3 DIA x 5.6 WT BS 3602 ERW	250	273	274
355.6 DIA x 25.4 WT API 5L X52 *	358	422	-

Notes: * Static yield properties ('preliminary tests') based on average or single values as available from 'standard' tests on certificates with a 12% reduction (ref dynamic/static yield ratios in Table 3.2).



6. REFERENCES

1. Johnson, R F and Murray, J D. 'The effect of rate of straining on the 0.2% proof stress and lower yield stress of steel', Conference on High Temperature Properties of Steels, ISI, Eastbourne, 1996.
2. BSEN 10002 - Part 1 'Tensile testing of metallic materials: Method of testing at ambient temperature', British Standards Institution, 1990.
3. Wimpey Offshore. 'Static strength of large scale tubular joints: test programme and results', OTI 89 543, HMSO, 1989.
4. BOMEL Ltd. 'Specification for static tensile coupon tests'. BOMEL reference C636\06\183S, Revision A, September 1997.
5. Steel Construction Institute. 'Joint Industry Tubular Frames Project - Phase I', Nine volume report, SCI reference SCI-RT-042, 1990.
6. Billington Osborne-Moss Engineering Limited. 'Joint Industry Tubular Frames Project - Phase II', Nine volume report, BOMEL reference C556R003.50 to .58, 1992.
7. BOMEL Ltd. 'Frames Project Phase III Nominal material properties', BOMEL reference C636\06\182U, Rev A, September 1997, Included in Appendix A to the Benchmark Analysis Work Plan, BOMEL reference C636\12\006S, Rev B, September 1997.
8. AKD Engineering Limited. 'Test specimen. Documentation package', AKD reference 4065/4413-2/4570, October 1998 and Supplements November 1998 (BOMEL Incoming Documents 11900 and 12108 - File C636\37).
9. Materials Engineering Limited. 'Static tensile coupon test results', Batch 1, December 1997; Batch 2, March 1998; and Batch 3, January 1999 (BOMEL Incoming Documents 8523, 9377 and 12633 - File C636\23).
10. Billington Osborne-Moss Engineering Limited. 'Joint Industry Tubular Frames Project, Phase II, Part 2 Testing and analysis of frame behaviour, Volume II BOMEL Specifications and fabrication and test house reports', BOMEL Reference C556R003.52, Rev. A, 1992.

APPENDIX A

FRAME MEMBER PROPERTIES AT START OF EACH TEST

(C636\06\294w-b.XLS, 14 pages)

Initial Build Data - Member properties for LC1 test

Member Number	Segment One						Segment Two						Segment Three						All Segment Analysis										
	Pipe Ref. P	Material Yield (N/mm ²)	Dia. (mm)	Wall Thck. (mm)	Area (mm ²)	Yield Load (kN)	Modulus (mm ²)	Yield Moment (kNm)	Pipe Ref. P	Material Yield (N/mm ²)	Dia. (mm)	Wall Thck. (mm)	Area (mm ²)	Yield Load (kN)	Modulus (mm ²)	Yield Moment (kNm)	Pipe Ref. P	Material Yield (N/mm ²)	Dia. (mm)	Wall Thck. (mm)	Area (mm ²)	Yield Load (kN)	Modulus (mm ²)	Yield Moment (kNm)	Max. Yld Load (kN)	Min. Yld Load (kN)	Max-Sept / Seg 1 +%	Min-Sept / Seg 1 -%	
2	4	326.7	355.8	12.70	13689	4472	1133821	370.4	7	320.8	355.8	12.38	13355	4284	1107942	355.4								4472	4284	4472	0.0	-4.2	
3	4	326.7	355.8	12.70	13689	4472	1133821	370.4	7	320.8	355.8	12.38	13355	4284	1107942	355.4								4472	4284	4472	0.0	0.0	
5	6	326.7	355.8	12.70	13689	4472	1133821	370.4	7	320.8	355.8	12.38	13355	4284	1107942	355.4								4472	4284	4472	0.0	0.0	
5/6 Can	12	355.3	452.2	12.81	17884	6354	1932797	886.7																6354	6354	6354	0.0	0.0	
6	6	326.7	355.8	12.70	13689	4472	1133770	371.0																4472	4472	4472	0.0	0.0	
8	5	327.5	356.2	12.81	13819	4528	1145281	375.1	7	320.8	355.8	12.38	13357	4285	1108268	355.5								4528	4285	4528	0.0	-5.3	
9	5	327.5	356.2	12.81	13819	4528	1145281	375.1	7	320.8	355.8	12.38	13357	4285	1108268	355.5								4528	4285	4528	0.0	0.0	
10	44	275.5	168.5	4.50	2319	639	92601	25.5																639	639	639	0.0	0.0	
11	44	275.5	168.5	4.50	2319	639	92601	25.5																639	639	639	0.0	0.0	
12	42	278.9	169.5	4.57	2354	656	93935	26.2																656	656	656	0.0	0.0	
13	42	278.9	169.5	4.57	2354	656	93935	26.2																656	656	656	0.0	0.0	
14	41	275.5	167.7	4.50	2322	640	92852	25.6																640	640	640	0.0	0.0	
15	69	277.8	168.5	4.50	2318	644	92578	25.7																644	644	644	0.0	0.0	
15/17 Can	19.11	347.3	168.3	9.30	4739	1846	178169	61.9																1846	1846	1846	0.0	0.0	
16	70	257.3	168.5	4.42	2278	566	91051	23.4																566	566	566	0.0	0.0	
17	66	261.4	168.7	4.42	2281	566	91254	23.9	40	288.9	168.3	4.41	2271	624	93303	27.0							566	566	566	0.0	0.0		
18	103	277.8	168.6	4.50	2320	644	92681	25.7																644	644	644	0.0	0.0	
19	107	273.8	168.7	4.55	2346	642	93708	25.7																642	642	642	0.0	0.0	
20	62	267.4	168.7	4.43	2285	611	91433	24.4																611	611	611	0.0	0.0	
20/22 Chord N16	76	277.3	168.7	4.55	2347	650	93812	26.0																650	650	650	0.0	0.0	
21	62	267.4	168.7	4.43	2286	611	91444	24.5	58	275.0	168.3	4.41	2271	624	90860	24.9							624	624	624	0.0	0.0		
22	76	277.1	168.6	4.55	2345	650	93850	26.0																650	650	650	0.0	0.0	
23	73	277.8	168.7	4.50	2321	645	92772	25.8																645	645	645	0.0	0.0	
23/25 Can	19.11	347.3	168.3	9.50	4739	1846	178169	61.9																1846	1846	1846	0.0	0.0	
24	65	281.1	168.7	4.80	2371	687	94099	26.8	58	275.0	168.3	4.41	2271	624	90860	24.9								687	687	687	0.0	-6.3	
25	72	277.8	168.8	4.50	2322	643	92875	25.8																643	643	643	0.0	0.0	
26	71	277.8	168.6	4.50	2320	644	92692	25.8																644	644	644	0.0	0.0	
27	66	289.4	168.5	4.52	2329	674	92667	26.9																674	674	674	0.0	0.0	
27/29 Chord N18	66	289.4	168.8	4.52	2333	675	93301	27.0																675	675	675	0.0	0.0	
28	77	261.4	168.5	4.33	2235	584	89342	23.4	56	275.0	168.6	4.41	2275	676	91019	25.0							584	584	584	0.0	0.0		
29	77	261.4	168.6	4.33	2235	584	89474	23.4	56	275.0	168.6	4.41	2275	676	91019	25.0							584	584	584	0.0	0.0		
30	67	289.7	168.7	4.57	2357	683	94179	27.3																683	683	683	0.0	0.0	
32	6	326.7	356.4	12.70	13713	4480	1137788	371.7	7	320.8	355.8	12.38	13357	4285	1108401	355.6							4480	4480	4480	0.0	0.0		
33	8	326.7	356.4	12.70	13715	4480	1138129	374.8																4480	4480	4480	0.0	0.0	
35	10	336.6	358.3	12.51	13511	4548	1121849	377.6																4548	4548	4548	0.0	0.0	
36	10	336.6	356.0	12.51	13501	4544	1120258	377.1																4544	4544	4544	0.0	0.0	
38	9	332.3	355.9	12.74	13733	4583	1137341	371.9	3	319.7	355.8	12.72	13711	4383	1135615	363.1								4583	4383	4583	0.0	-3.9	
39	9	332.3	355.9	12.74	13733	4583	1137341	371.9	3	319.7	355.8	12.72	13711	4383	1135615	363.1								4583	4383	4583	0.0	0.0	
40	43	283.5	168.7	4.48	2311	655	92450	26.2																655	655	655	0.0	0.0	
41	43	283.5	168.5	4.48	2310	655	92370	26.2																655	655	655	0.0	0.0	
42	13	324.1	169.7	4.80	2370	682	94833	26.7																682	682	682	0.0	0.0	
43	13	324.1	169.7	4.80	2370	682	94833	26.7																682	682	682	0.0	0.0	
44	13	324.1	169.7	4.80	2370	682	94833	26.7																682	682	682	0.0	0.0	
45	56	275.8	168.5	4.47	2303	630	91999	25.2	39	288.5	168.6	4.59	2386	682	94440	27.2	40	288.9	168.3	4.55	2341	676	93303	27.0	682	630	8.3	0.0	
45/47 Can	20	344.8	168.0	9.50	4731	1846	177526	59.4																1846	1846	1846	0.0	0.0	
46	57	283.9	168.6	4.53	2335	663	93260	26.5	69	277.8	168.6	4.50	2319	644	92669	25.7	54	275.6	168.6	4.37	2254	621	90191	24.9	663	621	663	0.0	-6.3
47	56	273.6	168.7	4.47	2306	631	92182	25.2	67	288.7	168.7	4.57	2356	683	94144	27.3	40	288.9	168.3	4.35	2344	677	93534	27.0	683	631	631	0.0	0.0
48	58	275.0	168.7	4.41	2279	628	91053	25.0	54	275.6	168.6	4.37	2254	621	90180	24.9	57	283.9	168.5	4.53	2334	662	93155	26.4	662	621	626	5.9	-0.7
49	59	266.9	168.5	4.45	2294	612	91654	24.5	71	277.8	168.7	4.50	2322	645	92841	25.8	40	288.9	168.3	4.55	2341	676	93303	27.0	676	612	612	10.5	0.0
49/51 Can	20	344.8	168.3	9.50	4739	1846	178169	59.7																1846	1846	1846	0.0	0.0	
50	60	286.4	168.6	4.60	2370	679	94617	27.1	81	283.3	168.9	4.54	2345	664	93830	26.6	58	275.0	168.3	4.41	2271	624	90860	24.9	679	624	679	0.0	0.0
51	58	266.9	168.6	4.45	2295	612	91756	24.5	79	280.7	168.5	4.49	2314	650	92434	25.9	40	288.9	168.8	4.55	2348	678	93856	27.1	678	612	612	10.7	0.0
52	60	286.4	168.6	4.60	2370	679	94629	27.1	80	277.5	168.7	4.52	2331	647	93163	25.9	58	275.0	168.3	4.41	2271	624	90860	24.9	678	624	678	0.0	-8.0
53	63	274.8	168.6	4.45	2300	632	91957	25.3	40	288.9	168.7	4.55	2346	678	93742	27.1								678	632	632	7.2	0.0	
53/55 Can	20	344.8	168.3	9.50	4739	1846	178169	59.7																1846	1846	1846	0.0	0.0	
54	64	274.5	168.6	4.50	2320	637	92727	25.5	54	275.6	168.6	4.37	2254	621	90191	24.9								621	621	621	0.0	-2.5	
55	63	274.8	168.7	4.46	2301	632	92014	25.3																					

3rd Repair Data - Member Properties for LC2C test

Repair Member Number (Note)	Segment One					Segment Two					Segment Three					All Segment Analysis									
	Pipe Ref. P	Material Yield (N/mm ²)	Di. (mm)	Wall Thick. (mm)	Area (mm ²)	Modulus (N/mm ²)	Yield Moment (kNm)	Yield Load (kN)	Modulus (mm ²)	Yield Moment (kNm)	Pipe Ref. P	Material Yield (N/mm ²)	Di. (mm)	Wall Thick. (mm)	Area (mm ²)	Modulus (N/mm ²)	Yield Moment (kNm)	Yield Load (kN)	Modulus (mm ²)	Yield Moment (kNm)	Max. Yld Load (kN)	Min. Yld Load (kN)	Max-Seg1 / Seg1 %	Min-Seg1 / Seg1 %	
2	4	326.7	355.8	12.70	13689	4472	113323	370.4			7	320.8	355.8	12.38	13355	4284	110784	355.4			4472	4284	4472	0.0	-4.2
3	4	326.7	355.8	12.70	13689	4472	113323	370.4													4472	4472	4472	0.0	0.0
5	6	326.7	355.8	12.70	13689	4472	113323	370.4													6354	6354	6354	0.0	0.0
5/6 Can.	12	355.3	457.2	12.81	17684	6354	183297	686.7													4476	4476	4476	0.0	0.0
6	6	326.7	355.8	12.70	13701	4478	113570	371.0													4526	4285	4526	0.0	-5.3
8	5	327.5	356.2	12.81	13819	4528	114528	375.1			7	320.8	355.8	12.38	13357	4295	1109269	355.5			4524	4524	4524	0.0	0.0
9	4	327.5	356.2	12.81	13813	4524	1144264	374.7													639	639	639	0.0	0.0
10	44	275.5	188.5	4.50	2318	639	92801	25.5													639	639	639	0.0	0.0
11	44	275.5	188.5	4.50	2319	639	92812	25.5													656	656	656	0.0	0.0
12	42	278.8	188.5	4.57	2354	656	93035	26.2													656	656	656	0.0	0.0
13	42	278.8	188.5	4.57	2353	656	93003	26.2													644	644	644	0.0	0.0
14	41	278.5	188.7	4.50	2321	640	92852	25.8													644	644	644	0.0	0.0
15	68	277.8	188.5	4.50	2318	644	92578	25.7													1563	1646	1646	0.0	0.0
15/17 Can	18	257.3	168.3	4.22	1739	585	81051	23.4													585	585	585	0.0	0.0
17	68	261.4	168.7	4.42	2281	596	81264	23.9			40	288.9	168.3	4.55	2341	619	93003	27.0			676	596	596	13.4	0.0
18	103	277.8	188.5	4.50	2320	644	92981	25.7													644	644	644	0.0	0.0
19	107	273.8	188.7	4.55	2348	642	93708	25.7													611	611	611	0.0	0.0
20	62	267.4	168.7	4.43	2285	611	81433	24.4													890	890	890	0.0	0.0
21	62	267.4	168.7	4.43	2286	611	81444	24.5			58	275.0	168.3	4.41	2271	624	90680	24.9			650	650	650	0.0	0.0
22	76	271.1	188.6	4.55	2345	650	93550	28.0													624	611	611	2.2	0.0
23	73	277.8	188.7	4.50	2321	643	92772	25.8													650	650	650	0.0	0.0
23/25 Can	19	287.3	168.3	4.33	1794	648	178169	61.9													650	650	650	0.0	0.0
24	65	281.1	168.7	4.60	2371	677	94699	26.6			58	275.0	168.3	4.41	2275	626	91019	25.0			636	594	594	7.2	0.0
25	72	277.8	188.6	4.50	2322	645	92975	25.9													1646	1646	1646	0.0	0.0
26	71	277.8	188.6	4.50	2320	644	92892	25.8													687	624	667	0.0	-6.3
27	66	288.4	168.5	4.52	2326	674	92867	26.9													644	644	644	0.0	0.0
27/28 Chord N18	68	288.4	168.8	4.52	2333	675	93361	27.0													674	674	674	0.0	0.0
28	77	261.4	168.5	4.33	2233	584	89342	23.4			58	275.0	168.6	4.41	2275	626	91019	25.0			636	594	594	7.2	0.0
29	77	261.4	168.6	4.33	2235	584	89474	23.4													636	594	594	7.2	0.0
30	67	288.7	168.7	4.57	2357	683	94179	27.3													4880	4265	4480	0.0	-4.3
32	8	326.7	356.4	12.70	13713	4480	113798	371.7			7	320.8	355.8	12.38	13357	4285	1108401	355.6			4880	4265	4480	0.0	0.0
33	8	326.7	356.4	12.70	13715	4480	1138125	371.8													4548	4548	4548	0.0	0.0
35	10	336.6	358.3	12.81	13511	4548	1121849	377.6													6375	6375	6375	0.0	0.0
35/36 Can	12	355.3	458.7	12.81	17944	6375	1948040	691.4													4548	4548	4548	0.0	0.0
36	10	336.6	358.0	12.81	13501	4544	1120258	377.1													6375	6375	6375	0.0	0.0
38	9	332.3	355.9	12.74	13733	4563	1137408	378.0			3	319.7	355.8	12.72	13711	4383	1135515	363.1			4563	4563	4563	0.0	-3.9
39	9	332.3	355.9	12.74	13733	4563	1137408	378.0													4563	4563	4563	0.0	0.0
40	43	283.5	168.7	4.48	2311	655	92450	26.2													655	655	655	0.0	0.0
41	43	283.5	168.6	4.48	2310	655	92370	26.2													655	655	655	0.0	0.0
42	13	358.3	168.7	4.80	6706	2822	288383	98.7													2822	2822	2822	0.0	0.0
43	13	358.3	168.7	4.80	6704	2821	288219	96.7													2821	2821	2821	0.0	0.0
44	13	358.3	168.7	4.80	6706	2822	288342	96.7													2822	2822	2822	0.0	0.0
45	56	273.6	168.5	4.47	2303	630	91889	25.2			39	288.5	168.6	4.58	2385	682	94440	27.2			2822	2822	2822	0.0	0.0
45/47 Can	20	324.8	168.0	4.30	1731	1584	177526	59.4													682	630	630	8.3	0.0
46	57	283.9	168.6	4.53	2335	663	92260	25.9													1584	1584	1584	0.0	0.0
47	56	273.6	168.7	4.47	2308	631	92192	25.2			66	277.8	168.6	4.50	2319	644	92689	25.7			663	621	663	0.0	-6.3
48	58	275.0	168.7	4.41	2275	626	91053	25.0			40	288.7	168.7	4.57	2356	683	94144	27.3			677	635	677	0.0	0.0
49	59	268.9	168.5	4.45	2294	612	91654	24.5			57	283.9	168.5	4.53	2334	662	93156	26.4			662	621	628	5.9	-0.7
49/51 Can	20	324.8	168.3	4.30	1738	1587	178169	59.7			40	288.9	168.3	4.55	2341	678	93303	27.0			678	612	612	10.5	0.0
50	20	286.4	168.6	4.60	2370	678	94617	27.1			63	283.3	168.9	4.54	2345	664	93830	26.6			1587	1587	1587	0.0	0.0
51	59	268.9	168.6	4.45	2295	612	91758	24.5			78	280.7	168.5	4.48	2314	650	92434	25.9			624	624	624	0.0	-4.0
52	60	268.4	168.6	4.80	2370	678	94629	27.1			59	275.0	168.3	4.41	2271	624	90680	24.9			678	612	612	10.7	0.0
53	63	274.8	168.6	4.46	2300	632	91957	25.3			40	288.9	168.7	4.55	2346	678	93742	27.1			624	624	624	0.0	-8.0
53/55 Can	20	324.8	168.3	4.30	1739	1587	178169	59.7													678	632	632	7.2	0.0
54	64	274.5	168.6	4.50	2320	637	92727	25.5			54	275.5	168.6	4.37	2254	621	90191	24.8			1587	1587	1587	0.0	0.0
55	63	274.8	168.7	4.46	2301	632	92014	25.3			40	288.9	168.3	4.55	2341	678	93303	27.0			637	621	637	0.0	-2.5
56	64	274.5	168.6	4.50	2320	637	92681	25.4			54	275.6	168.6	4.37	2254	621	90191	24.8			678	632	632	7.0	0.0
57	38	268.7	168.7	4.40	2271	612	90907	24.5			40	288.9	168.6	4.49	2315	661	92500	26.4			637	631	637	0.0	-2.4
57/59 Can	20	324.8	168.3	4.30	1739	1587	178169	59.7			40	288.9	168.6	4.49	2315	661	92500	26.4			678	632	632	7.2	0.0
58	55	248.2	168.6	4.41	2275	565	91018	22.8			54	276.8	168.5	4.49	2313	640	92355	25.6			1587	1587	1587	0.0	0.0
59	38	268.7	168.7	4.40	2271	612	90885	24.5			65	282.6	168.3	4.58	2355	668	93833	28.5			622	622	622	0.0	0.0
60	55	248.2	168.6	4.41	2274	564	90952	22.6			54	275.6	168.3	4.37	2251	620	89902	24.6			678	612	612	10.4	0.0

4th Repair Data - Member properties for LC3C test

Repair (Note)	Member Number	Segment One						Segment Two						Segment Three						All Segment Analysis										
		Pipe Ref. P	Material Yield (N/mm ²)	Di. (mm)	Wall Thk. (mm)	Area (mm ²)	Yield Load (kN)	Modulus (mm ²)	Yield Moment (kNm)	Pipe Ref. P	Material Yield (N/mm ²)	Di. (mm)	Wall Thk. (mm)	Area (mm ²)	Yield Load (kN)	Modulus (mm ²)	Yield Moment (kNm)	Pipe Ref. P	Material Yield (N/mm ²)	Di. (mm)	Wall Thk. (mm)	Area (mm ²)	Yield Load (kN)	Modulus (mm ²)	Yield Moment (kNm)	Max. Yield Load (kN)	Min. Yield Load (kN)	Max. Segt / Seg 1	Min. Segt / Seg 1	
	2	4	328.7	355.8	12.70	13686	4472	113821	370.4	7	320.8	355.8	12.38	13355	4284	110942	355.4								4472	4284	4472	0.0	-4.2	
	3	4	326.7	355.8	12.70	13686	4472	113821	370.4	7	320.8	355.8	12.38	13355	4284	110942	355.4								4472	4284	4472	0.0	0.0	
	5	6	326.7	355.8	12.70	13686	4472	113821	370.4	7	320.8	355.8	12.38	13355	4284	110942	355.4								4472	4284	4472	0.0	0.0	
	5/6 Can	12	355.3	457.2	12.81	17884	6354	153797	686.7																6354	6354	6354	0.0	0.0	
	6	6	326.7	355.8	12.70	13701	4472	113821	370.4																4472	4472	4472	0.0	0.0	
	8	5	327.5	358.1	12.81	13819	4526	1145281	375.1	7	320.8	355.8	12.38	13357	4285	1109269	355.5								4476	4285	4476	0.0	-5.3	
	9	5	327.5	358.1	12.81	13813	4524	1144264	374.7																4524	4524	4524	0.0	0.0	
	10	44	275.5	168.5	4.50	2319	639	92601	25.5																639	639	639	0.0	0.0	
	11	44	275.5	168.5	4.50	2319	639	92601	25.5																639	639	639	0.0	0.0	
	12	42	276.9	168.5	4.57	2354	656	93935	26.2																656	656	656	0.0	0.0	
	13	42	276.9	168.5	4.57	2353	656	93900	26.2																656	656	656	0.0	0.0	
	14	41	275.3	168.7	4.50	2322	640	92852	25.6																640	640	640	0.0	0.0	
	15	69	277.8	168.5	4.50	2318	644	92578	25.7																644	644	644	0.0	0.0	
	15/17 Can	18	287.3	168.3	4.50	2318	644	92578	25.7																644	644	644	0.0	0.0	
	16	70	257.3	168.5	4.42	2278	588	91051	23.4																588	588	588	0.0	0.0	
	17	68	261.4	168.7	4.42	2281	596	91254	23.9	40	288.9	168.3	4.95	2341	676	93303	27.0							596	588	588	0.0	0.0		
	18	103	277.8	168.6	4.50	2320	644	92861	25.7																644	644	644	0.0	0.0	
	19	107	279.8	168.7	4.55	2349	642	93708	25.7																642	642	642	0.0	0.0	
	20	62	267.4	168.7	4.43	2285	611	91433	24.4																611	611	611	0.0	0.0	
	20/22 Chord N18	76	277.1	168.7	4.55	2347	650	93612	26.0	58	275.0	168.3	4.41	2271	624	90860	24.9								650	650	650	0.0	0.0	
	21	62	267.4	168.7	4.43	2286	611	91444	24.5																611	611	611	0.0	0.0	
	22	76	277.1	168.6	4.55	2345	650	93650	26.0																650	650	650	0.0	0.0	
	23	70	277.8	168.7	4.50	2321	645	92772	25.8																645	645	645	0.0	0.0	
	23/25 Can	19	347.3	468.3	9.50	4739	1846	178169	61.9																1846	1846	1846	0.0	0.0	
	24	65	281.1	168.7	4.60	2371	667	94699	26.6	58	275.0	168.3	4.41	2271	624	90860	24.9								667	667	667	0.0	0.0	
	25	72	277.8	168.8	4.50	2322	645	92875	25.8																645	645	645	0.0	0.0	
	26	71	277.8	168.6	4.50	2320	644	92882	25.8																644	644	644	0.0	0.0	
	27	66	269.4	168.5	4.52	2328	674	92867	26.9																674	674	674	0.0	0.0	
	27/29 Chord N18	66	269.4	168.8	4.52	2333	675	93001	27.0																675	675	675	0.0	0.0	
	28	77	261.4	168.5	4.33	2233	584	89342	23.4	58	275.0	168.6	4.41	2275	628	91019	25.0								584	584	584	0.0	0.0	
	29	67	261.4	168.6	4.33	2236	594	89474	23.4																594	594	594	0.0	0.0	
	30	67	280.7	168.7	4.57	2357	683	94179	27.3																683	683	683	0.0	0.0	
	32	8	326.7	355.4	12.70	13713	4480	1137768	371.7																4480	4480	4480	0.0	0.0	
	33	8	326.7	355.4	12.70	13715	4480	1138125	371.8																4480	4480	4480	0.0	0.0	
	35	10	336.6	358.3	12.51	13511	4548	1121849	377.9																4548	4548	4548	0.0	0.0	
	35/37 Can	12	355.3	458.7	12.81	17944	6375	1546040	691.4																6375	6375	6375	0.0	0.0	
	38	10	338.6	358.0	12.51	13501	4544	1120256	377.1																4544	4544	4544	0.0	0.0	
	38	9	332.3	355.9	12.74	13733	4563	1137408	378.0	3	319.7	355.8	12.72	13711	4383	1135115	383.1								4563	4563	4563	0.0	-3.9	
	40	43	283.5	168.7	4.48	2310	653	92450	26.2																653	653	653	0.0	0.0	
	41	43	283.5	168.8	4.48	2310	655	92370	26.2																655	655	655	0.0	0.0	
	42	13	324.3	168.7	4.30	2262	583	88383	26.2																583	583	583	0.0	0.0	
	43	13	324.3	168.7	4.30	2262	583	88383	26.2																583	583	583	0.0	0.0	
	44	13	324.3	168.7	4.30	2262	583	88383	26.2																583	583	583	0.0	0.0	
	45	56	273.6	168.5	4.47	2303	630	91869	25.2	38	288.5	168.6	4.59	2385	682	94440	27.2								630	630	630	0.0	0.0	
	45/47 Can	20	344.8	168.0	9.50	4731	1584	17526	59.4																1584	1584	1584	0.0	0.0	
	46	57	283.9	168.6	4.53	2335	669	93300	26.5	68	277.8	168.6	4.50	2319	644	92866	25.7								669	669	669	0.0	0.0	
	47	56	273.6	168.7	4.47	2306	631	92182	25.2	67	288.7	168.7	4.57	2356	683	94144	27.3								631	631	631	0.0	-6.3	
	48	56	275.0	168.7	4.41	2275	628	91053	25.0	54	275.8	168.6	4.37	2254	621	90180	24.9								621	621	621	0.0	0.0	
	49	56	269.9	168.5	4.45	2294	612	91654	24.5	71	277.8	168.7	4.50	2332	645	92841	25.9								645	645	645	0.0	-0.7	
	49/51 Can	20	344.8	168.3	9.50	4736	1587	178169	59.7																	1587	1587	1587	0.0	0.0
	50	60	288.4	168.6	4.60	2370	678	94517	27.1	83	283.3	168.9	4.54	2345	664	93830	26.6								678	678	678	0.0	0.0	
	51	59	269.9	168.6	4.45	2295	612	91756	24.5	79	280.7	168.5	4.49	2314	650	92434	25.9								612	612	612	0.0	-8.0	
	52	80	286.4	168.6	4.60	2370	679	94629	27.1	90	277.5	168.7	4.52	2331	647	93163	25.9								679	679	679	0.0	0.0	
	53	83	274.8	168.6	4.46	2300	632	91967	25.3	40	288.9	168.7	4.55	2346	678	93742	27.1								632	632	632	0.0	-9.0	
	53/55 Can	20	344.8	168.3	9.50	4739	1587	178169	59.7																	1587	1587	1587	0.0	0.0
	54	64	274.3	168.6	4.50	2320	637	92221	25.9	54	275.6	168.6	4.37	2284	621	90181	24.9								637	637	637	0.0	-2.5	
	55	63	274.8	168.7	4.46	2301	632	92014	25.3	40	288.9	168.6	4.55	2348	678	93858	27.0								632	632	632	0.0	0.0	
	56	64	274.8	168.6	4.50	2320	637	92261	25.4	54	275.6	168.6	4.37	2284																

6th Repair Data - Member Properties for LC3CA and LC1CA tests

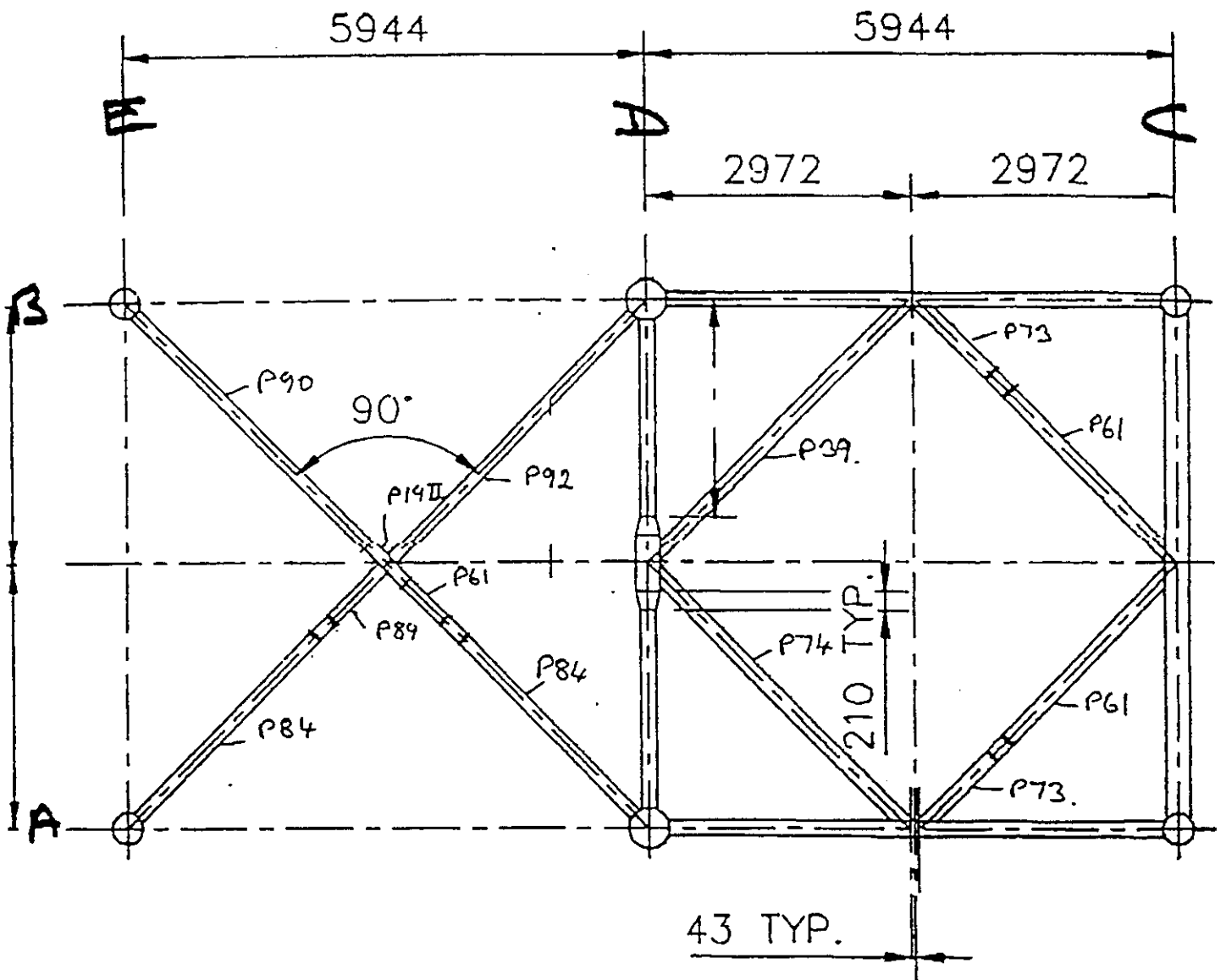
Repair (Note)	Member Number	Segment One						Segment Two						Segment Three						All Segment Analysis										
		Pipe Ref. P	Material Yield (N/mm ²)	Di. (mm)	Wall Thick. (mm)	Area (mm ²)	Yield Load (kN)	Modulus (mm ²)	Yield Moment (kNm)	Pipe Ref. P	Material Yield (N/mm ²)	Di. (mm)	Wall Thick. (mm)	Area (mm ²)	Yield Load (kN)	Modulus (mm ²)	Yield Moment (kNm)	Pipe Ref. P	Material Yield (N/mm ²)	Di. (mm)	Wall Thick. (mm)	Area (mm ²)	Yield Load (kN)	Modulus (mm ²)	Yield Moment (kNm)	Max. Yld Load (kN)	Max. Seg 1 / Seg 1 +/-	Max. Seg 1 / Seg 1 +/-	Max. Seg 1 / Seg 1 +/-	
	2	4	326.7	355.8	12.70	13689	4472	1133821	370.4	7	320.8	355.8	12.38	133555	4284	1107942	355.4								4472	4284	4472	0.0	-4.2	
	3	4	326.7	355.8	12.70	13689	4472	1133821	370.4																4473	4473	4473	0.0	0.0	
	5	6	326.7	355.8	12.70	13689	4472	1133821	370.4																4472	4472	4472	0.0	0.0	
	5/6 Can.	12	355.3	457.2	12.81	17684	6354	1932787	888.7																6354	6354	6354	0.0	0.0	
	6	6	326.7	355.8	12.70	13689	4472	1133821	370.4																4476	4476	4476	0.0	0.0	
	8	5	327.5	356.1	12.81	13819	4526	1145281	375.1	7	320.8	355.8	12.38	13357	4285	1108266	355.5								4476	4285	4476	0.0	-5.3	
	8	5	327.5	356.1	12.81	13819	4526	1145281	375.1																4524	4524	4524	0.0	0.0	
	10	44	275.5	368.3	4.50	2319	639	92601	25.5																639	639	639	0.0	0.0	
	11	44	275.5	368.3	4.50	2319	639	92601	25.5																639	639	639	0.0	0.0	
	12	42	278.0	368.5	4.57	2354	656	93905	26.2																656	656	656	0.0	0.0	
	13	42	278.0	368.5	4.57	2354	656	93905	26.2																656	656	656	0.0	0.0	
	14	41	275.3	368.7	4.50	2322	640	92852	25.8																640	640	640	0.0	0.0	
	15	69	277.8	368.3	4.50	2318	644	92578	25.7																644	644	644	0.0	0.0	
	15/17 Can	19 II	367.3	468.3	6.63	950	4739	1645	178189	61.9															1646	1646	1646	0.0	0.0	
	16	70	287.3	368.5	4.42	2278	596	91051	23.4																596	596	596	0.0	0.0	
	17	68	281.4	368.6	4.42	2281	596	91254	23.9	40	288.9	368.3	4.55	2341	675	93303	27.0								596	596	596	0.0	0.0	
	18	103	277.8	368.6	4.50	2330	644	92881	25.1																	644	644	644	0.0	0.0
	19	107	275.8	368.7	4.55	2346	642	93708	25.7																	642	642	642	0.0	0.0
	20	62	287.4	368.7	4.43	2285	611	91433	24.4																	611	611	611	0.0	0.0
	20/22 Chord N16	78	277.1	368.7	4.55	2347	650	93812	26.0																	650	650	650	0.0	0.0
	21	62	287.4	368.7	4.43	2285	611	91433	24.4	58	275.0	368.3	4.41	2271	624	90560	24.9								624	611	611	2.2	0.0	
	22	76	277.1	368.6	4.55	2345	650	93650	26.0																	650	650	650	0.0	0.0
	23	73	277.8	368.7	4.50	2321	645	92772	25.9																	645	645	645	0.0	0.0
	23/25 Can	19 II	367.3	468.3	6.63	950	4739	1645	178189	61.9																1646	1646	1646	0.0	0.0
	24	65	281.1	368.7	4.60	2371	667	94699	26.6	58	275.0	368.3	4.41	2271	624	90560	24.9									667	624	667	0.0	-8.3
	26	72	277.8	368.6	4.50	2322	645	92875	25.8																	645	645	645	0.0	0.0
	26	71	277.8	368.6	4.50	2322	644	92892	25.8																	644	644	644	0.0	0.0
	27	66	289.4	368.5	4.52	2329	674	93687	26.8																	674	674	674	0.0	0.0
	27/29 Chord N18	66	289.4	368.5	4.52	2329	674	93687	26.8																	674	674	674	0.0	0.0
	28	77	281.4	368.5	4.33	2283	584	89342	23.4	58	275.0	368.3	4.41	2271	624	90560	24.9									584	584	584	0.0	0.0
	29	77	281.4	368.5	4.33	2283	584	89342	23.4																	584	584	584	0.0	0.0
	30	67	289.7	368.7	4.57	2357	683	94176	27.3																	683	683	683	0.0	0.0
	32	6	326.7	355.4	12.70	13713	4480	1137188	371.7	7	320.8	355.8	12.38	13357	4285	1108266	355.5									4480	4285	4480	0.0	-4.3
	33	6	326.7	355.4	12.70	13713	4480	1137188	371.7																	4480	4285	4480	0.0	0.0
	35	10	338.8	368.3	12.51	13511	4549	1121849	377.8																	4549	4549	4549	0.0	0.0
	35/38 Can	12	355.3	457.2	12.81	17684	6354	1932787	888.7																	6354	6354	6354	0.0	0.0
	36	10	336.6	356.0	12.51	13501	4544	1120258	377.1	3	318.7	355.8	12.72	13711	4383	1135615	363.1									4544	4544	4544	0.0	0.0
	38	9	332.3	355.9	12.74	13733	4563	1137409	378.0	3	318.7	355.8	12.72	13711	4383	1135615	363.1									4563	4563	4563	0.0	-3.9
	39	9	332.3	355.9	12.74	13733	4563	1137409	378.0																	4563	4563	4563	0.0	0.0
	40	43	263.5	368.7	4.48	2311	655	92450	26.2																	655	655	655	0.0	0.0
	41	43	263.5	368.7	4.48	2310	655	92370	26.2																	655	655	655	0.0	0.0
	42	13	324.7	368.7	4.80	2370	688	94606	28.6																	688	688	688	0.0	0.0
	43	13	324.7	368.7	4.80	2370	688	94606	28.6																	688	688	688	0.0	0.0
	44	13	324.7	368.7	4.80	2370	688	94606	28.6																	688	688	688	0.0	0.0
	45	115	275.9	368.3	4.51	2321	640	92549	22.8	85	282.8	368.3	4.58	2356	696	93888	26.5	40	288.9	368.3	4.55	2341	676	93303	27.0	640	640	5.8	0.0	
	46	114	285.1	368.3	4.52	2326	663	92738	26.4																	663	663	663	0.0	0.0
	47	45 II	246.7	368.3	4.51	2321	572	92549	22.8	45 II	246.7	368.3	4.51	2321	572	92549	22.8									572	572	572	0.0	0.0
	48	114	285.1	368.3	4.52	2326	663	92738	26.4																	663	663	663	0.0	0.0
	49	101	277.8	368.3	4.50	2316	643	92361	25.7	82	288.4	368.3	4.51	2321	689	92548	26.7									643	643	643	0.0	0.0
	50	86	285.3	368.3	4.49	2311	659	92172	26.3																	659	659	659	0.0	0.0
	50/52 Chord N34	65	281.1	368.6	4.60	2370	688	94606	28.6																	688	688	688	0.0	0.0
	51	101	277.8	368.3	4.50	2316	643	92361	25.7	86	285.3	368.3	4.49	2311	659	92172	26.3									643	643	643	2.5	0.0
	52	30 II	253.9	368.3	4.48	2309	585	91983	23.4																	585	585	585	0.0	0.0
	53	115	275.9	368.3	4.51	2321	640	92549	22.8																	640	640	640	0.0	0.0
	54	113	283.7	368.3	4.50	2318	662	92301	26.4	75	277.8	368.3	4.62	2376	658	94619	28.3									662	659	662	0.0	-0.3
	55	102	277.8	368.3	4.50	2316	643	92361	25.7																	643	643	643	0.0	0.0
	56	113	285.7	368.3	4.50	2316	662	92351	26.4	31 II	253.0	368.3	4.57	2351	595	93860	23.7									662	585	662	0.0	-0.1
	57	30 II	253.9	368.3	4.48	2306	585	91953	23.4																					



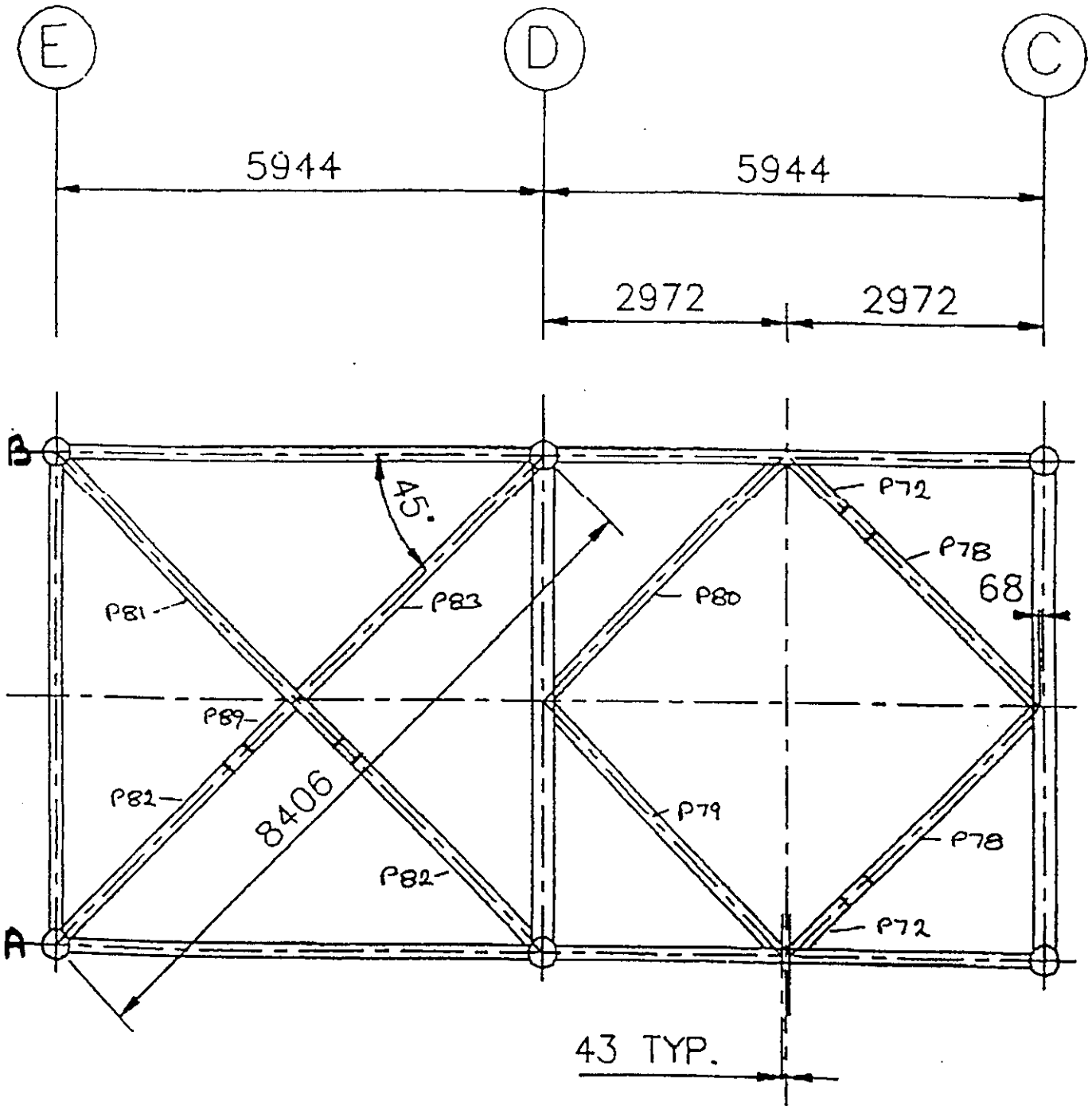
APPENDIX B

STRUCTURE - MATERIAL CROSS REFERENCING

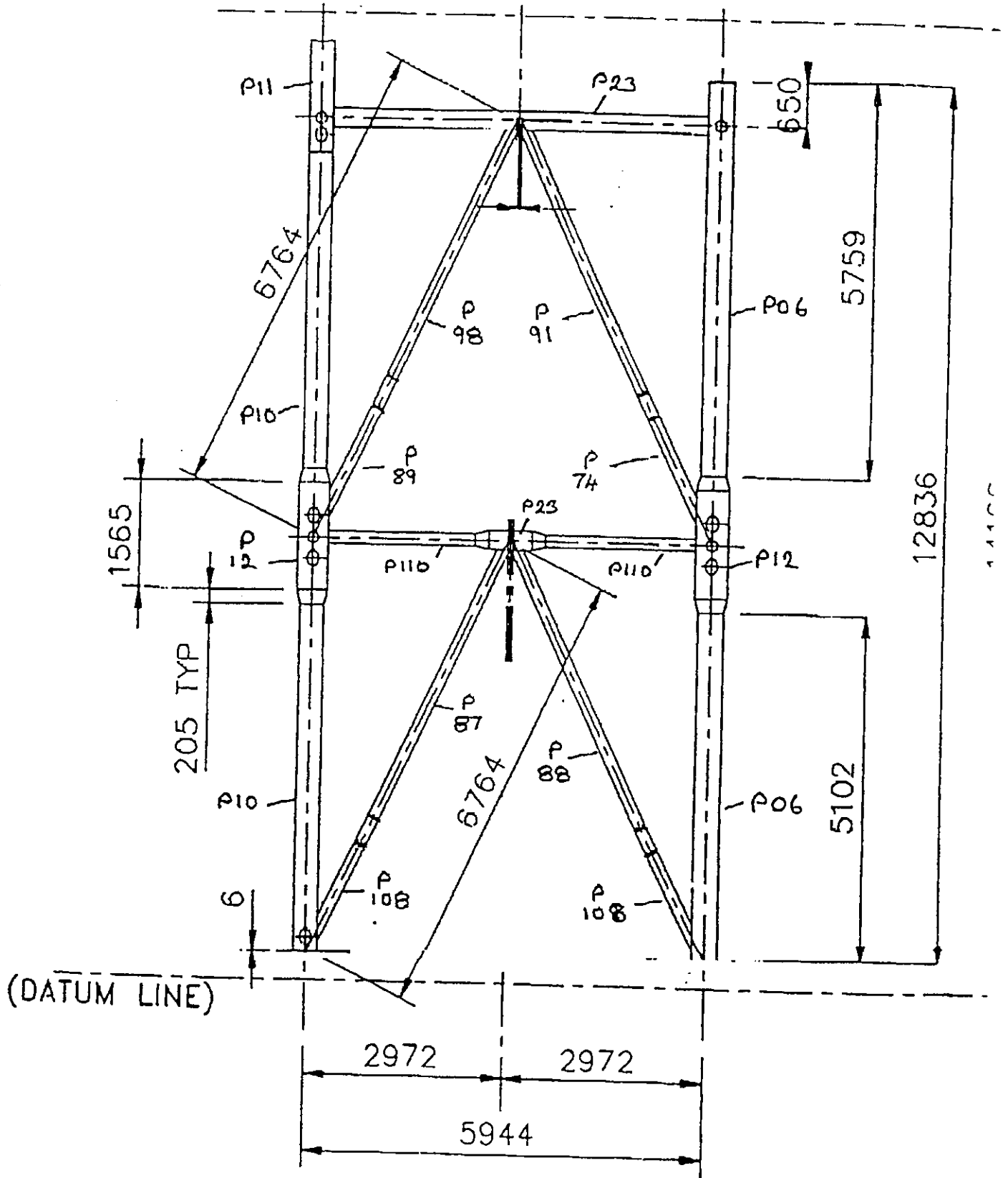
(BOMEL Incoming Document 9099 - 7 pages - initial build sketches from AKD)



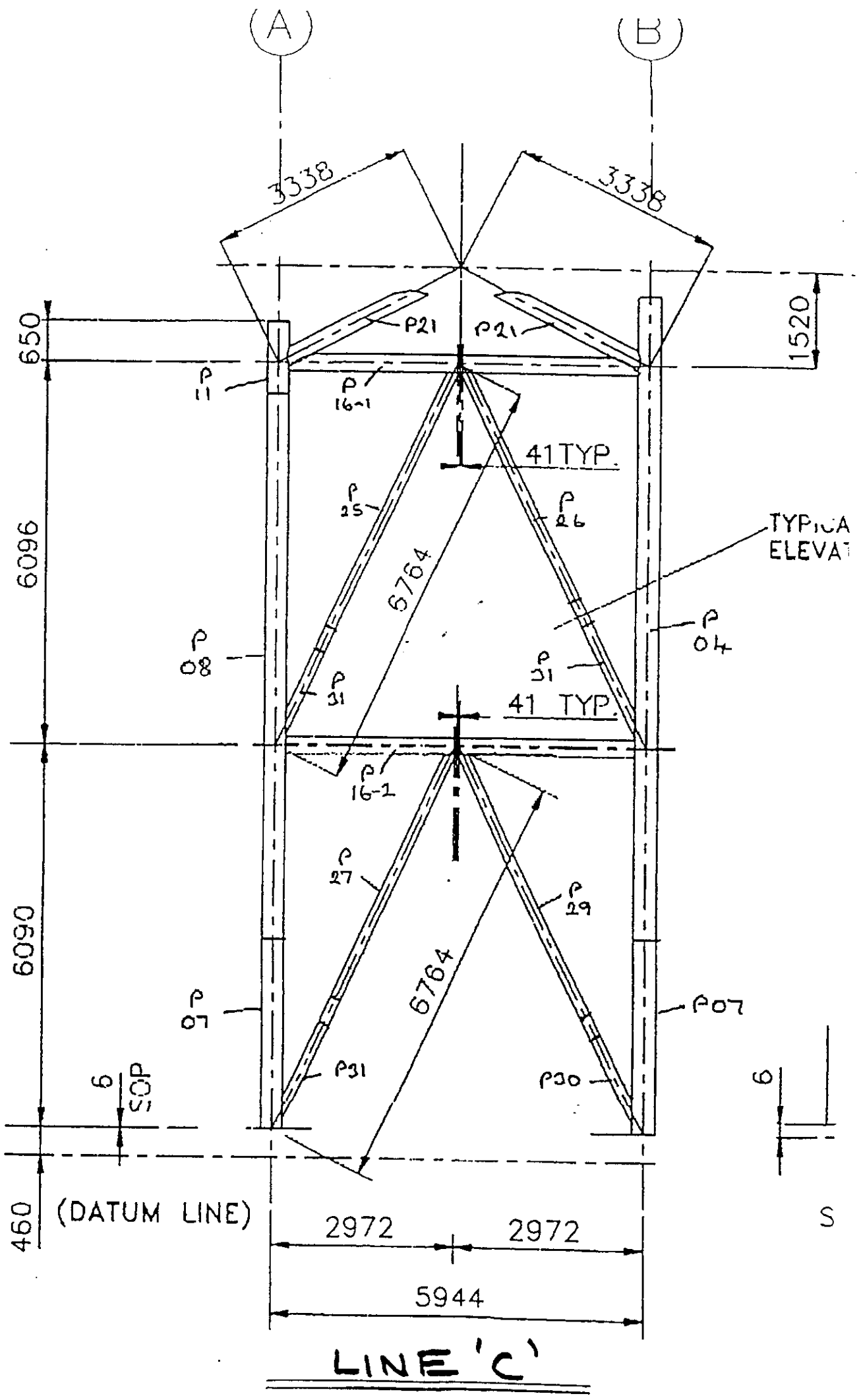
PLAN BRACING LEVEL 2

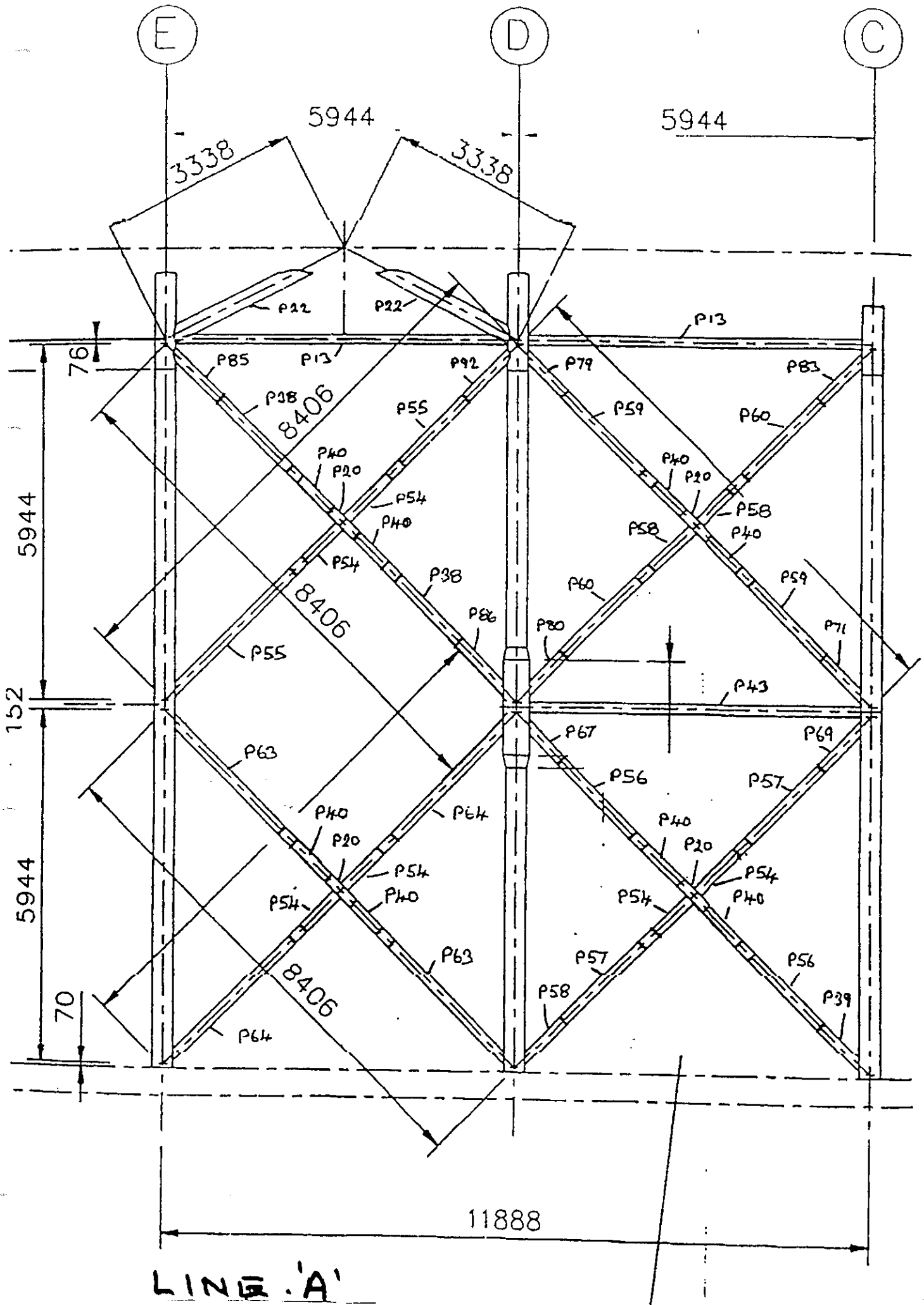


PLAN BRACING LEVEL 1



LINE 'D'







The contents of this document are confidential to Participants of the Frames Project - Phase III, under the terms of their contract for participation in the project

**JOINT INDUSTRY TUBULAR FRAMES PROJECT -
PHASE III**

ASSESSMENT OF LOCKED-IN FABRICATION STRESSES

C636\21\050R REV 0 JULY 1999

Purpose of Issue	Rev	Date of Issue	Author	Checked	Approved
Draft for Client comment	0	July 1999	JMB HMB	FHH FHH	CJB CJB

Controlled Copy	10	Uncontrolled Copy	
-----------------	----	-------------------	--

BOMEL LIMITED

Ledger House
Forest Green Road, Fifield
Maidenhead, Berkshire
SL6 2NR, UK

Telephone +44 (0)1628 777707
Fax +44 (0)1628 777877
Email bomel@compuserve.com

REVISION SHEET

REVISION	DETAILS OF REVISION	DATE
0	Draft for Client comment	July 1999

FILE SHEET

PATH AND FILENAME	DETAILS OF FILE
C636\26\PHASEI-X.pcx	Figure 2.1
C636\21\055U.pcx	Figure 2.2
C636\21\056U.pcx	Figure 2.3
C636\26\C476-7.pcx	Figure 3.1(a)
C636\26\C484-23.pcx	Figure 3.1(b)
C636\26\C514-7.pcx	Figure 3.1(c)
C636\46\001W.xls	Figure 3.2
C636\12\images\gui11.pcx	Figure 3.3(a)
C636\12\images\gui12.pcx	Figure 3.3(b)
C636\26\frame2.pcx	Figure 3.4
C636\21\044W.xls	Table 3.1
C636\26\C475-22.pcx	Figure 4.1
C636\21\041W.xls	Table 4.2
C636\21\042W.xls	Table 4.3
C636\21\046W.xls	Table 5.1
C636\21\052D.vsd	Figure 5.1
C636\26\C475-6.pcx	Figure B.1
C636\21\003S.wpd	Appendix C
C636\21\031W.xls	Appendix D



CONTENTS

	Page No.
FOREWORD	0.5
EXECUTIVE SUMMARY	0.8
1. INTRODUCTION	1.1
1.1 LOCKED-IN FABRICATION STRESSES	1.1
1.2 INFLUENCES OF LOCKED-IN FABRICATION STRESSES	1.1
1.3 LOCKED-IN STRESS MONITORING IN THE FRAMES PROJECT	1.2
2. FRAMES PROJECT PHASES I AND II - BACKGROUND	2.1
3. 3D FRAME CONFIGURATION	3.1
4. INITIAL BUILD / STRESS / FORCE MEASUREMENTS	4.1
4.1 SYSTEM SELECTION	4.1
4.2 THE DEMEC STRAIN MEASUREMENT SYSTEM	4.2
4.3 DEMEC SYSTEM MEASUREMENTS AND ACCURACY	4.4
4.4 SYSTEM VALIDATION	4.6
4.5 USE OF THE DEMEC SYSTEM	4.9
5. MEASUREMENTS OF INITIAL FORCES IN THE 3D FRAME	5.1
5.1 INITIAL BUILD LC1 TEST	5.1
5.2 1ST REPAIR - LC1C TEST	5.8
5.3 2ND REPAIR - LC2 TEST	5.8
5.4 3RD REPAIR - LC2C TEST	5.10
5.5 4TH REPAIR - LC3C TEST	5.11
5.6 5TH REPAIR - LC3 TEST	5.13
5.7 6TH REPAIR - LC3CA AND LC1CA TESTS	5.16
5.8 SUMMARY	5.20
6. CONCLUSIONS AND RECOMMENDATIONS	6.1
7. REFERENCES	7.1
APPENDIX A THE INFLUENCE OF LOCKED-IN FABRICATION STRESSES ON STRUCTURAL PERFORMANCE - EVIDENCE FROM FRAMES PROJECT PHASES I AND II	



CONTENTS CONTINUED

- APPENDIX B THE MAPS STRESS MEASUREMENT SYSTEM**
- APPENDIX C SPECIFICATION FOR DEMEC STRAIN GAUGE MEASUREMENTS**
- APPENDIX D CHRONOLOGICAL LOG OF DEMEC READINGS FOR 3D FRAME**



FOREWORD

This report is one of a series describing different aspects of Phase III of the Joint Industry Tubular Frames Project. Each report is self contained providing detailed information in the subject area and summarising relevant data from other documents. The following table lists and briefly describes the focus of each report for cross-referencing purposes.

Report Title	Reference	Circulation
Summary and Conclusions Overview report describing the project and principal findings	C636\04\478R	1
Background, Scope and Development Scene setting report summarising previous work, identified needs and Phase III programme definition and development	C636\04\435R	1
3D Test Set Up Brief description of the 3D test set up and structural configuration	C636\06\313R	1
Material Testing Report Description of material testing procedures, test results and disposition of specific materials within test structure	C636\23\004R	1
Assessment of Locked-In Fabrication Stress Explanation for the build up of locked-in fabrication stresses, description of their measurement and summary of the locked-in force values in key components at the start of each test	C636\21\050R	1
Test Frame Instrumentation Detailed description of all instrumentation systems used in the 3D frame, accuracy, sign conventions etc. Data on CD in final report	C636\25\071R	1
Loadcase 1 Test Report - Multiplanar K Joint Action Detailed description of the Loadcase 1 static test response and interpretation of the results and their significance	C636\37\014R	1
Loadcase 2 Test Report - Interaction Between X-Braced Planes Detailed description of the Loadcase 2 static test response and interpretation of the results and their significance	C636\39\011R	1
Loadcase 3 Test Report - Multiple Member Failures and 3D System Action Detailed description of the Loadcase 3 static test response and interpretation of the results and their significance	C636\40\021R	1



Report Title	Reference	Circulation
<p>Philosophy of Cyclic Testing Discussion of the background to cyclic response issues in the context of ultimate system strength and basis for specific loading scenarios</p>	C636\24\021R	1
<p>Loadcase 1 Cyclic Test Report Detailed description of the Loadcase 1 cyclic test response and interpretation of the results and their significance. Comparison with LC1 static results</p>	C636\38\010R	1
<p>Monotonic and Cyclic testing of Isolated K Joints Description and presentation of results from isolated component tests undertaken by SINTEF in Norway</p>	STF22 F98704 (C636\24)	1/2
<p>Loadcases 2 and 3 Cyclic Test Report Detailed description of the Loadcases 2 and 3 cyclic test responses and interpretation of the results and their significance. Comparison with LC2 and LC3 static results</p>	C636\41\011R	2
<p>Loadcases 1 and 3 'Alternative' Cyclic Tests Detailed description of the Loadcases 1 and 3 alternative cyclic test responses and interpretation of the results and their significance. Comparison with LC1 and LC3 static and cyclic tests</p>	C636\45\008R	3
<p>Multiplanar SCFs Joint BG / BOMEL report describing analytical work and experimental measurements of multiplanar SCFs. Includes comparison with 'standard' empirical approaches</p>	C636\18\018R	1
<p>Site Testing Programme results - Report to Benchmark Analysts Comprehensive report describing results for benchmark cases LC1, LC2 and LC3, including all pertinent data and providing response plots 'matching' the contributions from individual analysts</p>	C636\32\066R	4
<p>Benchmark Conclusions Report comparing blind and post test analyses with measured responses and assimilating learnings and recommendations for future practice identified by Benchmark Analysts</p>	C636\32\084R	1

Key to circulation.

Circulation	All participants	Participants in 1st extension	Participants contributing finance/analytical results to 2nd extension	Benchmark Analysts
1	✓	-	-	×
2	-	✓	-	×
3	-	-	✓	×
4	✓	-	-	✓



**JOINT INDUSTRY TUBULAR FRAMES PROJECT
PHASE III
ASSESSMENT OF LOCKED-IN FABRICATION STRESSES**

EXECUTIVE SUMMARY

As a redundant steel structure is fabricated, forces become locked-in to the members due to constraint effects as welds cool and shrink. These forces have been measured during the initial build and subsequent repairs to the Frames Project 3D test frame. This report describes the complementary mechanical and electrical measurement systems used and presents the results for critical components in each test.

It is shown that the pattern of forces can be readily understood but that it depends on the particular sequence of fabrication. The forces may be tensile or compressive and levels as high as 30% of the axial yield capacity of members were reached.

The influence on responses in the tests may be beneficial or detrimental depending on the direction of applied loading. The relative influence may be particularly great if joints without cans are the critical component in the loadpath.

As a result it is concluded that:

- the locked-in forces reached in the test frames must be taken into account when interpreting the measured capacities of components to applied loads
- the potential influence of these locked-in forces must be recognised in the comparison of benchmark analysis predictions to the test frame responses.

Table 5.12 summarises the measured locked-in fabrication forces acting at the start of each test. Table 3.1 presents the coacting forces due to gravity and a load cell offset calculated.

More generally when considering the conduct of ultimate strength analyses of jacket structures the potential influences of locked-in fabrication forces must be considered. Their magnitude and sense will never be known but some degree of sensitivity study may be appropriate to ensure that deterministic response predictions are valid.



1. INTRODUCTION

1.1 DEVELOPMENT OF LOCKED-IN FABRICATION STRESSES

It is a fundamental law of physics that a material contracts as it cools. In the case of weld metal forming a connection in a statically indeterminate structure, the surrounding members distort to give compatibility of the strain as the weld cools. As a result, a corresponding set of internal equilibrating forces is generated. A zone of self-equilibrating tensile and compressive residual stresses is also generated local to the weld. These stresses can reach yield level and can be very significant in fracture mechanics assessments of crack-like flaws. However it is the long range locked-in fabrication forces and their effect on the apparent capacity of structural components and systems that are the subject of this investigation.

Treatment of locked-in stresses in the open literature is not extensive. Nevertheless, the phenomenon is well-known to welders on fabrication sites. In preparing members for fit-up the distortion must be accounted for to ensure that the sequence of welds can be performed satisfactorily and that the straightness of members in the final structure is within specified tolerances. Similarly if there is a need to dismantle a welded structure, precautions are taken to avoid the effects of springback as members are cut and forces are released. The locked-in forces may be due to mechanical constraints, applied during fabrication to achieve fit-up, as well as weld shrinkage.

1.2 INFLUENCES OF LOCKED-IN FABRICATION STRESSES

In general component based design practice offshore, structural engineers take no explicit account of locked-in stresses. There are a number of reasons for this:

- Capacity equations for members, joints etc., are derived from isolated component tests where the specimens are statically determinate with free ends so no locked-in forces are present
- The magnitude and sense of locked-in forces depend on the sequence of fabrication. They would not be known before construction, nor are they generally monitored.
- The broad umbrella of a working stress safety factor may have been considered adequate to accommodate such random 'imperfections'.

However, if the effects of locked-in stresses are significant (and this report will show they can be), more rigorous account may be appropriate, particularly in a limit state scenario and where structural system reliabilities are being quantified.

In some structures instability in one weak load path may dominate the response. As a result, imperfections, such as locked-in stresses, which affect the capacity of the critical component, can have a direct influence on the system capacity. In others the redundancy may ensure that parallel load paths are evenly utilised such that, although the precise sequence of local failures leading to structural collapse may be sensitive to perturbations in the component properties, the ultimate collapse load may not be.

Ultimate strength (pushover) analyses are being performed increasingly to demonstrate the ability of a platform to withstand extreme events without catastrophic collapse and to prioritise and target inspection activity on key components for overall integrity. Detailed or accurate information about all aspects of system loading and resistance is generally not available and the need to perform sensitivity analyses is being recognised increasingly.

1.3 LOCKED-IN STRESS MONITORING IN THE FRAMES PROJECT

Having seen evidence of the potential influence of locked-in stresses on system performance in earlier phases of the Frames Project (see Section 2), the 3D programme included a specific monitoring activity:

1. To ensure the measured force responses were appropriately interpreted; and
2. To provide more general insight to the build up of locked-in stresses and their magnitude, and recommendations on their treatment in future analyses.

Section 3 provides a description of the 3D frame configuration and loading scenarios to define the state of stress in the structure at the start of each test. The ways in which the locked-in forces were measured and validated are described in Section 4. Section 5 then provides specific records for each test which are used in companion reports describing the test programme. Recommendations concerning the potential importance of these locked-in forces, in terms of their effects on component capacities and system responses recorded under applied load, are given in Section 6. In addition more general recommendations for considering the effect of locked-in stresses in jacket analyses are also presented.



2. FRAMES PROJECT PHASES I AND II - BACKGROUND

Attention was given to the potential influence of locked-in stresses on structural performance when interpreting the measured responses of the two-bay X braced frames tested in Phases I and II of the Frames Project^(1, 2) (Figure 2.1).

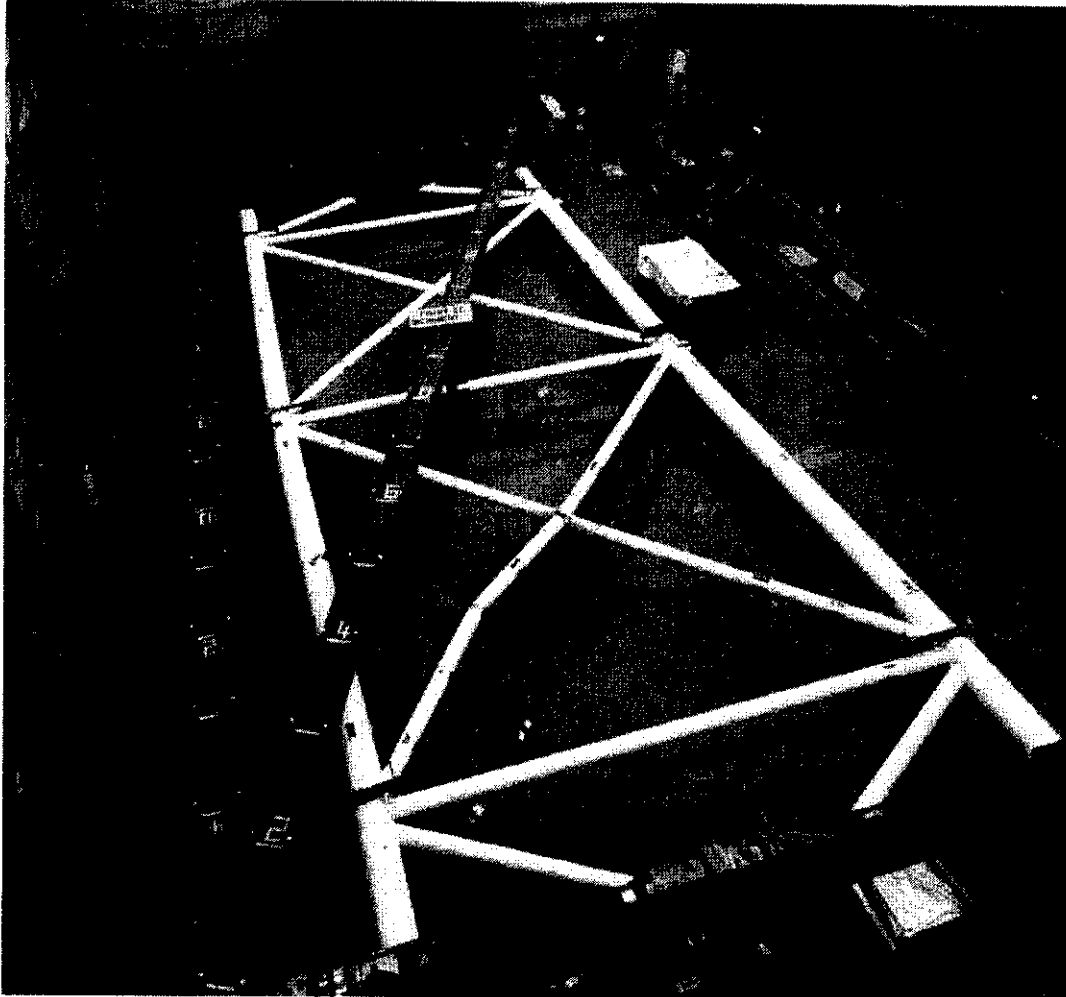


Figure 2.1 Frames Project Phase I - two bay X-braced frame

The issues are discussed in detail in Reference 3 which is reproduced here as Appendix A. However, in summary the sequence of component failures and capacity of individual members under applied frame loads were not as anticipated.

Figure 2.2 shows that in Frame I the top bay chord yields in tension (at Scan 9) before the corresponding brace buckles (at Scan 11). The members are moderately slender with very similar geometric and material properties. An initial pretension in the members would explain this (otherwise unexpected) sequence. Although locked-in forces were not measured in the Phase I project, evidence to support the findings was found in records of the construction sequence. For Frame I the mid-height horizontal was positioned before the top bay X-bracing

was introduced. The surrounding structure would therefore have resisted the pull as the X-brace welds cooled, inevitably resulting in pretension in these members.

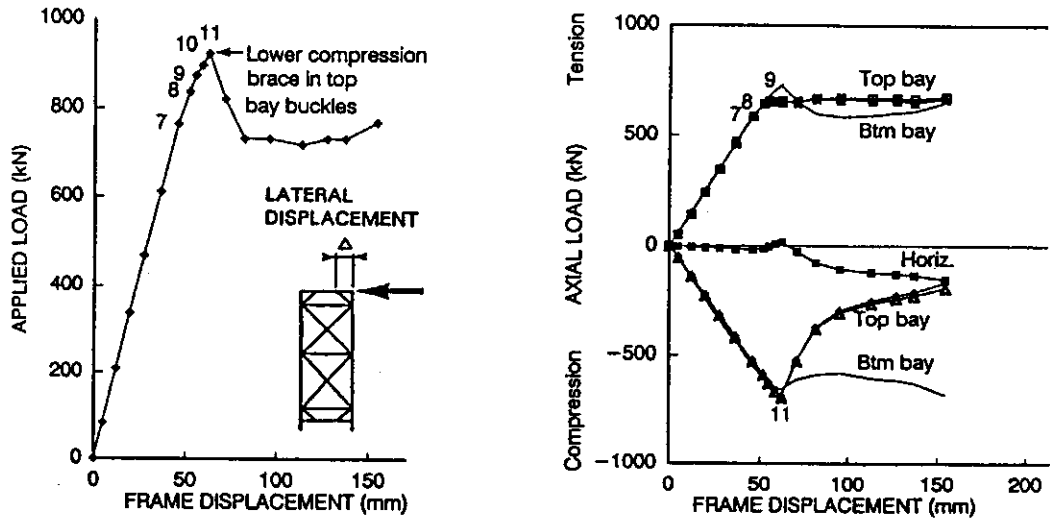


Figure 2.2 Frame I top bay brace loads through ultimate strength test

Conversely it can be seen from Figure 2.3 that in the case of Frame III (which did not have a mid-height horizontal) there appears to have been an initial pre-compression in the top bay bracing. The tension brace capacity in response to the applied force load is significantly greater than the measured yield stress and cross-sectional area would indicate. It is known that, to ensure the legs would be straight within tolerance, the frame legs were deliberately pulled outwards during fabrication to compensate for the inward force as the X-braces were welded. Once welding was complete the mechanical constraints were released and the legs moved in compressing the braces.

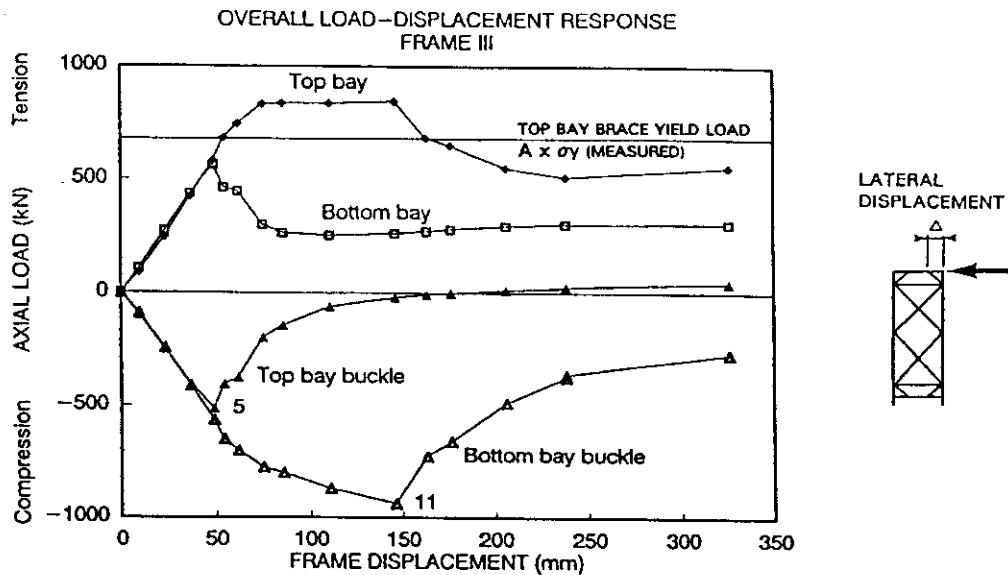


Figure 2.3 Frame III brace loads through ultimate strength test

In Phase II locked-in stresses were measured and provided a basis for accurately correlating recorded joint capacities within the frame to isolated component responses (see Appendix A). The stress levels were as much as 15% of the nominal yield of the brace materials and either tensile or compressive. It should be noted that the frame proportions and the geometric and material specification of the braces and legs in the 3D frame are nominally identical to the original 2D test structures.

Consideration was given to the potential effects of scale, and this was supported by a further investigation during the fabrication of a four leg X-braced Central North Sea jacket. The measured locked-in stresses were generally within $\pm 5\%$ of the nominal yield but levels as high as 12% were recorded which in absolute terms were as great as those recorded in the test frames. Had the jacket had more complex bracing, stiffer legs or an alternative construction sequence, higher levels of locked-in stress could be envisaged.

This early work therefore showed the effects locked-in fabrication stresses can have on ultimate structural performance and confirmed that the fabrication stress levels recorded in the test frames are representative of those in full-scale jacket structures.

On that basis it was recognised to be imperative that locked-in fabrication stresses were recorded in the 3D test structure, both to ensure the responses to applied load were correctly interpreted and to provide greater understanding of their potential influence on jacket behaviour.

3. 3D FRAME CONFIGURATION

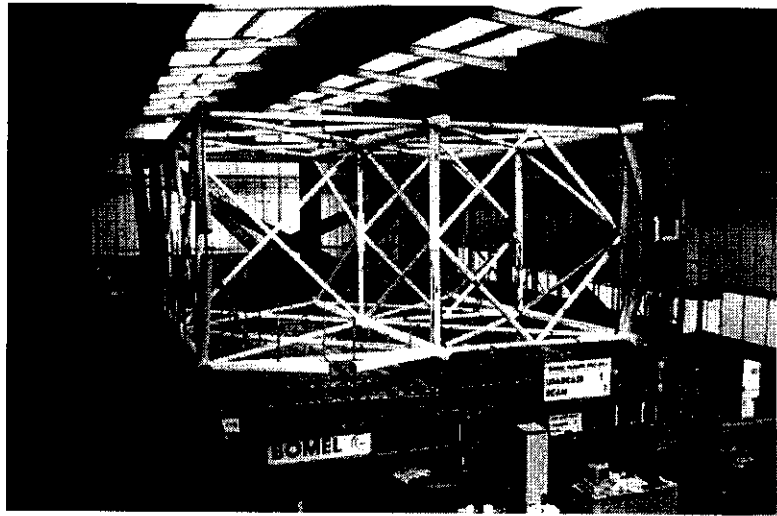
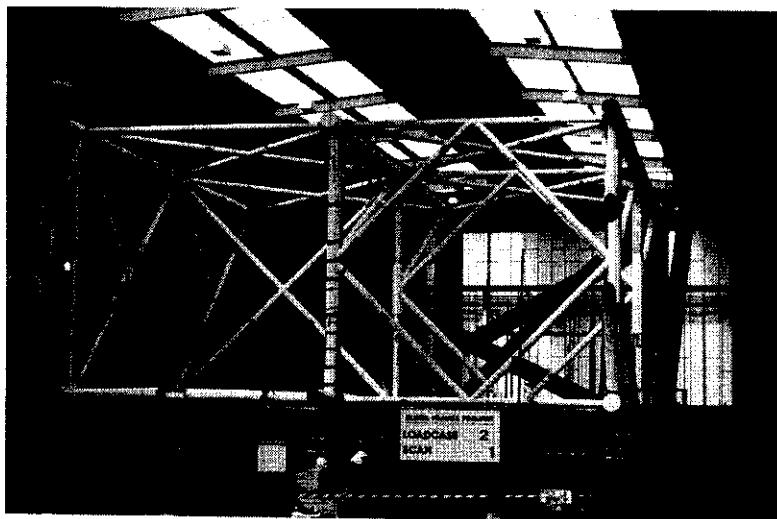
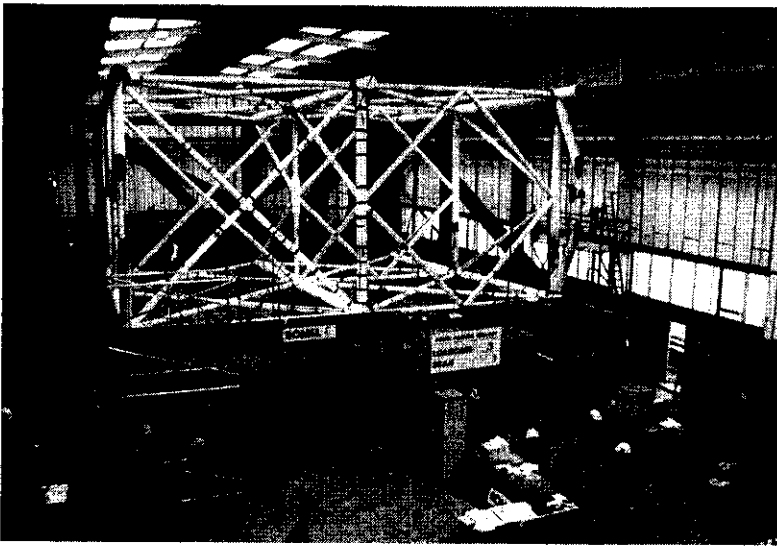
Before detailing the measurement of locked-in fabrication stresses, it is important to recognise all the elements contributing to the state of stress in the structure at the start of each test.

Eight frame tests were carried out in total with different patterns of load (static, cyclic etc) applied at three locations. The alternative loading beam positions in the three configurations are shown in Figure 3.1. The corresponding frame tests are listed in the captions. The test designations can be interpreted as follows:

a	b	c	d
LC	1	C	A
a	Loadcase		
b	Numeral '1' / '2' / '3' indicating loading position as per Figure 3.1		
c	' ' static test / 'C' cyclic test		
d	' ' static or basic cyclic test / 'A' alternative cyclic test		

Between consecutive tests, damaged areas of the frame were cut out and replaced in-situ. Figure 3.2 shows the sequence of frame tests and gives a diagrammatic representation of the repair locations.

No repairs were effected between Loadcases LC3CA and LC1CA. The 'critical' areas where members failed in each test are indicated by member number. Figure 3.3 gives the member and joint numbering schemes. It should be noted that X-braced members 98-101 at Level 1 were not present in the initial five tests LC1, LC1C, LC2, LC2C and LC3C; they remained in place for the final three tests. Similarly the loading configuration is shown for LC3** and differences from LC1** and LC2** tests are indicated in Figure 3.1.

	<p>LC1 LC1C LC1CA</p>
	<p>LC2 LC2C</p>
	<p>LC3 LC3C LC3CA</p>

Test	Date	Recording Times (MHz)	AVT Filename	Scan Numbers	BOMEL Working File C6361	Member Failures (Scan No)	Members Cut
LC1	T 26/04/98	17:35-23:05	LC1a_trial	1 to 10			
	T 26/04/98	09:30-10:44	LC1a_test	1 to 29	K38 (20), 72b (32) & K37 (softening)		
	C 20/04/98	10:44-16:43	LC1a_test	1 to 38			61, 62, 63, 64, 66, 67, 68, 69, 70, 71, 72
LC1C	T 23/05/98	14:23-17:50	LC1Ca_trial	1 to 26			
	T 30/05/98	13:45-21:18	LC1Ca_test	1 to 185	K38 (158) & K37 (164)		
	C 02/06/98	11:25-13:45					61, 62, 63, 64, 66, 67, 68, 69, 70, 71, 72
LC2	T 19/06/98	14:20-16:32	LC2a_T1	1 to 15			
	T 20/06/98	10:27-20:03	LC2a_test	1 to 49	X42 (14), 81/82y (21), 78b (38) & 82b (43)		
	C 20/06/98	20:03-22:34	LC2a_cut	50 to 59			78, 81 & 82
LC2C	T 19/07/98	17:30-18:44	LC2Ca_trial	1 to 22			
	T 20/07/98	08:47-09:40	LC2Ca_test1	1 to 9			
	T 20/07/98	09:41-21:13	LC2Ca_test1	1 to 143	X42 (116) & 81/83y (134)		
	T 21/07/98	06:52-20:44	LC2Ca_test2	144 to 292			
	C 21/07/98	20:44-21:42	LC2Ca_cut	293 to 300			81, 82, & 84
LC3C	T 04/08/98	19:56-23:47	LC3Ca_trial	1 to 35			
	T 05/08/98	09:40-10:47	LC3Ca_test1	1 to 33			
	T 06/08/98	13:14-21:45	LC3Ca_test1	1 to 133	51b (125), 57b (127), 50/52y (126), 54/56y (126) & 46/48y (126)		
	T 06/08/98	08:25-18:18	LC3Ca_test2	134 to 252			
	C 06/08/98	18:18-20:19	LC3Ca_cut	253 to 265			49, 51, 52, 57, 58 & 60
LC3	T 28/08/98	14:45-17:42	LC3a_trial	1 to 26			
	T 28/08/98	09:34-20:47	LC3a_test	1 to 73	49/51y (19), 45/47y (31), 57/59y (37), 50b (37), 60b (41), 54b (44), X16 (55), X44 (59), X18 (51) & 61b (62)		
	C 10/09/98	10:15-18:32	LC3a_cut	1 to 41			45, 46, 47, 49, 50, 51, 53, 54, 55, 57, 58, 59 & 61
LC3CA	T 23/10/98	10:38-11:32	LC3Cab_trial	1 to 25			
	T 24/10/98	12:12-21:07	LC3Cab_test	1 to 205	X36_comp (60), X35_comp (154), 58/57y (164), X33_comp (165), X34_comp (165) with possible 50/52y (165) & 46/48y (165)		
	T 24/10/98	08:16-15:10	LC3Cab_cut	1 to 205			
LC1CA	T 08/11/98	09:28-10:33	LC1Cab_trial	1 to 22			
	T 09/11/98	10:46-22:00	LC1Cab_test	1 to 166	K37 (69), K38 (125), 72b (140), 70b (146) & K38 severed (162)		
	C 10/11/98	08:10-09:56	LC1Cab_cut	169 to 174			57, 60, 54, 55, 46, 51, 47, 50, 61, 63, 69, 71, 98 & 100

KEY:
t: Loadcase trial
T: Loadcase test
c: Loadcase cut
K: K Joint number
X: X Joint number
b: Member buckled
y: Member yielded
Material has been tested
eg X42 = X Node 42 failed
81y = Member 81 yielded

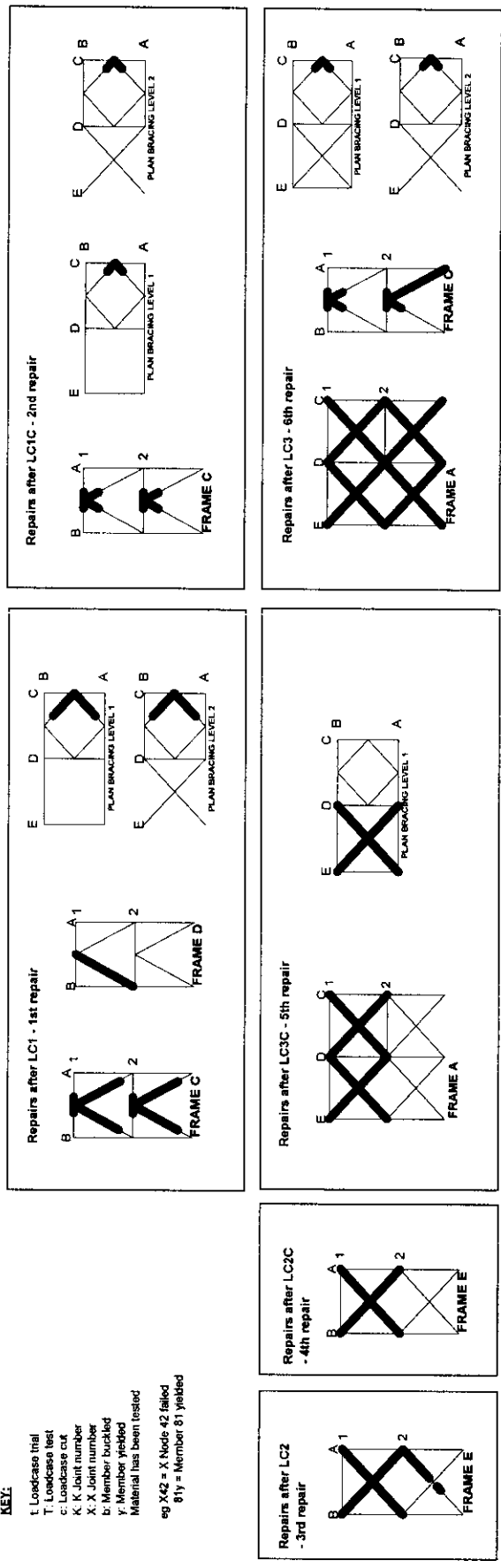


Figure 3.2 Summary of test sequence, member failures, cuts and repairs

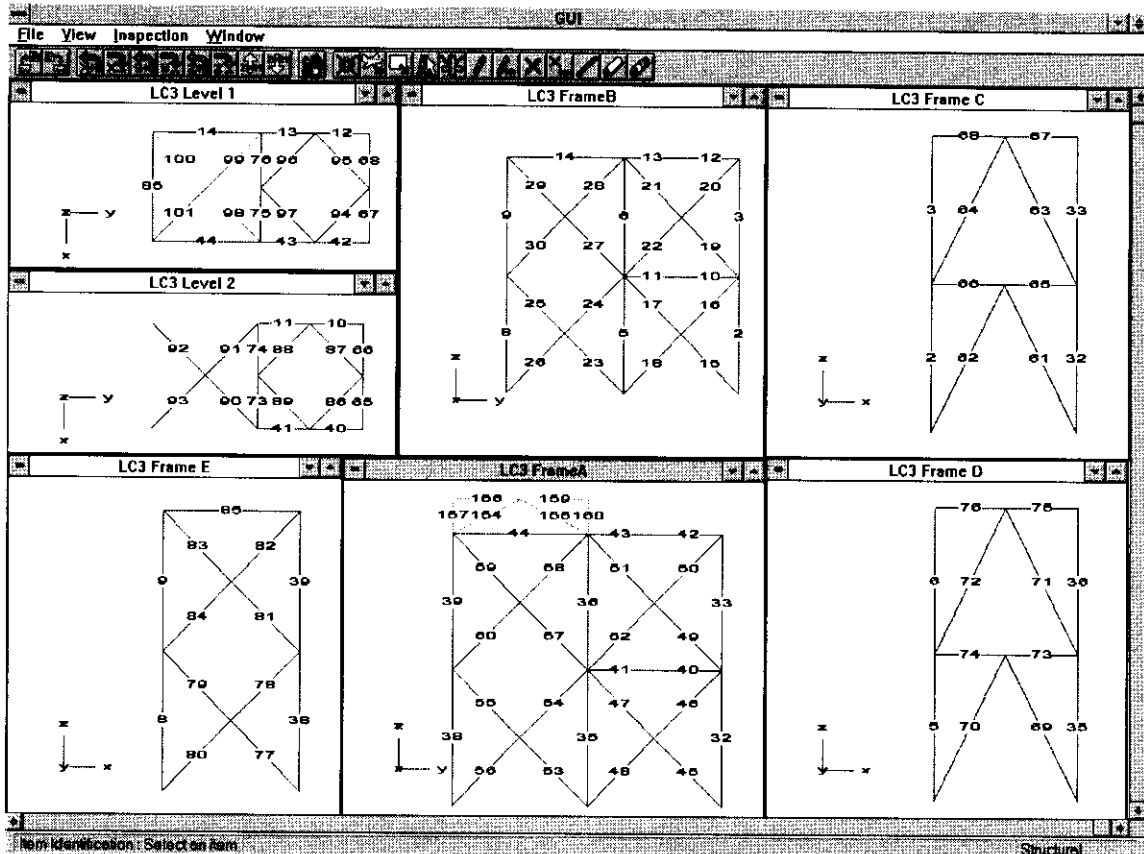


Figure 3.3(a) Member numbering scheme (Members 98-101 only in LC3, LC3CA and LC1CA tests)

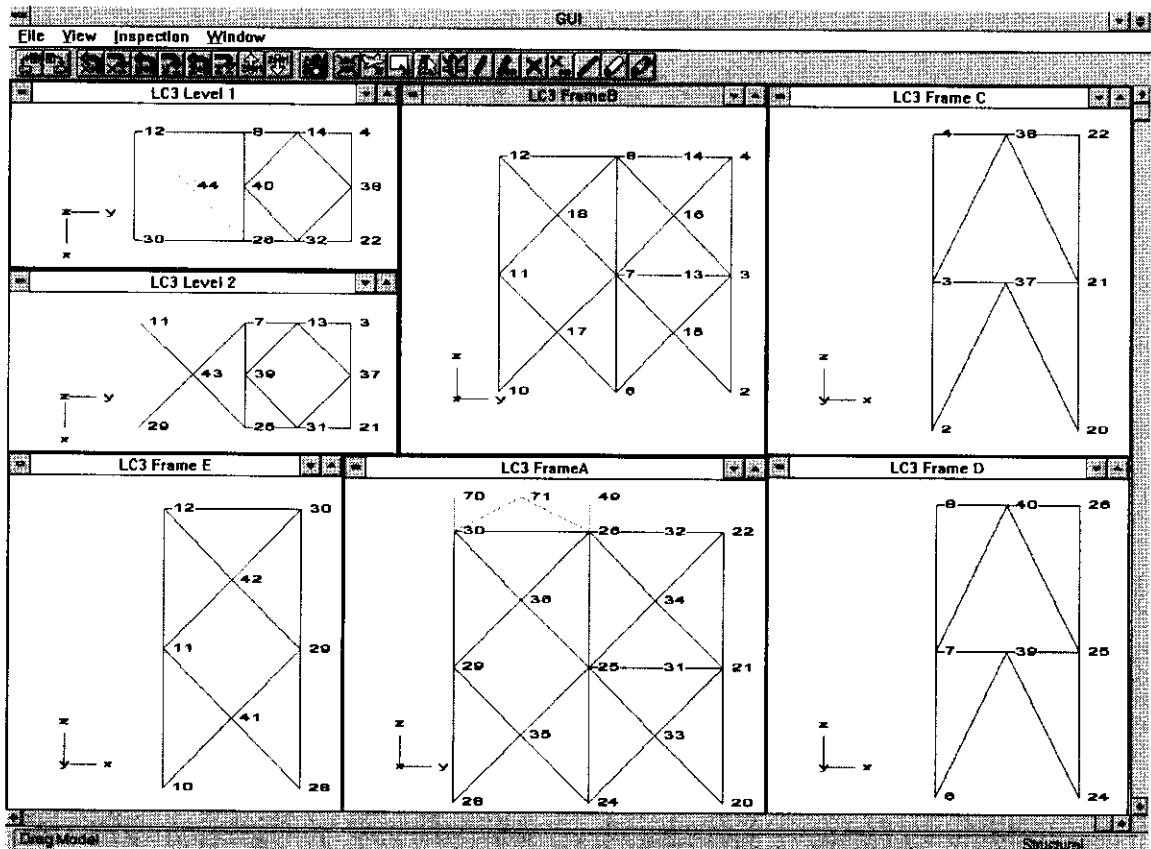


Figure 3.3(b) Node numbering scheme (Node 44 only present in LC3, LC3CA and LC1CA tests)

It can be seen from the side view of the model in Figure 3.4 that the tubular frame test specimen (white) is slightly higher near the actuator than at the point of connection to the rig. This is to provide clearance for cyclic loading in the 'vertical' plane. Furthermore the six frame legs are welded to the reaction rig (brown) and this rig in turn rests on a number of support stools. It can also be seen that, apart from at the actuator position, the frame has no supports and is effectively hanging as a cantilever from the rig. When there is zero applied load the members therefore carry self-weight gravitational loads in addition to any locked-in forces from fabrication.

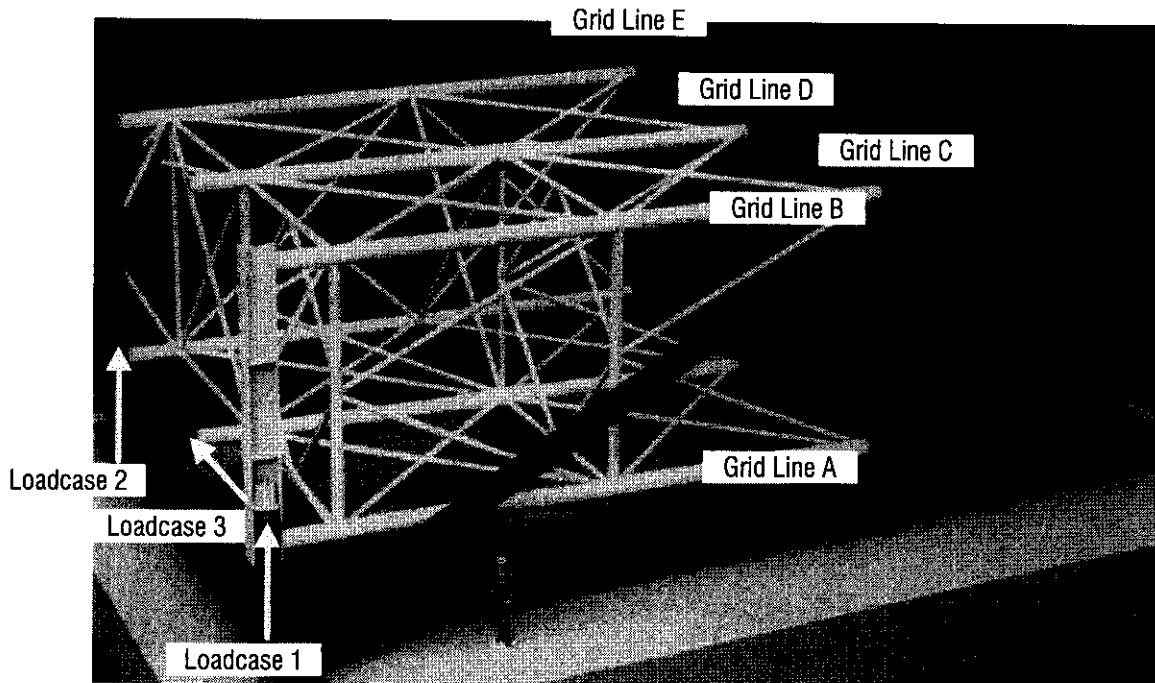


Figure 3.4 Side view of 3D frame model

The structural self-weight is taken to comprise the white tubular frame plus the loading beam to which the actuator is connected. For Loadcases 1 and 2 the same tubular beam was used but at different locations. A heavy I section was used for Loadcase 3 scenarios (Figure 3.1(c)). Care also needs to be taken when considering the contribution to internal forces from the actuator assembly, particularly for Loadcases 1 and 2. It can be seen in Figure 3.1(a) that the actuator (blue) stands on an articulation unit which is fixed to the rig and provides a direct reaction route for the actuator self-weight to ground.

A second articulation unit is located within the tubular loading beam at a level corresponding to the mid-height of the frame. However the actuator load cell sits at the top of the actuator shaft but **below** this second articulation unit. When the load cell gives a zero reading the top articulation unit is therefore hanging from the structure and the correct datum for the tests (zero applied load) requires a 15 kN offset to account for the unit self-weight. In test LC1CA the system datum was corrected; for tests LC1, LC1C, LC2 and LC2C the recorded values have to be adjusted.

The sequence of fabrication and stress/strain measurements adopted for the structure was as follows. Reference is made to DEMEC and electrical instrumentation systems to record member forces; further details are provided in Section 4.

1. The reaction rig was fabricated in entirety.
2. As each member was cut and prepared datum lengths were measured using the DEMEC strain measurement system.
3. The transverse two leg two bay X and K-braced frames C, D and E were fabricated in turn in plan. Each frame was rolled on its side, positioned in the rig and welded at the feet to the rig.
4. The lower legs of the 2D frames were supported at their node points to take up self-weight deflections and provide the correct inclination of the frame with respect to the rig.
5. The X and diamond bracing at Levels 1 and 2 was fabricated in-situ.
6. Finally bracing in the longitudinal Frames A and B was also fabricated in-situ.
7. The whole assembly (rig and frame) was then jacked up onto the support stools surmounted by sliding bearings. The props between the frame and rig were retained throughout.
8. The loading beam and actuator were positioned on Frame C for Loadcase 1. A forklift truck supported the weight of the beam and actuator throughout the welding operation.
9. The frame was instrumented and prepared for testing.
10. The state of stress in the structure was determined in comparison with the datum (Step 2) using the DEMEC system (see Section 4) [Reading A]. At the same time datum readings for the instrumentation systems were taken.
11. The frame supports were removed and the actuator was powered and positioned to give a datum reading in the load cell. The change in the state of stress within the frame between Steps 10 and 11 was recorded by the instrumentation [Reading B].
12. Subsequent changes due to applied actuator loads were also recorded by the instrumentation [Reading C].
13. The instrumentation system was specifically programmed not to reinitialise the gauges

each time the system was powered. Therefore the change in readings between the end of one test and the start of the next [Reading D] indicated the net change in individual members due to repairs within the structure, repositioning of the loading beam or supports etc. The exception was if gauges had to be repositioned or replaced due to damage or malfunction as the datum effectively altered.

14. Check readings on the state of initial stress are also given by the instrumentation from a comparison of values when members were cut with those at the start of each test [Reading E].

The combination of readings gathered in the above sequence therefore provides a cross-checked system. Equation 3.1 shows how the accumulated force in a member, from initial construction and 'N-1' cycles of structural testing and repair, can be compared with the force released when it is finally cut from the structure after test N.

$$A + B \sum_{n=1}^{N-1} (C_n + D_n) = -E \quad (3.1)$$

where n = test number

Reading	Source
A = Initial build force	DEMECs
B = Force changes due to positioning for first (LC1) test	Instrumentation
C _n = Force changes due to applied load from start to end of test n	Instrumentation
D _n = Force change due to repairs to structure or repositioning of actuator from the end of test n to start of test n + 1	Instrumentation
E = Force change in member between start of test N and cut out of member after the test	Instrumentation

Additional 'build' readings associated with repairs also provide intermediate checks.

The means by which the initial state of stress [Reading A] was established are described in Section 4. Reference 4 provides further details of the on-line instrumentation [Readings B to E]. However it is clear that together the measurements enabled the state of strain, stress or forces throughout the structure to be determined at any stage of the test programme.

Once welding and assembly were underway the values were due to a combination of locked-in fabrication, gravitational and applied load effects. It was therefore important to determine a reference point at which the contributions could be distinguished.

The point at which the structure was hanging unsupported with zero applied load was chosen, as the system could be readily analysed for each of the three configurations to determine the self-weight member forces. Instrumentation readings at Step 11 also correspond to this

Table 3.1 Continued

32	-47	-30	-49	63	-10	12	-2
33	-7	-1	-2	18	-3	-1	0
34	-63	-52	-61	54	-8	35	-5
35	-26	-17	-16	29	-4	7	-1
36	-3	-4	-12	1	0	3	-1
37	-95	-125	-138	58	-9	160	-24
38	-55	-87	-91	35	-5	135	-20
39	-9	-28	-28	7	-1	59	-9
40	4	-1	-1	-5	1	6	-1
41	2	2	3	0	0	2	0
42	3	-1	-2	-9	1	-2	0
43	-5	9	22	23	-3	-10	1
44	-2	4	6	7	-1	-8	1
45	4	-7	-9	-12	2	12	-2
46	-9	3	3	19	-3	-8	1
47	4	-7	-9	-12	2	12	-2
48	-9	3	3	19	-3	-8	1
49	4	-1	-2	-12	2	-1	0
50	-4	1	3	13	-2	2	0
51	4	-1	-2	-12	2	-1	0
52	-4	1	3	13	-2	2	0
53	13	-5	3	-18	3	26	-4
54	-15	-1	-7	22	-3	-11	2
55	13	-5	3	-18	3	27	-4
56	-15	-1	-7	22	-3	-11	2
57	4	-6	0	-11	2	13	-2
58	0	7	4	11	-2	-4	1
59	4	-6	0	-11	2	13	-2
60	0	7	4	11	-2	-4	1
61	-76	-56	-73	68	-10	14	-2
62	76	56	73	-68	10	-14	2
63	-53	-29	-47	73	-11	9	-1
64	54	29	47	-74	11	-9	1
65	31	21	28	-32	5	-4	1
66	-32	-21	-29	33	-5	4	-1
67	25	8	8	-48	7	0	0
68	-24	-5	-5	48	-7	0	0
69	-45	-37	-43	27	-4	17	-2
70	45	37	43	-27	4	-17	2
71	-34	-16	-30	36	-5	-6	1
72	34	16	43	-36	5	6	-1
73	16	15	12	-8	1	-7	1
74	-17	-17	-25	10	-2	12	-2
75	10	11	51	1	0	-2	0
76	-7	-7	0	0	0	1	0
77	-40	-53	-59	10	-2	46	-7
78	38	54	50	-8	1	-57	9
79	-39	-52	-58	10	-2	46	-7
80	39	55	51	-8	1	-57	8
81	-13	-40	-39	1	0	80	-12
82	10	32	39	0	0	-57	9
83	-12	-39	-38	1	0	80	-12
84	11	34	40	0	0	-57	9
85	2	2	9	0	0	-7	1
86	0	4	4	4	-1	-3	0
87	0	-4	-4	-4	1	3	0
88	-2	2	1	4	-1	-3	0
89	2	-2	-2	-4	1	3	0
90	15	4	4	-10	2	15	-2
91	-12	-1	-7	8	-1	-23	3
92	16	5	6	-10	2	15	-2
93	-13	-2	-8	8	-1	-23	3
94	-4	9	19	23	-3	-6	1
95	4	-8	-18	-23	3	6	-1
96	-6	6	16	23	-3	-6	1
97	7	-5	-15	-23	3	6	-1
98			15				
99			-10				
100			16				
101			-11				

Ref: C636\25\021W, 022W, 023W for LC1, 2, and 3 setups respectively
* calculated pro rata from 100kN SAFJAC values



4. INITIAL BUILD STRAIN / STRESS / FORCE MEASUREMENTS

The use of strain gauge instrumentation systems is well established in structural testing. Specific features of the instrumentation installed on the test frame to monitor changes in the fabricated structure are described in Reference 4. More unusual however is the measurement of strains during the process of fabrication as plain pipes with free ends are welded into a structure, experiencing shrinkage effects and finally hanging as part of a skeletal frame. This section presents the considerations underlying the selection of the DEMEC system for this purpose. The system itself is also described with an indication of its accuracy and validation.

4.1 SYSTEM SELECTION

The principal objective was to measure the change in axial strain, stress or force in each member from the stage it was a free tubular until it became an integral component of the 3D structural frame. Specific requirements of the measurement system were that it needed:

1. Not to impede the process of fabrication.
2. To be sufficiently accurate for locked-in stress levels that might affect component performance to be recorded.
3. To be robust enough to withstand 'handling' during fabrication.
4. Not to be expensive or time consuming to use.
5. To be portable in view of potentially limited access to the completed structure.
6. To be unaffected by general temperature changes over the course of fabrication or by local heat effects of welding.

Four measurement systems were evaluated on this basis:

- **Electric resistance strain gauges** (ie. conventional gauges) did not fulfill Criteria 1 nor 3. Standard gauges are very delicate and the presence of cabling would have severely hampered fabrication. The need for specialist application coordinating with fabrication activity further precluded this option.
- **Spot welded vibrating wire gauges** do not require cabling and can be 'read' with a

simple hand held excitation unit. They offer long term stability and are typically used for taking intermittent readings of this nature. However significant capital investment and specialist services are required and so the system failed to meet Criterion 4.

- The **MAPS System** is a newly developed technique for directly measuring biaxial stress and is described further in Appendix B. At the time of fabrication the ability to accurately measure low levels of stress in thin walled structures was not proven casting doubt on the ability to satisfy Criterion 2. Although nominally 'portable' the prototype equipment was cumbersome with limited reach violating Criterion 5. Finally, although a site trial of the system was undertaken it was shown not to be practical in light of Criterion 4; use of the system was physically time consuming and a two man team was only able to take readings for eight of the 100 or so members in one working day with a third man preparing the surface of the members. As a result the trial was halted.
- The **DEMEC System** comprises a simple mechanical gauge and four unobtrusive reference points on each member. The system was used successfully in Phase II of the project (see Section 2) and satisfied all six criteria for the 3D frame test.

The DEMEC system was therefore selected and specific details on the system and its use are presented below.

4.2 THE DEMEC STRAIN MEASUREMENT SYSTEM

The DEMEC system was developed by W H Mayes and Sons of Windsor, and is now used widely throughout the civil engineering industry, particularly to monitor cracks or measure deformations in concrete structures for which local strain measurements are inappropriate. It comprises a DEMountable MEChanical strain gauge with one fixed point and one moveable measuring point at the gauge end. Changes in the gauge length are transmitted through a pivot to the measuring dial gauge (see Figure 6 in Appendix A). The ratio between real movement and the reading on the dial gauge is calibrated and converted to strain. Gauges from 50mm to 2000mm are available and are selected depending on the magnitude of strains to be measured and the accuracy required. The datum length over which measurements are to be taken can be defined by adhering proprietary pips with a drilled hole to the structure (Appendix A, Figure 7), or alternatively by drilling a 1mm by 1.5mm hole directly into the member. The latter was not an option for the 3D frame given the relatively thin brace walls (4.5mm).

Figure 4.1 shows the system being used by BOMEL personnel prior to the 3D frame test.

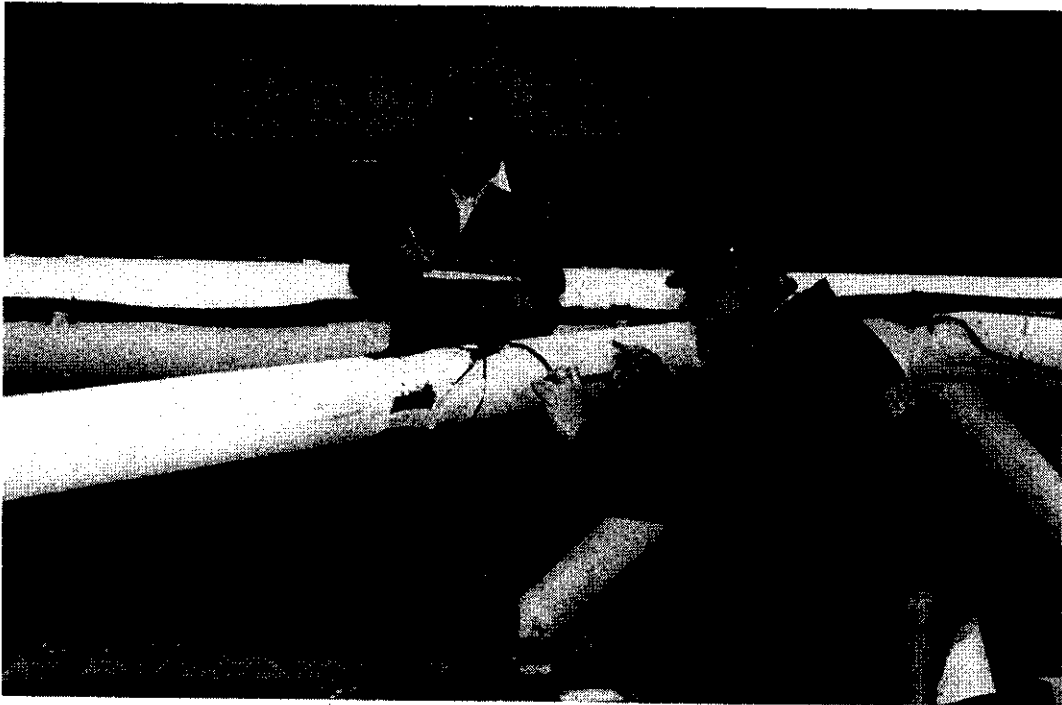


Figure 4.1 The DEMEC system in use on the Phase III 3D frame

It offered a number of advantages against the system selection criteria:

1. The system is cable-less and the pips are inconspicuous on the member surface. Furthermore the skills required to use the system are available within the fabricator's team. After a series of trials BOMEL was able to subcontract the measurements to the fabricator, AKD Engineering Limited, and the machine shop inspector worked to the BOMEL specification (see Appendix C). Scheduling the measurement and fabrication activities was then entirely in the control of AKD.
2. Use of an instrument with a 300mm gauge length was practical for use on site and gave acceptable resolution (see Section 4.3 below).
3. The only evidence of the system during fabrication was the pips positioned with two pairs on opposite sides of each member but almost flush with the tubular surface. The locations were highlighted to ensure slings were not used in the vicinity and only six pips (from over 400) were lost in the handling process.
4. The DEMEC gauge was made available free of charge by the Civil Engineering Department at City University. The pips and adhesive were inexpensive and the system could be used rapidly. Final readings for all members (three sets at two locations per member) were completed within the course of one working day. The



integration of the activity within the fabrication team, without the need for third party specialists, was a further advantage.

5. The DEMEC gauge, as shown in Figure 4.1, is hand held and readily portable. Positioning of the reference pips was specifically planned to give good access and to avoid overhead measurements in the fabricated structure (see BOMEL specification in Appendix C).
6. The gauge is mounted on a bar made from invar which is relatively inert to temperature changes. However a reference invar bar ensures that any temperature changes are corrected for and an unconstrained reference sample from each tubular is used to compensate for temperature fluctuations affecting the tubulars between initial and final readings. The positioning of the pips ensured they were not affected by local heat due to welding.

Set against these advantages, the system is positioned manually and depends on a visual reading of a dial gauge. The specification for using the DEMEC system presented in Appendix C details the way in which the system is used. The description below explains how the readings are combined and indicates the degree of accuracy that can be expected.

4.3 DEMEC SYSTEM MEASUREMENTS AND ACCURACY

Pairs of pips are adhered to opposite sides of each member once it has been cut. DEMEC readings are taken and recorded for both positions. Once the member is finally fabricated within the structure the readings are repeated. The difference between the readings gives the strain at each location and the average from opposite pairs indicates the axial strain. The conversion of the change in DEMEC reading to strain is effected using a calibration factor. The gauge used in the 3D test programme was re-calibrated by the manufacturer W H Mayes, just prior to use. The calibration certificate (No 79672) gave a conversion factor of 0.69×10^{-5} strain/division⁽⁵⁾. Readings were taken to the nearest half division and presented without a decimal point. The factor for use with the recorded readings is therefore:

$$\text{Calibration factor} = 0.69 \times 10^{-6} \text{ strain / decimal subdivision}$$

At the time each measurement (M) is taken, reference readings are also taken from the invar bar (I) and an unrestrained sample of tubular corresponding to the member (R), see Table 4.1. By subtracting changes in these readings between the start and completion of fabrication, temperature effects or adjustments to the gauge setting are compensated for.

Table 4.1 Gauge measurements used to determine change in strain

Measurement	Purpose	DEMEC Readings	
		Datum	Final
Invar bar	Instrument check	I_D	I_F
Reference sample	Temperature compensation	R_D	R_F
Member gauge	Change in strain	M_D	M_F

The change in reading across a pair of pips due to locked-in fabrication effects/gravity, C , is therefore given by:

$$C = (M_F - M_D) - (R_F - R_D) - (I_F - I_D) \quad (4.1)$$

The axial calculation also requires readings from the opposite pairs of pips (A and B) so in total twelve readings are combined. The impact of errors in readings on the final calculations are investigated below.

The calculation through to stress and strain proceeds through the following steps

- Axial strain, $\epsilon = 0.69 \times 10^{-6} \frac{(C_A + C_B)}{2}$ (4.2)

where C_A and C_B are calculated using Equation 4.1.

- Axial stress, $\sigma = \epsilon E$ (4.3)

where ϵ comes from Equation 4.2 and Young's modulus = $210 \times 10^3 \text{ N/mm}^2$.

- Axial force, $F = \sigma A$ (4.4)

where σ comes from Equation 4.3 and A is the member cross-sectional area.

The potential error in each DEMEC reading is an absolute amount independent from the magnitude of the reading. It can arise for example through ill-positioning of the instrument, mis-reading of the gauge etc., although the procedure for check readings should mitigate against this. Within the calibrated range of the gauge, no percentage error is given.

It is considered that in ideal conditions readings can be taken to ± 5 decimal subdivisions. However, when reaching for readings in situ the error may be significantly greater. As twelve readings combine in the axial force calculations the maximum error could be some 120 decimal subdivisions, although in the general case any errors may well compensate.

Based on Equations 4.2 to 4.4 this exceeded error of 120 decimal subdivisions in one of the 168mm \emptyset x 4.5mm WT braces of principal interest equates as follows:

$$\begin{aligned} \text{Maximum error} &= 120 \text{ decimals} \\ &= 41.4 \mu\epsilon \\ &= 8.7 \text{ N/mm}^2 \\ &= 20 \text{ kN.} \end{aligned}$$

In absolute terms the potential errors may seem significant particularly when only modest initial strain levels are being recorded. However the purpose of the readings is to identify whether locked-in stresses are of a level to affect the capacity of components under applied load. If the maximum error (8.7 N/mm²) is compared with the average yield stress level (278 N/mm²) for the bracing tubulars⁽⁶⁾ as a measure of the 'ultimate' condition, it amounts only to 3% (8.7 x 100/278). The accuracy of the DEMEC system is therefore acceptable for the purposes of this investigation.

4.4 SYSTEM VALIDATION

Extensive use was made of the DEMEC system throughout the programme. Figure 3.2 shows a chronological log of the readings taken indicating the stage of testing and reference for the source data. A repeat of all AKD data sheets is contained in Reference 7. An extensive spreadsheet was developed to reduce all the readings to units of stress and force⁽⁸⁾. For ease of presentation relevant results are extracted and tabulated in this report for particular locations and at different stages of the programme. In addition to the basic measurements of initial stress arising during fabrication, check readings were taken by different operatives and comparisons with the electrical instrumentation system were made. These steps to validate the system are presented below.

Initial checks were made on the use of the equipment by the fabricator AKD in taking datum readings on the prepared members prior to fabrication. These readings were generally straightforward to take and the checks showed use of the system to be satisfactory.

Once the structure was fully fabricated AKD took a complete set of final readings. BOMEL asked for a number of readings to be repeated on two occasions; the selection was made to include

different locations in the structure without reference to the data recorded. BOMEL personnel then used the DEMEC system independently. Table 4.2 shows a comparison of the stress levels from all three measurement sets based on nominal geometric properties for the members. It should be noted that the same datum values for the unrestrained tubulars were used in all three cases and the comparison indicates the consistency in the as-built readings.

Table 4.2 Check on DEMEC readings pre-test same / different days / operators

Member Locations		Calculated Stress from Demec Readings (N/mm ²)				Comparison Stresses (N/mm ²)			
Member Types	Member No	Final Reading 21/04/98	AKD Check 1 22/04/98	AKD Check 2 24/04/98	BOMEL Check 24/04/98	Maximum	Minimum	Range	% range / Nom. Yield
Fr B X bracing	15	83.0		83.0	84.4	84.4	83.0	1.4	0.5%
	16	37.7		31.9	34.4	37.7	31.9	5.8	2.1%
	17	80.1		87.7	89.8	89.8	80.1	9.7	3.5%
	18	29.3		32.6	29.0	32.6	29.0	3.6	1.3%
	19	41.3		35.9	38.4	41.3	35.9	5.4	2.0%
	20	35.5		26.4	27.5	35.5	26.4	9.1	3.3%
	21	45.6		43.8	48.2	48.2	43.8	4.4	1.6%
	22	26.1		29.7	30.1	30.1	26.1	4.0	1.4%
	23	40.6	54.7	37.3	38.0	54.7	37.3	17.4	6.3%
	24	48.2	63.4	43.1	42.7	63.4	42.7	20.7	7.4%
	25	30.1	32.2	34.4	31.9	34.4	30.1	4.3	1.6%
	26	24.6		31.5	30.8	31.5	24.6	6.9	2.5%
	28	30.1	37.0	19.2	23.5	37.0	19.2	17.8	6.4%
	29	54.0		56.9	54.3	56.9	54.0	2.9	1.0%
30	12.3	17.8	13.0	12.0	17.8	12.0	5.8	2.1%	
Fr A X bracing	54	65.9	64.8			65.9	64.8	1.1	0.4%
	56	63.4	61.9			63.4	61.9	1.5	0.5%
Fr C K bracing	61	-3.3	-0.7			-0.7	-3.3	2.5	0.9%
	62	21.0	20.7			21.0	20.7	0.4	0.1%
Fr E X bracing	77	-30.8	-33.7		-38.0	-30.8	-38.0	7.2	2.6%
	78	-11.7	-10.7		-12.8	-10.7	-12.8	2.2	0.8%
	79	-22.8	-22.8			-22.8	-22.8	0.0	0.0%
	81	24.3	23.9		22.8	24.3	22.8	1.5	0.5%
	82	36.2			27.2	36.2	27.2	9.0	3.2%
	83	35.9			14.9	35.9	14.9	21.0	7.5%

Reference C636\21\017W-e.wk4
Average yield = 278 N/mm² Reference C636\23\004R Rev. B

In general there is reasonable consistency between the readings and the range as a percentage of yield is within the bounds anticipated; the X-braced bay comprising members 15-18 is an example. Furthermore it can be seen that opposite braces within the 90° X-braced bays generally experience corresponding stress levels as equilibrium requires. It can be seen from Figure 3.3(a) that Braces 15/17 and 16/18 are paired, and Table 4.2 gives corresponding stress levels of 84/86 and 35/30 N/mm². There are occasional rogue readings for which no explanation is evident (eg. Braces 23 and 24, AKD Check 1). Therefore although the DEMEC data were generally good it was appropriate to apply equilibrium and other checks wherever possible.

A check against the electrical instrumentation system was also made. The readings in Table 4.2 correspond to the time the logger for the instrumentation system was switched on. The actuator loading system was then activated, the supports propping the frame were removed, and at Scan 5 the structure was hanging (albeit with a 15 kN offset due to the weight of the top hinge unit, see Section 3). At that stage BOMEL retook DEMEC readings for the readily accessible bracing in Frame A. Scan 6 followed immediately after. Table 4.3 shows the comparisons between DEMEC readings and the output from load cells and surface mounted strain gauges.

Table 4.3 Comparison between DEMEC and instrumentation systems as frame supports are removed

Member No	Stresses (N/mm ²)								% difference / Nom. Yield i=(h-c)/278
	From DEMEC readings			From Load Cells		From Strain Gauges		Average	
	AKD final	After support removal at Scans 5 to 6	Change	Scan 5	Scan 6	Scan 5	Scan 6	LC-SG & Scans 5-6	
	a	b	c=b-a	d	e	f	g	h=avg(defg)	
45	67.0	78.5	11.5	10.0	11.0	-	-	10.5	-0.4%
46	59.8	44.5	-15.3	-9.2	-8.3	-11.4	-11.5	-10.1	1.9%
47	65.6	77.5	11.9	10.0	11.1	-	-	10.5	-0.5%
48	54.7	46.3	-8.4	-9.0	-8.1	-10.9	-11.1	-9.8	-0.5%
49	-4.4	4.6	9.0	7.2	7.8	-	-	7.5	-0.5%
50	45.6	42.3	-3.3	-3.1	-2.1	-4.0	-4.2	-3.4	0.0%
51	-4.0	6.1	10.1	7.0	7.4	-	-	7.2	-1.1%
52	48.5	44.1	-4.4	-3.3	-2.2	-5.1	-5.3	-4.0	0.2%
53	9.4	15.9	6.5	6.1	7.2	-	-	6.7	0.1%
54	65.9	60.8	-5.1	-3.3	-2.8	-1.8	-1.4	-2.3	1.0%
55	6.5	12.6	6.1	6.0	6.5	-	-	6.3	0.1%
56	63.4	58.6	-4.8	-3.5	-2.5	-4.4	-3.9	-3.6	0.4%
57	34.8	39.8	5.0	6.1	6.6	-	-	6.3	0.5%
58	17.8	17.0	-0.8	-1.7	-1.2	-3.2	-2.8	-2.2	-0.5%
59	37.3	43.4	6.1	6.0	6.4	-	-	6.2	0.0%
60	13.8	13.3	-0.5	-1.6	-1.2	-3.3	-2.8	-2.2	-0.6%

Reference C636\21\017W-a.wk4 for Columns a and b
 Reference C636\AVT\LC1a_Trial.xls for Columns d, e, f, and g
 Nominal yield = 278 N/mm² Reference C636\23\004R Rev. B

It is important to recognise that the magnitude of the changes is very small. Nevertheless the DEMEC system can be seen to be correctly tracking the trends with equilibrating changes between opposite brace pairs as highlighted. In addition the DEMEC performance correlated at least as well with the high specification load cells as the conventional linear strain gauges.

Finally checks were also made during and after the Loadcase 3 test to validate the DEMEC system when significant deformations were present in the members. Table 4.4 presents the changes in DEMEC and load cell readings at different scans within the test in comparison with those at the start of the trial. Figures are only presented for members which had not been subject to plastic deformations.

Table 4.4 Comparison of member forces indicated by DEMEC and load cell systems in Loadcase 3 test

Member No.	Change in member force (kN)			
	Scan 60		Scan 73	
	DEMEC	Load Cell	DEMEC	Load Cell
52	-	-	5.1	4.1
54	-305.4	-328.4	172.6	179.0
55	667.7	694.6	-	-
56	-	-	169.4	172.6
58	-	-	107.2	111.8

The excellent correspondence between the DEMEC and load cell instrumentation systems is evident. In particular it should be noted that, whereas previous tables presented stresses, the above figures are in units of force. The load cells are pre-calibrated whereas the DEMEC measurements are converted on the basis of nominal areas hence some discrepancy, increasing in absolute terms with load level, may be anticipated.

As described previously two pairs of DEMEC pips are applied to either side of a member (either in- or out-of-plane). Strain gauges and load cells are installed as sets of four positioned orthogonally in- and out-of-plane. For small deflections, when plane sections remain plane, the four gauges provide redundancy and any set of opposite pairs can be averaged to give the axial force. However, if there are gross deformations this no longer holds true and, whilst the average of four gauges may give a dependable measure of axial force, two DEMEC readings will not. For the initial force measurements this presents no problem but indicates care is needed in extended use.

4.5 USE OF THE DEMEC SYSTEM

On the basis of the investigations presented above it is clear that, used with care, the DEMEC system offered a satisfactory method to determine initial stresses in the 3D structure.

5. MEASUREMENTS OF INITIAL FORCES IN THE 3D FRAME

Section 3 described the construction sequence for the 3D frame and explained the combination of locked-in fabrication forces and gravitational loads as well as applied load offsets in some tests from the presence of the hinge unit. In this section the measurement and breakdown of these force components is detailed to define the state of the structure at the start of each test. For the initial build the complete force distribution throughout the frame is given in order that general conclusions about the residual effects of fabrication can be drawn (Section 5.1). For the subsequent tests attention focuses on those components and areas of the structure where failures occurred to provide information directly relevant to the interpretation of the test results.

5.1 INITIAL BUILD LC1 TEST

Contributions to the state-of-stress in the test frame members at the start of the LC1 test are as indicated in Equation 3.2. Table 5.1 presents the calculations. The locked-in fabrication stresses in the final column are determined from the DEMEC measurements between the start and finish of fabrication (a) plus the changes indicated by the instrumentation as the frame supports were removed (b), less calculated elements due to self-weight gravitational loads and the 15 kN offset from the top hinge unit.

From a review of the results it can be seen that the agreement between load cell (LC) and strain gauge (SG) measurements as the supports are removed is reasonable. For determining the general level of stress use of nominal section properties is valid particularly given the accuracy of the DEMEC system.

Figure 5.1 provides a pictorial presentation of the locked-in fabrication forces calculated in Table 5.1. This is instructive and shows in Frame A, for example, how opposite force pairs in the X-bracing balance each other. In the construction sequence (Section 3) the 'horizontal' levels 1 and 2 were inserted before the Frame A and B infill X-bracing. Not surprisingly the horizontals carry significant compression whereas the X members have an initial pretension. The lower bay members in Frames A and B generally have higher tensile forces reflecting the greater constraint of the rig to shrinkage than the brace members at the top of the structure. In Frame E the lower bay was installed before the upper; in the former case the X braces are in compression, the latter in tension.

Table 5.1 LC1 locked-in fabrication forces (kN)

Member	DEMECs a	Logger b	Gravity c	LIS d=a+b-c
1		71 RSG	137	
2	208	35 SG	64	180
3	451	-23 SG	11	417
4		-14 RSG	14	
5	74	-19 SG	-9	64
6	45	-29 SG	-7	23
7		47 RSG	119	
8	144	41 SG	72	112
9	-307	1 SG	15	-321
10	-92	3 SG	-1	-88
11	-109	7 SG	1	-103
12	-32	-1 SG	1	-34
13	-154	22 SG	9	-141
14	-55	11 SG	6	-50
15	192		7	
16	87	5 SG	-1	93
17	185	-14 LC	7	165
18	68	2 SG	-1	71
19	96	-8 SG	3	84
20	82	3 LC	-2	87
21	106	-7 LC	3	96
22	60	-4 SG	-2	59
23	94	-29 SG	-22	87
24	112	22 LC	27	106
25	70	-26 SG	-22	66
26	57		27	
27	Pip missing	-18 SG	-9	
28	70	15 LC	8	77
29	125	-16 LC	-9	118
30	29	14 SG	8	35
31		-9 RSG	-113	
32	50	-18 SG	-47	79
33	5	5 SG	-7	17
34		-82 RSG	-63	
35	Pip missing	-86 SG	-26	
36	411	-13 SG	-3	402
37		-28 RSG	-95	
38	-139	-11 SG	-55	-95
39	-208	-13 SG	-9	-212
40	-78	7 SG	4	-75
41	-59	2 SG	2	-59
42	Can't reach	4 SG	3	
43	-81	-18 SG	-5	-94
44	-103	-8 SG	-2	-109
45	155	15 LC	4	166
46	138	-26 LC	-9	121
		-28 SG		
47	152	16 LC	4	164
48	127	-25 LC	-9	110
		-27 SG		
49	-10	14 LC	4	0
50	106	-23 LC	-4	87
		-24 SG		
51	-9	15 LC	4	2
52	112	-22 LC	-4	94
		-26 SG		
53	22	9 LC	13	18
54	153	-13 LC	-15	155
		-7 SG		
55	15	8 LC	13	10
56	147	-13 LC	-15	149
		-16 SG		
57	81	-4 LC	4	73
58	41	-3 LC	0	38
		-5 SG		
59	86	-4 LC	4	79
60	32	-3 LC	0	29
		-6 SG		

Table 5.1 Continued

61	-9	-72	LC	-76	-5
		-74	SG		
		-72	SG		
62	60	69	LC	76	54
		72	SG		
		72	SG		
63	2	-80	LC	-53	-25
		-79	SG		
		-76	SG		
64	20	74	LC	54	40
		75	SG		
		76	SG		
65	Pip missing	34	SG	31	
66	-31	-36	SG	-32	-35
67	Pip missing	106	SG	25	
68	Pip missing	-20	SG	-24	
69	26	-29	LC	-45	42
70	-40	26	LC	45	-60
71	61	-37	LC	-34	58
72	-37	32	LC	34	-38
73	-4	No datum	SG	16	
74	Pip missing	-14	SG	-17	
75	-20	-3	SG	10	-32
76	-70	-7	SG	-7	-70
77	-71	-13	LC	-40	-45
78	-27	4	LC	38	-61
		4	SG		
79	-53	-13	LC	-39	-27
80	3	4	LC	39	-32
		2	SG		
81	56	-5	LC	-13	64
82	84	-3	LC	10	71
		-8	SG		
		-4	SG		
83	83	-5	LC	-12	90
84	93	-4	LC	11	78
		-9	SG		
		-4	SG		
85	-36	-2	SG	2	-40
86	18	-3	LC	0	14
		-5	SG		
		-7	SG		
87	-3	5	LC	0	3
		4	SG		
		4	SG		
88	7			-2	
89	-24			2	
90	-45	13	LC	15	-47
91	-3			-12	
92	-11			16	
93	-15	-4	LC	-13	-6
94	47	-20	LC	-4	31
		-22	SG		
		-22	SG		
95	-30	20	LC	4	-14
		19	SG		
		17	SG		
96	57	-21	SG	-6	42
97	-19	20	SG	7	-5

Notes:

1. DEMEC readings based on AKD initial and final readings⁽⁷⁾. BOMEL calculations C636\21\017W-E.
2. Logger readings based on AVT files LC1a-trial.xls (switch on) to LC1a-test (Scan 1 corrected for 15 kN offset). BOMEL calculations C636\21\045W.
3. Self-weight calculations as per Table 3.1.
4. Instrumentation codes: RSG = rosette strain gauge; SG = strain gauge; LC = pre-calibrated load cell.
5. DEMEC, RSG and SG force calculations from strains based on nominal cross-sectional areas and Young's modulus, $E = 210 \times 10^3 \text{ N/mm}^2$. Calibrated load cells give a direct force measurement⁽⁸⁾.

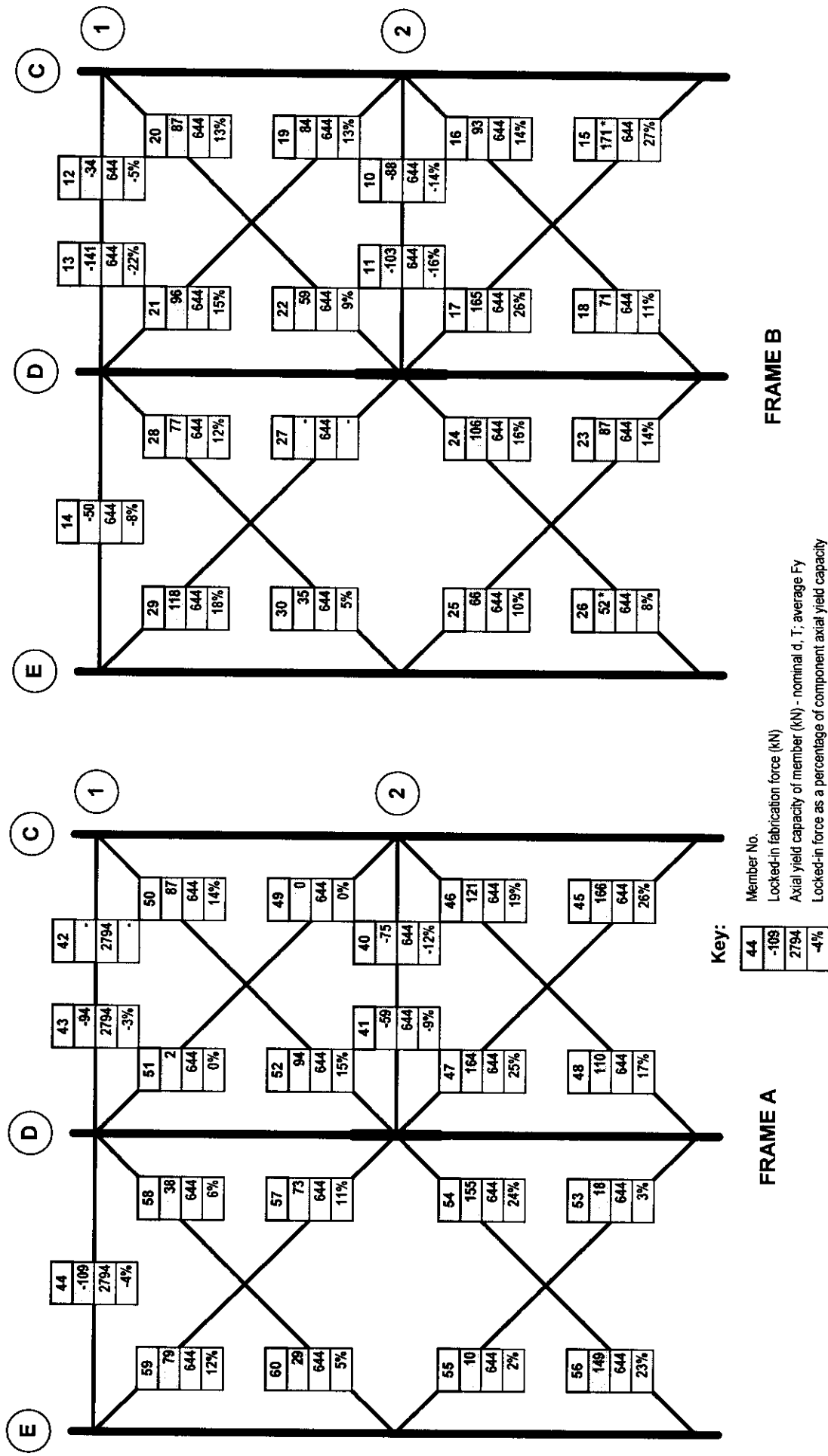
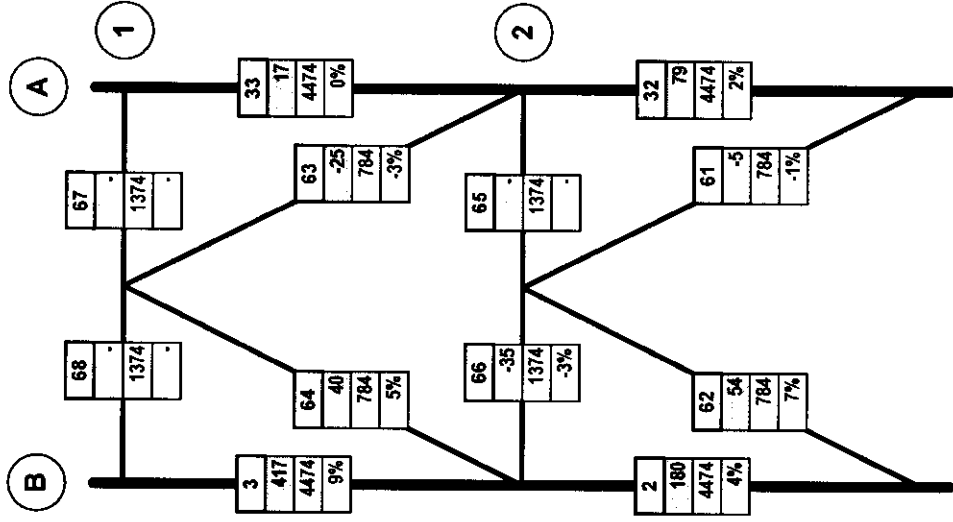
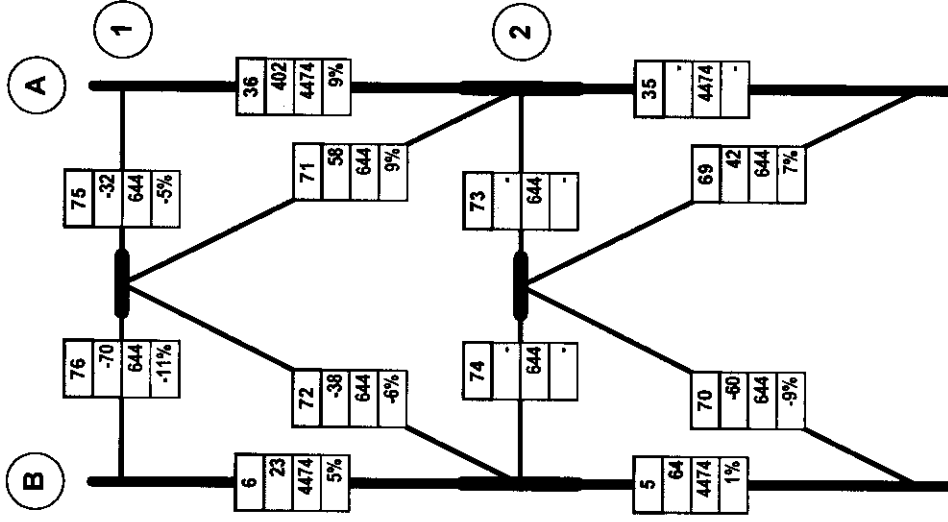


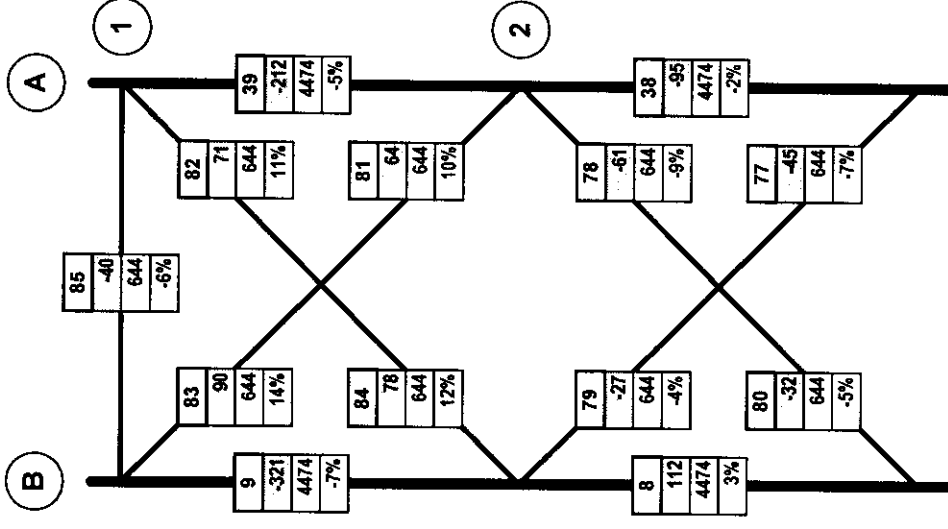
Figure 5.1 Initial build locked-in fabrication forces and comparison with member axial capacity (Page 1 of 3)



FRAME C



FRAME D



FRAME E

Figure 5.1 Initial build locked-in fabrication forces and comparison with member axial capacity (Page 2 of 3)

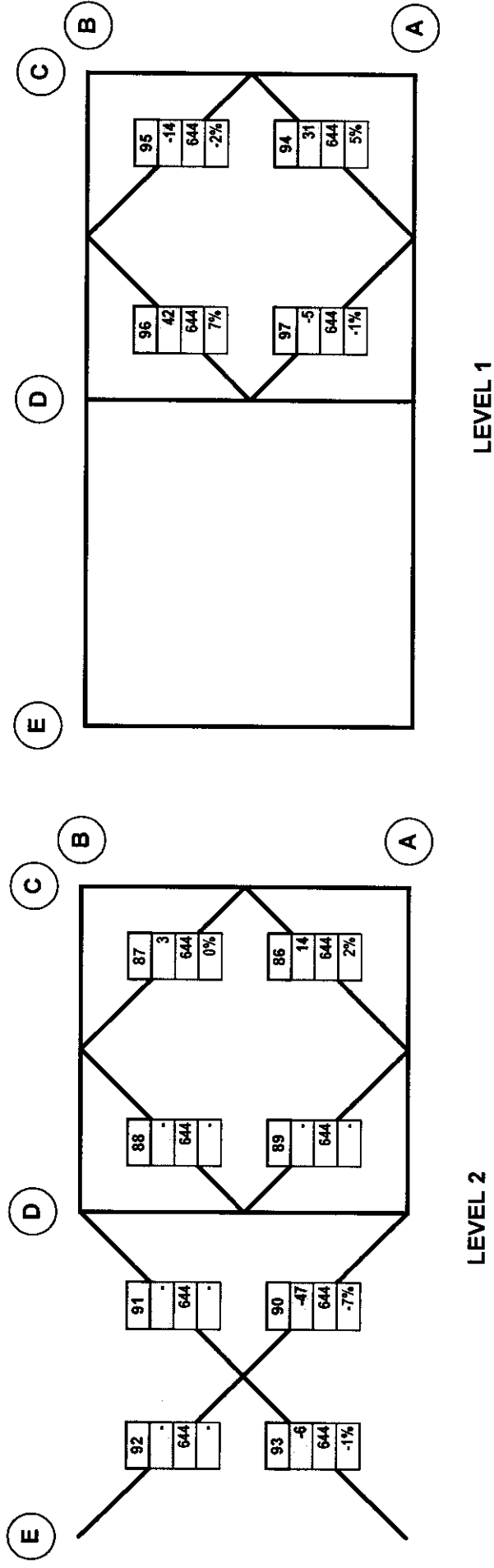


Figure 5.1 Initial build locked-in fabrication forces and comparison with member axial capacity (Page 3 of 3)



The locked-in force patterns in the Frame D bracing indicate reasonably balanced K action at the primary nodes. This condition is less clear in Frame C (particularly Braces 61/62); however the final DEMEC readings were checked, and the load cell and strain gauge values were consistent, as shown in Tables 4.2 and 5.1. It is important to recognise that equilibrating forces can arise from out-of-plane members, for example at the primary K nodes in Frame C.

Although in Frame E for example the leg forces are reasonably understandable given the brace forces recorded in Frames A, B and E, the readings are not entirely satisfactory. It is important to recognise that the DEMEC system was principally selected and validated to quantify initial forces in comparison with failure capacities for members which may contribute to the collapse mechanism (ie. the smaller braces). In the translation of strains to forces the same error in DEMEC strain measurement is compounded by a factor of 5.9 (ratio of leg to brace areas) in the initial force calculations for the legs. Where a 'maximum' absolute error of 20 kN is accepted for the primary braces the corresponding 'error' of 118 kN for the legs means that equilibrium checks between members of different sizes are not meaningful based on the values in Figure 5.1.

Considering the more appropriate comparison with component capacity, it is clear that the magnitude of initial fabrication forces can vary considerably and will certainly be influenced by build sequence. To get a consistent reference measure for illustrative purposes, component axial capacities, based on tensile yield for nominal geometries and average material properties⁽⁶⁾, are also included in Figure 5.1. In addition, the relative magnitude of the locked-in fabrication force as a proportion of the reference capacity is presented as a percentage.

Whether the effect is beneficial or detrimental depends on the relative sense of the locked-in force and may be more significant if the load path is limited by (lower) joint capacities or buckling. However, as a coarse measure it can be seen from Figure 5.1 that the locked-in forces in the primary X-bracing (168mm \emptyset x 4.5mm WT - 278 N/mm² yield - 644 kN axial tension capacity) range from -141 kN to +166 kN or -22% to + 26% of yield capacity. The locked-in forces in the legs (maximum +417 kN, minimum -321 kN) constitute only -7% to +9% of their tensile capacity. (355.6mm \emptyset x 12.7mm WT - 327 N/mm² yield - 4474 kN axial tension capacity).

Statistics of the mean and CoV could be assessed for the bracing but are not considered to be particularly helpful given the strong dependence on build sequence. The principal conclusion is that these forces, which are almost always neglected in structural design and assessment, can be considerable and their significance in terms of the response of components to applied load in the tests needs to be examined.



5.2 1ST REPAIR - LC1C TEST

Figure 3.2 illustrates the extent of the 1st repair. Brace 72 (in Frame D) was replaced in entirety and the load cell was re-welded into the new member. New DEMEC readings were taken. In Frame C and at Levels 1 and 2 the load cells remained within the frame and repairs were effected from the load cells to the multiplanar K nodes. Unfortunately several of the load cell gauges were damaged and it was determined in the post-processing⁽⁹⁾ that the measurements could not be relied upon. However, the limited constraint in K bracing, the higher component capacities in Frame C and evidence from the Frame II K-braced tests⁽²⁾ all indicate that the initial forces may be expected to have negligible influence on the LC1C component response.

5.3 2ND REPAIR - LC2 TEST

Figure 3.2 again shows the extent of the second repair and lists the component failures occurring in Frame E in the LC2 test.

Two approaches were taken to assessing the total forces in the members at the start of the LC2 test:

1. Accumulation of the change in instrumentation readings from initialisation of the logger to the start of the LC2 test with the initial build DEMEC values.
2. Measurement of the change in force as members are cut following the test compared with the start of the LC2 test (the force released is equal and opposite to the initial force).

Both approaches should be equally valid for determining the initial condition. Table 5.2 presents the comparison.

It can be seen from Table 5.2 that the total accumulated forces from the DEMEC and load cell systems correspond extremely well with the load cell forces determined at the cut out. The DEMEC values are determined on the basis of nominal section properties and the potential for absolute errors was discussed in Section 3. Nevertheless this comparison increases confidence in the use of either approach.

Table 5.2 Comparison of LC2 initial force calculations for Frame E bracing

Member	Force accumulation (kN)			Cut members	Force released (kN) Instrumentation LC2 start - LC2 cut [3]
	DEMEC initial build [1]	Instrumentation LC2 start - switch on [2]	Total		
77	-71.3	-30.2	-101.5		not free
78	-27.2	39.9	12.7	*	4.7
79	-52.8	-31.4	-84.2		not free
80	3.4	37.1	40.5		14.0
81	56.2	-43.5	12.1	*	10.2
82	83.9	26.2	110.1	*	127.1
83	83.0	-44.4	38.6		15.6
84	93.1	30.2	123.3		123.8

Notes:
 [1] See Table 5.1
 [2] Load cell data from AVT files: LC2a-test.xls Scan 1 and LC1a-trial.xls Scan 0 - see C636\21\032W.xls
 [3] Load cell data from AVT files: LC2a-cut.xls Scan 1 compared with Scan 59

The figures in Table 5.2 indicate the total force present in the members at the start of each test: ie. locked-in fabrication forces, gravitational loads and the initial load cell offset. Adopting the initial forces determined from the load cells as the members are cut, and where possible taking the gravitational and load cell offset forces given in Table 3.1, the components of locked-in fabrication force acting in the LC2 test can be determined as shown in Table 5.3. Average values in the final column reflect the expectation that forces in opposite pairs with 90° X bracing should equilibrate.

Table 5.3 Locked-in fabrication forces in critical LC2 components (kN)

Member	Initial force from cutout (Table 5.2 uno) a	LC2 gravity (Table 3.1) b	LC2 15 kN offset (Table 3.1) c	Locked-in fabrication force (kN)	
				a-b-c	average
77*	-102	-53	-7	-42	-33
78	5	54	9	-58	-54
79*	-84	-52	-7	-25	-33
80	14	55	8	-49	-54
81	10	-40	-12	62	64
82	127	32	9	86	83
83	16	-39	-12	67	64
84	124	34	9	81	83

* from DEMECs

5.4 3RD REPAIR - LC2C TEST

As shown in Figure 3.2, Braces 78 and 81 to 84 were completely replaced in the 3rd repair so the original DEMEC readings were no longer relevant.

Having demonstrated the validity of using load cell readings from start of test to cut out as a basis for determining the initial state of stress (see Section 5.3), this approach was adopted for LC2C. As shown in Table 3.2, the top bay bracing in Frame E (Members 81 to 84) are the critical components in the LC2C tests. Table 5.4 shows the full results separating the contribution from fabrication forces, gravity and the load cell offset.

Table 5.4 Locked-in fabrication forces in critical LC2C components (kN)

Member	Initial force from cutout [1] a	LC2C 15 kN offset (Table 3.1) b	LC2C gravity (Table 3.1) c	Locked-in fabrication force	
				a-b-c	average
81	111	-12	-40	163	166
82	78	9	32	37	34
83	117	-12	-39	168	166
84	75	9	34	32	34

Notes: [1] Load cell data from AVT files: LC2Ca-cut.xls Scan 300 (end of cutout) compared with Scan 1 (start of test)

5.5 4TH REPAIR - LC3C TEST

The LC3C test was the first applying horizontal load to the structure on Frame A. The load cell offset is no longer of concern as the actuator system is rotated through 90° (Figure 3.1(c)). Prior to the LC3C test, repairs were effected in Frame E (Figure 3.2 - 4th repair). The primary bracing in Frame A where member failures occurred in the LC3C test remained from the initial build. Table 5.5 provides a comparison between the initial forces recorded with the DEMEC system and subsequent changes recorded by the logger from switch on of the system to start of the LC3C test, with the forces measured during the cutout. In addition check readings from the DEMECs taken just prior to LC3C trial and subsequent instrumentation changes to the start of the test are shown. Some caution is needed in interpreting these, as discussed below.

Comparing first the two 'accumulated' force calculations a consistent shift between the results can be seen. However it is known that the reference sample was replaced after the original fabrication⁽⁷⁾ and the initial and pre-LC3C DEMEC readings used different samples. Comparison of datum values from the two reference samples in Reference 9, indicates a correction of some 30 N/mm² is required in the latter case. On this basis the two sets of readings would correspond (ie. Table 5.5 Column 4 compared with Column 7 values plus 30 N/mm²). However comparing the first accumulated readings (which do not need correction) from the fourth column with the forces determined from the cut out, further differences remain. In particular the cut out suggests Braces 49 and 51 were in a state of pre-compression at the start of the test.

Considerable effort has been expended to resolve the discrepancy but no explanation can be found. Investigations have confirmed that:

- the readings provide a meaningful pattern of initial stresses
- the incremental forces indicated by the instrumentation are balanced, and the changes with each previous test and repair are small and understandable in light of the specific activity
- the performance of the instrumentation in the LC3C test itself was satisfactory with no jumps in the recording and was satisfactory in subsequent tests.

At this stage the cut out forces are carried forward for use in the interpretation of the LC3C results, consistent with the approach in other tests.

Table 5.6 shows the separation of locked-in fabrication and gravitational elements using Table 3.1.

Table 5.5 Comparison of initial forces from key members in the LC3C test (kN)

Member	Force accumulated (kN)						Force released LC3 test start - LC3C cut [3]
	DEMEC C636\21\017W-E Initial	Instrumentation LC3C test start - switch on [1]	Total	DEMEC C636\21\017W-E Pre LC3C	Instrumentation LC3C test start - LC3C trial start [2]	Total	
49	-10.1	33.7	23.6	-9.2	5.0	-4.2	-41.1
50	105.7	-19.4	86.3	60.4	-14.8	45.6	53.6
51	-9.2	40.7	31.5	-10.1	5.1	-5.0	-47.8
52	112.4	-19.6	92.8	67.1	-14.4	52.7	45.0
<i>average</i>			<i>58.6</i>			<i>22.3</i>	
57	80.5	23.0	103.5	81.4	-14.4	67.0	65.5
58	41.1	12.2	53.3	16.8	4.6	21.4	19.6
59	86.4	19.2	105.6	83.0	-16.6	66.4	79.0
60	31.9	14.8	46.7	0.8	4.8	5.6	24.9
<i>average</i>			<i>77.3</i>			<i>40.1</i>	<i>47.3</i>

Notes:

- [1] Instrumentation change from completion of initial fabrication to start of LC3C test (AVT file LC3Ca-test.xls Scan 1 and LC1a-trial.xls Scan 0)
- [2] Instrumentation change from start of LC3C trial to start of LC3C test (Scan 1 from AVT files LC3C-test.xls and LC3Ca-trial)
- [3] Instrumentation change from start of LC3C test to completion of the cut out (Scans 1 and 265 from LC3Ca-cut.xls)

Table 5.6 Locked-in fabrication forces in critical LC3C components (kN)

Member	Initial force from cutout (Table 5.5) a	LC3C gravity (Table 3.1) b	Locked-in fabrication force (kN)	
			a - b	average
49	-41	-2	-39	-42
50	54	3	51	47
51	-48	-2	-46	-42
52	45	3	42	47
57	66	0	66	72
58	20	4	16	18
59	79	0	79	72
60	25	4	21	18

5.6 5TH REPAIR - LC3 TEST

Figure 3.2 shows that the X bracing in Level 1 and the top bays of Frame A was newly fabricated prior to the LC3 test. Critical components failing in the test were in Frame A, Frame B (top bays), Level 1 and Frame C (Brace 61). From the listing of members cut at the end of the test, it can be seen that the initial state of stress can be inferred from a combination of accumulated forces based on the DEMEC system and direct measurements of the cut out force. Table 5.7 summarises the results.

The correlation between the two systems is extremely good particularly for the new members following the 5th repair. Using the initial DEMEC measurements and sequence of instrumentation changes through the test gives a similar initial force level and pattern when compared with the cut out forces, but, as the averages for Frame A show, appear to be overstating the force level by some 20 kN (tension). Although the potential for problems associated with the initial DEMEC readings and long term functioning of the instrumentation system have been investigated, there appears to be no obvious cause and checks confirm to the contrary that the systems have continued to function well. In general, reliance will be placed on the cut out forces but for the X bracing in Frame B, where such data are not available, the potential that the locked-in fabrication stresses are overstated by 20kN will be considered in the LC3 results interpretation⁽¹⁰⁾.

Finally locked-in fabrication force and gravity contributions to the initial forces at the start of LC3 are separated out in Table 5.8.

Table 5.7 Comparison of initial forces for key members in LC3 test

Member	Stage of fabrication	Force accumulated (kN)			Force released (kN) Instrumentation [2] LC3 start - cut
		DEMEC C636\21\017W-E	Instrumentation to start of LC3 test [1]	Total	
19	Initial build	95.6	-11.0	84.6	n/a
20	Initial build	82.2	-4.4	77.8	n/a
21	Initial build	105.7	-14.8	90.9	n/a
22	Initial build	60.4	-2.2	58.2	n/a
27	Initial build	-	-84.5	-	n/a
28	Initial build	69.6	-2.8	66.8	n/a
29	Initial build	125.0	-65.3	59.7	n/a
30	Initial build	28.5	12.1	40.6	n/a
45	Initial build	155.2	-137.6	17.6	-3.8
46	Initial build	138.4	-78.5	59.9	19.8
47	Initial build	151.8	-110.3	41.5	-10.3
48	Initial build	126.7	-107.7	19.0	10.6
			<i>Average</i>	34.5	16.3
49	5th repair	168.3	9.1	177.4	165.7
50	5th repair	132.3	21.0	153.3	182.9
51	5th repair	167.5	7.7	175.2	162.1
52	5th repair	140.7	42.0	182.7	181.7
			<i>Average</i>	172.2	173.1
53	Initial build	21.8	65.6	87.4	31.2
54	Initial build	152.7	-79.3	73.4	56.1
55	Initial build	15.1	39.8	54.9	37.0
56	Initial build	146.8	-66.1	80.7	64.6
			<i>Average</i>	74.1	47.2
57	5th repair	115.5	6.2	121.7	108.8
58	5th repair	47.7	1.7	49.4	53.7
59	5th repair	113.0	5.5	118.5	110.6
60	5th repair	45.2	1.6	46.8	51.2
			<i>Average</i>	84.1	81.1
61	2nd repair	-	-	-	-6.2
98	5th repair	148.5	1.0	149.5	189.5
99	5th repair	140.1	-0.5	139.6	156.5
100	5th repair	197.1	-1.7	195.4	194.2
101	5th repair	136.7	2.6	139.3	134.7

Notes:

[1] Instrumentation change from completion of repair indicated to start of LC3 test (AVT file LC3a-test.xls Scan 1)
Reference files: 5th repair LC3a-trial Scan 1, Initial build LC1a-trial Scan 0

[2] Instrumentation data from AVT files: LC3a-cut.xls except for 98-101 - released force calculated from LC1CA cut and change in instrumentation from start of LC3 test (LC3a-test.xls Scan 1) to start of LC3CA test (LC3Cab-test.xls Scan 1)

Member	LC3CA test start - LC1CA cut out	LC3C test start - LC3CA test start	Total
98	99.5	90.0	189.5
99	90.5	66.0	156.5
100	110.7	83.5	194.2
101	67.0	67.7	134.7

Table 5.8 Locked-in fabrication forces in critical LC3 components at start of LC3 test (kN)

Member	Initial force from cut out uno (Table 5.7) a	LC3 gravity (Table 3.1) b	Locked-in fabrication force (kN) LC3 start	
			a - b	Average
19 [1]	85	5	80	83
20 [1]	78	-10	88	78
21 [1]	91	5	86	83
22 [1]	58	-10	68	78
27 [1]	-	-5	-	65
28 [1]	67	1	66	53
29 [1]	60	-5	65	65
30 [1]	41	1	40	53
45	-4	-9	5	2
46	20	3	17	13
47	-10	-9	-1	2
48	11	3	8	13
49	166	-2	168	166
50	183	3	180	180
51	162	-2	164	166
52	182	3	179	180
53	31	3	28	31
54	56	-7	63	68
55	37	3	34	31
56	65	-7	72	68
57	109	0	109	110
58	54	4	50	48
59	111	0	111	110
60	51	4	47	48
61	-6	-73	67	67
98	190	15	175	177
99	157	-10	167	156
100	194	16	178	177
101	135	-11	146	156

Note:
[1] Force accumulation from initial build - too positive by 20 kN?

5.7 6TH REPAIR - LC3CA AND LC1CA TESTS

Following completion of the LC3 test extensive repairs were undertaken for the test frame as shown in Figure 3.2. Tests LC3CA and LC1CA proceeded with the actuator first on Frame A (see Figure 3.1(c)) then repositioned on Frame C (see Figure 3.1(a)). DEMEC readings were taken for all members replaced in the 6th repair; in addition cuts were made to determine the locked-in forces released on completion of the final test. These are used to determine the locked-in fabrication forces present in the frame for the two tests; the gravitational component of the initial forces is different in the two tests because of the repositioning of the actuator (see Table 3.1). The actuator datum was reset for the LC1CA test so no offset is required as in the earlier LC1 and LC1C tests.

Table 5.9 provides a comparison between the accumulated forces calculated from the DEMEC readings and subsequent changes between completion of fabrication and start of the LC3CA test, with the corresponding forces determined from the instrumentation at the LC1CA cut out.

The agreement is generally good and the pattern of high / low tensile / compressive forces is confirmed by the two systems.

The DEMEC readings come from different stages of the programme as shown therefore for consistency reference is made to the cut out readings from the instrumentation as a basis for determining locked-in fabrication forces.

Although the Frame B top bay X joints were loaded beyond their elastic limit in the LC3 test they were not replaced prior to the LC3CA test. The joints were again loaded into the nonlinear regime in this test; the initial loads can be determined from the condition shown in Table 5.7 plus changes in the recorded loads from the instrumentation between the start of the two tests. These are summarised in Table 5.10.

Table 5.11 subtracts the gravity forces (see Table 3.1) from the total force in the members at the start of the LC3CA test to give the component of locked-in fabrication force.

When interpreting the responses in LC1CA the new position of the actuator needs to be taken into account. The alternative pattern of gravitational forces is also shown in the table.

Table 5.9 Comparison of LC3CA initial forces for key members in LC3CA and LC1CA tests (kN)

Member	Stage of fabrication	Cut after LC1CA?	Force accumulation (kN)			Force released (kN) Instrumentation [2] LC3CA start - LC1CA cut
			DEMEC C636\21\017W-E	Instrumentation to start of LC3CA test [1]	Total	
45	6th repair		128.1	-0.9	127.2	135.9
46	6th repair	*	72.8	-0.9	71.9	38.1
47	6th repair	*	125.6	-0.8	124.8	131.7
48	6th repair		76.2	-1.0	75.2	52.6
49	6th repair		115.5	-1.2	114.3	119.0
50	6th repair	*	180.0	-2.2	177.8	153.2
51	6th repair	*	105.5	0.9	106.4	119.5
52	6th repair		180.9	-2.1	178.8	146.5
53	6th repair		116.4	0.1	116.5	113.7
54	6th repair	*	150.7	-2.1	148.6	173.1
55	6th repair	*	115.5	-0.1	115.4	116.0
56	6th repair		154.1	- (assume -2.1)	152.0	152.3
57	6th repair	*	93.8	-0.4	93.4	115.9
58	6th repair		7.5	0.2	7.7	10.4
59	6th repair		87.1	-0.7	86.4	100.1
60	6th repair	*	21.8	0.4	22.2	10.3
61	6th repair	*	14.5	-0.7	13.8	6.0
62	2nd repair [3]		-	-	-	-36.6
63	2nd repair	*	-	-	-	-2.0
64	2nd repair [3]		-	-	-	-38.6
69	Initial build	*	26.0	-95.3	-69.3	-94.3
70	Initial build [3]		-40.3	118.0	77.7	22.6
71	Initial build	*	61.2	-91.6	-30.4	-74.5
72	1st repair [3]		52.0	31.4	83.4	-50.3
98	5th repair	*	148.5	-98.5	50.0	90.0
99	5th repair		140.1	-91.0	49.1	66.0
100	5th repair		197.1	-112.4	84.7	83.5
101	5th repair	*	136.7	-64.4	72.3	67.7

Notes:

[1] Instrumentation change from completion of repair indicated to start of LC3CA test (AVT file: LC3CA-test Scan 1). Release files: 6th repair: LC3CAB-trial Scan 1
5th repair: LC3a-trial Scan 1
1st repair: LC1Ca-trial Scan 1
Initial build: LC1a-trial Scan 0

[2] Load cell data from AVT files: LC1CAB-cut.xls Scan 174 compared with LC3CAB-test.xls Scan 1

[3] Comparison not valid - although other primary K brace is cut, out-of-plane braces/leg/horizontal maintain some constraint - problem particularly for braces 70 and 72 which buckled in LC1CA test.

Table 5.10 Initial forces in Frame B X bracing at start of LC3CA test (kN)

Member	Force accumulation (kN)		Total
	At start of LC3 test (Table 5.7) [1]	Instrumentation Start of LC3CA test - start of LC3 test [2]	
19	84.6	4.5	89.1
20	77.8	8.1	85.9
21	90.9	22.0	112.9
22	58.2	-9.0	49.2
27	-	13.6	-
28	66.8	28.1	94.9
29	59.7	35.7	95.4
30	40.6	29.1	69.7

Note:
 [1] Force accumulation from initial build - too positive by 20kN?
 [2] Instrumentation change from start of LC3CA test to start of LC3 test.
 AVT files LC3CAB-test.xls Scan 1 and LC3a-test.xls

Table 5.11 Locked-in fabrication forces in critical LC3CA / LC1CA components at start of LC3CA test (kN)

Member	Initial force from cut out uno (Tables 5.10 & 5.11) a	LC3CA gravity (Table 3.1) b	Locked-in fabrication force (kN) LC3CA start		LC1CA gravity (Table 3.1)
			a - b	Average	
19 [1]	89	5	84	96	3
20 [1]	86	-10	96	78	-2
21 [1]	113	5	108	96	3
22 [1]	49	-10	59	78	-2
27 [1]	-	-5	-	100	-9
28 [1]	95	1	94	81	8
29 [1]	95	-5	100	100	-9
30 [1]	70	1	69	81	8
45	136	-9	145	143	4
46	38	3	35	43	-9
47	132	-9	141	143	4
48	53	3	50	43	-9
49	119	-2	121	121	4
50	153	3	150	146	-4
51	120	-2	122	121	4
52	147	3	144	146	-4
53	114	3	111	112	13
54	173	-7	180	170	-15
55	116	3	113	112	13
56	152	-7	159	170	-15
57	116	0	116	108	4
58	10	4	6	6	0
59	100	0	100	108	4
60	10	4	6	6	0
61	6	-73	79	n/a	-76
63	-2	-47	45	n/a	-53
69	-94	-43	-51	n/a	-45
71	-75	-30	-45	n/a	-34
98	90	15	75	72	-
99	66	-10	76	78	-
100	84	16	68	72	-
101	68	-11	79	78	-

Note: [1] Force accumulation from initial build - too positive by 20kN?

5.8 SUMMARY

Based on the foregoing evaluations, Table 5.12 summarises the averaged locked-in fabrication forces in critical components at the start of each frame test. Gravitational forces act in addition to the fabrication forces when the applied load is at the zero datum; these value are given in Table 3.1. It is important to note that where no locked-in fabrication forces are given the values are not zero. The table only presents selected values relevant to the interpretation of the failure sequence observed in the tests.

Table 5.12 Summary of locked-in fabrication forces at the start of each test for key members

Member	Locked-in fabrication force (kN) at start of test						
	LC1	LC1C	LC2	LC2C	LC3C	LC3	LC3CA [2]
Frame B [1]							
Top CD 19						83	96
20						78	78
21						83	96
22						78	78
Top DE 27						65	100
28						53	81
29						65	100
30						53	81
Frame A							
Btm CD 45						2	143
46						13	43
47						2	143
48						13	43
Top CD 49					-42	166	121
50					47	180	146
51					-42	166	121
52					47	180	146
Btm DE 53						31	112
54						68	170
55						31	112
56						68	170
Top DE 57					72	110	108
58					18	48	6
59					72	110	108
60					18	48	6

Member	Locked-in fabrication force (kN) at start of test						
	LC1	LC1C	LC2	LC2C	LC3C	LC3	LC3CA [2]
Frame C							
Btm 61	-5	-				67	79
62	54	-					
Top 63	-25	-					45
64	40	-					
Frame D							
Btm 69	42						-51
70	-60						
Top 71	58						-45
72	-38						-
Frame E							
Btm 77			-33				
78			-54				
79			-33				
80			-54				
Top 81			64	166			
82			83	34			
83			64	166			
84			83	34			
Level 1							
X 98						177	72
99						156	78
10						177	72
0						156	78
10							
1							
Notes:							
[1] Force accumulation from initial build - too positive by 20kN?							
[2] No repairs between LC3CA and LC1CA tests - LC1CA interpretation is with respect to datum at start of LC3CA test							
- Data not available							



6. CONCLUSIONS AND RECOMMENDATIONS

The measurement schemes adopted during the initial build and subsequent repairs of the 3D test structure have provided sound information on the level of forces locked-in to the members as a result of shrinkage and deformations during fabrication. The DEMEC and electric resistance systems have provided a means to cross-check the results. Specific values have been extracted for those key components within the frame which play a part in subsequent failure sequences; these are tabulated in Table 5.12. In addition to the fabrication forces, self-weight gravitational loads are also present when the structure is in the datum position prior to the application of external actuator loads in each test; the gravity components are presented in Table 3.1.

The pattern of fabrication forces can be understood in terms of the sequence of fabrication, ie. tensile forces are present in members installed when the surrounding structure is well braced and conversely compressive forces are measured in the first installed bracing. Equilibrium checks confirm the validity of the forces; opposite pairs of braces within an X bay carry similar force levels; in K braces the forces are generally equal and opposite.

The magnitude of the forces is considerable, reaching as much as 30% of the nominal axial tensile capacity of some members. Depending on the sense of applied loads these may act to increase or decrease the apparent resistance of components. As a proportion of component capacity the relative effects may be even greater if joints along the loadpath have no cans and are therefore weaker than the members.

The principal conclusions for the Frames Project are that:

- the locked-in forces reached in the test frames must be taken into account when interpreting the measured capacities of components under applied loads
- the potential influence of these locked-in forces must be recognised in the comparison of benchmark analysts' predictions to the test frame responses.

More generally when considering the conduct of ultimate strength analyses of jacket structures, the potential influence of locked-in fabrication forces must be considered. Their magnitude and sense will never be known but some degree of sensitivity study may be appropriate to ensure that deterministic response predictions are valid.

7. REFERENCES

1. 'Joint Industry Tubular Frames Project - Phase I', Nine volume report, SCI Reference SCI-RT-042, 1990.
2. BOMEL Limited. 'Joint Industry Tubular Frames Project - Phase II', Nine volume report, BOMEL Reference C556R003.50 to .58, 1992.
3. Bolt, H M and Smith, J K. 'The influence of locked-in fabrication stresses on structural performance', Offshore Mechanics and Arctic Engineering Conference, Copenhagen, 1995.
4. BOMEL Limited. 'Joint Industry Tubular Frames Project - Phase III - Test Frame Instrumentation', BOMEL Document No. C636\25\071R, Rev O, June 1999.
5. Mayes Instruments Limited. DEMEC Calibration Certificate No 79672. BOMEL Incoming Document 8461, File C636\21, December 1997.
6. BOMEL Limited. 'Joint Industry Tubular Frames Project - Phase III - Material Testing report', BOMEL Document No. C636\23\004R, Rev B, April 1999.
7. AKD Engineering Limited. 'Test specimen documentation package', AKD Reference 4065/4413-2/4570, BOMEL Incoming Document 11900, File C636\31, November 1998.
8. BOMEL Limited. 'Reduction of DEMEC readings', BOMEL Document No. C636\21\017W-E.xls, May 1999.
9. BOMEL Limited. 'Evaluation of locked-in stress measurements - calculations', BOMEL Document No. C636\21\054W, May 1999.
10. BOMEL Limited. 'Loadcase 3 test report - Multiple member failures and 3D system action', BOMEL Document No. C636\40\021R, Rev O, August 1999.

APPENDIX A

**THE INFLUENCE OF LOCKED-IN FABRICATION STRESSES
ON STRUCTURAL PERFORMANCE
- EVIDENCE FROM FRAMES PROJECT PHASES I AND II**

Reference 3 (11 Pages)

THE INFLUENCE OF LOCKED-IN FABRICATION STRESSES ON STRUCTURAL PERFORMANCE

Helen M Bolt
Billington Osborne-Moss Engineering Limited
Maidenhead, Berkshire
UK

J K Smith
Amoco (UK) Exploration Company
London
UK

ABSTRACT

The potential influence of locked-in fabrication stresses on the ultimate response of structural frames is investigated. Whilst local shrinkage at welded connections has been quantified to some extent in the past, the effect on the capacity of structural components and frames has not been illustrated. The investigation reported here was prompted by the results from some large scale ultimate load tests of tubular frames. Some of the components within these frames failed at loads significantly different from values predicted simply on the basis of geometry and yield stress. The discrepancies between measured and predicted capacities were attributed to locked-in fabrication stresses which are an inherent feature of the welded construction of redundant frames. This conclusion was reached on the basis of detailed measurements during the fabrication of subsequent specimens.

The paper demonstrates the influence of locked-in stresses on the test frames and discusses the potential significance for the prediction of the ultimate response of jacket structures with reference to previous findings in the open literature. A principal difficulty is to quantify the influences of scale in the test frames as welds cool and shrink, compared with full scale jacket construction. To elucidate this a unique set of measurements of the locked-in strains accumulating during the fabrication of an Amoco structure were taken. A mechanical system of strain measurement was used and this and alternative approaches are evaluated.

Based on the findings, it is recommended that future frame testing projects include thorough measurements of fabrication stresses to ensure that results are properly interpreted. Furthermore, it may be appropriate to include sensitivity studies (encompassing locked-in fabrication stresses and other realistic factors) in the assessment of the ultimate strength of a jacket structure.

INTRODUCTION AND BACKGROUND

As a welded joint cools, its contraction is resisted in all directions by the surrounding cooler material generating a stress field in the structure with equilibrating zones of tension and compression. Local to the weld the residual stress distribution reaches the yield value and becomes very important in the fracture mechanics assessment of flaws. If the shrinkage is resisted by the surrounding structure, the long-range stresses can generate net forces in the members. It is the latter case with which this study is concerned.

The complexity of the stress distribution and the broad umbrella of a working stress safety factor means that to date their influence has been largely ignored in structural analysis. In a limit state scenario, and particularly where a mean representation of behaviour is required for assessment purposes (as in the new API RP2A Section 17.0), the significance of these locked-in stresses and other inherent imperfections needs to be quantified.

Treatment of locked-in stresses in the open literature is not extensive. Nevertheless, the phenomenon is well known to welders on fabrication sites. In preparing the members for fit-up the distortion must be accounted for to ensure that the sequence of welds can be performed satisfactorily. Of course it is the shrinkage from the closing welds which results in locked-in fabrication strains along the members.

Reference 1 by White, Dwight and Leggatt and the background material assimilated in the paper, constitutes the principal source of information on locked-in fabrication stresses revealed in a literature search as part of the present study. The work is described in some detail to demonstrate the build-up of locked-in stresses due to weld shrinkage but the shortcomings of the proposed calculation method in practical application are also highlighted.

Potential significance of locked-in stresses

Ultimate strength (pushover) analyses are being performed increasingly to demonstrate the ability of a platform to withstand extreme events without catastrophic collapse. Nonlinear analysis programs such as the Frames Project software SAFJAC (4) are used to predict the ultimate response. Detailed or accurate information about all aspects of system loading and resistance is generally not available and the need to perform sensitivity analyses is being recognised increasingly (6). In some structures instability in one weak load path may dominate the response (7). As a result, imperfections, such as locked-in stresses, which affect the capacity of the critical component can have a direct influence on the system capacity (3). In others the redundancy may ensure that parallel load paths are evenly utilised such that, although the precise sequence of local failures leading to structural collapse may be sensitive to perturbations in the system properties (6), the ultimate collapse load may not.

If confidence is to be placed in reserve strength predictions (eg. to form part of an inspection scheduling prioritisation), it is important to ensure that the range of possible responses is established, reflecting the probable range of system parameters. The Frames Project findings indicated that locked-in fabrication stresses could be important. Furthermore because their influence could be detrimental or beneficial in terms of component capacities, it cannot be concluded that it is conservative to ignore locked-in prestress. It was recognised that geometric scale differentiated the frame test specimens and jacket structures. However, no method for calculating the relative effects of weld shrinkage or cooling appeared to be readily available.

Given the potential implications for practice in terms of the confidence that can be placed in pushover analysis predictions and the need for sensitivity analyses, the build-up of locked-in fabrication stresses was investigated further with full-scale measurements in the course of fabricating Amoco's Lomond jacket structure. In this paper the Frames Project results are discussed in the context of the literature review, the selected measurement system is described and the full scale results are presented.

FRAMES PROJECT FINDINGS

The Joint Industry Tubular Frames Project was established to examine the reserve and residual strength of jacket structures through a series of ultimate load tests on first two-dimensional and now three-dimensional frames (4, 5). The project is being undertaken by Billington Osborne-Moss Engineering Limited (BOMEL) and Amoco (UK) Exploration Company (Amoco) is one of the Participants. Both member and joint collapses have been investigated, and the tests have afforded new insight into the ultimate response of frames.

However, in some instances the apparent capacities of components within the 2D frames were significantly different from predicted values. Subsequent investigations, including detailed measurements, revealed that the differences were largely attributable to locked-in pre-stress in the brace members arising in the course of fabrication. The potential influence of locked-in stresses can be illustrated with examples from the Frames Project test programme.

Frame geometry and fabrication

The X-braced frames tested in Phase I of the Frames Project are shown in Figure 2. In non-dimensionalised terms the member properties were representative of offshore jacket structures. The specimens were fabricated in accordance with standard procedures and were not stress relieved. The sequence was generally for the legs to be welded first between the top and bottom beams. The horizontals and stub diagonals to the beams were then introduced before the primary diagonals were fully welded. The exact sequence varied from frame to frame, but generally the surrounding frame was stiff at the stage the primary braces were welded.

Frame I - Phase I

Figure 3 shows the variation of axial loads in the top bay bracing in Frame I, in response to a lateral load applied at the top of the frame. It can be seen that a yield plateau was reached in the tension member before the rapid fall off in load associated with compression buckling. Given the slenderness of the members this result was unexpected but could be explained by a small pre-tension in the bracing which would increase the external load necessary to precipitate buckling and reduce the applied load to give tensile yield. The sensitivity of the failure sequence to small initial loads can be seen. Unfortunately the build up of fabrication stresses was not recorded in Phase I of the Frames Project and so the above explanation, although probable based on later findings, could not be concluded categorically.

Frame III - Phase I

A more extreme discrepancy between idealised analysis and tests is shown in Figure 4 for Frame III. Frame III was identical to Frame I, except for the omission of the mid-height horizontal. In contrast to Frame I, the compression brace buckled very much earlier than predicted and the tensile capacity was apparently much higher. However, once the externally applied loads precipitated instability, the frame capacity was limited. The remaining capacity in alternative loadpaths (the tension chord in this simple framed structure) was unable to compensate for the post-buckling load shedding from the brace. The explanation for the presence of such significant pre-compression in the specimen can be found in the fabrication sequence.

The sequence was generally as noted above, but the fabricator was concerned that without the mid-height horizontal the shrinkage associated with welding the primary bracing might bow the legs inwards and the fabricated structure would be outwith the specification. Accordingly mechanical restraints were applied to the legs, drawing the legs outwards at mid-height to compensate for any subsequent shrinkage. After welding was complete the mechanical restraint was released and it would appear that the legs sprang back, introducing significant initial pre-compression in the braces.

The comparison between Frames I and III shows the influence that mechanical intervention to improve fit-up and the stiffness of the surrounding structure can have on the build-up of locked-in fabrication stresses.

MEASUREMENT OF LOCKED-IN STRAINS

System selection

The principal objective of the full-scale measurements was to indicate the level of locked-in stresses arising in jacket fabrication. The study was made possible by the kind permission of Amoco (UK) Exploration Company and Highlands Fabricators Limited (HiFab), who gave BOMEL access to the HiFab site from October 1991 to June 1992 as the Lomond Jacket was built for Amoco's CATS, Central Area Transmission System (Figure 5). The premise in being given access was that the fabrication should not be impeded. In choosing a measurement system full consideration had to be given to an unobtrusive but 'permanent' datum system, the ability to take rapid measurements, equipment portability in view of limited access, the changing temperatures and exposed environment, as well as the accuracy required for meaningful results to be obtained.

Three measurement systems were evaluated on the basis of the above:

- Electric resistance strain gauges - although conventionally used in structural testing, rejected because of the long term instability of gauges or malfunction and the need for permanent cabling.
- Spot welded vibrating wire gauges - although waterproof and offering long term stability, rejected because of the capital cost of equipment and specialist services.
- The Demec system - recommended on the basis of its practicality, unobtrusiveness and environmental tolerance and based on satisfactory performance in the Frames Project tests where accuracy was confirmed in comparison with strain gauged load cells.

The Demec strain measurement system

The Demec system was developed by W H Mayes and Sons of Windsor, and is now used widely throughout the civil engineering industry. It comprises a mechanical strain gauge with one fixed point and one moveable measuring point at the gauge end. Changes in this gauge length are transmitted through a pivot to the measuring dial gauge, Figure 6. The ratio between real movement and the measurement on the dial gauge is calibrated and converted to strain. Gauges from 50mm to 2000mm are available and are selected depending on the magnitude of strains to be measured and the accuracy required.

A 250mm gauge length was adopted in this work. This was practical for use on site and gave sufficient resolution. The length over which measurements are to be taken can be defined by adhering proprietary pips with a drilled hole to the structure (Figure 7), or alternatively by drilling a 1mm by 1.5mm hole directly into the member.

It should be noted that a very similar system for measuring locked-in strains was adopted in Reference 2.

FULL SCALE MEASUREMENTS

The Lomond jacket is shown in Figure 5. The structure is X-braced with X framing in plan, without midheight horizontals in the face frames.

The frames comprise four X-braced bays with the top three bays and associated legs fabricated initially and the lower bay

constructed in the final stages. The lower bay legs are pre-fabricated as a unit along with the pile guides.

The four face frames are referred to as Frames A, B, 1 and 2. Frames 2 and 1 were fabricated first and in that order. Each of the X-braces was made up from a through member and two shorter members welded at the centre to form the X-brace. For each of the Frames 2 and 1, three X-braces were placed in position and subsequently welded to the legs. These are Stages 1 and 2 respectively in the fabrication process as outlined in Figure 8. Stages 3 and 4 involved welding the Frame A and B X-braces to Frames 1 and 2, respectively. The plan braces which house the conductor guides were also welded to Frame 2 at this stage. Stage 5 followed during which the structure was welded in the rolled-up position and finally, at Stage 6, the jacket lower bays were introduced.

Datum readings

Initial marking of members was necessary before they were used in the construction of any frames. Close liaison with HiFab was necessary to ensure that datum readings could be taken as required after the plate became identifiable as a tubular member but before it was welded into a frame.

It was clear from the fabrication plan (Figure 8) that although access to the full length of the diagonal bracing would be afforded for Frames 1 and 2 during early stages of fabrication, once the jacket roll-up commenced access would be extremely limited. Platforms were erected around each node to enable the welds to be as close to the intersections as possible without being directly influenced by residual strains local to the weld. For this reason a minimum offset of a half brace diameter was stipulated for the closest measurement point from the intersection ($0.5d \sim 500\text{mm}$). However, establishing the in-plane datums for the acute side of the member beyond $0.5d$, set the orthogonal measurement position more than $1.5d$ (1.5m) away from the intersection for the 45° brace angles.

Site observations

Many site visits each lasting several days were made by the BOMEL team. This ensured that datum readings could be established and retaken as the individual plane frames were completed and welded together to illustrate the 2D and 3D redistribution of the stresses as the restraints changed.

Work progressed on parallel fronts depending on other yard activity and the availability of welders. The chronological sequence of weld completion was noted but weld passes were laid in several tranches. Therefore the n th completed intersection may not have been free at the time the $n-4$ th was completed - root and subsequent passes may already have offered restraint. Furthermore where shrinkage is due to wrap up effects as well as transverse effects, the distribution will depend on the start and stop locations of the weld. This circumferential variation may only even out gradually along the member away from the intersection.

Example calculations, based on Roark (8) for a free cylinder with an applied end moment, indicate that the moment would dissipate over a 200mm length for a representative 1000mm OD

10N/mm² may be taken to indicate reasonable agreement. Furthermore it indicates that the member end measurement strategy was valid and that the level of stresses indicated in the tables and figure are representative of the distribution in the structure.

For plan members at the lowest level, the stresses were alternately tensile and compressive and were at around 4% of yield on jacket completion. Had these welds been laid fast, it might have been expected that large tensile forces would have been generated given the greater stiffness of the surrounding structure. However it can be seen from Figure 8 that Frames 2 and B had not been connected at the time the plan bracing welds were completed. Hence the moderate level of stresses in these members can be understood.

DISCUSSION

Volumetric changes or distortion of components in the course of assembling a redundant structure will result in residual forces being locked-in to the structure once the governing influences (eg. changes in ambient temperature) reverse. Some of fabrication which can have this effect on jacket structures are:

- Mechanical handling and alignment (fit up) forces
- Preheat prior to welding
- Weld shrinkage related to welding procedure (rate of heat input, root gap, etc)
- Fabrication sequence
- Relative component stiffnesses and support conditions
- Ambient temperature

Each factor and the variation it may induce, is discussed in detail in the final project report (9) on the basis of which this aggregate view is assimilated.

The picture of the development of locked-in stresses is complicated by the number of factors involved. The measurements in this study have encompassed them all as they 'naturally' occur in practice. The findings indicate that the various influences can, and do, counteract each other such that both tensile and compressive stresses are generated. Furthermore where possible, the effects have been quantified and in all cases these have confirmed the finding that the Lomond jacket experienced a somewhat lower level of stress than the test frames.

The effects of scale

The scale of the structure is influential on the level of locked-in stresses developed. For the test frames the bay width was 6m and the minimum brace to leg root gap was 3mm. For the Lomond jacket the span was 25m but the minimum root gap was set in the range 3 to 6mm.

The extent of the gap in relation to the length along which shrinkage strains are to be distributed is quite different. The absolute magnitude of the weld area in relation to electrode size affects the accumulation of shrinkage with each pass, so that at large scale a more significant locked-in stress gradient may be generated through the thickness from resisting wrap-up.

Furthermore, 'scale' affects the approach to fabrication and the resulting control over locked-in stress development. Simultaneous welding is an inevitable aspect of jacket fabrication. The outdoor site also means that changes in the weather, leeward versus

windward sides of the structure, direct sunshine, etc., may contribute more significantly to in-built stresses arising during fabrication.

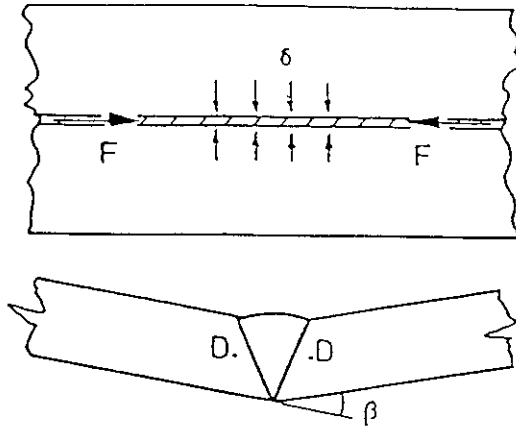
Influences on ultimate response

Just as locked-in fabrication stresses influenced the mode and sequence of component failures in the Frames Project test frames, so too could the ultimate response of jacket structures be influenced. Although the measurements for the Lomond jacket indicated that the average level of pre-stress in the jacket was low and within $\pm 5\%$ of yield, in some members average values as great as 12% of yield were found. These values were a function of the structure configuration and proportions, and the specific sequence of fabrication. A structure with horizontal and diagonal bracing in the same plane might be expected to have higher levels of locked-in stresses because of the restraint. Nevertheless arguments associated with scale have been presented suggesting that, in general, the stress levels would be unlikely to reach those recorded for the test frames.

It may reasonably be concluded that no radical change should be made to pushover analysis procedures, although the need to perform sensitivity studies is underlined. The influence of locked-in stresses depends on the system redundancy and the mode of component failures. It has been demonstrated that where system capacity is governed by instability, for example member buckling, locked-in stresses may have a direct influence on both component and system capacities. However, where the ultimate response mode is ductile, such that alternative loadpaths can compensate for a premature failure in one component, the self-equilibrating locked-in stresses may have no net effect on system capacity. Even if there is no influence on the ultimate capacity, the sequence of component failures may be altered by locked-in fabrication stresses. In a complex structure with evenly balanced failure modes which each may involve a sequence of component failures, it is possible that the limiting sequence may be altered with a potential influence on system capacity. It is therefore suggested that locked-in prestress should be considered as a factor in sensitivity studies which may already encompass variations in material properties, geometries, loading, etc.

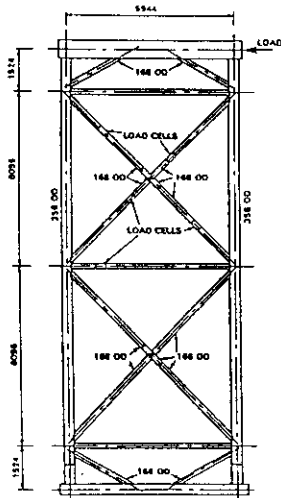
Discrepancies between actual and nominal material yield values can be considerable and may be accounted for in ultimate strength analysis, but generally they offer additional capacity. Furthermore in critical situations for a specific structure, certificates may be traceable for individual members. Locked-in fabrication stresses are different, however, in that they may be tensile or compressive and it is unlikely that fabrication records and the available analytical methods will enable the extent of shrinkage to be calculated with any accuracy. It would therefore be necessary to develop 'worst case' scenarios based on different distributions through the structure. In this way, bounds to the possible failure modes could be developed.

This procedure would not necessarily be followed routinely but for hindcasting analyses or analyses which will determine appropriate inspection, maintenance or repair scheduling, inclusion of locked-in prestresses in sensitivity studies may be appropriate. A suitable approach to such sensitivity studies is presented by the authors in Reference 10.



BASIC SHRINKAGE PARAMETERS F = TENDON FORCE,
 δ = TRANSVERSE SHRINKAGE = DECREASE IN DD, β = WRAP UP

Figure 1 Shrinkage effects at a weld



Frame	Configuration	Objective
I	Horizontal Strong joint can	Member failure
II	Horizontal Weak joint can	Joint failure sequence
III	No horizontal Strong joint can	Role of redundancy
IV	Horizontal Crack at weak joint	Influence of crack on joint

Figure 2 Frames Project Phase I X-braced frames

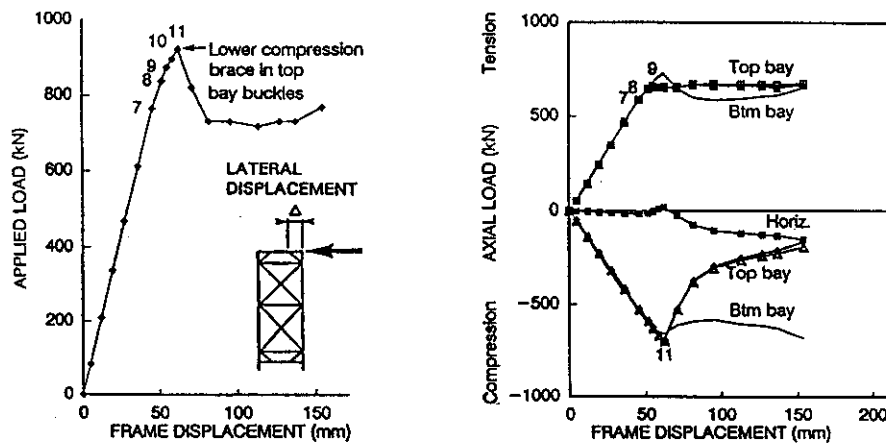


Figure 3 Frame I top bay brace loads through ultimate strength test

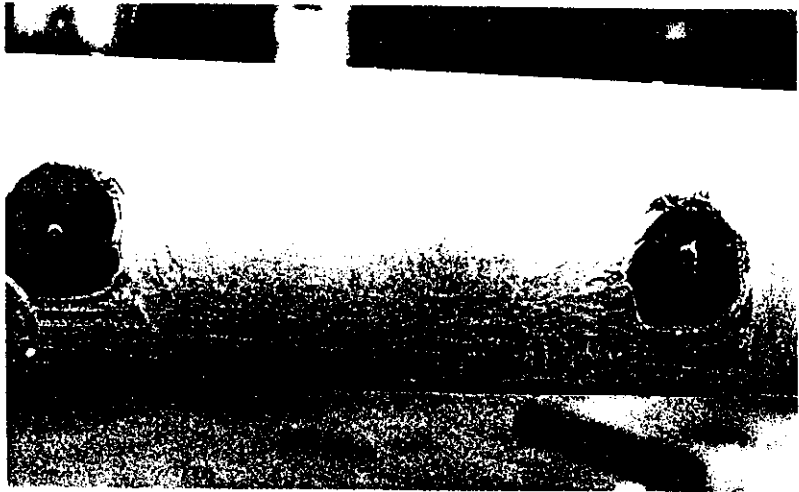


Figure 7 Locating pips for Demec gauge

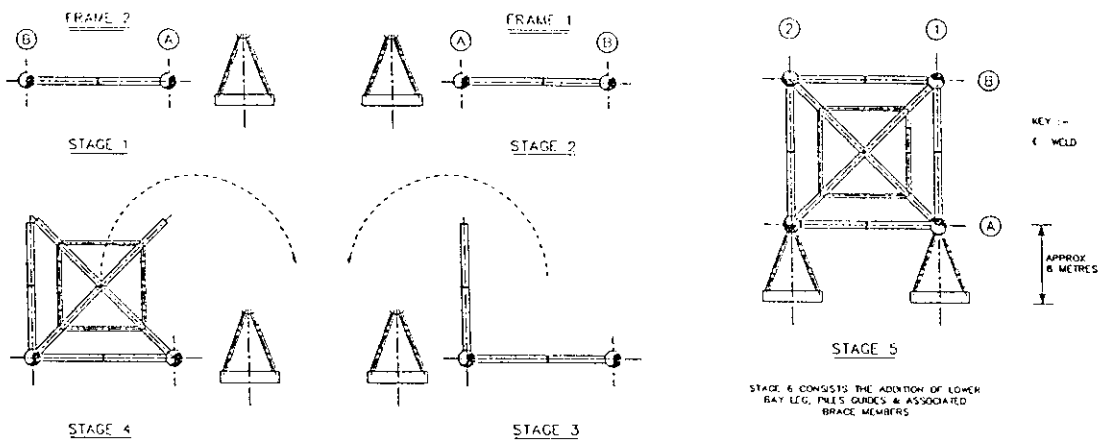


Figure 8 Lomond jacket fabrication sequence

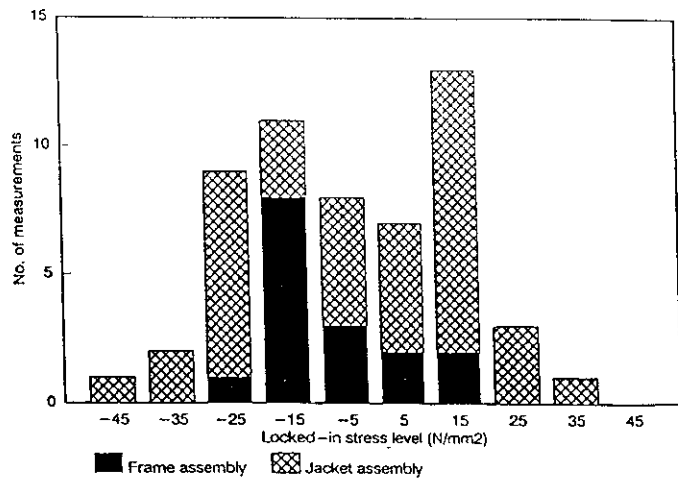


Figure 9 Spread of locked-in stresses at different stages of fabrication

APPENDIX B

THE MAPS STRESS MEASUREMENT SYSTEM



APPENDIX B THE MAPS STRESS MEASUREMENT SYSTEM

THE MAPS MEASUREMENT SYSTEM

The MAPS system was developed by AEA Technology and is described as a non-destructive, readily portable device to measure bi-axial stress.

The device consists of a magnetic probe and is based on the principle that the presence of stress in a material changes its domain structure through the effect known as magnetostriction so that quantities such as magnetic permeability become functions of the total component stress. MAPS can be used on structural steels and a wide range of other ferromagnetic materials. Laboratory and in-field prototype systems have been used by AEA Technology to measure stresses resulting from material processing, fabrication and in-service loading.

The MAPS probe comprises a magnetic yoke to apply an alternating field to the specimen, together with a series of coils to measure inductance and flux linkage from which permeability and anisotropy can be derived. There is also a coil for measuring coercivity in order to guard against material variation, and one for reference measurements and to correct for variations in probe lift-off from the surface. When in use, initialisation measurements are first made to compensate for lift-off and back-off. The probe then rotates through 360° while seven magnetic parameters are measured at discrete intervals. After the measurement is completed, these parameters can be plotted as a function of orientation. This step enables the principal stress axes to be identified, since the anisotropy is zero along the bisectors between the axes. The next step is to derive the three main parameters (presently identified as magnetic anisotropy and permeability components along the principal axes).

Calibration data need to be available. These take the form of calibration maps for the three main magnetic parameters as a function of biaxial tensile and compressive stress. The maps are constructed using a theoretical model linked to measurements on a similar steel during a simple bend test. The model corrects for texture, and compensates for variations in back-off due for instance to microstructure. The analysis program then fits the measured values of the three main parameters to the calibration maps, using a least squares routine (inversion). This procedure delivers the best fit for the absolute magnitude of the two principal stress components (whose directions were deduced previously).

Use of the system has generally been envisaged to define a stress field (for example in a plate) based on a series of MAPS measurements over a grid of points. The experimental data are then inverted to stress values as before, and the resulting matrix of tensor values plotted as a function of position. The variation of stress with depth can also be determined by scanning the magnetic field frequency. This is useful for discriminating surface effects where surface damage is indicated by the presence of high near-surface tensile stress levels.

In the case of the 3D test frame interest is in determining the net axial stress by averaging these corresponding components of stress from readings at diametrically opposed points around the member circumference. AEA Technology technicians conducted selected on-site measurements using the MAPS system as seen in Figure B.1.

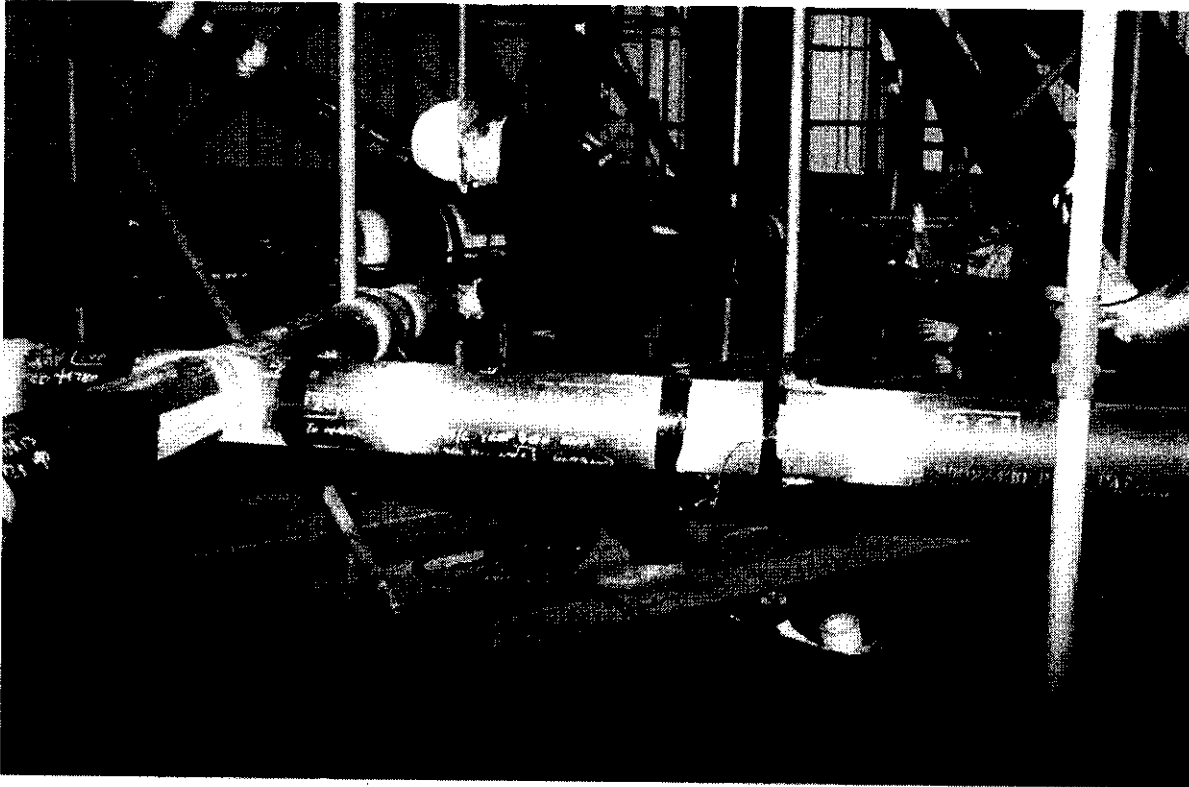


Figure B.1 Use of the AEA Technology MAPS system prior to testing of the 3D frame

Although the direct measurement of stress was attractive, the system proved to be slow to use, cumbersome for use at height and from scaffolding, and demanding in manpower resources to prepare the specimen surfaces, take repeated readings and move equipment. Use of the DEMEC system, as described in the main body of this report, was therefore preferred.

APPENDIX C

SPECIFICATION FOR DEMEC STRAIN GAUGE MEASUREMENTS

BOMEL Specification Reference C636\21\003S, Rev O, November 1997
as implemented by AKD Engineering Limited during the 3D frame fabrication

**JOINT INDUSTRY TUBULAR FRAMES PROJECT
PHASE III**

**SPECIFICATION FOR
DEMEC STRAIN GAUGE MEASUREMENTS**

C636\21\003S REV 0 NOVEMBER 1997

Purpose of Issue	Rev	Date of Issue	Author	Checked	Approved
For quotation	0	November 1997	<i>HMB</i> HMB	<i>JADC</i> JADC	<i>CJB</i> CJB

Controlled Copy		Uncontrolled Copy	
-----------------	--	-------------------	--

BILLINGTON OSBORNE-MOSS ENGINEERING LIMITED

Ledger House
Forest Green Road, Fifield
Maidenhead, Berkshire
SL6 2NR, UK

Telephone + 44 (0) 1628 777707
Fax + 44 (0) 1628 777877

REVISION SHEET

REVISION	DETAILS OF REVISION	DATE
0	First issue for AKD quotation	4.11.97

FILE SHEET

PATH AND FILENAME	DETAILS OF FILE
C636\15\014D	Demec measurement location drawing
C636\21\004U	Appendix A - Templates for the recording of Demec readings
C636\12\048V-A	Appendix B - Member numbering scheme

CONTENTS

		Page No
1	INTRODUCTION	1.1
2	SCOPE OF WORK	2.1
2.1	FAMILIARISATION WITH DEMEC EQUIPMENT AND MEASUREMENT TECHNIQUES	2.1
2.2	SETTING OUT OF DEMEC PIPS AND SUPPLY OF REFERENCE SAMPLES	2.2
2.3	DATUM READINGS	2.3
2.4	FINAL READINGS	2.4
2.5	REPLACEMENT MEMBERS	2.4
3	DOCUMENTATION	3.1
DRAWING	C636\15\014D	
APPENDIX A	TEMPLATES FOR THE RECORDING OF DEMEC READINGS	
APPENDIX B	MEMBER NUMBERING SCHEME FOR USE WITH DEMEC MEASUREMENTS	

1 INTRODUCTION

As part of the Phase III Frames Project, the build-up of locked-in fabrication stresses in the tubular frame are to be measured using the Demec system.

These locked-in stresses arise in the course of fit-up, welding and shrinkage on cooling, and may be either tensile or compressive. The forces can be substantial and may enhance or degrade the apparent response of the structure to applied loads. By measuring the locked-in stresses their effect can be accounted for in the interpretation of the results of the main test programme.

The Demec system has been selected because it is simple to use and involves no permanent instrumentation which might impede fabrication. The system was used successfully by a junior BOMEL engineer in the previous phase of the Frames Project. The Demec system is used to record the change in the separation of two points. The gauge is calibrated so that each division movement equates to a certain value of strain. For this strain, the associated stress is calculated.

Measurement locations need to be set up and datum readings taken for each member within the structure before its fabrication is closed-out. Final readings will be taken once the full fabrication of the 3D frame is complete. The change in the readings will be used to determine the locked-in stresses in the manner described above.

It is important to account for the effects of ambient temperature on the readings and to check for any drift in the gauge readings. This is achieved by taking reference readings from unstressed samples of the same material and using the Invar bar in the Demec set.

This specification concerns the conduct of the Demec readings.

2 SCOPE OF WORK

Principal items in the scope of work are as follows:

- 1 Familiarisation with Demec equipment and measurement techniques
- 2 Setting-out of Demec pips and supply of reference samples
- 3 Datum readings
- 4 Final readings
- 5 Documentation.

Further details are provided below.

2.1 FAMILIARISATION WITH DEMEC EQUIPMENT AND MEASUREMENT TECHNIQUES

Appropriate AKD personnel shall attend a demonstration of the Demec system and its use, as outlined in this procedure, before work commences. The Demec gauge, setting out bar and reference bar are to be provided free-issue by BOMEL, together with sufficient Demec pips. The Demec gauge is provided with a current NAMAS calibration certificate.

The gauge shall be treated with care at all times and when not in use shall be stored in a safe place in the wooden case provided by BOMEL. AKD shall be responsible for making good any damage that may be caused in the course of its work and for any remeasurement that may be necessary if the gauge has to be replaced.

If at any point in the work AKD have any concerns or queries about the system and its use, BOMEL shall be notified immediately to provide assistance.

The Demec system shall be returned to BOMEL on completion of the work.

To take a reading the pivot end of the gauge should be placed in the indentation of one pip and the other end should be moved and located in the second pip. The gauge should be rocked slightly about its longitudinal axis until a steady reading is obtained. The gauge should be held firmly in position; no applied force is required. The gauge should then be removed and replaced

and a further reading obtained. If the readings differ by more than half a subdivision the process shall be repeated until consistent measurements are obtained.

The dial gauge reading should be taken in the usual way:

- The divisions on the small inner dial give the thousands, a
- The main divisions on the large outer dial give the hundreds, b
- The sub-divisions on the large outer dial give the tens, c
- The position between two sub-divisions gives the units; however sufficient accuracy is achieved if readings are given to the nearest half division
- Readings shall be recorded thus:
abc0 or abc5

As with all dial gauges, particular care should be taken to ensure that the clockwise increase in readings is remembered when taking readings.

2.2 SETTING OUT OF DEMEC PIPS AND SUPPLY OF REFERENCE SAMPLES

Two measurement locations shall be set up for each member in the Frame. This requires four pips to be used in opposite pairs on the axis of the member (see Drawing C636\15\014D bound within this specification). On Frames A and B pips shall be placed on the in-place axis but for Frames C, D and E and the Level 1 and 2 plan bracing, pips shall be placed on the out-of-plane axis. This strategy will ensure final results can be based on readings from either side in the rolled up position.

The pips shall be affixed using a superglue suitable for metals, to be supplied by AKD. The drilled hole shall be outermost. The longitudinal spacing of the pips shall be determined using the 12" setting out bar. A tolerance of ± 2 mm can be accommodated in the circumferential and longitudinal positions.

The pips shall be positioned away from any weld locations as illustrated schematically in Drawing C636\15\014D; exact positions shall be selected by AKD in light of cutting plans.

The pips shall be circled with a permanent paint marking to help locate them for further readings and to ensure they are not damaged in the course of fabrication/lifting, etc. One pair of pips shall be labelled 'A', the other 'B'. The marking shall be large and clear so that the orientation in the final frame will be clearly distinguishable. The location of the pips shall be recorded on a drawing as illustrated in Drawing C636\15\014D. The measurement given shall be from the closest pip to the reference point/intersection. A tolerance of ± 10 mm can be accommodated.

Offcuts of each tubular type (size/specification) at least 350 mm long shall be provided. No distinction need be made between different batches, i.e. one sample of the 168 mm dia x 4.5 mm WT BS3602 ERW will be sufficient. One measurement location shall be set up on each offcut by placing a pair of pips longitudinally. The samples shall be clearly and permanently identified and shall be kept safe from damage, in the vicinity of the structure/members.

2.3 DATUM READINGS

A template for the recording of Demec readings is presented in Appendix A. To ensure that current and relevant reference readings are used, it is proposed that new sheets are used hourly with separate sheets for each material type. BOMEL would give consideration to alternative proposals from AKD.

The procedure for taking readings is as follows:

- 1 Ensure reference samples are in the vicinity of structure/members to be measured.
- 2 Identify tubular type for members to be measured (reference drawing C636\15\002D). Select appropriate logsheet.
- 3 Record name, date and time. Take and record measurement from the Invar bar. Take and record measurement from the appropriate material reference sample. At least two readings shall be taken before recording the measurement to ensure the gauge is positioned correctly and recordings are consistent.
- 4 Record the member number. The member reference scheme is provided in Appendix B.
- 5 Record with (✓) confirmation that member and log sheet materials correspond. Record with (✓) confirmation that member reading is being taken within one hour of reference readings.

If either is not confirmed, a new log sheet should be started.

- 6 Take and record measurement across the A pair of Demec pips. Take and record measurement across the B pair of Demec pips. At least two readings shall be taken before recording the measurement to ensure the gauge is positioned correctly and recordings are consistent.

- 7 Repeat Steps 4 to 6 until additional log sheets are necessary. For each new log sheet return to Step 3.

Datum readings for all members shall be taken before the associated fabrication is closed-out.

To check the procedures and use of the system, the first readings (say four members) shall be repeated a day or two after the initial datum readings are taken. The log sheets shall be faxed to BOMEL for review and approval. BOMEL will revert within one working day.

2.4 FINAL READINGS

Once fabrication of the 3D structure is complete all the Demec measurements shall be repeated. Steps 1 to 7 of the procedure in Section 2.3 shall be repeated as necessary.

The timing of the final readings shall be discussed and agreed with BOMEL before work commences.

2.5 REPLACEMENT MEMBERS

As for the initial frame fabrication there is the same requirement to measure locked-in stresses for the replacement members introduced following the loadcase 1 and 2 tests. Demec pips shall be applied and datum readings taken for the new members in accordance with Sections 2.2 and 2.3. Once fabrication of the repaired structure is complete, final readings for only the new members shall be taken in accordance with Section 2.4. Strain measurements for the remainder of the structure will be obtained automatically from the wired gauges that will then be in place.

3 DOCUMENTATION

AKD shall provide the following to BOMEL:

- Layout drawings indicating the location of the pips on each member (see Drawing C636\15\014D)
- Completed log sheets for all Demec readings (see Appendix A).

Original hand-written sheets shall be provided to BOMEL on completion of all measurements. The handwriting must be clear but the records shall not be transposed or otherwise typed up to avoid errors.

Copies of the log sheets relating to the initial and check readings as required under Section 2.3 shall be provided to BOMEL by fax.

Copies of layout drawings and completed log sheets shall be made available to BOMEL at interim stages upon request, either by fax or to the BOMEL site representative, as appropriate.



The contents of this document are confidential to Participants of the Frames Project - Phase III, under the terms of their contract for participation in the project

**JOINT INDUSTRY TUBULAR FRAMES PROJECT -
PHASE III**

TEST FRAME INSTRUMENTATION

C636\25\071R REV 0 JULY 1999

Purpose of Issue	Rev	Date of Issue	Author	Checked	Approved
Draft for Client Comment	0	July 1999	LMB HMB	FHH FHH	 CJB

Controlled Copy	10	Uncontrolled Copy	
-----------------	----	-------------------	--

BOMEL LIMITED

Ledger House
Forest Green Road, Fifield
Maidenhead, Berkshire
SL6 2NR, UK

Telephone +44 (0)1628 777707

Fax +44 (0)1628 777877

Email bomel@compuserve.com

REVISION SHEET

REVISION	DETAILS OF REVISION	DATE
0	Draft for Client Comment	30.7.99

FILE SHEET

PATH AND FILENAME	DETAILS OF FILE
C636\26\C476-7.pcx	Figure 1.1
C636\26\C468-24.pcx	Figure 3.1
C636\26\C473-5.pcx	Figure 3.2
C636\26\C475-7.pcx	Figure 3.3
C636\26\C488-4.pcx	Figure 3.4
C636\26\C476-34.pcx	Figure 3.5
C636\26\C472-36.pcx	Figure 3.6
C636\26\C476-15.pcx	Figure 3.7
C636\26\C476-14.pcx	Figure 3.8
C636\26\C514-22.pcx	Figure 3.9
C636\26\C518-17.pcx	Figure 3.10
C636\26\C515-11.pcx	Figure 3.11
C636\26\C514-29.pcx	Figure 3.12
C636\25\072U.vsd (original plus Revs A to D)	Table 4.1
C636\AVT\LC2a_Test.xls - Raw sheet	Figure 5.1
C636\AVT\LC2a_Test.xls - Data sheet	Figure 5.2
C636\AVT\LC2a_Test.xls- Data sheet	Figure 5.3
C636\AVT\LC2a_Test.xls - Global sheet	Figure 5.4
C636\AVT\LC2a_Test.xls - FrA TED For sheet	Figure 5.4
C636\AVT\LC2a_Test.xls - FrE TB Comp sheet	Figure 5.4
C636\AVT\LC2a_Test.xls - FrA DC BBL Mom sheet	Figure 5.4
C636\AVT\LC2a_Test.xls - Lev 2-X For sheet	Figure 5.4
C636\AVT\LC2a_Test.xls - N29 Disp sheet	Figure 5.4
C636\12\images\gui7.pcx to gui12.pcx	Appendix A Figures A.1 to A.6
C636\15\011D-D	Appendix A
C636\15\012D-B	Appendix A
C636\15\013D-B	Appendix A
C636\18\017D	Appendix A
C636\15\016D	Appendix A
C636\25\075D (using C636\12\images\base.pcx)	Appendix A
Inc Document 9084 (File C636\25)	Appendix B
Inc Document 12291 (File C636\25)	Appendix C



CONTENTS

	Page No.
FOREWORD	0.6
EXECUTIVE SUMMARY	0.9
1. INTRODUCTION	1.1
2. INSTRUMENTATION LAYOUT AND SPECIFICATION	2.1
3. TECHNICAL DETAILS OF INSTRUMENTATION	3.1
3.1 LOAD CELLS	3.1
3.2 SITE INSTALLED LINEAR STRAIN GAUGES	3.3
3.3 STRESS CONCENTRATION FACTORS	3.4
3.4 DISPLACEMENT TRANSDUCERS AT JOINTS	3.4
3.5 LOAD PATH MONITORING	3.6
3.6 GLOBAL STRUCTURAL DISPLACEMENTS	3.6
3.6.1 Test Frame	3.6
3.6.2 Reaction Rig	3.7
3.7 DATA LOGGING AND VALIDATION	3.9
3.8 DATA PROCESSING	3.11
3.9 OTHER MONITORING SYSTEMS	3.11
3.9.1 Paint System	3.11
3.9.2 Video Footage	3.12
3.9.3 Audio	3.13
3.10 SUMMARY	3.13
4. SIGN CONVENTION	4.1
4.1 GLOBAL AXES	4.1
4.2 STRAIN GAUGE CONVENTION	4.1
4.3 ROSETTE POSITIONING	4.3
4.4 DISPLACEMENT MONITORING	4.3
4.5 SUMMARY	4.3
5. SPREADSHEET DATA LOGGING SYSTEM	5.1
5.1 SPREADSHEET LAYOUT	5.1
5.2 PROCEDURES FOR DATA CAPTURE	5.6
5.3 FINAL DATAFILES	5.6



CONTENTS CONTINUED

	Page No.
6. REFERENCES	6.1
APPENDIX A INSTRUMENTATION SUMMARY	
APPENDIX B AVT LOAD CELL CALIBRATION REPORT - EXCLUDING APPENDICES	
APPENDIX C AVT REPORT - DATA COLLECTION AND PRESENTATION OF FINAL DATA FILES	



FOREWORD

This report is one of a series describing different aspects of Phase III of the Joint Industry Tubular Frames Project. Each report is self contained providing detailed information in the subject area and summarising relevant data from other documents. The following table lists and briefly describes the focus of each report for cross-referencing purposes.

Report Title	Reference	Circulation
Summary and Conclusions Overview report describing the project and principal findings	C636\04\478R	1
Background, Scope and Development Scene setting report summarising previous work, identified needs and Phase III programme definition and development	C636\04\435R	1
3D Test Set Up Brief description of the 3D test set up and structural configuration	C636\06\313R	1
Material Testing Report Description of material testing procedures, test results and disposition of specific materials within test structure	C636\23\004R	1
Assessment of Locked-In Fabrication Stress Explanation for the build up of locked-in fabrication stresses, description of their measurement and summary of the locked-in force values in key components at the start of each test	C636\21\050R	1
Test Frame Instrumentation Detailed description of all instrumentation systems used in the 3D frame, accuracy, sign conventions etc. Data on CD in final report	C636\25\071R	1
Loadcase 1 Test Report - Multiplanar K Joint Action Detailed description of the Loadcase 1 static test response and interpretation of the results and their significance	C636\37\014R	1
Loadcase 2 Test Report - Interaction Between X-Braced Planes Detailed description of the Loadcase 2 static test response and interpretation of the results and their significance	C636\39\011R	1
Loadcase 3 Test Report - Multiple Member Failures and 3D System Action Detailed description of the Loadcase 3 static test response and interpretation of the results and their significance	C636\40\021R	1



Report Title	Reference	Circulation
<p>Philosophy of Cyclic Testing Discussion of the background to cyclic response issues in the context of ultimate system strength and basis for specific loading scenarios</p>	C636\24\021R	1
<p>Loadcase 1 Cyclic Test Report Detailed description of the Loadcase 1 cyclic test response and interpretation of the results and their significance. Comparison with LC1 static results</p>	C636\38\010R	1
<p>Monotonic and Cyclic testing of Isolated K Joints Description and presentation of results from isolated component tests undertaken by SINTEF in Norway</p>	STF22 F98704 (C636\24)	1/2
<p>Loadcases 2 and 3 Cyclic Test Report Detailed description of the Loadcases 2 and 3 cyclic test responses and interpretation of the results and their significance. Comparison with LC2 and LC3 static results</p>	C636\41\011R	2
<p>Loadcases 1 and 3 'Alternative' Cyclic Tests Detailed description of the Loadcases 1 and 3 alternative cyclic test responses and interpretation of the results and their significance. Comparison with LC1 and LC3 static and cyclic tests</p>	C636\45\008R	3
<p>Multiplanar SCFs Joint BG / BOMEL report describing analytical work and experimental measurements of multiplanar SCFs. Includes comparison with 'standard' empirical approaches</p>	C636\18\018R	1
<p>Site Testing Programme results - Report to Benchmark Analysts Comprehensive report describing results for benchmark cases LC1, LC2 and LC3, including all pertinent data and providing response plots 'matching' the contributions from individual analysts</p>	C636\32\066R	4
<p>Benchmark Conclusions Report comparing blind and post test analyses with measured responses and assimilating learnings and recommendations for future practice identified by Benchmark Analysts</p>	C636\32\084R	1

Key to circulation.

Circulation	All participants	Participants in 1st extension	Participants contributing finance/analytical results to 2nd extension	Benchmark Analysts
1	✓	-	-	×
2	-	✓	-	×
3	-	-	✓	×
4	✓	-	-	✓



JOINT INDUSTRY TUBULAR FRAMES PROJECT - PHASE III TEST FRAME INSTRUMENTATION

EXECUTIVE SUMMARY

A comprehensive set of instrumentation was installed on the Frames Project 3D test frame to provide detailed data on forces, bending moments, stress concentration factors and displacements throughout the ultimate strength tests. The 880 channel system comprised:

- 46 pre-calibrated load cells (184 gauges)
- ~ 400 site installed linear strain gauges
- ~ 300 site installed rosette strain gauges
- 30 displacement transducers
- 22 km of cabling
- ~ 1600 complete scans of all 880 data channels
- 166 Mb of Excel spreadsheet data capture files.

This report describes the basis for the system design and the techniques used. Detailed drawings indicate the locations of all the instrumentation. The sign convention and channel referencing schemes are defined and the structure of the spreadsheet used for data capture, reduction and graphing is explained.

The final data files supplied by the instrumentation contractor AV Technology Limited are listed. These are provided on the project CD.



1. INTRODUCTION

The Joint Industry Tubular Frames Project was established to investigate the ultimate strength behaviour of 3D jacket type structures and to benchmark analytical predictions of the response. An accurate and dependable system of instrumentation was therefore essential to measure the forces and deflections. Figure 1.1 shows the set-up just prior to the first test.

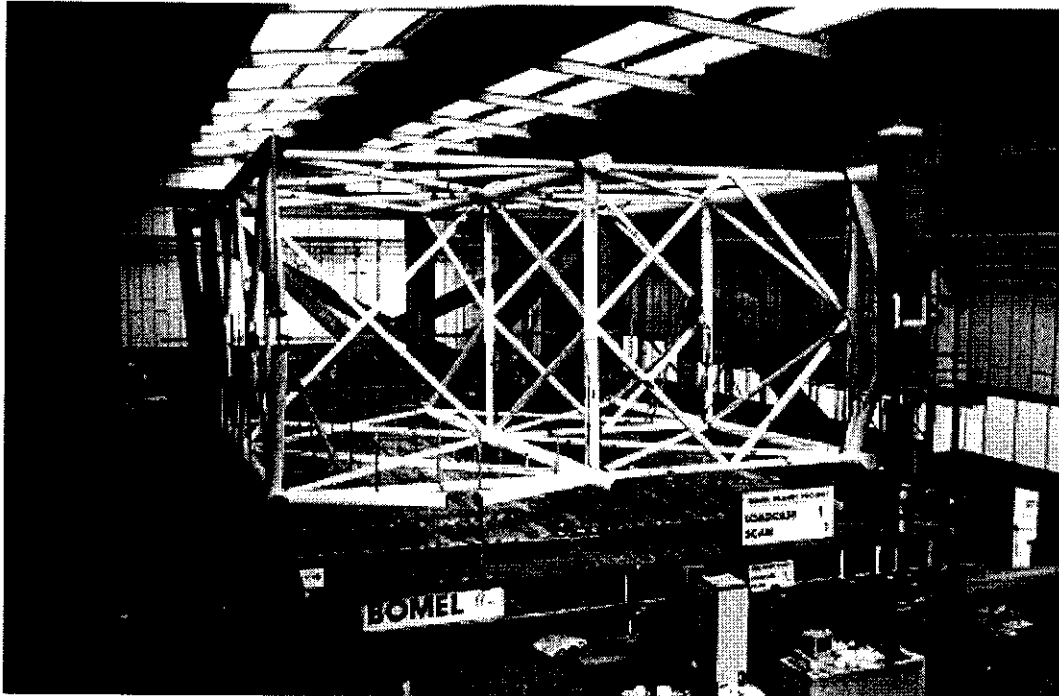


Figure 1.1 Instrumented 3D test frame prior to LC1 test

This report provides details of the instrumentation scheme adopted. Forces and moments were measured using a combination of pre-calibrated load cells welded into the structure and sets of linear strain gauges applied on site to the structural members. Rosette strain gauges were used to record the combination of shear and axial force acting at the connection of the frame legs to the reaction rig and to determine stress concentration factors at the multiplanar node at the top of the structure. Global deflections of the test frame nodes were recorded with potentiometers and supplementary information on the uplift of the reaction rig at support points was obtained from dial gauges. Local deformations at critical joints were measured with frame mounted potentiometers. All electrical instrumentation was connected to a central logging system providing direct output to an MS Excel spreadsheet which in turn was programmed to give on line graphing throughout each test. These spreadsheets contain comprehensive data scanned at many stages during each test and form the basis for interpreting the frame responses.

The supply, installation and data capture activities were sub-contracted to AV Technology Limited based on a competitive tender. The programme overall involved:



- 46 pre-calibrated load cells (184 gauges)
- ~ 400 site installed linear strain gauges
- ~ 300 site installed rosette strain gauges
- 30 displacement transducers
- 22 km of cabling
- 8 multi-day tests
- ~ 1600 complete scans of all 880 data channels
- 166 Mb of Excel spreadsheet data capture files.

This report describes the underlying basis of the instrumentation specification and layout (Section 2). Section 3 provides technical details of the measurement devices adopted and Section 4 sets down the sign convention adopted to be consistent with the benchmark analysis scheme. In Section 5 the logging system and data file structure are described and the audit trail from raw measurements to final deliverables is presented. It concludes with a summary of the load effect data available and their use in interpreting the test frame responses.



2. INSTRUMENTATION LAYOUT AND SPECIFICATION

BOMEL prepared a specification for instrumentation of the 3D frame⁽¹⁾ based on the following requirements:

1. Accurate and dependable measurements of axial forces in primary members for elastic and nonlinear regimes.
2. Information on axial force-moment distribution in members subject to bending (legs) or susceptible to buckling (compression braces).
3. Measurement of stress concentration factors at central multiplanar node.
4. Local response data for tubular joints.
5. Complete tracking of loadpath through structure under applied forces.
6. Determination of global structural deformations.
7. On-line monitoring facilities.
8. Automated data reduction.

The above were required not only for local interpretation of the responses but also for comparison with global response predictions from benchmark analysts.

To achieve these objectives the specified system (see Appendix A) comprised the following elements in each case:

1. Thick-walled, high yield pre-calibrated load cells instrumented with four orthogonal strain gauges welded into primary brace members during fabrication (see Drawing C636\15\011D in Appendix A).
 - the section properties ensure the load cells remain elastic (and the strain gauge readings valid) even if the surrounding member becomes plastic
 - installation at the point of contraflexure where buckling to occur ensures the influence of the thick-walled section on structural response is negligible
 - four gauges provide redundancy within the load cell as averaging opposite gauges should give equivalent axial readings under small deflection conditions



- pre-calibration of instrumented load cells under known loads provides a direct measure of force independent from local section properties and a very high degree of accuracy
 - high specification gauges and sufficient load cell length ensure gauges are unaffected by welded fabrication
 - installation of load cells in 'opposite' braces within X-braced bays provides a further degree of redundancy / validation.
2. Site installation of orthogonal (in-plane/out-of-plane) pairs of linear strain gauges (see Drawings C636\15\012D and 013D in Appendix A).
- good accuracy but less costly than integral load cells
 - orthogonal pairs to monitor bending and give redundancy in axial force calculations
 - nominal forces or adjusted using measured D and T values at local section
 - interpretation not valid if local strains exceed elastic limit (see 7).
3. Site installed pairs of rosette gauges at locations corresponding with HSE convention⁽²⁾ together with sets of four linear strain gauges on incoming braces (see Drawings C636\18\017D and C636\15\013D in Appendix A).
- determination of SCFs by linear extrapolation
 - comprehensive calculation of axial forces and moments acting at the multiplanar node.
4. Site installation of displacement transducers straddling joint intersections at critical nodes (see Drawing C636\15\016D in Appendix A for details in each test) and local strain gauges to track bending moments (see Drawing C636\15\013D in Appendix A):
- sufficient stroke to capture full nonlinear deflection response (to ~150mm)
 - caution on accuracy in initial elastic range (<1mm)
 - welded attachment to give continuous readings throughout tests
 - measurement of any bending contributions to ensure (axial) capacity is appropriately interpreted.
5. Gauging (load cells and/or site installed strain gauges) to give axial forces through all primary loadpaths and rosette gauges at connection of the frame legs to the reaction rig to comprehensively record axial force, moment and shear transfer (see Drawing C636\15\013D in Appendix A).
6. Potentiometers monitoring spatial movement of primary frame nodes (with respect to ground) at lower levels and draw wire measurements for relative movement between nodes within the frame. Potentiometers and supplementary dial gauges recording



uplift of reaction rig from supports (for comparison with analysis predictions) - see Drawing C636\25\075D in Appendix A.

7. Integrated logging of all electrically powered instrumentation enabled tests to proceed efficiently and capturing simultaneous data (particularly important as the structure deforms plastically). A high rate of scanning and averaging of multiple readings through an AC cycle ensures stability and accuracy. For purposes of safety and engineering control of the tests, on line monitoring was essential.
8. Automated data reduction was essential for the programme to be viable and direct transfer to an MS Excel spreadsheet system enabled interpretation and reporting functions to be integrated.

As noted above, Appendix A provides comprehensive drawings detailing the instrumentation layouts. Figures in Appendix A also give the member and node numbering scheme adopted for the frame in order that the location of specific instrumentation can be cross-referenced. The key for referencing each of the eight tests is included in order that the instrumentation modifications loadcase to loadcase can be interpreted.

It will be seen in Section 5 that the scheme used in the data acquisition and processing software provides a clear and comprehensive cross-reference between specific readings and frame location.



3. TECHNICAL DETAILS OF INSTRUMENTATION

3.1 LOAD CELLS

Load cells were used primarily to measure axial forces in bracing members; in addition bending moments at the load cell positions could be deduced. The 46 load cells were fabricated from a higher grade, thicker walled section than the bracing to ensure the load cells remained elastic (and gave reliable readings) even if the surrounding member buckled and yielded. Typical / nominal properties were:

- bracing: 168 mm O.D x 4.5mm W.T. BS 3602 ERW, $F_y = 278 \text{ N/mm}^2$
- load cell: 168 mm O.D x 5.0mm W.T. BS 4848 G50, $F_y = 395/457 \text{ N/mm}^2$

The load cells were welded into the bracing at anticipated points of contraflexure to eliminate any influence of the section on buckling characteristics. The load cell locations are shown in Appendix A. Two lengths of load cell were prepared (350mm and 500mm). The longer load cells were located in members which were expected to fail and which would therefore have to be replaced during the testing programme. The additional length of these load cells, which were to be cut out of the damaged member and re-used, was to accommodate re-preparation of the ends prior to welding into the replacement member.

The load cells were strain gauged with two pairs of diametrically opposed TML FLA6-11 gauges. These were applied with TML CN adhesive and protected with a three stage coating system consisting of 'Bofors' Barrier B, M-Group F-Coat and finally, a layer of aluminium foil. Figure 3.1 shows one of the instrumented load cells.

Subsequent to strain gauging, each load cell was calibrated in a NAMAS certificated 300 kN capacity press. Calibration commenced following a number of applications of a shake down load of approximately 6% greater than the maximum calibration load. Shakedown cycles were applied to ensure that (a) all strain gauges were operating, and (b) that the load cells were positioned such that any bending stresses were less than 5% of the nominal axial stress. Maximum load was applied in six equal increments then removed in three equal decrements, strain gauge readings being recorded at each stage. The maximum loads were set beyond the elastic limit of the braces into which the load cells were to be installed. During the calibration operation, all strain gauge elements were individually configured into full bridge circuits using three dummy strain gauges per actual element. The dummy gauges were bonded to an unstressed steel block to provide automatic temperature correction.

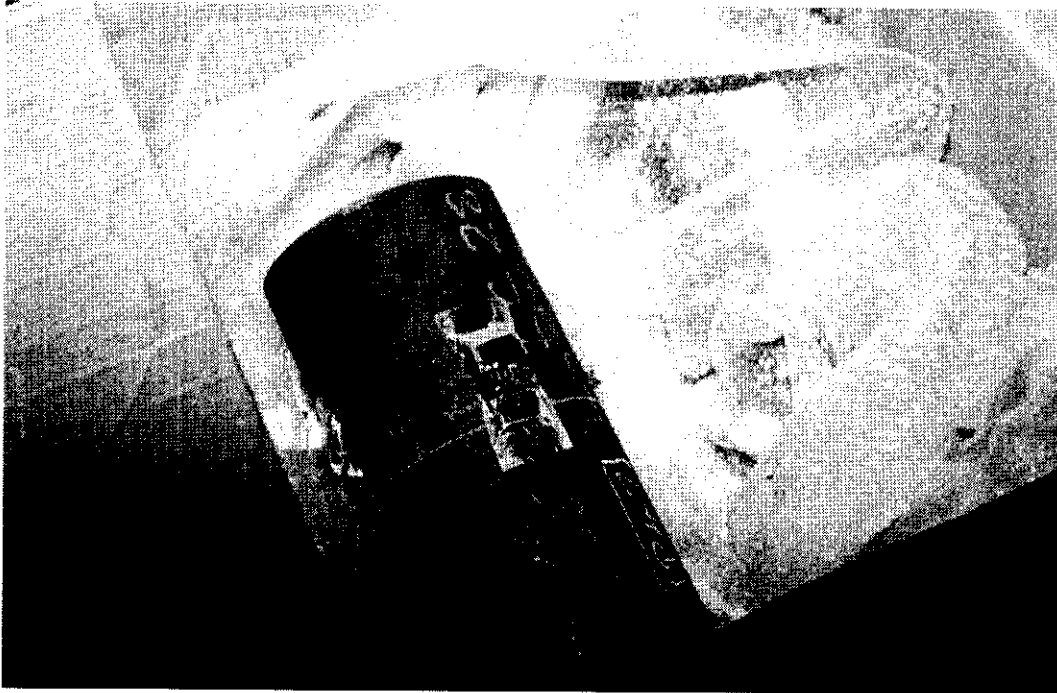


Figure 3.1 Load cell

The calibration factor for each load cell, in micro strain per kN force, was calculated using the average slope of the load versus axial strain relationship over the six load increments. Following calibration, the ends of each load cell were prepared for welding into the structure.

The text of the AVT's calibration report⁽³⁾ is presented as Appendix B. The voluminous test records from AVT's report are not reproduced. However Table 3.1 summarises the axial force calibration factors calculated for each load cell and carried forward into the data processing software.

Table 3.1 Load calibration factors

Load cell ID	Calibration factor $\mu\epsilon$ per kN	Load cell ID	Calibration factor $\mu\epsilon$ per kN	Load cell ID	Calibration factor $\mu\epsilon$ per kN	Load cell ID	Calibration factor $\mu\epsilon$ per kN
LC 1	1.779	LC 13	1.787	LC 25	1.959	LC 37	1.978
LC 2	1.792	LC 14	1.815	LC 26	2.001	LC 38	1.994
LC 3	1.810	LC 15	1.785	LC 27	1.833	LC 39	1.809
LC 4	1.786	LC 16	1.806	LC 28	1.789	LC 40	1.783
LC 5	1.692	LC 17	1.811	LC 29	1.828	LC 41	1.976
LC 6	1.780	LC 18	1.812	LC 30	1.829	LC 42	1.971
LC 7	1.826	LC 19	1.834	LC 31	1.925	LC 43	1.918
LC 8	1.795	LC 20	1.815	LC 32	1.980	LC 44	1.982
LC 9	1.778	LC 21	1.795	LC 33	1.912	LC 45	1.939
LC 10	1.785	LC 22	1.831	LC 34	1.953	LC 46	1.935
LC 11	1.837	LC 23	1.987	LC 35	1.937		
LC 12	1.795	LC 24	1.931	LC 36	1.942		

3.2 SITE INSTALLED LINEAR STRAIN GAUGES

To augment the data obtained from the load cells, in particular to measure axial forces and bending moments in members at joints of particular interest, strain gauges were positioned as detailed in Appendix A. Linear gauges were TML WFLA-6-11-1L pre-encapsulated pre-wired strain gauges.

Figure 3.2 shows the site installed gauges on Brace 27. Three dummy strain gauges per active strain gauge were installed on pre-prepared dummy blocks mounted adjacent to the measuring site. The full bridge circuit was selected on the basis of a number of calibration trials over alternative half-bridge or dummy resistor configurations. The chosen set up was shown to deliver good accuracy and resolution of measured strains with compensation for all possible sources of errors. The accuracy was well within the required $\pm 2\frac{1}{2}\%$, even at low levels of strain. The dummy blocks are visible in the picture and the linear strain gauges are protected under the green tape. The fixing of the cabling to protect against the wires becoming detached is evident as are the white tags fixed at either end of the cable and marked up with the gauge ID.



Figure 3.2 Member strain gauges

3.3 STRESS CONCENTRATION FACTORS

To determine SCFs at selected locations at the multiplanar Node 7 on Line B, a combination of rosette and linear gauges was applied as set out in Appendix A. The 48 rosettes were three element (45°) type TML FRA-3-11-1L strain gauges to enable them to be affixed at the precise positions close to the weld toe. The additional strain gauges to define bending moments in the incoming braces were linear gauges as described in Section 3.2. All gauges were provided with dummy blocks. Figure 3.3 shows one view of Node 7, fully gauged prior to testing.

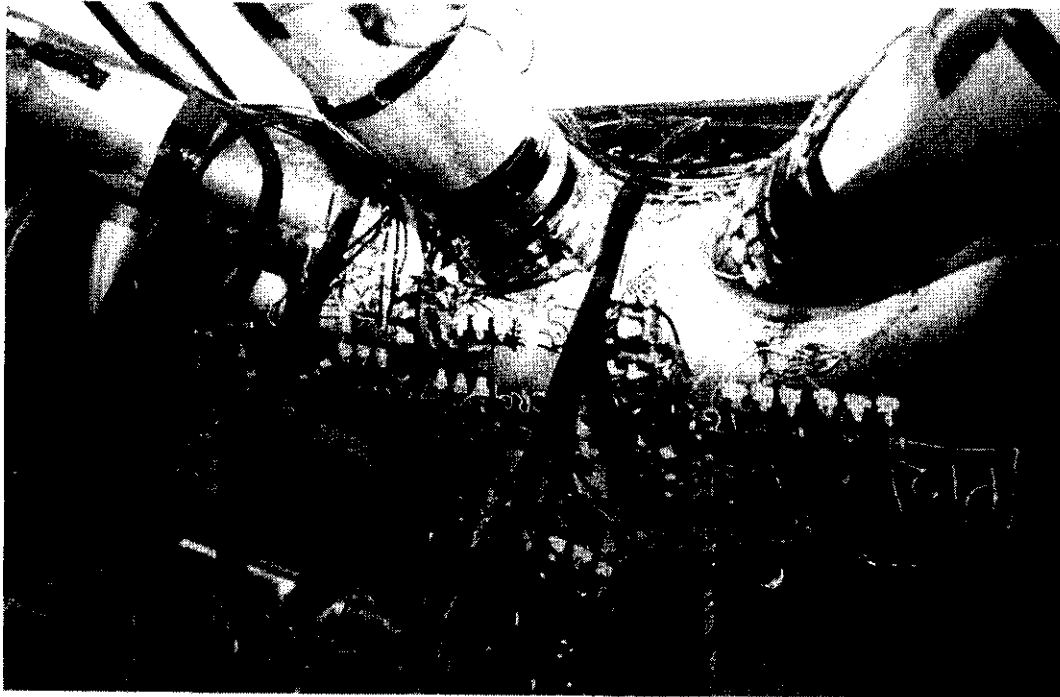


Figure 3.3 SCF gauging at primary multiplanar node

3.4 DISPLACEMENT TRANSDUCERS AT JOINTS

A number of tubular joint intersections were expected to experience significant deformations in the tests. They had been fabricated without joint cans replicating construction practice for many older jacket structures. Information on the local load-deformation ($P-\delta$) response of the joints is very important to interpret the global behaviour and to provide a basis for future predictions. To measure local displacements, Penny and Giles linear potentiometers were connected directly to swivel mountings spot welded to the structure on the centre line of the incoming braces and / or chord as appropriate. The potentiometers were calibrated by AVT prior to use in the test programme. Figures 3.4 and 3.5 show the typical arrangement for monitoring at X and K nodes. Output from the load cells provided corresponding data on member forces.

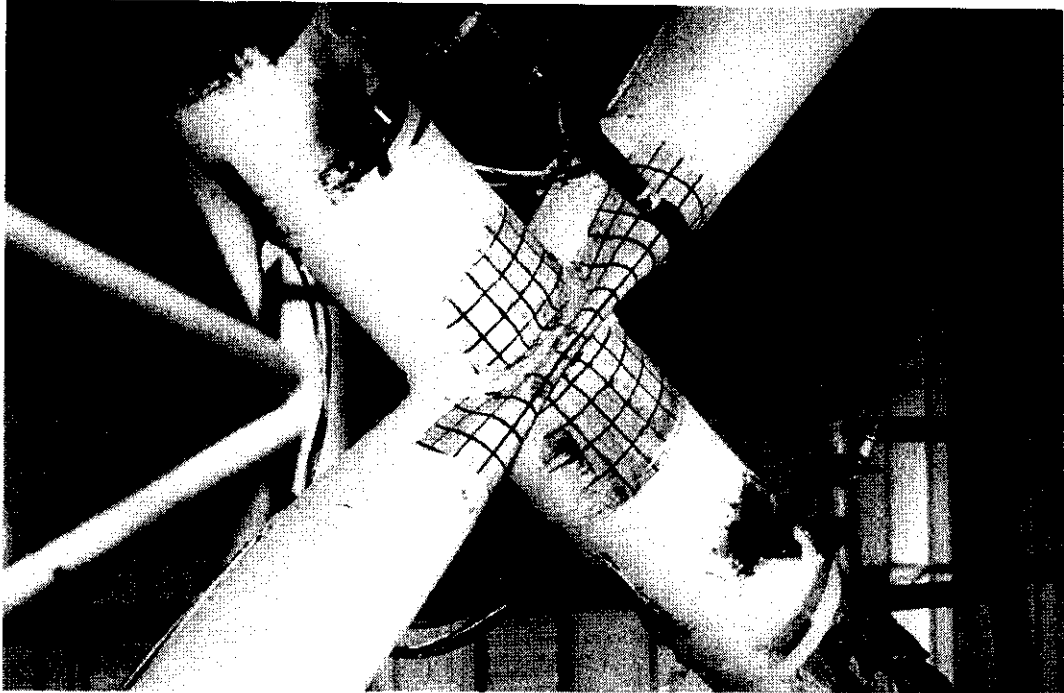


Figure 3.4 Joint deformation measurements at X Node 42 in LC2 test

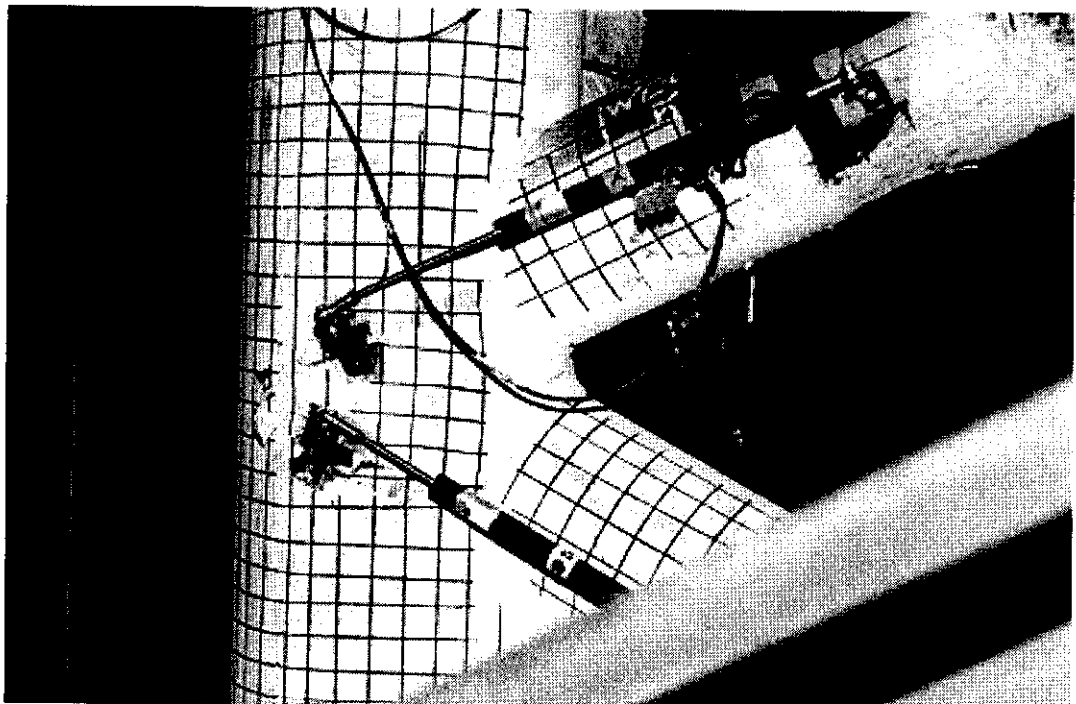


Figure 3.5 Joint deformation measurements at K Node 37 in LC1 test

Also visible is the gridline drawn on the X node prior to testing. Although relatively crude these grids were effective in highlighting the pattern of deformation and were used extensively in subsequent tests.

3.5 LOAD PATH MONITORING

The instrumentation drawings in Appendix A demonstrate that the load path coverage was comprehensive. In addition to the load cells and site-installed linear strain gauges, rosette gauges were positioned at locations where the leg sections connected with the rig. It was important here to record the axial forces, moments and shears being transferred to the reaction rig. The layout is shown in the Appendix A drawings.

Figure 3.6 shows the complex arrangement of rosettes (45° TML Wfra-6-11-1L pre-encapsulated pre-wired gauges).

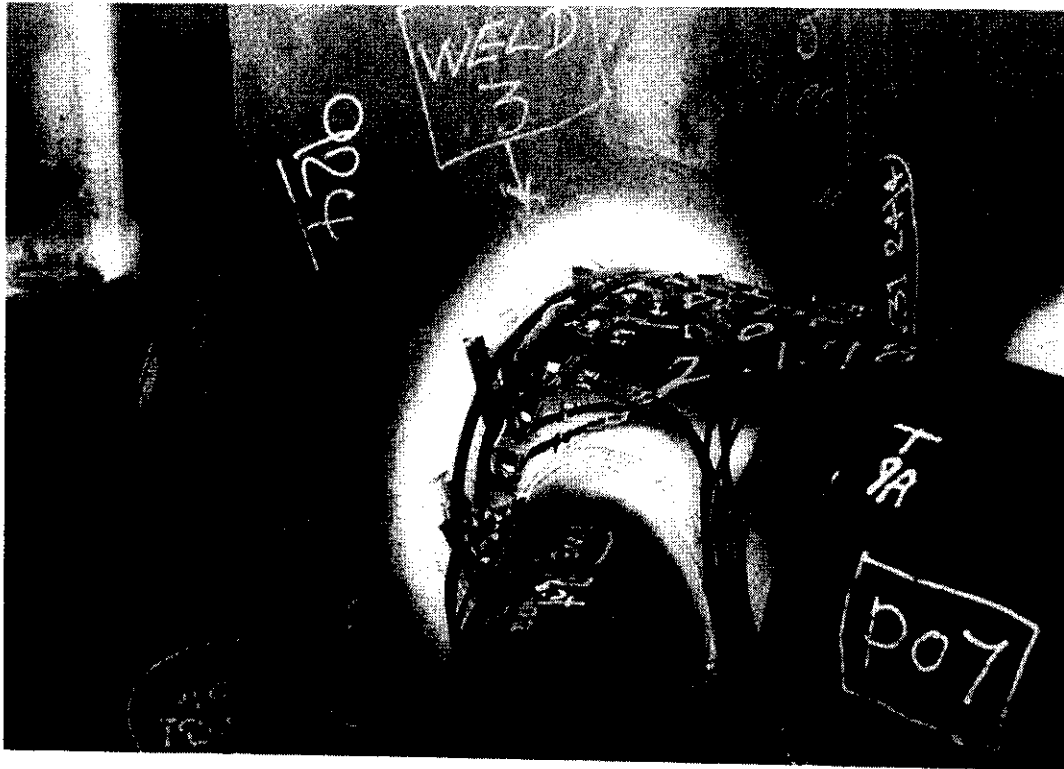


Figure 3.6 Rosette gauging at the base of the frame legs at the reaction rig connection

3.6 GLOBAL STRUCTURAL DISPLACEMENTS

3.6.1 Test Frame

Global displacements of the test specimen in the two lateral and vertical directions (see numbering scheme in Appendix A) were measured at Nodes 21, 22, 29 and 30 by means of linear transducers. The results were processed to obtain the x, y, z co-ordinates of the new position. At Nodes 25 and 26 a single axis of displacement was monitored corresponding to the plane of load application (ie. for LC1 and LC2 vertical displacements, for LC3 horizontal



displacements). A combination of Penny and Giles linear potentiometers and uni-measure type LX-PA draw wire potentiometers (DWP) was used. Each transducer was calibrated prior to use and was connected to a self-aligning mounting bracket attached to a fixed support independent of the test specimen/loading rig structure. Steel cables were used to connect the DWP transducers to each node position. Figure 3.7 is a photograph of the arrangement at Node 30. This shows a linear potentiometer for the measurement of z displacements and two draw wires connected to DWPs to measure x and y displacements. The accuracy of measurement for all transducers was better than $\pm 2\frac{1}{2}\%$.



Figure 3.7 Monitoring of global frame displacements

Although monitoring of the frame displacements at the uppermost level was uneconomic, some measure of the frame distortion was determined with draw wires between corresponding Nodes in Frames A and B. Depending on the location of loading and anticipated deformations, draw wires connected Nodes 3 and 21, 4 and 22 or 11 and 29.

3.6.2 Reaction Rig

The reaction rig rested on 'frictionless' bearing pads at twelve node points. It could therefore lift up from these supports depending on the applied load. At one point, Node 61, lateral movements were prevented but uplift was allowed. The changing support conditions influence the stiffness of the system response and therefore uplift information was relevant to the interpretation of the tests and comparison with analytical predictions. Further details regarding the 3D test set up are given in a companion report⁽⁵⁾.

Global displacements of the base of the loading rig were measured in the x, y and z directions with Penny and Giles potentiometers at Nodes 45 and 48, the most distant points from the fixed Node 61 (see Appendix A figures). The results were processed to obtain the x, y and z coordinates of the displaced position as before. Figure 3.8 shows a typical configuration at Node 45.

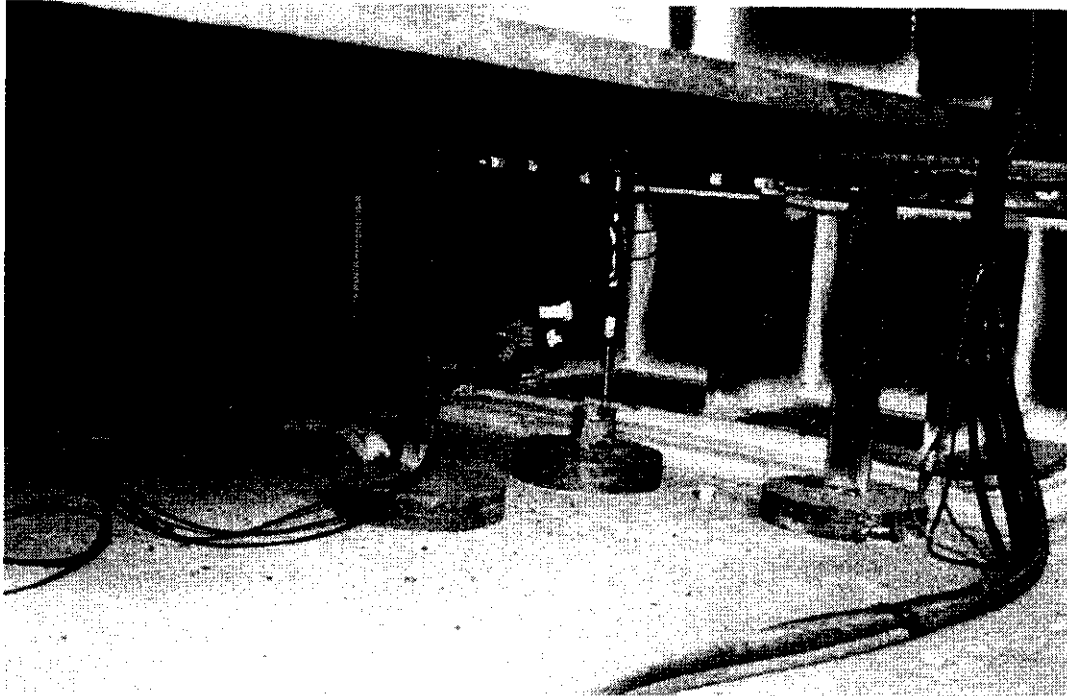


Figure 3.8 Monitoring of global displacements of reaction rig

Displacements of the loading rig base in the vertical direction were also measured near Nodes 51, 52, 54, 56, 57 and 58 by means of mechanical dial gauges with a resolution of 0.01 mm. Each gauge was fixed, by means of a magnetic base, to a steel plate resting on the floor. The principal purpose of these was to detect where and when uplift occurred.

For the LC3 configuration the horizontal displacement of the stub beam to which the actuator was connected, was measured relative to the base beam along the centre line of the actuator by a mechanical dial gauge of 0.01 mm resolution. The dial gauge can be seen in position at the top right of Figure 3.9.

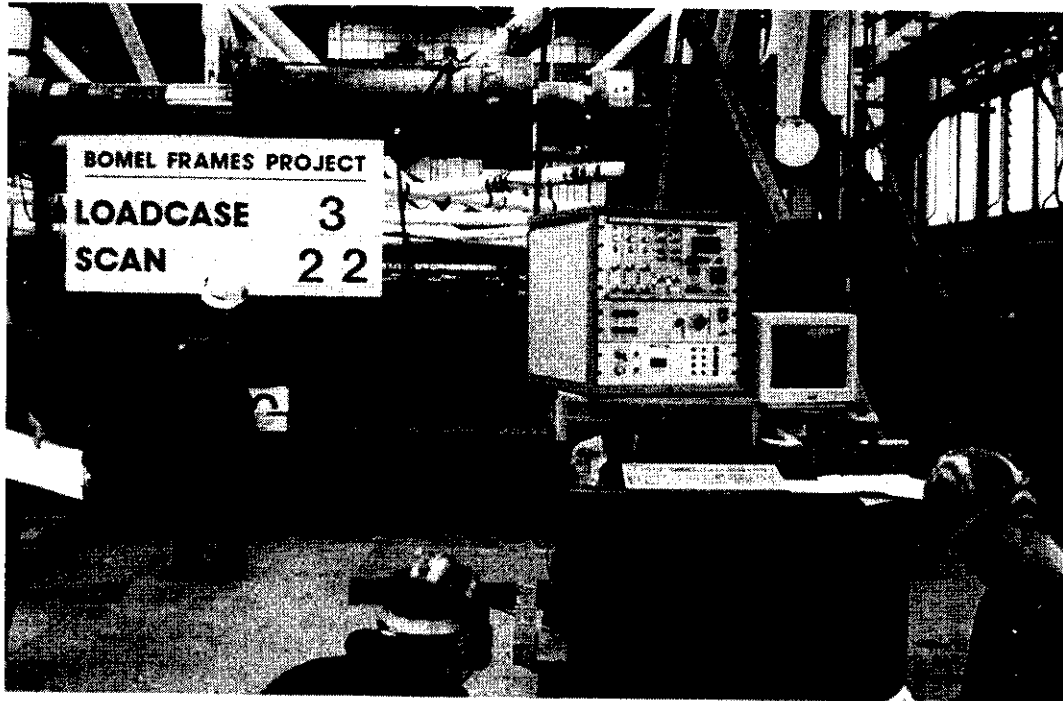


Figure 3.9 Monitoring deflection of the actuator mounting in LC3 test scenarios

The dial gauges were monitored and recorded manually whereas all other systems were scanned automatically by the logging system.

3.7 DATA LOGGING AND VALIDATION

All strain gauges and displacement transducers were wired in to an 880 channel logger supplied by Sunnyside Systems Limited (see Figure 3.10). The bespoke system was developed combining a number of smaller units. Excitation voltages for strain gauge and transducer channels were pre-set. Averaging of multiple samples through an AC cycle minimised fluctuations. Output signals were passed directly to a Microsoft Excel spreadsheet, pre-programmed to assign and convert raw values to displacements, strain measurements and force data as described in Section 4. Each scan of the instrumentation was activated at the controlling PC and was completed for all 880 channels within 15 seconds. Importantly the system was initialised when first activated. At subsequent stages through the test, whether the system remained energised or not, the same reference datum was used.

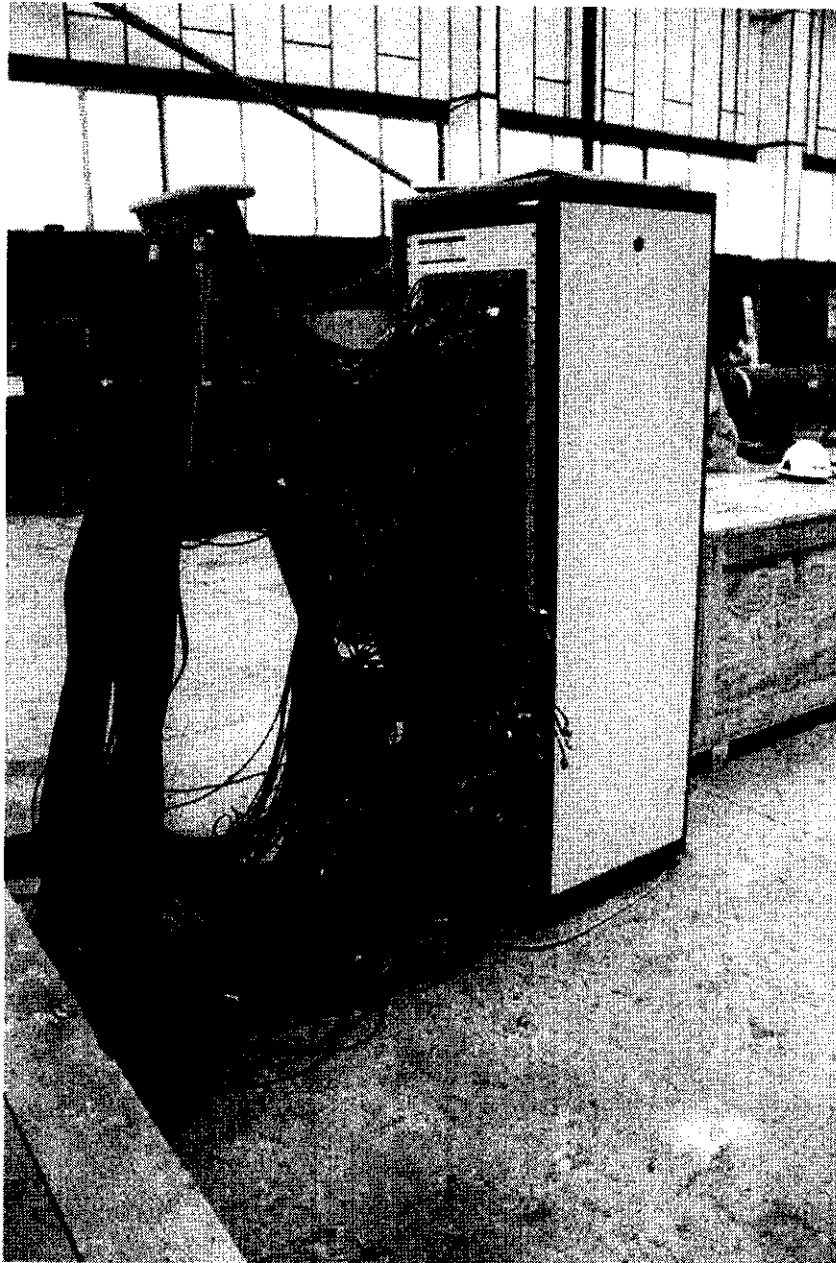


Figure 3.10 Data logger with improvised cable support

With the complexity of the system great care was taken to ensure cables were labelled at both ends and that the channel assignment and connector wiring were correct. Furthermore as the system was dismantled on completion of the test programme the excitation voltages at every channel were measured and cross-checked with the values within the logging spreadsheet.

Voltages from the load and displacement signals from the actuator were also connected directly into the logging system to provide for simultaneous data capture.



At the start of individual tests a number of checks were performed:

- comparison with data at end of previous test (allowing for expected changes due to repairs)
- repeatability of readings to ensure system was fully warmed up
- detection of extreme or out of range values. Where necessary connections were checked or gauges replaced. Only when the system was functioning satisfactorily did testing commence.

In addition the AVT site team monitored the system throughout each test. BOMEL personnel similarly interrogated the data in comparison with predicted values and on the basis of equilibrium checks.

3.8 DATA PROCESSING

As noted above and described more fully in Section 5, the Microsoft Excel spreadsheet into which the raw signals were channelled was pre-programmed by AVT and BOMEL to determine displacements, forces, etc. In addition graphs were set up to plot measurements at specific locations within the structure as the tests progressed and to superimpose these on predicted values. The software provided an important basis for controlling the tests and is used extensively in the interpretation of the responses in companion reports.

3.9 OTHER MONITORING SYSTEMS

In addition to the instrumentation outlined above, a number of other 'systems' provided important information on structural performance.

3.9.1 Paint System

Prior to each test the frame was painted, firstly for clarity in photographic and video footage but secondly to provide an indication of plasticity. If the member strains are large, the paint flakes from the surface of the steel. Furthermore, as shown in Figure 3.11, zones of yielding develop clear diagonal striations or Lüders lines providing an important indication of the extent of plasticity to supplement the load level data from load cells.

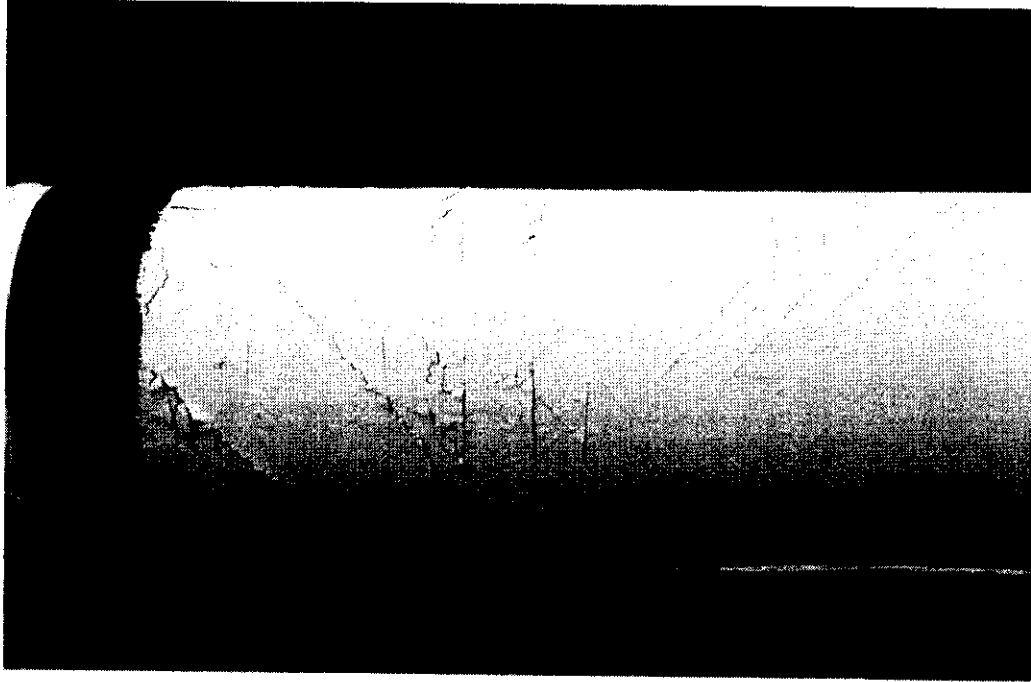


Figure 3.11 Plasticity indicated in the striations of the paint coating

3.9.2 Video Footage

Video recordings were taken of all aspects of every test. Global shots were supplemented with local views from fixed camera positions. The movement of key components within the shot and globally against the fixed surround are instructive. In addition the relay of the video to remote monitors (see Figure 3.12) enabled local deformations and cracks to be detected whilst keeping people clear of the heavily loaded structure.

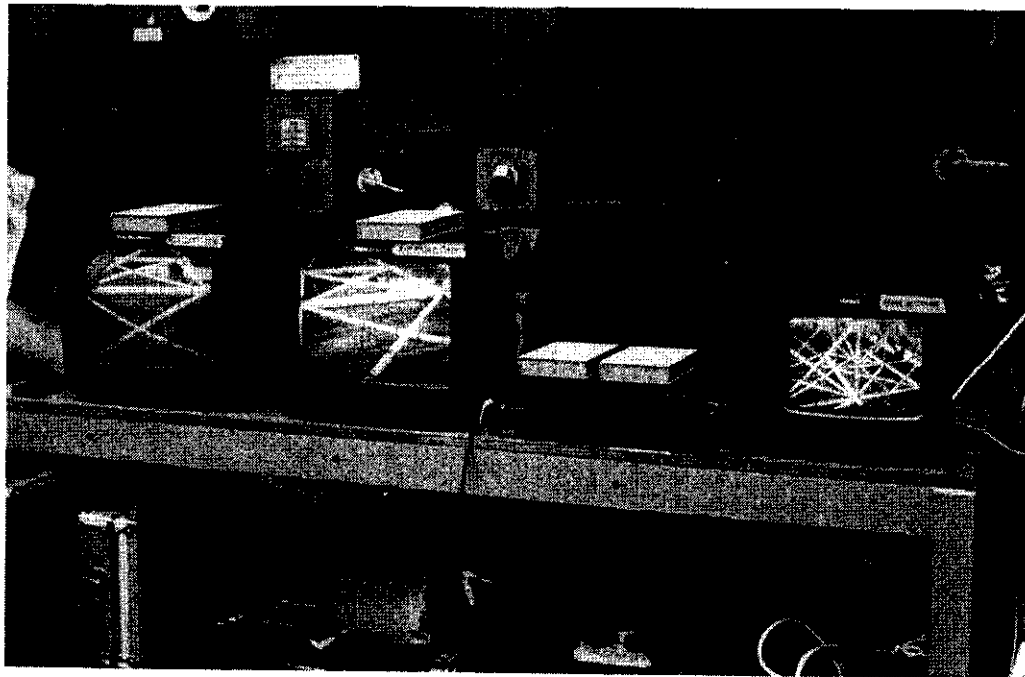


Figure 3.12 Remote monitors relaying local and global shots of the frame test



The timing of the video shots was directly synchronised with the loading and instrumentation scan records made for each test.

3.9.3 Audio

Another important aspect when monitoring the tests was sound. Creaking of the test frame and reaction rig was clearly audible and helped identify zones of significant displacements or cracking.

3.10 SUMMARY

The above descriptions have demonstrated that monitoring of the 3D frame tests was carefully planned and executed. The systems were specified to a high standard and were validated and cross-checked at every opportunity. It can also be seen from companion test reports that the stability and consistency of the gathered data are exceptionally good and provide an important basis for confident interpretation of the findings.



4. SIGN CONVENTION

A very important aspect in correctly interpreting the output from the instrumentation is definition of the sign convention adopted. The scheme adopted by AVT based on the global x, y, z coordinate system defined by BOMEL and used by the benchmark analysts is as follows.

4.1 GLOBAL AXES

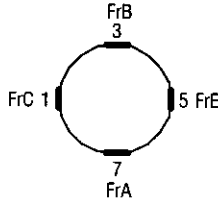
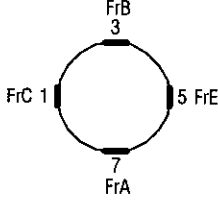
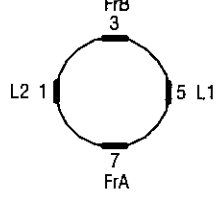
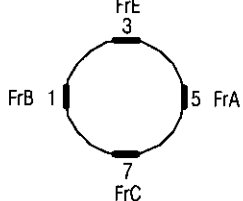
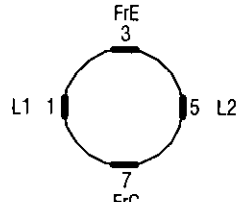
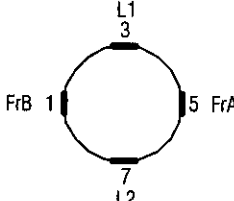
The x, y, z coordinate scheme for the frame is shown in the node and member numbering diagrams in Appendix A. Considering the test frame in-situ within the reaction rig (see Figure 1.1) the definition is:

x direction = vertical	Positive downwards (Frame B to A)
y direction = horizontal (side to side)	Positive from left to right (Frame E to C) looking into the frame
z direction = horizontal (lengthways)	Positive from back to front (Level 2 to Level 1)

4.2 STRAIN GAUGE CONVENTION

For the load cells and site installed strain gauges eight positions at 45° intervals around the member circumference were identified. Rosette gauges were installed at the feet of the frame at its connection to the rig at all eight locations (see drawings in Appendix A). In general, for axial force and moment measurements, only alternate positions 1, 3, 5 and 7 were used. The axis definition for all members is described in Table 4.1 below. The diagrams are illustrative; looking along the member in the given direction the numbered gauge positions are noted and other parts of the frame generally to that side of the member are indicated. For diagonal bracing (which includes all load cells) Gauges 1 and 5 are positioned in-plane with 3 and 7 out-of-plane. In all cases positive moments are defined based on $\epsilon_1 - \epsilon_5$ in-plane and $\epsilon_3 - \epsilon_7$ out-of-plane, where ϵ_1 , ϵ_3 , ϵ_5 and ϵ_7 are the recorded strains at positions 1, 3, 5 and 7 respectively.

Table 4.1 Sign convention and numbering scheme for linear strain gauges

Frames	Members	Viewing Direction	Illustration
A, B	Legs	Towards z	
	Diagonal braces	Towards z	
	Transverse braces	Towards y	
C, D, E	Legs - defined in Frames A & B		
	Diagonal braces	Towards z	
	Transverse braces	Towards x	
1, 2	Diagonal braces	Towards y	
	Horizontal braces - defined as transverse braces in Frames A & B		
	Vertical braces - defined as transverse braces in Frames C, D & E		



4.3 ROSETTE POSITIONING

Rosettes at the base of the legs are positioned at 45° intervals around the circumference. Principal positions 1, 3, 5 and 7 etc., are defined as for Frames A and B in Table 4.1. The intermediate gauges 2, 4, 6 and 8 provide additional data for shear and moment calculations. The 45° rosette Element A is aligned with the leg axis with a clockwise convention giving Element C in the hoop direction.

SCF rosettes are oriented with Element A parallel to the weld toe, again with a clockwise convention, giving Element C perpendicular to the weld toe. Appendix A provides further details.

4.4 DISPLACEMENT MONITORING

Global displacements are monitored and resolved using the axis system defined in Section 4.1. For local displacements at a joint, compressive displacements are negative and tensile elongations positive.

4.5 SUMMARY

The above convention was implemented in the installation and logging of the instrumentation. The convention stems from the definition used by BOMEL in analysis and provided for use by benchmark analysts. The interpretation of the test results follows the given scheme.



5. SPREADSHEET DATA LOGGING SYSTEM

As described in Section 3 the 880 instrumentation channels on the test frame were scanned by the electronic logging system and the raw results were written to a Microsoft Excel spreadsheet. The same spreadsheet was also programmed to reduce the raw values to forces, displacements etc., and to plot various parameters through each test. Understanding the information contained within, and the structure of, the spreadsheet is therefore essential for interrogating the frame responses.

5.1 SPREADSHEET LAYOUT

The same basic spreadsheet was used for all tests. The sequence and content of sheets within each file is as follows:

Revisions: Sheet inserted by AVT after all tests were completed to note any special features, changes or malfunctions identified post test.

All subsequent changes made by BOMEL (eg. to correct for initial load offsets) have also been logged on this sheet.

The sequence of file references from on-site records, to AVT 'final deliverable' files, to BOMEL output is also logged.

Raw: Sheet captured raw voltages at each scan of the logging system, automatically inserting a new column of values. Figure 5.1 shows an example, where:

Channel: sequential channel No. in logger

Sensor type: SG-FLA 6 6mm linear strain gauge

SG-FRA 3 3mm rosette strain gauge

DT-PG 150 150mm stroke Penny & Giles displacement transducer

DT-UM 30 Uni-measure draw wire potentiometer, etc.

Actuator load and displacement signals are in the final channels 879 and 880.

Tag No: LC1 load cell number 1

SG17 site installed linear strain gauge on Member 17

SG35-4 fourth set of rosette strain gauges at 'foot' of frame on Member 35

SCF30 SCF rosette at position 30 as specified by BG

ASG29 additional strain gauge numbered 29 associated with Node 7 SCF reading.

DT21 displacement transducer monitoring at Node 21



SG84A surface mounted strain gauges on Member 84 near joint (A =near, B = far)

Ref: 1, 5 in-plane linear strain gauges
 3,7 out-of-plane linear strain gauges
 A,B,C rosette gauge elements A to C clockwise, A parallel to weld toe for SCFs and along axis of leg at frame feet

Ten,Comp indicator for surface mounted displacement transducers

x,y,z orientation of global displacement monitoring transducers

Member: 23 member number for strain gauges, node number for transducers

Location: FrA 1E-2D members in Frame A running from Level 1 on Frame E to Level 2 on Frame D
 Rig E 1 A node of rig defined by coincidence of Frame A, Level 1 and Frame E axes

Max yield: value) For strain gauges: *Max* and *Min* voltage recorded
Min yield: value) across all columns for this channel - used to check strains have not exceeded nominal yield value for member

For displacements transducers: *Max* column gives range setting and *Min* column gives initial position for transducer

Units: Volts in all cases

Two blank columns

Data columns: Scan 'n' numbers increment automatically. Date and time entered manually with each scan. Raw voltages below. Maximum scans per datafile 245.

Data: Conversion sheet calculating microstrain and displacement values - rows have one-to-one correspondence with 'Raw' sheet. Figure 5.2 shows an example:
Channel, Sensor type, Tag no, Ref,
Member: All as per Raw
Range: Measuring range in engineering units
Calibration factor: Conversion factor from volts to engineering units
Units: Engineering units eg microstrain, mm etc
Tension/compression: Cell highlighted for strains outside elastic range $\pm 1350 \mu\epsilon$
Diff check: Check to highlight minimal ($<20\mu\epsilon$) change in reading possibly indicating faulty gauge
Graph label: '54 measured' - axial force measured in Member 54 -

label used in graph legend. '54 IP measured' - in-plane bending moment in Member 54 etc

Scan data: Difference between raw measurements at scan 'n' and the datum Scan 1 are used to determine the incremental strain under applied load

Subsequent rows calculate member forces etc., as shown in Figure 5.3

AXLC1: In these rows the initial columns are used to indicate the calculation being performed (eg. AXLC1 - load cell one axial force) using average of four channels (eg. channels 1 to 4) as noted and conversion factor from load cell calibration test (eg. 0.562 from Table 3.1) to give force in kN.

Pred 1: Provides a matrix of nodal displacements and member forces for different levels of applied load from analytical predictions. These can be plotted in combination with the measured values in subsequent graphs

Global xyz: Calculates global x, y and z movements of node points from three transducers based on 'raw' values. These 'resolved' measurements are presented in the 'Data' sheet.

Graphs: Subsequent sheets present pre-defined graphs. The following examples interpret the naming scheme on the spreadsheet tabs. Figure 5.4 presents some examples from the Loadcase 2 test and AVT file LC2a-test.xls.

N45 Disp	displacements at Node 45
Global	overall load deflection response from actuator
FrA TED For	member forces in the top bay (Levels 1 to 2) of Frame A between Frames E and D
FrA ED TBU Mom	moments in the upper part of the top bay compression brace (ie. X node to Level 1) of Frame A between Frames E and D
FrE TB Comp	load deformation response across compression joint in top bay (Levels 1 to 2) of Frame E
Fr E Leg For	member forces in Frame E legs
Lev 2-Dia For	member forces in the diamond bracing in Level 2
Lev 1 - LC3X For	forces in Level 1 X braces installed for Loadcase 3
Fr Feet	axial forces calculated at base of frame legs at connection to rig from rosette

BOMEL 3D FRAMES PROJECT

Loadcase 2 - Test

20-Jun-98

Revision 'Final Master' 10 Oct 98 10:20

Scan 1 Scan 2 Scan 3

CHANNEL	SENSOR TYPE	TAG No.	REF	MEMBER	LOCATION	MAX Yield	MIN Yield	UNITS	20-Jun 10:33	10:44	10:46
1	SG - FLA 6	LC1	1	59	FRAME A 1E-2D	0.00080007	5.8838E-05	Volts	5.88E-05	8.88E-05	0.000114
2	SG - FLA 6		3			0.00067546	-0.0007893	Volts	0.000342	0.000363	0.000384
3	SG - FLA 6		5			0.00086057	0.00019456	Volts	0.000195	0.000218	0.000241
4	SG - FLA 6		7			0.00222605	0.00028123	Volts	0.000281	0.000314	0.000341
5	SG - FLA 6	LC2	1	58	FRAME A 1D-2E	0.00012444	-0.0003231	Volts	-8.93E-05	0.000113	-0.000119
6	SG - FLA 6		3			0.00131516	-4.18E-05	Volts	1.98E-05	7.06E-06	6.35E-07
7	SG - FLA 6		5			0.00025393	-0.0002482	Volts	9.74E-05	7.76E-05	6E-05
8	SG - FLA 6		7			-0.0006211	-0.0019153	Volts	-0.000621	-0.000651	-0.000665
9	SG - FLA 6	LC3	1	57	FRAME A 1E-2D	0.00035652	-0.0002386	Volts	-0.000187	-0.000161	-0.000137

Figure 5.1 Structure of Raw sheet

BOMEL 3D FRAMES PROJECT

Loadcase 2 - Test

20-Jun-98

Revision 'Final Master' 10 Oct 98 10:20

Scan 2

CHANNEL	SENSOR TYPE	TAG No.	REF	MEMBER	LOCATION	RANGE	CAL FACTOR	UNITS	TENSION	COMP	DIFF	Graph Label
1	SG - FLA 6	LC1	1	59	FRAME A 1E-2D	2000	400000	Microstrain	0	0	296	12
2	SG - FLA 6		3			2000	400000	Microstrain	0	0	586	8
3	SG - FLA 6		5			2000	400000	Microstrain	0	0	266	9
4	SG - FLA 6		7			2000	400000	Microstrain	0	0	778	13
5	SG - FLA 6	LC2	1	58	FRAME A 1D-2E	2000	400000	Microstrain	0	0	179	-9
6	SG - FLA 6		3			2000	400000	Microstrain	0	0	543	-5
7	SG - FLA 6		5			2000	400000	Microstrain	0	0	201	-8
8	SG - FLA 6		7			2000	400000	Microstrain	0	0	518	-12
9	SG - FLA 6	LC3	1	57	FRAME A 1E-2D	2000	400000	Microstrain	0	0	238	10

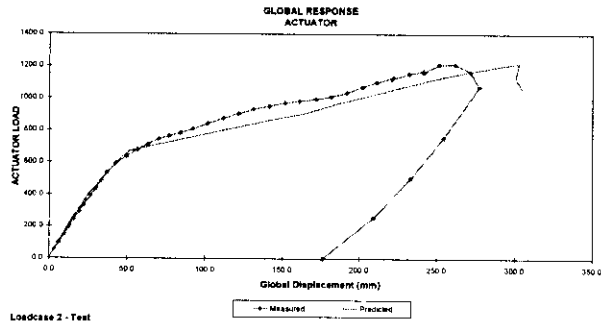
Figure 5.2 Structure of Data sheet presenting raw values in engineering units

881	AXLC 1	AVERAGE 4 CHANNELS	1	4	0.562	kN	59 Measured	6.0
882	AXLC 2	AVERAGE 4 CHANNELS	5	8	0.558	kN	58 Measured	-4.8
883	AXLC 3	AVERAGE 4 CHANNELS	9	12	0.552	kN	57 Measured	5.9
973	OPBLC 1	DIFFERENCE CHANNELS	2	6	0.010526	kNm	59 Measured	-0.1
974	OPBLC 2	DIFFERENCE CHANNELS	6	10	0.010526	kNm	58 Measured	0.1
975	OPBLC 3	DIFFERENCE CHANNELS	10	14	0.010526	kNm	57 Measured	0.0
927	IPBLC 1	DIFFERENCE CHANNELS	1	3	0.010526	kNm	59 Measured	0.0
928	IPBLC 2	DIFFERENCE CHANNELS	5	7	0.010526	kNm	58 Measured	0.0
929	IPBLC 3	DIFFERENCE CHANNELS	9	11	0.010526	kNm	57 Measured	0.0

Figure 5.3 Subsequent presentation of calculated forces in Data sheet

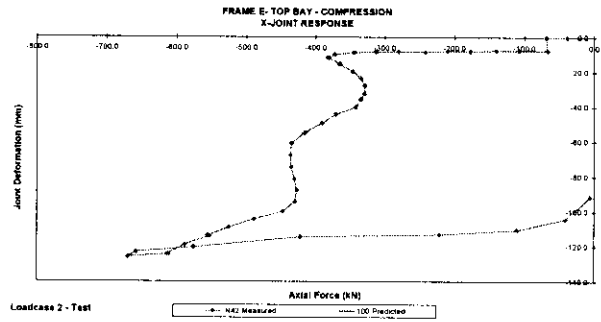
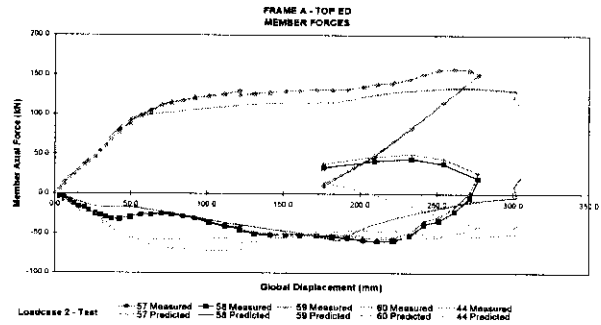


BOMEL ENGINEERING CONSULTANTS



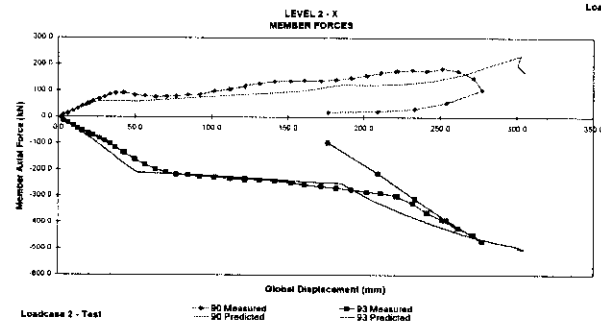
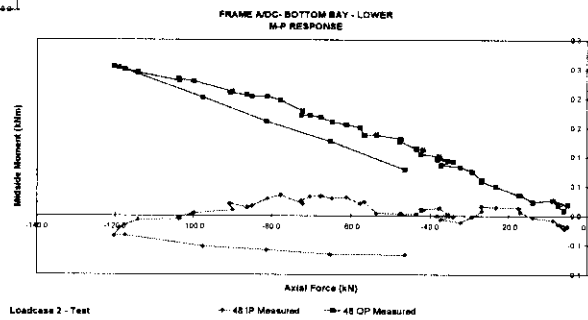
FrA TED For sheet

Global sheet



FrA DC BBL Mom sheet

FrE TB Comp sheet



N29 Disp sheet

Level 2-X For sheet

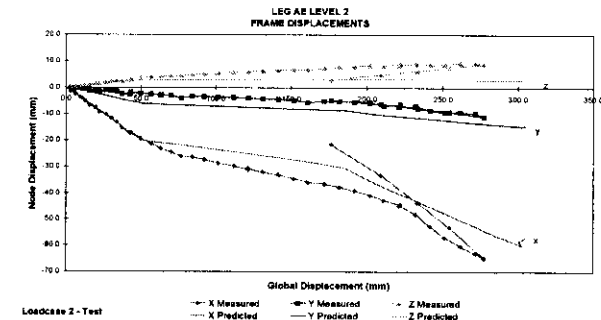


Figure 5.4 Example plots showing measured and predicted values



5.2 PROCEDURES FOR DATA CAPTURE

The scan numbers associated with each set of results uniquely define the point in the test. Records from the actuator system were logged against scan number. The number was displayed on the board (Figure 1.1) and used in photographic and video records.

After each scan during the test the spreadsheet file was saved out to ensure that if there were corruption previous records would not be affected. In the event no such problems arose.

For speed and ease of file handling not all scans were saved to one spreadsheet. However, once the data were validated post test by AVT, the scans were consolidated. In the case of some cyclic tests the number of scans exceeded the spreadsheet size limit and two sequential files are retained.

In general the records from the trials, during which the frame was set to the datum position and the system functionality was tested, are separated from the test. Similarly the records from the cutout subsequent to the test are stored separately.

5.3 FINAL DATAFILES

An initial and final issue of the spreadsheet files was made by AVT. The final version (denoted a or b) are provided on the project CD. The file names are as follows:

LC1a_Test	Loadcase 1 test
LC1a_Trial	Loadcase 1 trial
LC1Ca_Test	Loadcase 1 cyclic test
LC1Ca_Trial	Loadcase 1 cyclic trial
LC1CAb_Cut	Loadcase 1 cyclic A cut out
LC1CAb_Test	Loadcase 1 cyclic A test
LC1CAb_Trial	Loadcase 1 cyclic A trial
LC2a_Cut	Loadcase 2 cut out
LC2a_Test	Loadcase 2 test
LC2a_Trial	Loadcase 2 trial
LC2Ca_Cut	Loadcase 2 cyclic cut out
LC2Ca_Test1	Loadcase 2 cyclic test - part 1
LC2Ca_Test2	Loadcase 2 cyclic test - part 2
LC2Ca_Trial	Loadcase 2 cyclic trial
LC3a_Cut	Loadcase 3 cut out
LC3a_Test	Loadcase 3 test



LC3a_Trial Loadcase 3 trial
LC3Ca_Cut Loadcase 3 cyclic cut out
LC3Ca_Test1 Loadcase 3 cyclic test - part 1
LC3Ca_Test2 Loadcase 3 cyclic test - part 2
LC3Ca_Trial Loadcase 3 cyclic trial
LC3CAb_Test Loadcase 3 cyclic A test
LC3CAb_Trial Loadcase 3 cyclic A trial

Appendix C contains AVT's final report⁽⁴⁾ which accompanies the data files. Further explanation of changes or reconnections highlighted within the spreadsheet are presented.

In subsequent investigation BOMEL introduced corrections for load cell offsets in the 'data' sheet, additional graphs to extend the presentation and calculations for SCF evaluation. In addition minor corrections to labelling were made. Such changes are fully documented on the 'Revisions' sheet and are traceable back to the final AVT supplied files.

These modified files form part of the deliverables on the project CD and are called up from the relevant investigative reports.



6. REFERENCES

1. BOMEL Limited. 'Joint Industry Tubular Frames Project - Phase I/II - Specification for strain and displacement measurement', BOMEL Reference C636\06\217S Rev 0, November 1997.
2. Health and Safety Executive (Department of Energy). 'Background Notes to New Fatigue Design Guidance for Steel Welded Joints in Offshore Structures', HMSO, 1984.
3. AV Technology Limited. 'BOMEL Frames Project - Load Cells', AVT Reference AVT/3581/S1, February 1998.
4. AV Technology Limited. '3D Frames Project - Data collection and presentation of final data files', AVT Reference AVT/3581/R1, November 1998.
5. BOMEL Limited. '3D test set up', BOMEL Reference C636\06\313R, August 1999.



APPENDIX A

INSTRUMENTATION SUMMARY

Frame Test / Loadcase Nomenclature
Node and Member Numbering Schemes
Load Cell Details - C636\15\011D Rev D
Strain Gauging Details - Sheet 1 of 2 - C636\15\012D Rev B
Strain Gauging Details - Sheet 2 of 2 - C636\15\013D Rev B
Node 7 SCF Gauge Positions - C636\18\017D
Joint Deformation Monitoring - C636\15\016D Rev 0
Rig Node Displacement Monitoring - C636\25\075D

FRAME TEST / LOADCASE NOMENCLATURE

LC	x	y	z
----	---	---	---

LC = Loadcase

x = 1, 2 or 3 indicating line of actuator loading (Line C, E or A respectively)

y = blank = static test
 = C = cyclic test

z = blank for static and baseline cyclic tests
 = A for alternative cyclic loading scenarios

Figure A.1 to A.6 show the member and node numbering schemes adopted in each test. In general the numbering is consistent. The principal changes are associated with the stub bracing for each loading position and the addition of the Level 1 X bracing for the Loadcase 3, Loadcase 3CA and Loadcase 1CA scenarios.

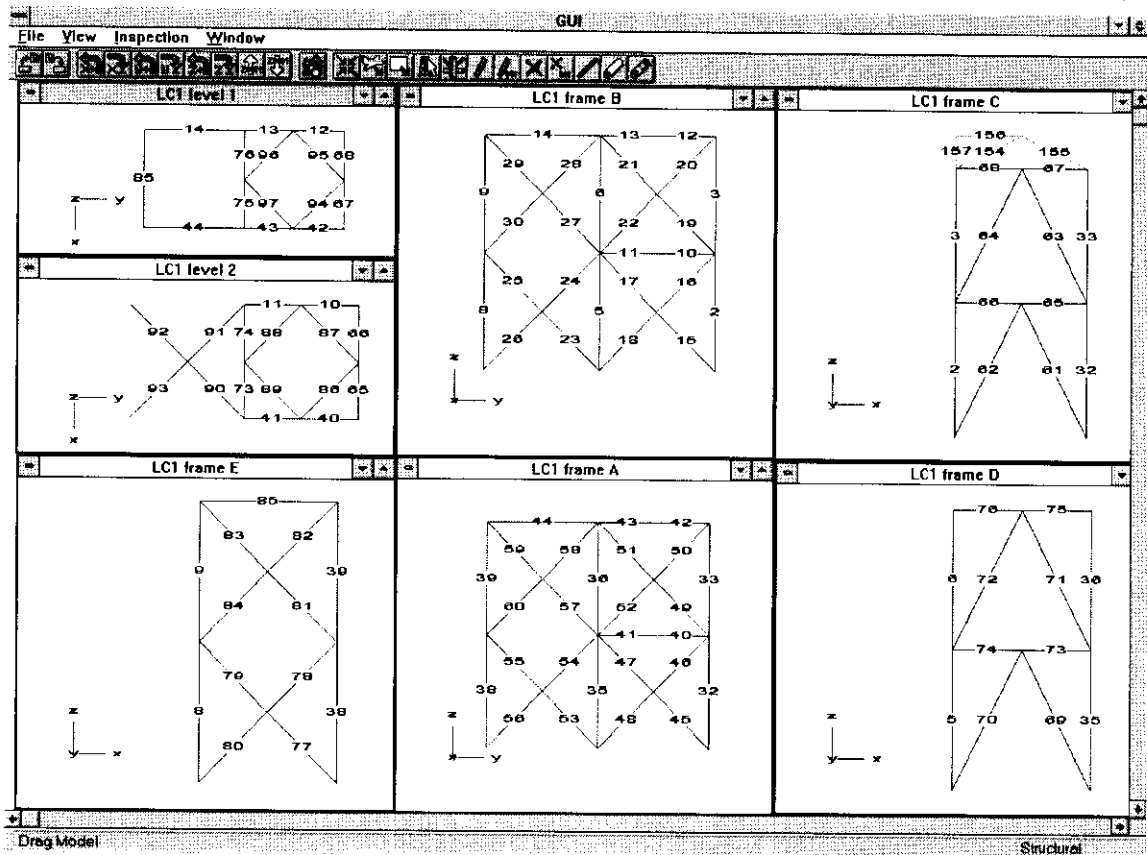


Figure A.1 Member numbering system Loadcase 1

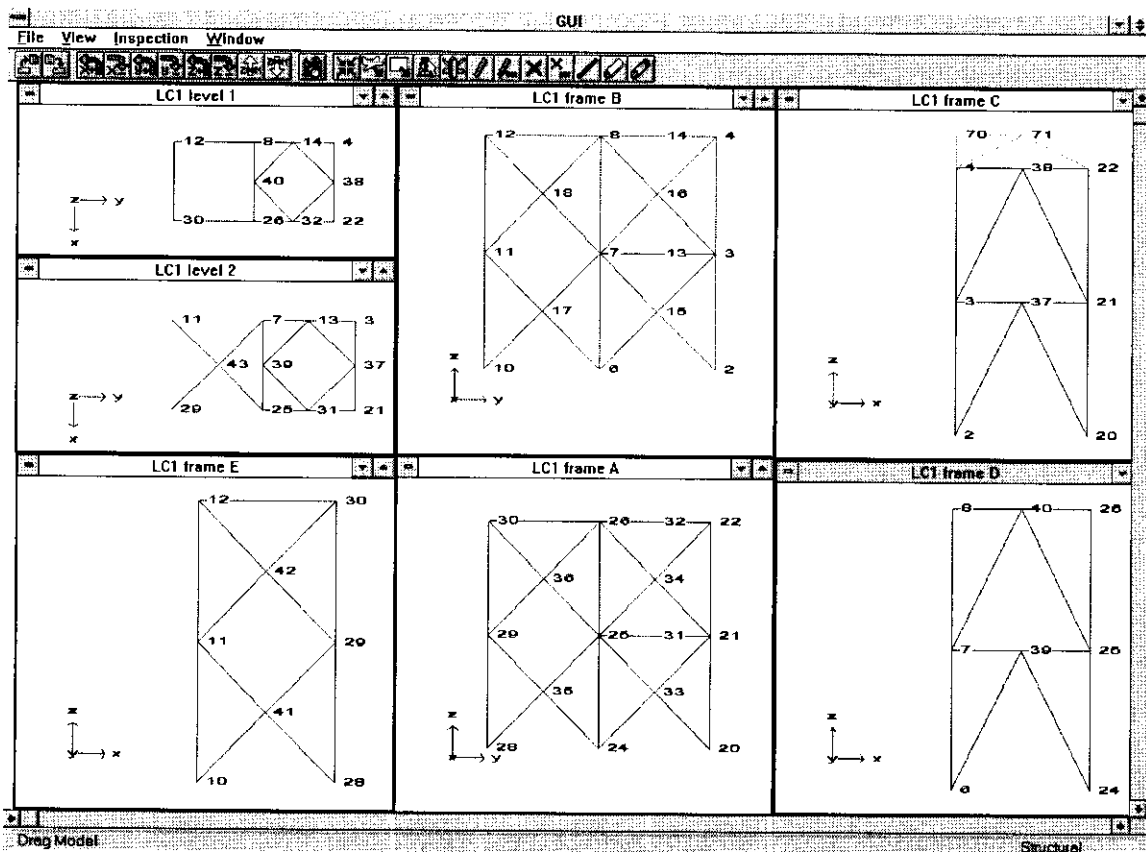


Figure A.2 Node numbering system Loadcase 1

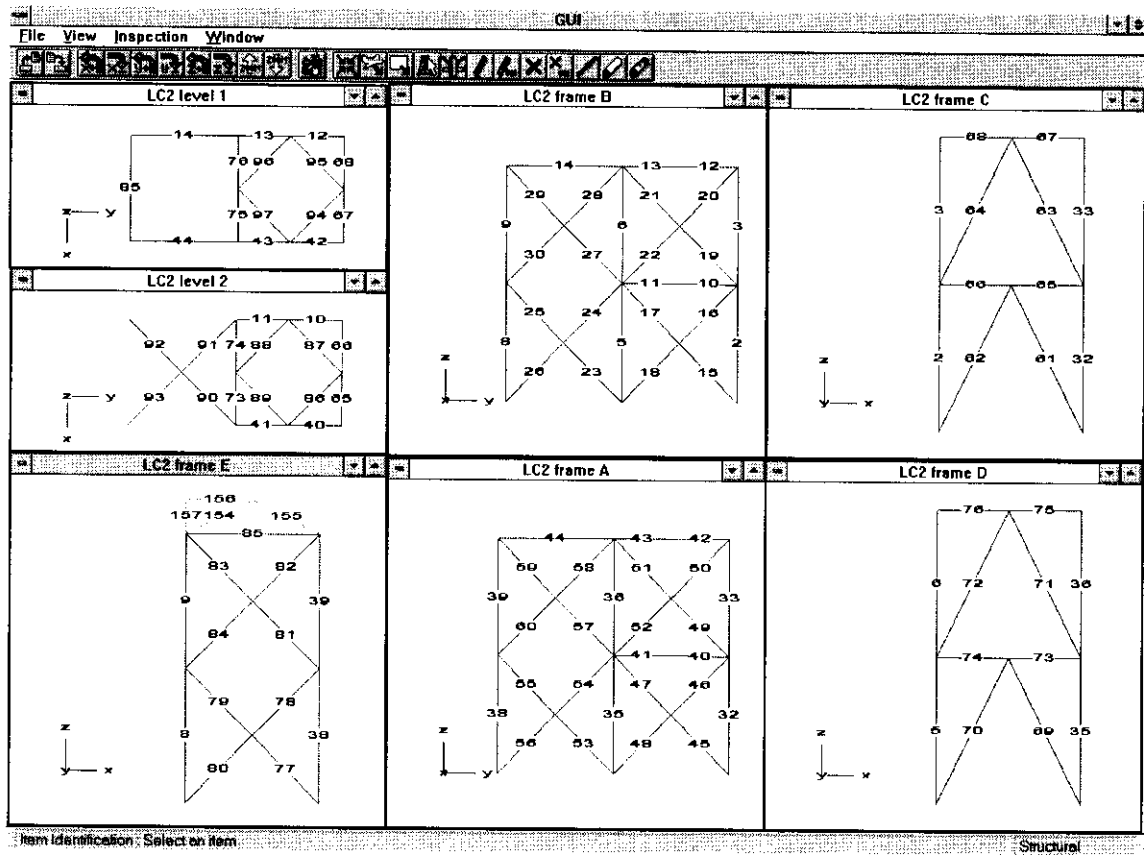


Figure A.3 Member numbering system Loadcase 2

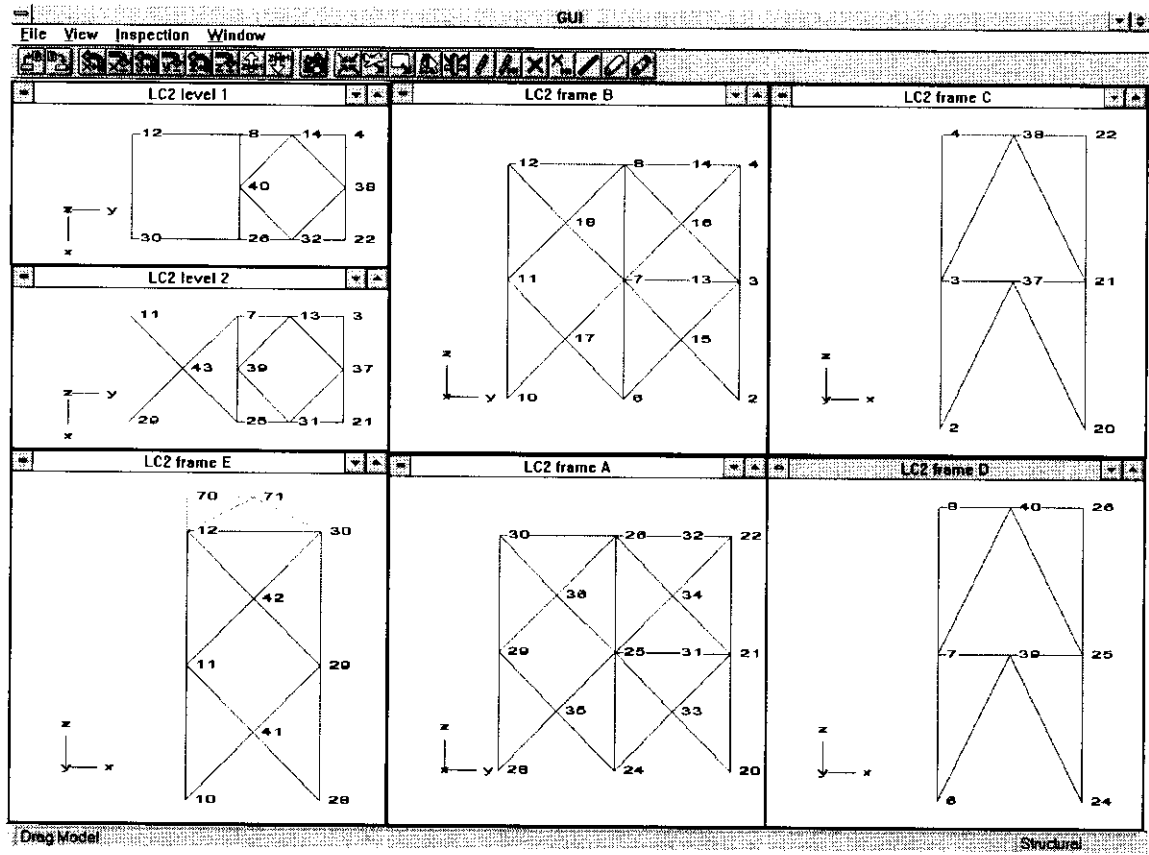


Figure A.4 Node numbering system Loadcase 2

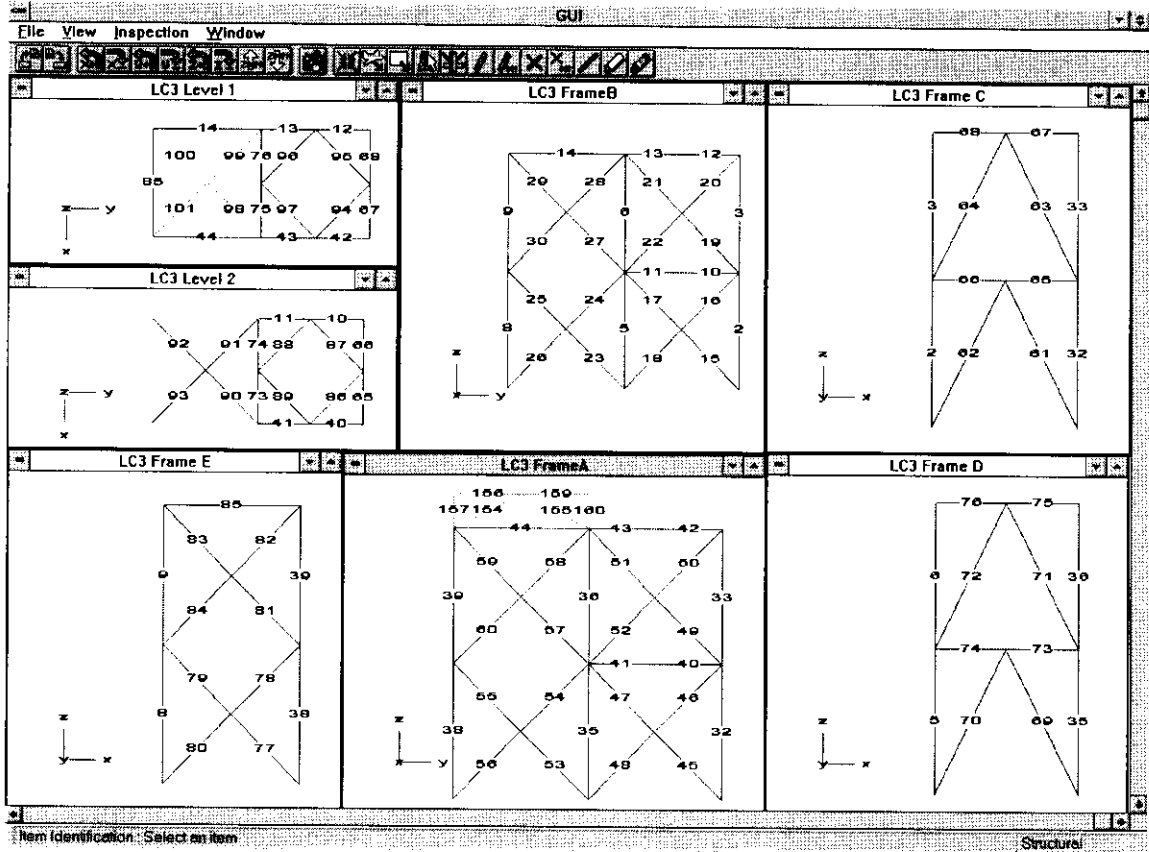


Figure A.5 Member numbering system Loadcase 3

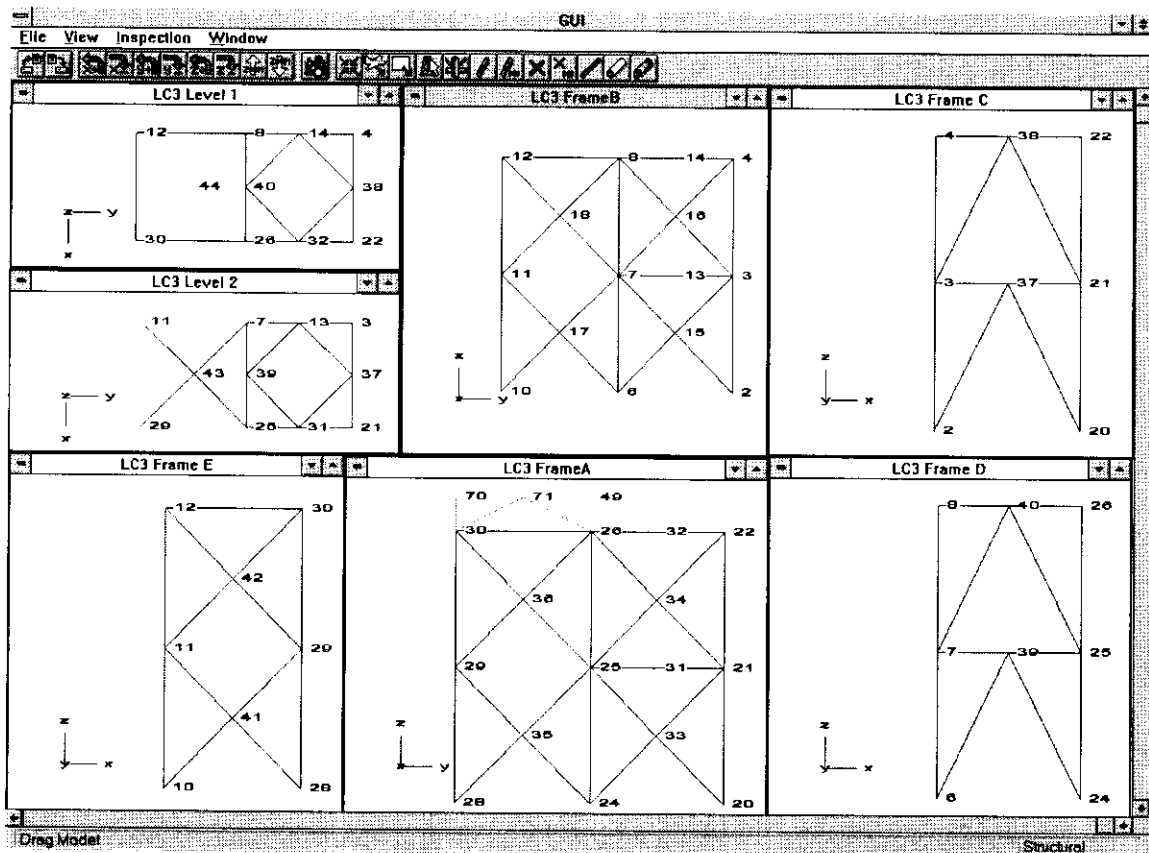


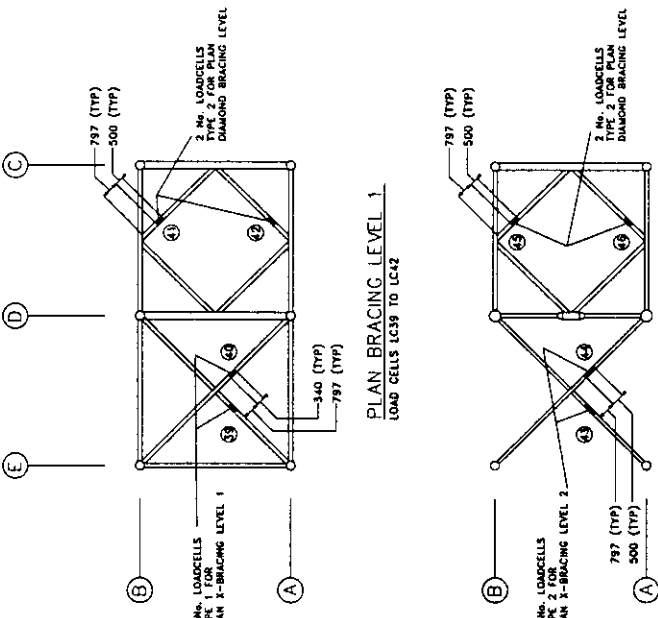
Figure A.6 Node numbering system Loadcase 3

NOTES

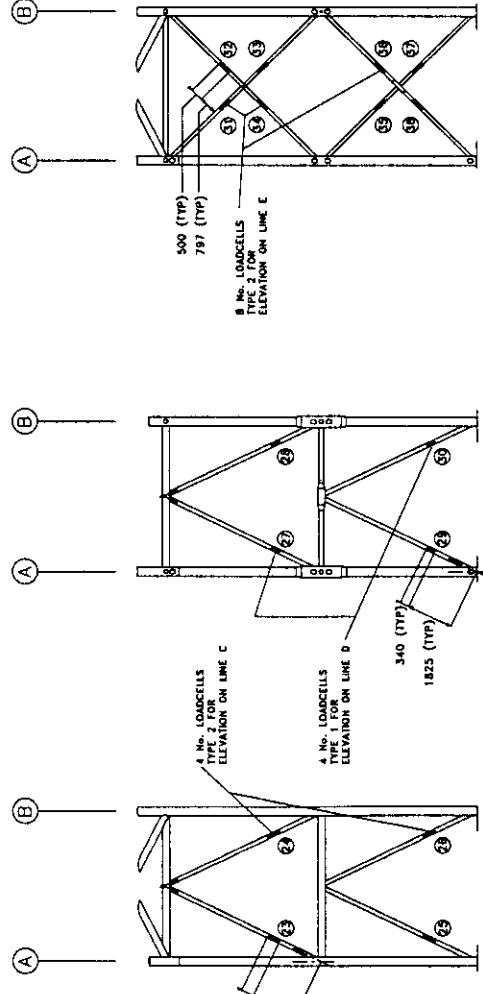
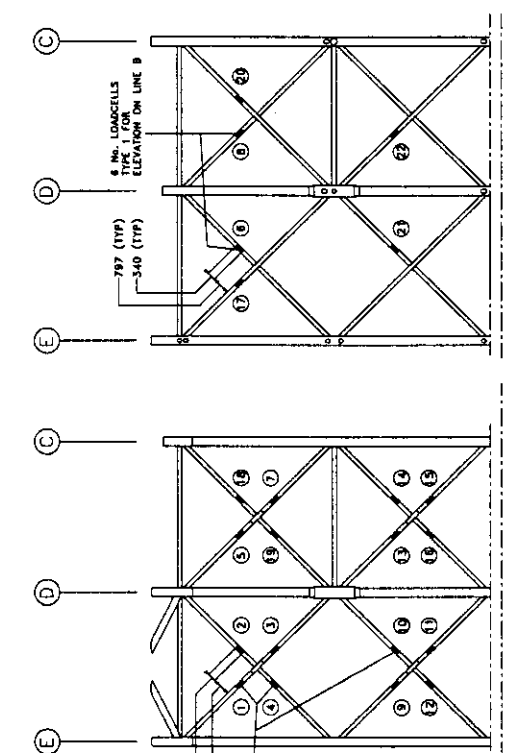
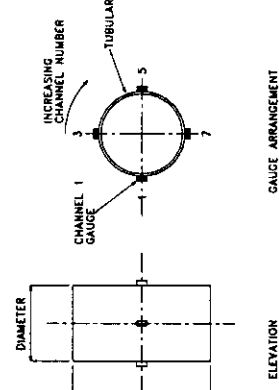
1. ALL LOAD CELLS TO BE MANUFACTURED FROM HOT FINISHED HOLLOW CIRCULAR SECTION TO BS4606 PART 2 MADE FROM STEEL TO BS4360 GRADE 50C.
2. ALL LOAD CELLS TO BE MANUFACTURED WITH ENDS MACHINED FLUSH AND SQUARE END PREPARATION FOR WELDING WILL NOT TAKE PLACE UNTIL AFTER CALIBRATION.
3. ALL DIMENSIONS ARE IN MM.
4. ALL GAUGES TO BE APPLIED IN ACCORDANCE WITH BOMEL DOCUMENT No. C638/08/21/15.
5. TOTAL NUMBER OF STRAIN GAUGE CHANNELS PER LOAD CELL = 4.
6. LOAD CELLS TO BE CLEARLY AND PERMANENTLY IDENTIFIED AS LCI TO LC46.
7. EACH LOAD CELL TO BE IDENTIFIED ON THIS DRAWING THUS - (4) LOAD CELL No. IDENTIFIED ON THIS DRAWING THUS - (4) LOAD CELL No. IDENTIFIED ON THIS DRAWING THUS - (4) AND PERMANENTLY IDENTIFIED IN THE FOLLOWING MANNER - LCI1, 11 - 14 etc LCI2, 21 - 24 etc LCI3, 31 - 34 etc LCI4, 41 - 44 etc LCI5, 51 - 54 etc LCI6, 61 - 64 etc LCI7, 71 - 74 etc LCI8, 81 - 84 etc LCI9, 91 - 94 etc LCI10, 101 - 104 etc LCI20, 201 - 204 etc
8. LOAD CELLS TO BE CLEARLY AND PERMANENTLY IDENTIFIED AS LCI TO LC46.
9. EACH LOAD CELL TO BE IDENTIFIED ON THIS DRAWING THUS - (4) LOAD CELL No. IDENTIFIED ON THIS DRAWING THUS - (4) AND PERMANENTLY IDENTIFIED IN THE FOLLOWING MANNER - LCI1, 11 - 14 etc LCI2, 21 - 24 etc LCI3, 31 - 34 etc LCI4, 41 - 44 etc LCI5, 51 - 54 etc LCI6, 61 - 64 etc LCI7, 71 - 74 etc LCI8, 81 - 84 etc LCI9, 91 - 94 etc LCI10, 101 - 104 etc LCI20, 201 - 204 etc
10. GAUGE POSITIONS AND CHANNEL NUMBERS TO BE CLEARLY IDENTIFIED.
11. FOR GENERAL NOTES REFER TO DRG. C638/15/0020

LOAD CELL SCHEDULE

LOAD CELL	DIAMETER (mm)	WT. (mm)	LENGTH (mm)	No. OFF
TYPE 1	168.3	5.0	340	28
TYPE 2	168.3	5.0	500	18



PLAN BRACING LEVEL 2
LOAD CELLS LC43 TO LC46



Drawing No. C638/15/0110

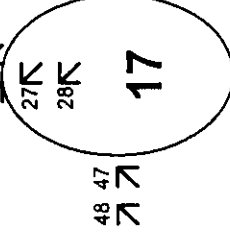
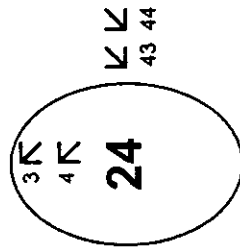
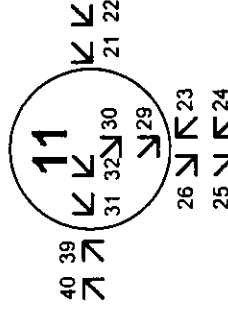
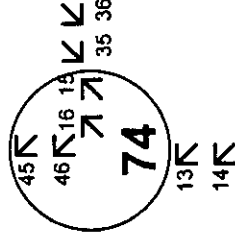
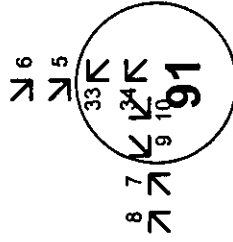
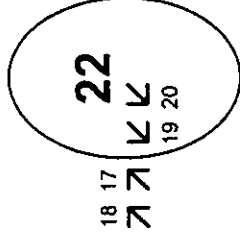
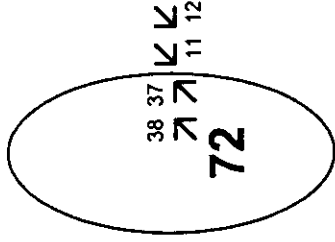
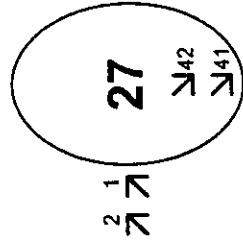
1 OF 2
B 920.5 x 650 FAB. BEAM
(DATUM LINE)

5 4 3 2 1 A B C D

BOMEL CONSULTING
15000 Victoria Road
Pittville, Mansfield, Nottingham, Notts, UK
Tel: +44 (0)1430 77707
Fax: +44 (0)1430 77707
Drawing No. C638/15/0110

PROJECT: JOINT INDUSTRY PROJECT
CLIENT: B. CALDWELL
BOMEL CONTRACT No. C043808
DATE: 27/8/09
SCALE: 1:100
DRAWING TITLE: **FRAMES PHASE III**
LOAD CELL DETAILS

NODE 7 - SCF GAUGE POSITIONS



Key:

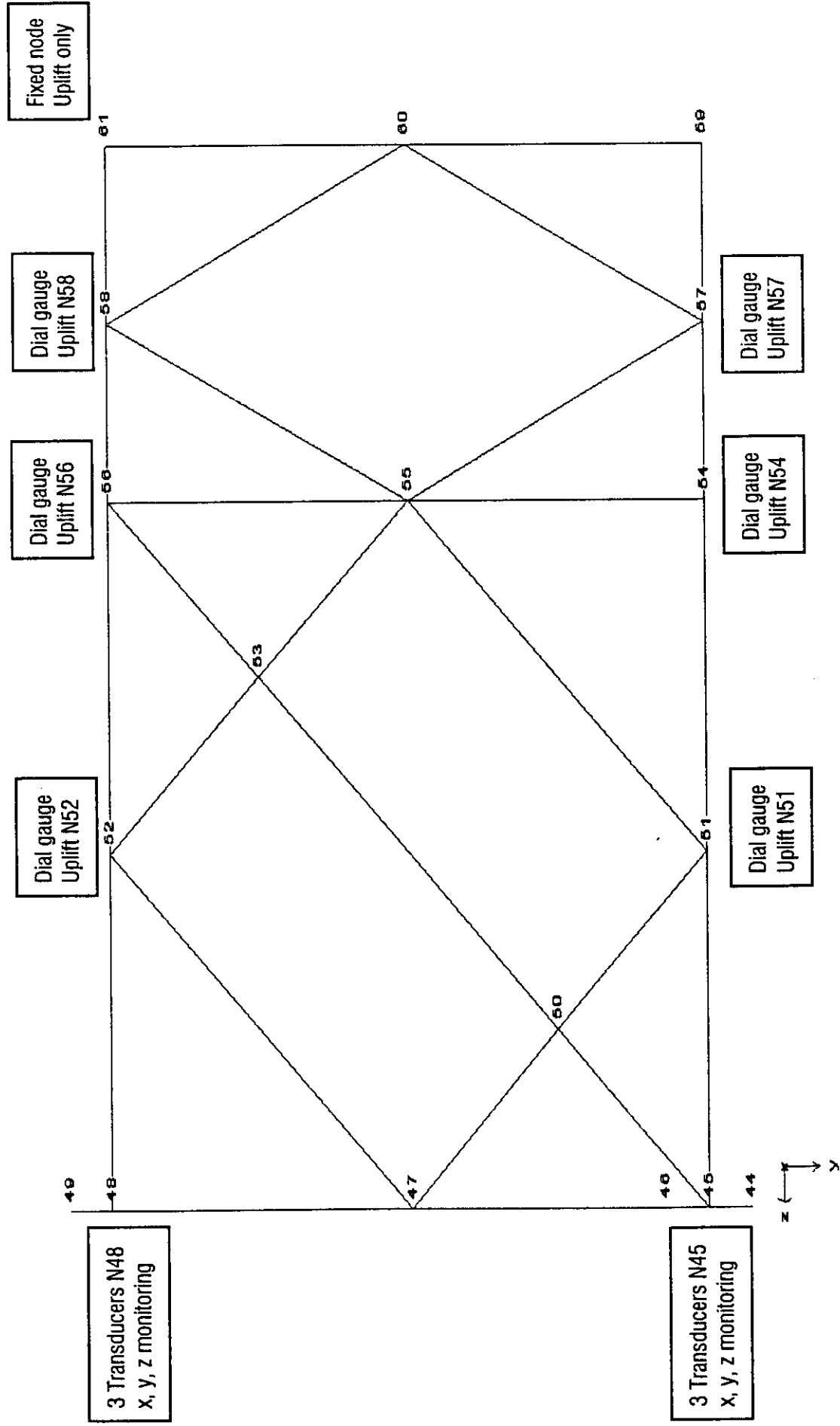


- 41 SCF gauge number
- A, B, C rosette gauge ID, clockwise from A
- A parallel to weld toe

Gauge positions:

- All brace side gauge pairs: 4mm and 12.7mm from weld toe
- Chord side gauge pairs at saddle location: 4mm and 19.9mm from weld toe
- Chord side gauge pairs at crown location: 4mm and 13.0mm from weld toe

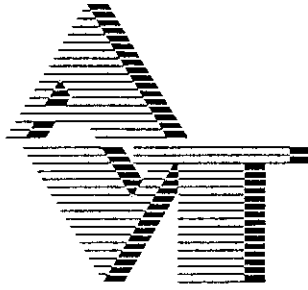
RIG NODE DISPLACEMENT MONITORING - PLAN ON BASE OF RIG



APPENDIX B

**AVT LOAD CELL CALIBRATION REPORT⁽³⁾
- EXCLUDING APPENDICES**

(11 pages)



A V TECHNOLOGY LIMITED

AVTECH House, Birdhall Lane, Cheadle Heath, Stockport, Cheshire SK3 0XU

Telephone: 0161 491 2222 Fax: 0161 428 0127

PROJECT NO. AVT/3581/S1

REVISION NO. 0

PREPARED FOR BOMEL Ltd
Ledger House
Forest Green road
Fifield
Maidenhead
Berkshire
SL6 2NR

ATTENTION OF Mr D. Caldwell
Associate Director

BOMEL FRAMES PROJECT

LOAD CELLS

17 February 1998

APPROVED BY:

Neil Parkinson
Eur Ing Neil Parkinson BSc CEng MIMechE
Technical Director

ABERDEEN OFFICE: A V Technology Ltd, Roevin House, 43 Dee Street, Aberdeen AB11 6DY
Telephone: 01224 583569 Fax: 01224 583572

Registered in England No. 1829338. Registered office: AVTECH House, Birdhall Lane, Cheadle Heath, Stockport, Cheshire SK3 0XU



1. INTRODUCTION

This report details the strain gauging, electrical testing and calibration of the 46 No. load cells supplied to BOMEL for subsequent welding into the 3D frame.

All 46 No. load cell bodies were supplied free-issue to AVT for strain gauging at AVT's premises in Stockport on 8 December 1997. Following calibration by AVT at Hevilifts in Aldridge, West Midlands, load cell Nos. 23 - 26 inclusive were delivered to AKD Engineering in Lowestoft on 23 December and all other load cells were delivered by AVT to AKD Engineering on 9 January 1998.

All work was performed against BOMEL purchase order No. 4787.

2. GENERAL REQUIREMENTS

A total of 46 No. load cells are required, each with 4 No. uni-axial active strain gauges equally spaced. 2 types of load cells are required, in lengths of 350 or 500 mm.

2.1 Strain Gauges

The strain gauging of all 46 load cells are identical, as follows:

- Strain gauges: TML FLA6-11
- Adhesive: TML CN
- Local terminal tags: M-Group CPF- 75C
- Extension cabling: 30 mm lengths of twisted 2 cores (7/0.2) PVC sheathed cable

2.2 Coatings

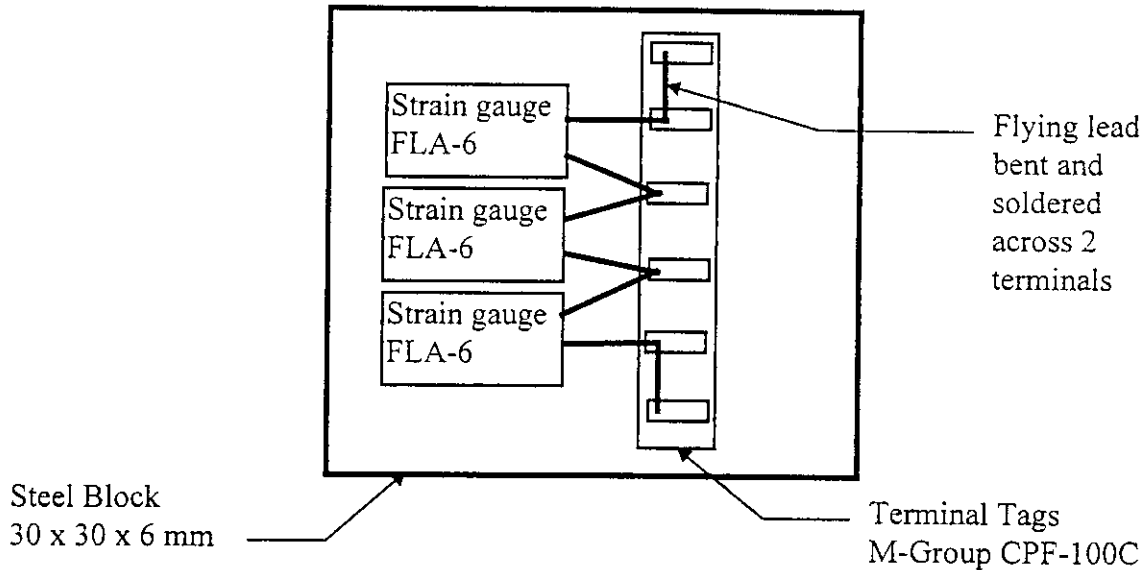
3 stage coating system:

1. 'Bofors' Barrier B
2. M-Group F-Coat
3. Aluminium Foil

3. BRIDGE COMPLETION

All strain gauge elements were individually configured into full bridge circuits using 3 no. dummy strain gauges per active element. The dummy gauges were bonded to an unstressed steel block to provide automatic temperature correction.

3.1 Dummy Block General Arrangement



3.2 Steel Block

30 mm x 30 mm x 6 mm (steel type BS970 1983 080A15)

3.3 Strain Gauges

- Strain gauges: TML FLA6-11
- Adhesive: TML CN
- Local terminal tags: M-Group CPF-100C

3.4 Coatings

3 stage coating system:

1. 'Bofors' Barrier B
2. M-Group F-Coat
3. Aluminium Foil

3.5 Cable Attachment

No flying leads have been connected. On-site extension cables will be soldered directly onto the terminal tags on the dummy blocks.

4. TEMPORARY CABLING

To minimise the risk of accidental damage to the strain gauges, the load cells have been supplied with no extension cables.

3m lengths of temporary 4 core cable type 16-2-4C have been soldered to the exposed terminal tags on the bridge completion block for the purposes of electrical testing and calibration. These temporary cables have been removed prior to delivery to BOMEL

5. ELECTRICAL TESTING

5.1.1 Bridge Balancing

Each full bridge has been individually balanced using 'Zeranin' wire to produce a datum offset of < 500 microstrain (in accordance with a separate AVT procedure)

5.2 Electrical Testing

Following bonding, coating with Barrier B and connection onto the bridge completion block, all strain gauge full bridge circuits have been electrically tested and the following results recorded:

Test Parameter	Instrument	Acceptance Criteria
Resistance to Ground (RTG)	GIT1300	> 2kMOhms
Datum Offset	P3500, GF=2.0, FB	< 500 microstrain

6. ACCELERATED DRIFT TESTING

All strain gauges have been electrically tested to ensure excellent long term stability, using AVT's 'accelerated drift test procedure'. This testing was performed after the insertion of any balance Zerain wire into the full bridge circuit.

6.1 Test Method:

1. Perform testing in a laboratory environment at constant temperature around 20°C.
2. Load cells must have been stored in the test environment for at least 4 hours prior to testing to allow temperatures to stabilise.
3. Apply a $\pm 6V$ dc supply across each full bridge in turn, using the Farnell bench supply
4. Allow to stabilise for 10 minutes
5. Measure supply voltage (P+ to P-) using a DVM to a resolution of 2 decimal places e.g. 11.98 V
6. Measure Full Bridge output using S+/S- terminals of a P3500 (FB GF=2, BR Excitation OFF)
7. Calculate normalised value of output: = Microstrain * 12 / excitation Voltage
8. Wait for a further 20 minutes
9. Repeat steps 5 - 7 inclusive
10. Compute difference in readings over the 20 minute period
11. Acceptance criterion is indicated difference < 10 indicated microstrain (equivalent to \approx 1.5 true microstrain at normal P3500 excitation of 2V)

7. CALIBRATION

7.1 Types

There are 2 types of load cells:

LOAD CELL	PIPE SIZE	LOAD CELL LENGTH	QUANTITY
Type 1	168.3 x 5.0 mm	340 mm	28
Type 2	168.3 x 5.0 mm	500 mm	18

Load cell Nos. 23 - 26 inclusive are expected to transmit higher loads have been manufactured from a higher grade steel.

7.2 Load Ranges

LOAD CELL	LOAD CELL I.D.	SHAKEDOWN LOAD	CALIBRATION LOAD
Type 1	23 - 26 inclusive	950	900
Type 2	1 - 46 inclusive, excluding 23 - 26	800	750

7.3 Expected Strains

For $E = 207,000 \text{ N/mm}^2$, expected sensitivity = 1.88 microstrain per kN

Calibration/Shakedown Load	Expected Strain Output
750 kN	1410
800 kN	1500
900 kN	1690
950 kN	1786

7.4 Test Rig

All load cells have been calibrated using the NAMAS calibrated 3000kN press at Hevilifts Ltd, Brickyard Road, Aldridge, West Midlands, WS9 8TA. The NAMAS calibration certificate for this test machine is presented in Appendix A

7.5 Data Logging

During calibration, the load cell strain gauges have been monitored using a Measurement Group P3500, calibrated using a NAMAS traceable strain gauge indicator calibrator type 1550A, set up to match the strain gauge Gauge Factor of 2.12, to read the correct strain in the load cell.

7.6 Calibration Procedure

Load cells were delivered to Hevilifts the day before calibration to allow load cells to stabilise at test rig ambient temperature for at least 12 hours prior to calibration.

1. Position 1 Load cell in test rig, and connect 4 strain gauge circuits to data logger
2. Note datum reading at zero load
3. Apply load of 250 kN and note bending as % axial
4. If bending X or Y exceeds 5% axial, unload and re-position load cell in rig
5. Repeat steps 2 - 4 until bending X & Y is less than 5% axial
6. When acceptable, continue to load to Shakedown load and note strains
7. Unload to zero load and note strains
8. Re-apply Shakedown load a further 2 times, or until strain range is repeatable within 15 microstrain
9. Reduce load to zero and hold for 60 seconds, note time
10. Increase load in 6 equal increments to Calibration load, holding load constant at each load increment for at least 30 seconds, noting time.

750 kN range	Increments: 0, 125, 250, 375, 500, 625 & 750 kN
900 kN range	Increments: 0, 150, 300, 450, 600, 750 & 900 kN
11. Reduce load in 3 equal increments, holding load constant at each load increment for at least 30 seconds, noting time.

750 kN range	Increments: 750, 500, 250, 0 kN
900 kN range	Increments: 900, 600, 300, 0 kN
12. Upload stored data to PC and import into Excel spreadsheet and graph to verify.

7.7 Calibration Results

During calibration, the measured strain results were manually input into an Excel spreadsheet in order to compute on-line the X & Y bending strains as percentage of average axial strain at each load increment.

Using the 'SLOPE' function within Excel, the average slope of the 6 loading increments of load versus average axial strain has been computed (expected = 1.88 microstrain per kN)

All electrical testing accelerated drift testing, shakedown, and calibration results per load cell are recorded on a single spreadsheet page, included in Appendix B.

7.7.1 Summary of Load Cell Calibration factors

Load Cell I.D.	Calibration Factor Microstrain per kN
LC 1	1.779
LC 2	1.792
LC 3	1.810
LC 4	1.786
LC 5	1.692
LC 6	1.780
LC 7	1.826
LC 8	1.795
LC 9	1.778
LC 10	1.785
LC 11	1.837
LC 12	1.795
LC 13	1.787
LC 14	1.815
LC 15	1.785
LC 16	1.806
LC 17	1.811
LC 18	1.812
LC 19	1.834
LC 20	1.815
LC 21	1.795
LC 22	1.831
LC 23	1.987

Load Cell I.D.	Calibration Factor Microstrain per kN
LC 24	1.931
LC 25	1.959
LC 26	2.001
LC 27	1.833
LC 28	1.789
LC 29	1.828
LC 30	1.829
LC 31	1.925
LC 32	1.980
LC 33	1.912
LC 34	1.953
LC 35	1.937
LC 36	1.942
LC 37	1.978
LC 38	1.994
LC 39	1.809
LC 40	1.783
LC 41	1.976
LC 42	1.971
LC 43	1.918
LC 44	1.982
LC 45	1.939
LC 46	1.935

8. HANDLING & STORAGE PRECAUTIONS

The load cells each have strain gauges and thermal compensation blocks bonded to the outside of the pipes and should be treated as extremely delicate.

The strain gauged areas must not be handled during lifting of the load cells, nor must the load cells be allowed to lie in their sides.

The strain gauges are very sensitive to moisture and must be stored indoors in a dry area.

During welding of the tubes into the frame, the temperature at the mid section of the load cells must not exceed 100°C, or else the strain gauged may be permanently damaged.

APPENDIX C

AVT REPORT

DATA COLLECTION AND PRESENTATION OF FINAL DATA FILES⁽⁴⁾

(AVT/3581/R1 - 38 pages)

REPORT NO. AVT/3581 R1 BOMEL

REVISION NO. 1

PREPARED FOR BOMEL Ltd
Ledger House
Forest Green Road
Fifield
Maidenhead
Berkshire
SL6 2NR

ATTENTION OF Dr Helen M. Bolt
Director

**3D FRAMES PROJECT
DATA COLLECTION AND
PRESENTATION OF FINAL
DATAFILES**

18 November 1998

APPROVED BY:
Eur Ing Neil Parkinson BSc CEng MIMechE
Technical Director

CONTENTS

1	SUMMARY	5
2	INTRODUCTION	7
2.1	Standardised Data Cell locations	7
2.2	Standardised Spreadsheet Formats	8
3	LOADCASE 1 SUMMARY	9
3.1	Loadcase 1 - Pre-Test Summary	9
3.2	Loadcase 1 - Test Summary	9
3.3	Loadcase 1 – Cut-Outs	9
3.4	Re-assigned Channels	9
3.5	Spreadsheet Modifications	9
4	LOADCASE 1C SUMMARY	10
4.1	Loadcase 1C- Pre-Test Summary	10
4.2	Loadcase 1C – Test Summary	10
4.3	Loadcase 1C – Cut-Outs	10
4.4	Re-assigned Channels	10
4.5	Spreadsheet Modifications	10
5	LOADCASE 2 SUMMARY	11
5.1	Loadcase 2- Pre-Test Summary	11
5.2	Loadcase 2 – Test Summary	11
5.3	Loadcase 2 – Cut-Outs	11
5.4	Re-assigned Channels	11
5.5	Spreadsheet Modifications	11
6	LOADCASE 2C SUMMARY	12
6.1	Loadcase 2C- Pre-Test 1 Summary	12
6.2	Loadcase 2C- Pre-Test 2 Summary	12
6.3	Loadcase 2C – Test Summary	12
6.4	Loadcase 2C – Cut-Outs	13
6.5	Re-assigned Channels	13
6.6	Suspect/Faulty Gauges	13
6.7	Spreadsheet Modifications	13
7	LOADCASE 3C SUMMARY	14
7.1	Loadcase 3C- Pre-Test 1 Summary	14
7.2	Loadcase 3C- Pre-Test 2 Summary	14

7.3	Loadcase 3C – Test Summary	14
7.4	Loadcase 3C – Cut-Outs	15
7.5	Re-assigned Channels	15
7.6	Suspect/Faulty Gauges	15
7.7	Spreadsheet Modifications	15
8	LOADCASE 3 SUMMARY	16
8.1	Loadcase 3- Pre-Test Summary	16
8.2	Loadcase 3 – Test Summary	16
8.3	Loadcase 3 – Cut-Outs	17
8.4	Re-assigned Channels	17
8.5	Suspect/Faulty Gauges	17
8.6	Spreadsheet Modifications	18
8.7	Displacement Transducer Relocations	18
9	LOADCASE 3C.A SUMMARY	19
9.1	Loadcase 3C.A- Pre-Test Summary	19
9.2	Loadcase 3C.A – Test Summary	19
9.3	Loadcase 3C.A – Cut-Outs	19
9.4	Re-Assigned Channels	20
9.5	Re-Connected Channels	20
9.6	Suspect/Faulty Gauges	20
9.7	Spreadsheet Modifications During Loadcase 3C.A	20
9.8	Spreadsheet Modifications carried forward from previous Tests	21
10	LOADCASE 1C.A SUMMARY	22
10.1	Loadcase 1C.A- Pre-Test Summary	22
10.2	Loadcase 1C.A – Test Summary	22
10.3	Loadcase 1C.A – Cut-Outs	23
10.4	Re-Assigned Channels	23
10.5	Re-Connected Channels	23
10.6	Suspect/Faulty Gauges	23
10.7	Spreadsheet Modifications During Loadcase 1C.A	24
10.8	Spreadsheet Modifications carried forward from previous Tests	24
11	SPREADSHEET REVISION RECORD	25
12	RE-ISSUED ‘FINAL’ DATAFILES	27
13	EXCITATION VOLTAGE CHECKS	29
13.1	Strain Gauge Channels	29

13.2	Displacement Channels	29
13.3	Displacements	30
14	GLOBAL XYZ	31
14.1	Definition of Problem	31
14.2	Transformation Equations	31
15	RETROSPECTIVE EFFECTS	32
15.1	Loadcase 2 Retro Changes	32
15.2	Loadcase 3C Retro Changes	32
15.3	Loadcase 3 Retro Changes	32
15.4	Loadcase 1C.A Retro Changes	32
16	MODIFICATIONS TO 'FINAL' VERSION DATAFILES	33
16.1	Loadcase 1	33
16.2	Loadcase 1C	33
16.3	Loadcase 2	34
16.4	Loadcase 2C	35
16.5	Loadcase 3C	35
16.6	Loadcase 3	36
16.7	Loadcase 3C.A - Spreadsheet Modifications to Final Version 'b'	37
16.8	Loadcase 1C.A - Spreadsheet Modifications to Final Version 'b'	38

1 SUMMARY

This report relates to the collection of data during the testing of the 3D Frames for the following Loadcases:

Loadcase 1	25 & 26 April 1998
Loadcase 1C	29 – 31 May 1998
Loadcase 2	20 June 1998
Loadcase 2C	19 – 21 July 1998
Loadcase 3C	4 – 6 August 1998
Loadcase 3	28 & 29 August 1998
Loadcase 3C.A	23 & 24 October 1998
Loadcase 1C.A	9 & 10 November 1998

All test data was supplied to BOMEL immediately following each Loadcase, however, this data has been subsequently been re-formatted for final presentation with this report.

This report presents the following information, which supplements the data as provided on ZIP disk.

Section 1 presents standardised cell references for all data contained within the datafiles, together with a pro-forma 'worksheet' layout for each of the datafile 'folders'.

Sections 3 to 10 present a summary of the key information for each Loadcase Test, including key milestone Scans (with dates and times), details of any spreadsheet highlights or anomalies, including any channel re-assignments or deviations from the standard pro-forma.

Each Loadcase 'Test' Summary also includes any Pre-Test 'Trial' information as well as details of the monitoring of 'Cut-Outs'.

Section 11 presents a summary of the historical development of the master spreadsheet from original version 'a' through to the most recent version 'ab' used during Loadcase 3 Cut-Outs and finally to the latest versions 'a' and 'b' developed for the transfer of final data to BOMEL.

Section 12 presents a summary of the 44 original datafiles that have been used to produce the 22 'final' datafiles for all of the Loadcases.

Section 13 presents details of the logger excitation voltages as measured for each channel upon completion of the final test on 10 November 1998. This information has been used to apply corrected calibration factors to all affected channels.

Section 14 presents the method statement used for the derivation of the Global XYZ Space transformation equations. These are required to transform the transducer x, y & z measurements (in the axis of the individual transducers), to Global components with reference to the 3D frame co-ordinates.

Section 15 presents details of a number of system anomalies, which, at the time of their discovery, had 'Retrospective Effects' on earlier datafile versions. Such effects include the discovery of low sensor excitation voltages on specific logger channels. Assuming that these voltages must always have been low since the very first measurements, then it has been necessary to retrospectively alter calibration factors in earlier (and later) datafile versions in order to compensate.

Finally, Section 16 presents a summary of all spreadsheet modifications that have been applied in order to convert the original datafiles to the 'final' version.

This report Revision 1 supersedes Revision 0, through the addition of information for the final 2 tests, Loadcases 3C.A and 1C.A.

2 INTRODUCTION

2.1 Standardised Data Cell locations

COLUMN	RAW SHEET	DATA SHEET	DESCRIPTION
A	CHANNEL	CHANNEL	Logger Input No. 1 - 880
B	SENSOR TYPE	SENSOR TYPE	Sensor Type and Make and Model e.g. SG-FLA6 = Strain Gauge type FLA6 (6mm, single element) SG-FRA3 = Strain Gauge type FRA3 (3mm, stacked 3 element rosette) DT-PG150 = Displacement Transducer type Penny & Giles 150mm range
C	TAG No.	TAG No.	Unique Reference = sensor type followed by Unique position No. e.g. LC30 = Load Cell No. 30 SG8-5 = SG on Member No. 8 in orientation 5 DT45 = Displacement Transducer on Node 45
D	REF	REF	Orientation Reference e.g. 1, 3, 5 or 7 for SG X, Y or X for DT
E	MEMBER	MEMBER	BOMEL Member No.
F	LOCATION	LOCATION	Global Location Reference e.g. FRAME B 1C-2D is on Frame B, between points 1C and 2D
G	MAX YIELD	RANGE	Measuring range in Engineering Units
H	MIN YIELD	CAL FACTOR	Conversion Factor from Volts to Engineering Units
I	UNITS	UNITS	Engineering Units e.g. microstrain, kN, kNm, mm
J		TENSION	Any peak tensile strains > 1350 microstrain are highlighted Red
K		COMP	Any peak compressive strains < - 1350 microstrain are highlighted Blue
L	SCAN 1	DIFF CHECK	Any SGs showing less than 20 microstrain are highlighted Yellow
M	SCAN 2	GRAPH LABEL	Label as it will appear on Graph Legend
N	SCAN 5 etc.	SCAN 4 etc.	

2.2 Standardised Spreadsheet Formats

All final sheets in Excel™ 7.0, MS-Office™ 97, Windows™ 97/98

2.2.1 Standardised Worksheets per Folder:

Revisions	Details of all revisions to convert the original sheets (as previously supplied to BOMEL) to Final Versions
Raw	Worksheet containing all raw data as imported directly from the Sunnyside 'Scan 8000' logger system
Data	Conversions to calibrated data
Pred1	Prediction Data as provided by BOMEL, used within graphs
Global XYZ	Transformation of measured displacements to Global XYZ Co-ordinates
Graphs	Various Graph sheets, showing measured versus predicted data

3 LOADCASE 1 SUMMARY

3.1 Loadcase 1 - Pre-Test Summary

Scan No.	Time	Date	Comments	Spreadsheet Reference
1	17:30	25/4/98	Datum	LC1Th_1
3	20:15		Supports Removed	
18	23:05		No Load at end of first day	LC1Th_18
19	09:35	26/4/98	Datum at start of second day ASG 54 re-assigned from Logger Ch 834 to Ch 777 and corrected within spreadsheet	LC1Th_19
20	09:45		New Datum	
29	10:44		Final Datum at end of Pre-Test	LC1Th_29

3.2 Loadcase 1 - Test Summary

Scan No.	Time	Date	Comments	Spreadsheet Reference
1	10:44	26/4/98	Datum (copy of Scan 29 from Pre-Test @ 10:44)	LC1i_1
12	13:23		LC25-3 & LC25-7 (Chs 98 & 100) Re-connected	
21	15:55		DT38-1 (Ch 852) Failed (dropped-off) DT38-2 (Ch 853) Failed (dropped-off) DT4-22 (Ch 876) Repaired (wire had been 'snagged' on preceding Scans)	
38	18:43		Final Scan	LC1i_38

3.3 Loadcase 1 - Cut-Outs

None

3.4 Re-assigned Channels

ASG 54 re-assigned from Logger Ch 834 to Ch 777.

3.5 Spreadsheet Modifications

Data sheet corrected for re-assignment of ASG 54 from Logger Ch 834 to Ch 777.

4 LOADCASE 1C SUMMARY

4.1 Loadcase 1C- Pre-Test Summary

Scan No.	Time	Date	Comments	Spreadsheet Reference
1	14:23	29/5/98	Datum	LC1CTm_1
26	17:50		Final Pre-Test Scan	LC1Cm_0
26	17:50		Final Datum, Corrected for Datum Zero	LC1Cm_0x

4.2 Loadcase 1C – Test Summary

Scan No.	Time	Date	Comments	Spreadsheet Reference
1	13:42	30/5/98	Datum	LC1Cn_1
30	20:58		Datum at end of first day	LC1Cn_30
31	08:26	31/5/98	Datum at start of second day	
50	10:24		Last Scan before start of new spreadsheet	LC1Cn_50
51	11:04		First Scan in continuation spreadsheet	LC1Co_0
99	14:54		Last Scan in spreadsheet containing Scans 1 & 51 – 100)	LC1Co_49
113			DT26X Repaired	
145			Last Scan in spreadsheet containing Scans 1 & 100 – 145)	LC1Cp_46
185			Last Scan in spreadsheet containing Scans 1 & 146 – 185) Final Datum at end of Test	LC1Cq_40

4.3 Loadcase 1C – Cut-Outs

None.

4.4 Re-assigned Channels

Ch 834 re-assigned to Ch 777 in Raw sheet.

4.5 Spreadsheet Modifications

Data sheet corrected for re-assignment of Ch 834 into Ch 777 in Raw sheet.

5 LOADCASE 2 SUMMARY

5.1 Loadcase 2- Pre-Test Summary

None

5.2 Loadcase 2 – Test Summary

Scan No.	Time	Date	Comments	Spreadsheet Reference
1 & 1a	10:30	20/6/98	Datum	LC2o_1
4	11:35		DT42 Reset	
15	12:55		SG 8-1 re-assigned from Ch 201 to Ch 477 and corrected within spreadsheet	LC2o_15
38	17:26		DT30z (Ch 866) re-set	
49	20:03		Final Scan at end of Test	LC2o_49

5.3 Loadcase 2 – Cut-Outs

Scan No.	Time	Date	Comments	Spreadsheet Reference
50	20:40	20/6	Datum at start of cut-outs	LC2o_50
53			End of Spreadsheet version 'o'	LC2o_53
54	21:20		Calibration Factor changed for SG 67-3 (Ch 346) to compensate for low excitation voltage	LC2p_54
59	22:34		Final Scan Loadcase 2	LC2p_59

5.4 Re-assigned Channels

ASG 54 re-assigned from Ch 834 to Ch 777.

SG 8-1 re-assigned from Ch 201 to Ch 477 from Scan 15 onwards.

5.5 Spreadsheet Modifications

Data sheet corrected for re-assignment of ASG 54 from Ch 834 to Ch 777.

Data sheet corrected for re-assignment of SG 8-1 from Ch 201 to Ch 477 from Scan 15 onwards.

Calibration Factor changed for SG67-3 (Ch 346) to compensate for low excitation voltage from Scan 54.

6 LOADCASE 2C SUMMARY

6.1 Loadcase 2C- Pre-Test 1 Summary

Scan No.	Time	Date	Comments	Spreadsheet Reference
1	17:30	19/7/98	Datum	LC2CTr_1
22	18:44		End of Pre-Test 1	LC2Cr_T1

6.2 Loadcase 2C- Pre-Test 2 Summary

Scan No.	Time	Date	Comments	Spreadsheet Reference
1	08:47	20/7/98	Datum	LC2Cr_1
7	09:41		DT42 Re-connected	
9	09:41		End of Pre-Test 2	LC2Cr_9

6.3 Loadcase 2C – Test Summary

Scan No.	Time	Date	Comments	Spreadsheet Reference
1	09:41	20/7/98	Datum (= Scan 9 of Pre-Test 2)	LC2C2r_1
14	10:53		LC46-3 (Ch182, Member 78) repaired	
17	11:45		Additional SGs installed SG82B (Chs 389 – 392) SG5-4c (Ch516) Repaired	
58	14:11		End of first spreadsheet (Scans 1 – 58)	LC2C2r_58
64 & 65			No Data for these 2 Scans	
65	14:31		Logger fault observed since Scan 48 (low excitation voltage on Chs 801-880, due to capacitor failure on Logger Ch 863)	
66	15:55		Logger problem fixed (Chs 850-853, 875 & 876 disconnected to avoid further problems)	
109	18:36		End of spreadsheet (Scans 1 & 59 – 109)	LC2C2r_109
143	21:14		End of first day End of spreadsheet (Scans 1 & 110 – 143)	LC2C2r_143
144	08:51	21/7/98	Start of second day	
203	13:19		End of spreadsheet (Scans 1 & 144 – 203)	LC2C2r_203

263	18:24		End of spreadsheet (Scans 1 & 204 – 163)	LC2C2r_263
292	20:44		End of spreadsheet (Scans 1 & 164 – 292) Final Datum at end of Test	LC2C2r_292

6.4 Loadcase 2C – Cut-Outs

Scan No.	Time	Date	Comments	Spreadsheet Reference
293	21:09	21/7/98	Start of Cut-Outs	
300	21:42		End of Test Final Scan	LC2C2r_300

6.5 Re-assigned Channels

ASG 54 re-assigned from Ch 834 to Ch 777.

SG 8-1 re-assigned from Ch 201 to Ch 477.

Additional SGs installed SG82B 1, 3, 5 & 7 re-assigned to Chs 389 – 392 from Scan 17 onwards (replacing unused SG84B).

6.6 Suspect/Faulty Gauges

Irretrievable loss of data for Chs 801-880 for Scan 48 –64 inclusive (due to logger fault causing low excitation voltage for these channels).

SG 30-5 (Ch 259) Failed.

LC 30-7 Failed.

6.7 Spreadsheet Modifications

Data sheet corrected for re-assignment of ASG 54 from Ch 834 to Ch 777.

Data sheet corrected for re-assignment of SG 8-1 from Ch 201 to Ch 477.

Additional SGs installed SG82B 1, 3, 5 & 7 (Chs 389 – 392) from Scan 17 onwards.

Calibration Factor for SG 67-3 (Ch346) increased to account for low excitation voltage (1.96V instead of 5.0V).

7 LOADCASE 3C SUMMARY

7.1 Loadcase 3C- Pre-Test 1 Summary

Scan No.	Time	Date	Comments	Spreadsheet Reference
1	19:55	4/8/98	First Scan	LC3Ctu_1
2	20:14		Datum, zero load, supports removed	
9	21:50		SG 58-3 (Ch330) & SG 60-1 (Ch 333) gauges replaced	
35	23:48		End of Pre-Test 1	LC3Ctu_35

7.2 Loadcase 3C- Pre-Test 2 Summary

Scan No.	Time	Date	Comments	Spreadsheet Reference
1	09:44	5/8/98	Datum	LC3Cu_1
35	12:40		Additional SG 49-1, 3, 5 & 7 & SG 51-1, 3, 5 & 7 installed (Chs 457 – 460 and 465-468) End of Pre-Test 2	LC3Cu_35

7.3 Loadcase 3C – Test Summary

Scan No.	Time	Date	Comments	Spreadsheet Reference
1	13:14	5/8/98	New Datum at start of Test	LC3Cv_1
50	18:28		End of spreadsheet (Scans 1 – 50)	LC3Cv_50
102	20:41		End of spreadsheet (Scans 1 & 51 – 102)	LC3Cv_102
116	21:43		End of first day	
117	08:20	6/8/98	Start of second day	
155	11:33		End of spreadsheet (Scans 1 & 102 – 155)	LC3Cv_155
167	12:24		Equation for Axial Load from LC30 (Row 913) modified (incorrectly) to ignore Ch 120	
195	13:42		End of spreadsheet (Scans 1 & 156 – 195)	LC3Cv_195
210	14:36		End of spreadsheet (Scans 1 & 196 – 210)	LC3Cv_210
245			End of spreadsheet (Scans 1 & 211 – 245)	LC3Cv_245
252			End of spreadsheet (Scans 1 & 246 – 252) Final Datum at end of Test	LC3Cv_252

7.4 Loadcase 3C – Cut-Outs

Scan No.	Time	Date	Comments	Spreadsheet Reference
253	18:42	6/8/98	Start of Cut-Outs	
265	20:20		Final Scan	LC3Cv_265

7.5 Re-assigned Channels

ASG 54 re-assigned from Ch 834 to Ch 777

SG 8-1 re-assigned from Ch 201 to Ch 477

DT 29-X re-assigned from Ch 861 to Ch 850 prior to Pre-Test

DT 30-Y re-assigned from Ch 865 to Ch 851 prior to Pre-Test

DT 30-Z re-assigned from Ch 866 to Ch 852 prior to Pre-Test

DT 48-Y re-assigned from Ch 871 to Ch 853 prior to Pre-Test

Additional SG 49-1, 3, 5, & 7 re-assigned to Chs 457 – 460, (replacing SG 87F), from Pre-Test Scan 35

Additional SG 51-1, 3, 5, & 7 re-assigned to Chs 465 – 468, (replacing SG 94F), from Pre-Test Scan 35

7.6 Suspect/Faulty Gauges

SG 30-5 (Ch 259) Failed

LC 30-7 Failed

7.7 Spreadsheet Modifications

Calibration Factor for SG 67-3 (Ch346) increased to account for low excitation voltage(1.96V instead of 5.0V)

Data sheet corrected for re-assignment of Ch 834 into Ch 777 in Raw sheet

Data sheet corrected for re-assignment of Ch 201 to Ch 477 in Raw sheet

Equation for Axial Load from LC30 (Row 913) modified to ignore failed gauge Ch 120 from Scan 166 onwards – This was incorrect and should have averaged Rows 120 + 122 (not Rows 124 + 126)

Data sheet corrected for re-assignment of Displacement transducers DT39-1, DT39-2, DT40-1 and DT 40-2

Additional strain gauges SG49 and 51 in Chs 457-460 and 465-468 from Test Scan 1

8 LOADCASE 3 SUMMARY

8.1 Loadcase 3- Pre-Test Summary

Scan No.	Time	Date	Comments	Spreadsheet Reference
1	14:55	28/8/98	Datum	LC3Tw_1
5 – 15			Low Excitation Voltage on Chs 801 – 880	
16	16:32		Chs 801– 880 OK (DT42 (Ch854) removed)	
28	17:30		LC20-5 (Ch 79) and SG97-3 (Ch 402) Repaired	
29	17:40		End of Pre-Test	LC3Tw_29

8.2 Loadcase 3 – Test Summary

Scan No.	Time	Date	Comments	Spreadsheet Reference
1	09:32	29/8/98	Datum	LC3x_1
1a	09:40		New Datum ASGs 61 – 64 re-assigned from Chs 841-844 to Chs 829-832	LC3y_2
15	11:10		Equations for Axial Load LC30 modified to <u>correctly</u> ignore failed LC30-7 (Ch 120)	LC3z_15
18-20			Low Excitation Voltage on Chs 401 – 480 (short circuit due to cable damage)	
21	12:25		Chs 401– 480 OK (short circuit on Ch450)	
26	13:01		Low Excitation Voltage on Chs 401 – 480 (short circuit due to cable damage)	
27	13:11		Chs 401– 480 OK (All cable screens disconnected to avoid further short circuits)	
40	15:02		DTs 21, 22, 29 & 30 reset (see below)	
50	17:23		New DT44 (Ch 877) installed to monitor joint deformation across Node 44	
51	17:34		DT44 moved to Ch 875	LC3aa_51
60			End of first spreadsheet (Scans 1–60)	LC3aa_60
64	19:18		DT21z post moved 5mm in –X direction	
73	20:46		Final Test End of second spreadsheet (Scans 1 & 61–73)	LC3aa_73

8.3 Loadcase 3 – Cut-Outs

Scan No.	Time	Date	Comments	Spreadsheet Reference
1	09:32	29/8/98	Datum from Loadcase 3	LC3ab_1
2	10:13	10/9/98	First Scan at start of cut-outs	
14	12:07		Member 49 Cut	
15	12:20		Member 51 Cut	
19	12:43		Member 54 Cut	
20	12:54		Member 46 Cut	
25	13:34		Member 61 Cut	
33	15:40		Member 55 Cut	
34	15:46		Member 53 Cut	
39	16:19		Member 45 Cut	
41	16:32		Final Scan	LC3ab_41

8.4 Re-assigned Channels

ASG 54 re-assigned from Ch 834 to Ch 777

SG 8-1 re-assigned from Ch 201 to Ch 477

DT 39-1 re-assigned from Ch 861 to Ch 850

DT 39-2 re-assigned from Ch 865 to Ch 851

DT 40-1 re-assigned from Ch 866 to Ch 852

DT 40-2 re-assigned from Ch 871 to Ch 853

ASG61 re-assigned from Ch 841 to Ch 829 from Scan 2

ASG62 re-assigned from Ch 842 to Ch 830

ASG63 re-assigned from Ch 843 to Ch 831

ASG64 re-assigned from Ch 844 to Ch 832

New DT44 (Ch 877) installed to monitor joint deformation on Node 44 from Scan 50

DT44 re-assigned to Ch 875 from Scan 51

8.5 Suspect/Faulty Gauges

SG 30-5 (Ch 259) Failed

LC 30-7 Failed

8.6 Spreadsheet Modifications

Calibration Factor for SG 67-3 (Ch346) increased to account for low excitation voltage (1.96V instead of 5.0V)

Data sheet corrected for re-assignment of Ch 834 into Ch 777 in Raw sheet

Data sheet corrected for re-assignment of Ch 201 to Ch 477 in Raw sheet from Scan 15 onwards

ASGs ASG61 – 64 re-assigned from Chs 841-844 to Chs 829-832 from Scan 1a

Eqn. for Axial Load LC30 modified to correctly ignore Ch 120 (LC30-7) from Scan 15

8.7 Displacement Transducer Relocations

The following adjustments were made at Scan 40 to permit greater mobility of DTs during subsequent loading:

DT22-Z	Frame Point moved 25 mm in X direction
DT21-X	Frame Point moved 40 mm in -Y direction
DT21-Z	Frame Point moved 40 mm in Y direction
DT30-Z	Frame Point moved 40 mm in -Y direction
DT29-X	Frame Point moved 40 mm in Y direction
DT29-Z	Frame Point moved 40 mm in -Y direction

9 LOADCASE 3C.A SUMMARY

9.1 Loadcase 3C.A- Pre-Test Summary

Scan No.	Time	Date	Comments	Spreadsheet Reference
1	09:32	29/8/98	Datum Scan From Loadcase 3	
2	16:32	22/10/98		
17	08:45	23/10/98		
23	10:30	23/10/98	End of AVT Pre-Trial tests – all channels OK	LC3CA_Pre Trial
1	10:38	23/10/98	Datum	
25	11:31			
25a	11:51		Repeat of Scan 25 with LC12-7 (Ch48) repaired	LC3CAT_25

9.2 Loadcase 3C.A – Test Summary

Scan No.	Time	Date	Comments	Spreadsheet Reference
1	12:08	23/10/98	Datum	
83	17:30		End of first Spreadsheet (At Zero Load)	LC3CA_83
84	17:49		New sheet, commencing from Scan 1 & 74 onwards	
138	21:07		End of second Spreadsheet	LC3CA_138
138	08:16	24/10/98	New Sheet, retaining Scan 1 from 23/10/98	
167	10:49		Repeat of Scan 166	
187	12:47		End of third Spreadsheet	LC3CA_187
195	14:00		New sheet, commencing from Scan 1 & 187 onwards	
205	15:12		End of Test	LC3CA_205

9.3 Loadcase 3C.A – Cut-Outs

None

9.4 Re-Assigned Channels

9.4.1 Strain gauges

SG95_7 re-assigned from Ch 472 into Ch 478

9.4.2 Frame C K-Joints

DT 37-1 re-assigned from Ch 850 to Ch 845

DT 37-2 re-assigned from Ch 851 to Ch 846

DT 38-1 re-assigned from Ch 852 to Ch 847

DT 38-2 re-assigned from Ch 853 to Ch 878

9.5 Re-Connected Channels

9.5.1 DTs across Frame A X Joints

DT Ref.	Across Member	Re-using Cable No.	Cable Disconnected from Ch No.	Re-Connected into Logger Channel No.
33	45-47	312	312	876
34	49-51	309	309	877
35	54-56	311	311	854
36	58-60	392	392	874

9.5.2 Re-Connected Load Cells:

LC1	LC5	LC9	LC13	LC25
LC2	LC7	LC10	LC14	
LC3	LC18	LC11	LC15	
LC4	LC19	LC12	LC16	

9.5.3 Re-Installed Strain Gauges:

61	86
62	87
63	94
64	95

9.6 Suspect/Faulty Gauges

SG76_7 Channel 368 (Inaccessible for repair)

SG80_3 Channel 374 (Inaccessible for repair)

SG 30-5 (Ch 259) Failed

LC 30-7 Failed

9.7 Spreadsheet Modifications During Loadcase 3C.A

New Graphs added for Frame A X-Joints and Frame C K-Joints from Scan 10 during Test.

9.8 Spreadsheet Modifications carried forward from previous Tests

Data sheet corrected for re-assignment of Ch 834 into Ch 777 in Raw sheet

Data sheet corrected for re-assignment of Ch 201 to Ch 477 in Raw sheet from Scan 15 onwards

ASGs ASG61 – 64 re-assigned from Chs 841-844 to Chs 829-832

Eqn. for Axial Load LC30 modified to ignore Ch 120 (LC30-7)

10 LOADCASE 1C.A SUMMARY**10.1 Loadcase 1C.A- Pre-Test Summary**

Scan No.	Time	Date	Comments	Spreadsheet Reference
1	12:08	23/10/98	Datum from Loadcase 3C.A	
2	9:29	9/11/98	Initial Scan prior to re-setting DT22	
3	9:53		All channels working OK Global Displacement (Ch880) copied as new datum into Scan 1	
22	10:36		End of Trial	LC1CA_Trial

10.2 Loadcase 1C.A – Test Summary

Scan No.	Time	Date	Comments	Spreadsheet Reference
1	12:08	23/10/98	Datum from Loadcase 3C.A	
2	10:48	9/11/98		
62	15:00		End of first Spreadsheet	LC1CA_62
63	15:07		Start of new Spreadsheet, retaining Scan 1	
115	18:07		End of second Spreadsheet	LC1CA_115
116	18:25		Start of new Spreadsheet, retaining Scan 1	
154	20:27		Re-Scan 153 with DT38_2 disconnected, DT25X & DT26X reset minus ≈ 150 mm	
156	20:51		DT37_2 disconnected	
159	21:07		DT21X reset minus ≈ 100 mm, DT21Z re-orientated to permit greater vertical deflections of frame	
164	21:33		Structure 'Failed'	
168	21:59		End of Test	LC1CA_168

10.3 Loadcase 1C.A – Cut-Outs

Scan No.	Time	Date	Comments	Spreadsheet Reference
169	08:13	10/11/98	Repeat of Scan 168 = Datum at start of cut-outs	
170	9:11		Members 57, 60, 54, 55, 51, 50, 47 & 46 Cut	
172	9:26		Members 61 & 63 Cut	
173	9:51		Members 99, 69, 100 & 71 Cut	
174	9:57		End of Test	LC1CA_Cutout

10.4 Re-Assigned Channels**10.4.1 Strain gauges**

SG95_7 re-assigned from Ch 472 into Ch 478

10.4.2 Frame C K-Joints

DT 37-1 re-assigned from Ch 850 to Ch 845

DT 37-2 re-assigned from Ch 851 to Ch 846

DT 38-1 re-assigned from Ch 852 to Ch 847

DT 38-2 re-assigned from Ch 853 to Ch 878

10.5 Re-Connected Channels**10.5.1 DTs across Frame A X Joints**

DT Ref.	Across Member	Re-using Cable No.	Cable Disconnected from Ch No.	Re-Connected into Logger Channel No.
33	45-47	312	312	876
34	49-51	309	309	877
35	54-56	311	311	854
36	58-60	392	392	874

10.6 Suspect/Faulty Gauges

SG76_7 Channel 368 (Inaccessible for repair)

SG80_3 Channel 374 (Inaccessible for repair)

SG 30-5 (Ch 259) Failed

LC 30-7 Failed

10.7 Spreadsheet Modifications During Loadcase 1C.A

New Graphs added for Frame A X-Joints and Frame C K-Joints from Scan 10 during Test.

10.8 Spreadsheet Modifications carried forward from previous Tests

Data sheet corrected for re-assignment of Ch 834 into Ch 777 in Raw sheet

Data sheet corrected for re-assignment of Ch 201 to Ch 477 in Raw sheet from Scan 15 onwards

ASGs ASG61 – 64 re-assigned from Chs 841-844 to Chs 829-832

Eqn. for Axial Load LC30 modified to ignore Ch 120 (LC30-7)

11 SPREADSHEET REVISION RECORD

SPREADSHEET VERSIONS	WHERE USED	MODIFICATIONS
a to g	Not used	Development versions
LC1T1h_0 to 18	LC1 Pre-Test	First Issue
L1T1h_19 to 29	LC1 Pre-Test	ASG54 Re-assigned from Ch 834 to Ch 777
LC1i_1 to 39	LC1 Test	New Sheet for Test
j, k, l & m	Not used	
LC1Cm_0	LC1C Pre-Test	Max & Min Yield detection
LC1Cm_0x	LC1C Pre-Test	Corrected for Datum Zero
LC1Cn_1 to 50	LC1C Test	New sheet for Scans 1 -50
LC1Co_1 to 49	LC1C Test	New sheet for Scans 51 - 99
LC1Cp_1 to 46	LC1C Test	New sheet for Scans 100 - 145
LC1Cq_1 to 40	LC1C Test	New sheet for Scans 146 - 185
LC2o_1 to 49	LC2 Test	LC2 Prediction data added Max & Min Yield detection and 'Difference' calculation
LC2p_50-59	LC2 Cut-Outs	Calibration Factor change for Ch 346
LC2CTr_1 to 22	LC2C Pre-Test 1	LC2C Prediction data added
LC2Cr_1 to 9	LC2C Pre-Test 2	New sheet for Test
LC2C2r_1 to 300	LC2C Test & Cut-Outs	New sheet for Test
LC3Tu_1 to 35	LC3 Pre-Test	LC3C Prediction data added DT39-1, DT39-2, DT40-1 and DT 40-2 (Chs 861, 865, 866 & 871) Re-assigned to Chs 850 - 853
LC3Cu_1 to 34	LC3C Test	New sheet for Test
LC3Cu_35	LC3C Test	Additional SG49 installed in Chs 457-460 and SG51 installed in Chs 465-468
LC3Cv_1 to 165	LC3C Test	New sheet for Test
LC3Cv_166 to 265	LC3C Test & Cut-Outs	Modified Axial Force equations for LC30 to ignore failed gauge (Ch120) - Data sheet Row 913
LC3Tw_1 to 29	LC3 Pre-Test	LC3 Prediction data added
LC3x_1	LC3 Test	New sheet for Test
LC3y_2 to 14	LC3 Test	ASGs 61 - 64 Re-assigned from Ch841-844 to Ch 829-832

LC3z_15 to 50	LC3 Test	Corrected Axial Force equations for LC30 to ignore failed gauge (Ch120) - Data sheet Row 913
LC3aa_51 to 73	LC3 Test	DT 44 re-assigned to Ch 875
LC3ab_1 to 41	LC3 Cut-Outs	New sheet for Cut-Outs
LC??Aa	LC1, LC1C, LC2, LC2C, LC3 & LC3C	New sheet for presentation of 'final' datafiles on 13 October 1998 Global XYZ added Revision sheet added
LC??Ab	LC1C.A & LC3C.A.	New sheet for presentation of 'final' datafiles on 18 November 1998 Cal Factor corrections based upon final logger excitation voltage measurements

12 RE-ISSUED 'FINAL' DATAFILES

LOADCASE DESCRIPTION	'FINAL' DATAFILE	TOTAL NO. SCANS	ORIGINAL DATAFILES:
Loadcase 1 Pre-Test Trial	LC1a_Trial	0 - 29	LC1Th_18, LC1Th_19, LC1Th_29
Loadcase 1 Test	LC1a_Test	1 - 38	LC1i_38
Loadcase 1C Pre-Test Trial	LC1Ca_Trial	1 - 18	LC1Cm_0, LC1Cm_0x
Loadcase 1C Test	LC1Ca_Test	1 - 185	LC1Cn_50, LC1Co_49, LC1Cp_46, LC1Cq_40,
Loadcase 2 Test	LC2a_Test	1 - 49	LC2o_49
Loadcase 2 Cut-Outs	LC2a_Cut	11 (1 & 50 – 59)	LC2p_59
Loadcase 2C Pre-Test Trial	LC2Ca_Trial	1 - 31	LC2Cr_T1, LC2Cr_9,
Loadcase 2C Test	LC2Ca_Test1	1 - 143	LC2C2r_58, LC2C2r_109, LC2C2r_143
Loadcase 2C Test	LC2Ca_Test2	151 (1 & 144 – 292)	LC2C2r_203, LC2C2r_263, LC2C2r_292,
Loadcase 2C Cut-Outs	LC2Ca_Cut	9 (1 & 293-300)	LC2C2r_300
Loadcase 3C Pre-Test Trial	LC3Ca_Trial	70	LC3CTu_35, LC3Cu_35
Loadcase 3C Test	LC3Ca_Test1	133	LC3Cv_50, LC3Cv_102, LC3Cv_155,
Loadcase 3C Test	LC3Ca_Test2	121 (1 & 134 – 252)	LC3Cv_155, LC3Cv_195, LC3Cv_210, LC3Cv_245, LC3Cv_252,
Loadcase 3C Cut-Outs	LC3Ca_Cut	13 (1 & 253 – 265)	LC3Cv_265
Loadcase 3 Pre-Test Trial	LC3a_Trial	1 - 29	LC3Tw_29
Loadcase 3 Test	LC3a_Test	1 - 73	LC3aa_60, LC3aa_73
Loadcase 3 Cut-Outs	LC3a_Cut	1 - 41	LC3ab_41

Loadcase 3C.A Pre-Test Trial	LC3CAb_Trial	1 - 23 & 1 - 25a	LC3CAT_25
Loadcase 3C.A Test	LC3CAb_Test	1 - 205	LC3CA_83, LC3CA_138, LC3CA_187, LC3CA_205,
Loadcase 1C.A Pre-Test Trial	LC1CAb_Trial	1 - 22	LC1CA_Trial
Loadcase 1C.A Test	LC1CAb_Test	1 - 168	LC1CA_62, LC1CA_115, LC1CA_168,
Loadcase 1C.A Cut Outs	LC1CAb_Cut	169 - 174	LC1CA_Cutout

13 EXCITATION VOLTAGE CHECKS

Upon completion of the final test (Loadcase 1C.A Cut-Outs) on 10 November 1998, Measurements were made to quantify the actual excitation voltages for all passive sensors (Load Cells, Strain Gauges and Displacement Transducers). Measurements were taken using Bodycote Ltd's WhiteGold DVM, Serial No. 24002243.

13.1 Strain Gauge Channels

Voltages were measured for each of up to 80 channels per rack with all sensors energised (i.e maximum rack loading).

13.2 Displacement Channels

Voltages were measured for each of the Displacement Transducer Channels (845 to 878) with only one DT connected at a time, but with all Strain Gauges in that rack energised to try to maximise rack loading.

For any channel with an excitation voltage of less than 5.0Volts, the measurements were repeated for each transducer type.

Results were as follows:

Rack No.	Channel Nos.	Comments
1	1 - 80	All 5.0 V
2	81 - 160	All 5.0 V
3	161 - 240	Channels 161 - 184 inc. all 2.50V, Others all 5.0 V
4	241 - 320	All 5.0 V
5	321 - 400	Channel 346 (SG67-3) 1.85V, Others all 5.0 V
6	401 - 480	All 5.0 V
7	481 - 560	All 5.0 V
8	561 - 640	All 5.0 V
9	641 - 720	All 5.0 V
10	721 - 800	All 5.0 V
11	801 - 880	All Strain Gauges 5.0 V. All DTs 5.0 V except those listed below

13.3 Displacements

Channel No.	PG 150 and UM20/30 (1kOhm)	PG 250 (2 kOhm)	Comments
861	4.03V	4.12V	DT29X Compensated for within Loadcases LC1, LC1C, LC2, LC2C Re-assigned to unaffected Channel for Loadcases LC3C, LC3, LC3C.A & LC1C.A
865	4.02V	4.11V	DT30Y Compensated for within Loadcases LC1, LC1C, LC2, LC2C Re-assigned to unaffected Channel for Loadcases LC3C, LC3, LC3C.A & LC1C.A
866	4.02V	4.11V	DT30Z Compensated for within Loadcases LC1, LC1C, LC2, LC2C Re-assigned to unaffected Channel for Loadcases LC3C, LC3, LC3C.A & LC1C.A
878	4.05V	4.18V	Not Used during Loadcases LC1, LC1C, LC2, LC2C, LC3, LC3C. DT38_2 Compensated for within Loadcases LC3C.A and LC1C.A
879	4.02V	4.11V	Global Load is not passive therefore has no affect

14 GLOBAL XYZ

The measured displacements of the 6 tri-axial groups of x, y & z transducers at each of Nodes 21, 22, 29, 30, 45 & 48 have been transformed to represent true components of displacements in the Global X, Y & Z space frame co-ordinates.

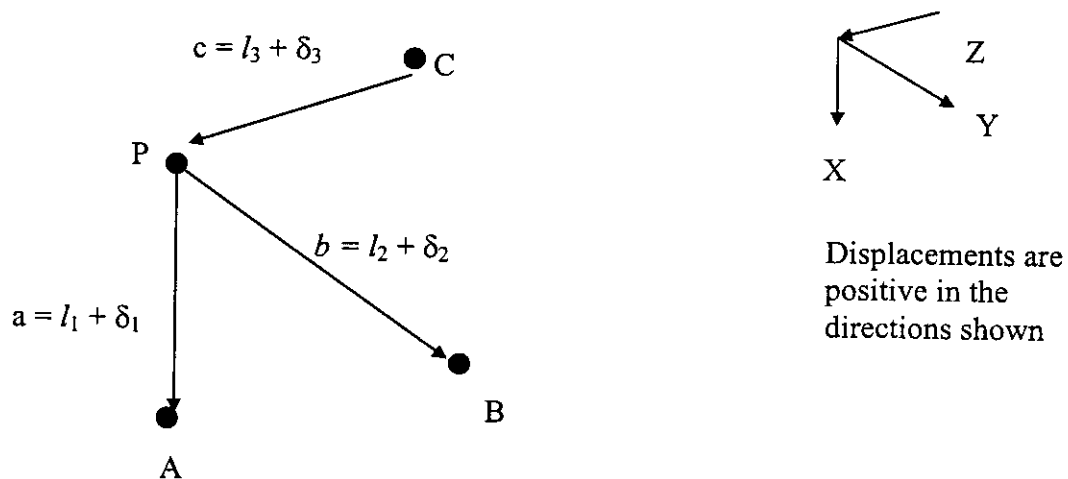
This transformation has been performed in accordance to the following specification:

14.1 Definition of Problem

Three displacement transducers meet at a point on a mobile structure, P, the other ends of each transducer being rigidly fixed to the reference frame at points A, B & C.

At the datum condition, the 3 transducers are nominally aligned with the reference X, Y & Z co-ordinates and each have a datum length, l .

However, when the fixed point, X moves in space, one or more of the 3 transducers will vary in length by amounts δl , such that the 3 transducer axes will no longer remain orthogonal. (At extreme displacements, it is estimated that the axes of the transducers may typically be misaligned from the global X, Y & Z axes by up to around 30°).



Knowns: Datum lengths of the 3 transducers l_1 , l_2 , & l_3

Transducer displacements in axes of transducers, δ_1 , δ_2 , & δ_3

Assumptions: All 3 transducers are aligned with X, Y & Z frame axes at datum condition

All transducers meet at a point.

Unknowns: Displacements x , y & z which are the resolved components of δ_1 , δ_2 , & δ_3 in the X, Y & Z frame axes.

14.2 Transformation Equations

AVT have produces a set of 3 independent quadratic transformation equations to resolve the 3 independent displacements into global X, Y & Z co-ordinates to describe the movement of a point in space, relative to a fixed 3D reference frame.

The transformation equations have been implemented in the Global XYZ worksheet, contained within each Final Version Loadcase spreadsheet folder.

15 RETROSPECTIVE EFFECTS

These are details of effects observed during testing which have implications for previous versions of datafiles.

15.1 Loadcase 2 Retro Changes

Low excitation voltage detected in SG 67-3 (Ch 346) 1.96 V instead of 5.0 V – must adjust Cal Factor (Cell H349) in all Data spreadsheets from 400,000 to 1,020,408.2

15.2 Loadcase 3C Retro Changes

Low excitation voltage detected on Ch 861 (DT39_1) (4.23 V), Ch 865 (DT39-2) (4.03 V), Ch 866 (DT 40-1) (4.23 V). Must apply corrected Calibration Factors for these channels for all Loadcases.

15.3 Loadcase 3 Retro Changes

Calibration Factors for ASG 61 – 64 (Chs 841-844) are too high by a factor of 100. Must amend Data sheet Cells H844 to H847 to 4000 for all other Loadcases (and for Loadcase 3 Pre-Test).

15.4 Loadcase 1C.A Retro Changes

Calibration Factor changes resulting from Final Voltage measurements:

Sensor	Channel	Cal Factor Cell Reference	Old Value	New Value
SG67-3	346	Data!H349	1020408.2	1081081.1
DT37-2	846	Data!H849	-30.0	+30.0
DT38-2	878	Data!H881	-30.0	+37.04

These changes only affect the final 2 Loadcase tests LC1C.A and LC3C.A.

16 MODIFICATIONS TO 'FINAL' VERSION DATAFILES

16.1 Loadcase 1

16.1.1 Worksheet Standardised Data Locations

Data Sheet - Standardised Cell References imposed (Data Scan 2 moved from Column L to Column N)

Prediction Data sheet - Standardised Cell References imposed (6 Rows inserted (Rows 11-16) for provision for Nodes 2 & 10)

16.1.2 Input Channel Re-assignment

Data sheet highlighted (green) to notify re-assignment of ASG 54 from Logger Ch 834 to Ch 777

16.1.3 Re-allocate spreadsheet for Correct ASGs Input Locations

Channels 813-816 Channel allocation previously ASGs 33-36 now Spares

Channels 829-832 Channel allocation previously ASGs 49-52 now Spares

Channels 837-844 Channel allocation previously Spares now ASGs 57-64

Channels 841-844 Calibration Factor previously 400,000 now 4000

16.1.4 Calibration Factors changed to compensate for measured low excitation voltage

Channel	Sensor	Data Cell Ref	Compensation Factor	Old Cal Factor	New Cal Factor
Ch 346	SG 67-3	H349	5.00/1.96	400,000	1,020,408.2
Ch 861	DT29_X	H864	5.00/4.23	50	59.1
Ch 865	DT30-Y	H868	5.00/4.03	157.6	195.5
Ch 866	DT 30-Z	H869	5.00/4.23	50	59.1

16.2 Loadcase 1C

16.2.1 Worksheet Standardised Data Locations

Data Sheet - Standardised Cell References imposed (Data Scan 2 moved from Column L to Column N)

Prediction Data sheet - Standardised Cell References imposed (6 Rows inserted (Rows 11-16) for provision for Nodes 2 & 10)

16.2.2 Input Channel Re-assignment

Data sheet highlighted (green) to notify re-assignment of ASG 54 from Logger Ch 834 to Ch 777

16.2.3 Re-allocate spreadsheet for Correct ASGs Input Locations

Channels 813–816 Channel allocation previously ASGs 33-36 now Spares
 Channels 829-832 Channel allocation previously ASGs 49-52 now Spares
 Channels 837-844 Channel allocation previously Spares now ASGs 57-64
 Channels 841-844 Calibration Factor previously 400,000 now 4000

16.2.4 Calibration Factors changed to compensate for measured low excitation voltage

Channel	Sensor	Data Cell Ref	Compensation Factor	Old Cal Factor	New Cal Factor
Ch 346	SG 67-3	H349	5.00/1.96	400,000	1,020,408.2
Ch 861	DT29_X	H864	5.00/4.23	50	59.1
Ch 865	DT30-Y	H868	5.00/4.03	157.6	195.5
Ch 866	DT 30-Z	H869	5.00/4.23	50	59.1

16.3 Loadcase 2

16.3.1 Worksheet Standardised Data Locations

Prediction Data sheet - Standardised Cell References imposed (6 Rows inserted (Rows 11-16) for provision for Nodes 2 & 10

16.3.2 Input Channel Re-assignment

Data sheet highlighted (green) to notify re-assignment of ASG 54 from Ch 834 to Ch 777.

Data sheet highlighted (green) to notify re-assignment of SG8-1 from Ch 201 to Ch 477 from Scan 15 onwards.

16.3.3 Re-allocate spreadsheet for Correct ASGs Input Locations

Channels 813–816 Channel allocation previously ASGs 33-36 now Spares
 Channels 829-832 Channel allocation previously ASGs 49-52 now Spares
 Channels 837-844 Channel allocation previously Spares now ASGs 57-64
 Channels 841-844 Calibration Factor previously 400,000 now 4000

16.3.4 Calibration Factors changed to compensate for measured low excitation voltage

Channel	Sensor	Data Cell Ref	Compensation Factor	Old Cal Factor	New Cal Factor
Ch 346	SG 67-3	H349	5.00/1.96	400,000	1,020,408.2
Ch 861	DT29_X	H864	5.00/4.23	50	59.1
Ch 865	DT30-Y	H868	5.00/4.03	157.6	195.5
Ch 866	DT 30-Z	H869	5.00/4.23	50	59.1

16.4 Loadcase 2C

16.4.1 Worksheet Standardised Data Locations

Prediction Data sheet - Standardised Cell References imposed (6 Rows inserted (Rows 11-16) for provision for Nodes 2 & 10

16.4.2 Input Channel Re-assignment

Data sheet highlighted (green) to notify re-assignment of ASG 54 from Ch 834 to Ch 777.

Data sheet highlighted (green) to notify re-assignment of SG8-1 from Ch 201 to Ch 477.

16.4.3 Re-allocate spreadsheet for Correct ASGs Input Locations

Channels 813-816	Channel allocation	previously ASGs 33-36	now Spares
Channels 829-832	Channel allocation	previously ASGs 49-52	now Spares
Channels 837-844	Channel allocation	previously Spares	now ASGs 57-64
Channels 841-844	Calibration Factor	previously 400,000	now 4000

16.4.4 Calibration Factors changed to compensate for measured low excitation voltage

Channel	Sensor	Data Cell Ref	Compensation Factor	Old Cal Factor	New Cal Factor
Ch 346	SG 67-3	H349	5.00/1.96	400,000	1,020,408.2
Ch 861	DT29_X	H864	5.00/4.23	50	59.1
Ch 865	DT30-Y	H868	5.00/4.03	157.6	195.5
Ch 866	DT 30-Z	H869	5.00/4.23	50	59.1

16.4.5 Additional Strain Gauges

Additional SGs installed SG82B 1, 3, 5 & 7 (Chs 389 – 392) from Scan 17 onwards. (Replacing SG84F). Datum Scan 17 copied into Column L. Changes are highlighted Yellow in Data sheet.

16.5 Loadcase 3C

16.5.1 Input Channel Re-assignment

Data sheet highlighted (green) to notify re-assignment of ASG 54 from Ch 834 to Ch 777

Data sheet highlighted (green) to notify re-assignment of SG8-1 from Ch 201 to Ch 477.

16.5.2 Re-allocate spreadsheet for Correct ASGs Input Locations

Channels 813-816	Channel allocation	previously ASGs 33-36	now Spares
Channels 829-832	Channel allocation	previously ASGs 49-52	now Spares
Channels 837-844	Channel allocation	previously Spares	now ASGs 57-64
Channels 841-844	Calibration Factor	previously 400,000	now 4000

16.5.3 Calibration Factors changed to compensate for measured low excitation voltage

Channel	Sensor	Data Cell Ref	Compensation Factor	Old Cal Factor	New Cal Factor
Ch 346	SG 67-3	H349	5.00/1.96	400,000	1,020,408.2

16.5.4 Additional Strain Gauges

Data sheet highlighted (Yellow) to indicate additional SG 49-1, 3, 5,& 7 re-assigned to Chs 457 – 460, (replacing SG 87F), from Test Scan 1.

Data sheet highlighted (Yellow) to indicate additional SG 51-1, 3, 5,& 7 re-assigned to Chs 465 – 468, (replacing SG 94F), from Test Scan 1.

16.5.5 Re-Assigned Displacement Transducers

Global XYZ sheet highlighted (Green) to indicate re-assigned displacement transducer inputs, as follows:

DT 29-X re-assigned from Ch 861 to Ch 850

DT 30-Y re-assigned from Ch 865 to Ch 851

DT 30-Z re-assigned from Ch 866 to Ch 852

DT 48-Y re-assigned from Ch 871 to Ch 853

16.5.6 Modified Equations for Processed Data

Calculation of Axial Load for LC30 corrected to ignore failed strain gauge LC30-7 (Ch120). (Highlighted Magenta in Data sheet).

16.6 Loadcase 3**16.6.1 Input Channel Re-assignment**

Data sheet highlighted (green) to notify re-assignment of ASG 54 from Logger Ch 834 to Ch 777

Data sheet highlighted (green) to notify re-assignment of SG8-1 from Logger Ch 201 to Ch 477.

16.6.2 Re-allocate spreadsheet for Correct ASGs Input Locations

Channels 813–816 Channel allocation previously ASGs 33-36 now Spares

Channels 829-832 Channel allocation previously ASGs 49-52 now Spares

Channels 837-844 Channel allocation previously Spares now ASGs 57-64

ASGs ASG61 – 64 re-assigned from Chs 841-844 to Chs 829-832 from Scan 1a AND Calibration Factor reverted to original value 400,000

16.6.3 Calibration Factors changed to compensate for measured low excitation voltage

Channel	Sensor	Data Cell Ref.	Compensation Factor	Old Cal Factor	New Cal Factor
Ch 346	SG 67-3	H349	5.00/1.96	400,000	1,020,408.2

16.6.4 Additional Strain Gauges

Data sheet highlighted (Yellow) to indicate additional SG 49-1, 3, 5,& 7 re-assigned to Chs 457 – 460, (replacing SG 87F), from Test Scan 1.

Data sheet highlighted (Yellow) to indicate additional SG 51-1, 3, 5,& 7 re-assigned to Chs 465 – 468, (replacing SG 94F), from Test Scan 1.

16.6.5 Re-Assigned Displacement Transducers

Global XYZ sheet highlighted (Green) to indicate re-assigned displacement transducer inputs, as follows:

DT 29-X re-assigned from Ch 861 to Ch 850

DT 30-Y re-assigned from Ch 865 to Ch 851

DT 30-Z re-assigned from Ch 866 to Ch 852

DT 48-Y re-assigned from Ch 871 to Ch 853

16.6.6 Modified Equations for Processed Data

Calculation of Axial Load for LC30 corrected to ignore failed strain gauge LC30-7 (Ch120). (Highlighted Magenta in Data sheet).

16.7 Loadcase 3C.A - Spreadsheet Modifications to Final Version 'b'

Calibration Factor for SG 67-3 (Ch346) increased to account for low excitation voltage (1.85V instead of 5.0V)

Calibration Factor for DT38_2 (Ch 878) increased to account for low excitation voltage (4.05V instead of 5.0V)

16.7.1 Changed Polarity of DTs

Ch	Sensor	Old Polarity	New Polarity
846	DT37_2	-	+
854	DT33	+	-
874	DT36	+	-
876	DT33	+	-
877	DT34	+	-
878	DT38_2	-	+

Revision Notes updated.

16.8 Loadcase 1C.A - Spreadsheet Modifications to Final Version 'b'

Calibration Factor for SG 67-3 (Ch346) increased to account for low excitation voltage (1.85V instead of 5.0V)

Calibration Factor for DT38_2 (Ch 878) increased to account for low excitation voltage (4.05V instead of 5.0V)

DT22 'NUM' Error from Scan 148 to end of test, Corrected in Final version 'b' (Highlighted Yellow)

16.8.1 Changed Polarity of DTs

Ch	Sensor	Old Polarity	New Polarity
846	DT37_2	-	+
854	DT33	+	-
874	DT36	+	-
876	DT33	+	-
877	DT34	+	-
878	DT38_2	-	+

Revision Notes updated.

*The contents of this document are confidential to Participants of the Frames Project -
Phase III, under the terms of their contract for participation in the project*

**JOINT INDUSTRY TUBULAR FRAMES PROJECT -
PHASE III**

**MULTIPLANAR JOINT
STRESS CONCENTRATION FACTORS**

C636\18\018R REV 0 AUGUST 1999

Purpose of Issue	Rev	Date of Issue	Author	Checked	Approved
For Client comment	0	August 1999	HMB HMB	FHH FHH	 CJB

Controlled Copy	10	Uncontrolled Copy	
-----------------	----	-------------------	--

BOMEL LIMITED

Ledger House
Forest Green Road, Fifield
Maidenhead, Berkshire
SL6 2NR, UK

Telephone +44 (0)1628 777707

Fax +44 (0)1628 777877

Email bomel@compuserve.com



REVISION SHEET

REVISION	DETAILS OF REVISION	DATE
0	Draft for Client comment and reference by BG in follow up analysis	August 1999

FILE SHEET

PATH AND FILENAME	DETAILS OF FILE
C636\18\024u.pcx	Figure 1.1
C636\12\images\gui11.pcx	Figure 2.1(a)
C636\12\images\gui12.pcx	Figure 2.1(b)
C636\26\C476-7.pcx	Figure 2.2(a)
C636\26\C484-23.pcx	Figure 2.2(b)
C636\26\C514-7.pcx	Figure 2.2(c)
C636\18\020u.pcx	Figure 2.3(a)
C636\18\019u.pcx	Figure 2.3(b)
C636\18\021u.pcx	Figure 2.4
C636\18\022u.pcx	Figure 2.5
BOMEL incoming document 11354 File No. C636\43	Table 2.1
C636\18\023u.vsd	Figure 2.6
C636\18\017d.vsd	Figure 3.1
C636\18\025u.pcx	Figure 3.2
C636\26\C475-7.pcx	Figure 3.3
C636\26\C475-10.pcx	Figure 3.4
C636\26\C517-13.pcx	Figure 3.5
C636\18\026u.vsd	Figure 3.6
C636\18\027u.vsd	Figure 3.7
C636\18\028u.vsd	Figure 3.8



FILE SHEET CONTINUED

PATH AND FILENAME	DETAILS OF FILE
C636\37\011W.xls sheet GLOBAL Scan nos	Figure 4.1
C636\39\008W.xls sheet GLOBAL Scan nos	Figure 4.2
C636\40\016W.xls sheet GLOBAL Scan nos	Figure 4.3
C636\43\scfsorce.xls Sheet location summary	Table 4.1
C636\43\012w-a-1.xls Sheet report summary	Table 4.2
C636\43\012w-a-2.xls Sheet report summary	Table 4.3
C636\43\012w-a-3.xls Sheet report summary	Table 4.4
C636\04\017u.wpd	Appendix A
BOMEL Incoming documents 9266, 9314, 11354 & 12127	Appendix B
File C636\18	
C636\11\011d.dwg	Appendix C
C636\15\012d.dwg	Appendix C
C636\15\013d.dwg	Appendix C
C636\18\017d.vsd	Appendix C
C636\43\027w.xls	Appendix D
C636\43\028w.xls	Appendix D
C636\43\029w.xls	Appendix D
C636\43\027w.xls	Appendix E
C636\43\028w.xls	Appendix E
C636\43\029w.xls	Appendix E
C636\43\012w-a-1.xls	Appendix E
C636\43\012w-a-2.xls	Appendix E
C636\43\012w-a-3.xls	Appendix E



CONTENTS

	Page No.
FOREWORD	0.5
EXECUTIVE SUMMARY	0.9
1. INTRODUCTION	1.1
1.1 BACKGROUND	1.1
1.2 SCF STUDY SCOPE	1.3
2. JOINT SELECTION	2.1
2.1 BASIS FOR JOINT SELECTION	2.1
2.2 PRELIMINARY INVESTIGATIONS	2.4
2.3 DETAILED INVESTIGATIONS	2.4
2.3.1 FE Analysis	2.4
2.3.2 Parametric SCF Assessment	2.4
2.3.3 Evaluation	2.7
2.3.4 Future Investigations	2.9
3. INSTRUMENTATION	3.1
3.1 GENERAL	3.1
3.2 SCF MONITORING INSTRUMENTATION	3.1
3.3 SIGN CONVENTION	3.5
3.4 SCF DATA REDUCTION	3.9
3.5 NOMINAL STRESS REDUCTION	3.11
4. PRESENTATION OF RESULTS	4.1
4.1 SAMPLED RESULTS	4.1
4.2 COMPARISON OF RESULTS	4.8
4.2.1 Nominal Forces and Moments	4.8
4.2.2 Nominal and Principal Stresses	4.8
4.2.3 Measured and Predicted Principal Stresses	4.9
5. REFERENCES	5.1



CONTENTS CONTINUED

APPENDIX A	BRIEFING NOTE ON SCFs FOR MULTIPLANAR JOINTS WITHIN THE FRAMES III PROJECT TEST PROGRAMME
APPENDIX B	BG COMPARISON OF WELD TOE STRESS PREDICTIONS - NODE 7 - LOADCASES 1, 2 AND 3
APPENDIX C	INSTRUMENTATION LAYOUT DETAILS
APPENDIX D	COMPARISON OF RESULTS
APPENDIX E	DETAILED RESULTS

FOREWORD

This report is one of a series describing different aspects of Phase III of the Joint Industry Tubular Frames Project. Each report is self contained providing detailed information in the subject area and summarising relevant data from other documents. The following table lists and briefly describes the focus of each report for cross-referencing purposes.

Report Title	Reference	Circulation
Summary and Conclusions Overview report describing the project and principal findings	C636\04\478R	1
Background, Scope and Development Scene setting report summarising previous work, identified needs and Phase III programme definition and development	C636\04\435R	1
3D Test Set Up Brief description of the 3D test set up and structural configuration	C636\06\313R	1
Material Testing Report Description of material testing procedures, test results and disposition of specific materials within test structure	C636\23\004R	1
Assessment of Locked-In Fabrication Stress Explanation for the build up of locked-in fabrication stresses, description of their measurement and summary of the locked-in force values in key components at the start of each test	C636\21\050R	1
Test Frame Instrumentation Detailed description of all instrumentation systems used in the 3D frame, accuracy, sign conventions etc. Data on CD in final report	C636\25\071R	1
Loadcase 1 Test Report - Multiplanar K Joint Action Detailed description of the Loadcase 1 static test response and interpretation of the results and their significance	C636\37\014R	1
Loadcase 2 Test Report - Interaction Between X-Braced Planes Detailed description of the Loadcase 2 static test response and interpretation of the results and their significance	C636\39\011R	1
Loadcase 3 Test Report - Multiple Member Failures and 3D System Action Detailed description of the Loadcase 3 static test response and interpretation of the results and their significance	C636\40\021R	1



Report Title	Reference	Circulation
<p>Philosophy of Cyclic Testing Discussion of the background to cyclic response issues in the context of ultimate system strength and basis for specific loading scenarios</p>	C636\24\021R	1
<p>Loadcase 1 Cyclic Test Report Detailed description of the Loadcase 1 cyclic test response and interpretation of the results and their significance. Comparison with LC1 static results</p>	C636\38\010R	1
<p>Monotonic and Cyclic testing of Isolated K Joints Description and presentation of results from isolated component tests undertaken by SINTEF in Norway</p>	STF22 F98704 (C636\24)	1/2
<p>Loadcases 2 and 3 Cyclic Test Report Detailed description of the Loadcases 2 and 3 cyclic test responses and interpretation of the results and their significance. Comparison with LC2 and LC3 static results</p>	C636\41\011R	2
<p>Loadcases 1 and 3 'Alternative' Cyclic Tests Detailed description of the Loadcases 1 and 3 alternative cyclic test responses and interpretation of the results and their significance. Comparison with LC1 and LC3 static and cyclic tests</p>	C636\45\008R	3
<p>Multiplanar SCFs Joint BG / BOMEL report describing analytical work and experimental measurements of multiplanar SCFs. Includes comparison with 'standard' empirical approaches</p>	C636\18\018R	1
<p>Site Testing Programme results - Report to Benchmark Analysts Comprehensive report describing results for benchmark cases LC1, LC2 and LC3, including all pertinent data and providing response plots 'matching' the contributions from individual analysts</p>	C636\32\066R	4
<p>Benchmark Conclusions Report comparing blind and post test analyses with measured responses and assimilating learnings and recommendations for future practice identified by Benchmark Analysts</p>	C636\32\084R	1

Key to circulation.

Circulation	All participants	Participants in 1st extension	Participants contributing finance/analytical results to 2nd extension	Benchmark Analysts
1	✓	-	-	×
2	-	✓	-	×
3	-	-	✓	×
4	✓	-	-	✓



JOINT INDUSTRY TUBULAR FRAMES PROJECT - PHASE III

MULTIPLANAR JOINT STRESS CONCENTRATION FACTORS

EXECUTIVE SUMMARY

The Joint Industry Tubular Frames Project Phase III was undertaken to provide realistic data on the performance of 3D jacket type structures. Alongside the principal activities examining ultimate system strength performance, the demonstration structure was instrumented to provide data on realistic stress concentrations (SCFs) developed at multiplanar tubular joint intersections for comparison with simplified approaches used in design.

Analytical and interpretative work was undertaken by BG plc as part of their contribution to the project. BG worked closely with BOMEL personnel who were responsible for implementing the instrumentation recommendations and data reduction. This report, prepared by BOMEL, is therefore a bridging document between the main body of project reports and the specific investigation reported in a comparison document by BG. It outlines the full scope of the activity and then describes the basis on which a multiplanar node was selected for monitoring. The chosen joint (Node 7) comprised eight intersections in three planes with K, T, N and KT configurations. Twenty four different brace/chord crown/saddle locations were selected to monitor stress concentrations providing insight to inter-plane interactions and addressing anomalies between prediction methods.

This report sets out the instrumentation system installed by AV Technology comprising 48 number 45° rosettes from which to determine weld toe principal stresses, and some 56 additional linear strain gauges to determine nominal axial and bending stresses. The sign conventions adopted in the experimental work are defined and the theories underlying the data reduction are set down.

Sample results are presented for initial stages in each of the Loadcase 1, 2 and 3 tests. Comparisons are made between the nominal load effects determined from the test and BOMEL SAFJAC and BG ABAQUS analyses. The nominal stresses are then compared with the weld toe principal stress to give an indication of the stress concentration factors. Direct comparison is also made between measured and predicted levels of weld toe stress. The report highlights a number of areas which may contribute to discrepancies from this first pass comparison. Nevertheless there is reasonable correlation between the average absolute stress levels across all the cases considered. Where values in the test average 59N/mm², for example, FE analysis give some 44N/mm² and predictions using Efthymiou parametric predictions average 50N/mm².



Whilst encouraging, further investigation is required as reported in the companion BG report to help interpret and generalise the findings. The BG report describes in detail the criteria for node selection. The underpinning finite element analyses using ABAQUS and USFOS comparisons are presented, together with a detailed description of the calculations using industry standard parametric formulae for both planar and multiplanar SCF predictions. In addition to complete structural analyses, the findings from component calculations are presented in which the contribution from individual brace loads to stress levels at other intersections were investigated. These and the comparison between measured and predicted values from this report provide the basis for assessing the significance and ability for industry to determine realistic SCFs at multiplanar joints in jacket structures.

The volume of data gathered is enormous and the quality is shown in this report to be exceptional. The extension of the Frames Project Phase III programme to encompass eight instead of the planned four tests has enabled twice as much data to be gathered at no extra cost, although the data interpretation falls beyond the present scope.

In addition the BG work included finite element analysis of two other multiplanar nodes, determination of SCFs and comparison with conventional parametric predictions. The SINTEF tests in support of the Loadcase 1 cyclic scenarios also captured SCF data for a similar geometry. In addition to addressing the specific scope within the project the work has resulted in a large body of data for future use to expand industry understanding of multiplanar influences on stress concentrations and fatigue performance.



1. INTRODUCTION

1.1 BACKGROUND

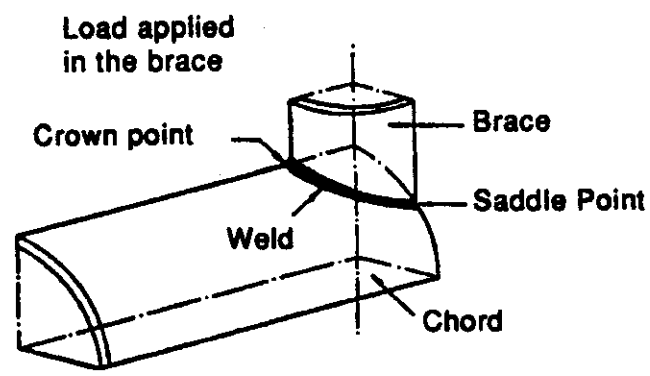
Phase III of the Joint Industry Tubular Frames Project was established to examine the ultimate response characteristics of jacket type offshore structures. In order to provide a realistic demonstration of the behaviour, a large scale 3D structure was built and tested under multiple loading scenarios. To date offshore design practice in terms of both strength and fatigue has been based on results of idealised component tests^(eg. 1, 2). Only recently have these been supplemented with data on 2D frame responses^(3, 4). The Frames Project 3D facility therefore provided a unique opportunity to investigate many aspects of 'real' structural behaviour.

Offshore structures are designed to withstand ultimate and fatigue limit states. Although survival of extreme events may be crucial to life safety, degradation due to fatigue may have significant economic and operational consequences. During the early years of North Sea oil and gas production some fatigue damage was experienced requiring a number of structural repairs and changes to engineering practice. However with fuller recognition of fatigue loading mechanisms and improved design methods based on extensive laboratory tests⁽²⁾, these problems have now largely been eliminated. Nevertheless with an ageing population of offshore platforms there has been renewed attention on fatigue. In particular it now appears that fatigue performance is better than anticipated and there is interest in quantifying the influence of factors which are not accounted for in current methods.

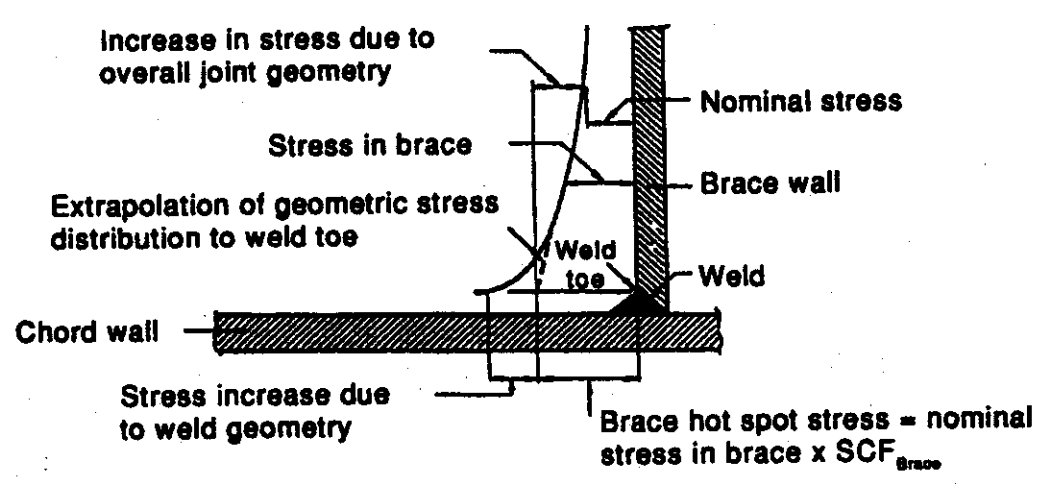
For example, the stress concentrations around welded intersections which precipitate fatigue damage are usually determined from parametric formulae for joints in a plane. Figure 1.1 illustrates the local development of stresses up to the weld toe of tubular joint intersections.

The influence of out-of-plane braces, either stiffening the chord or modifying the local loadpaths, is rarely considered. Some research effort has been directed at determining multiplanar effects both with experimental and analytical investigations and to develop formulae for general application. However, these are not used routinely in practice.

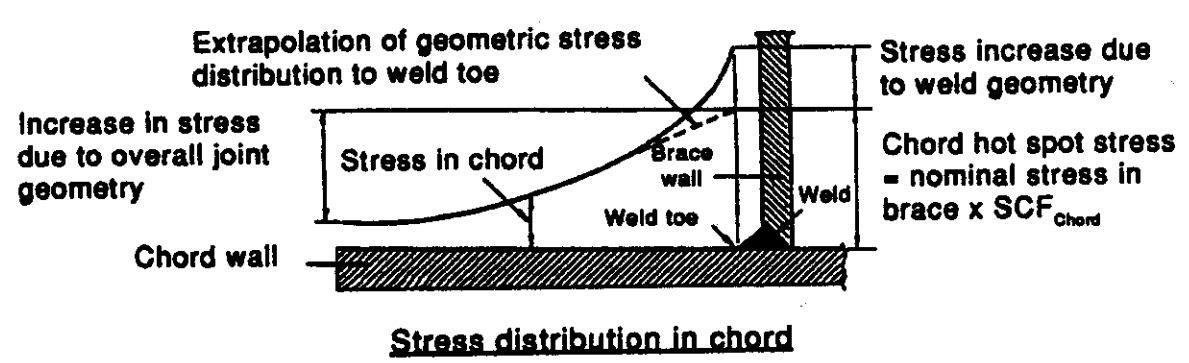
On this basis the Frames Project Participants agreed that the 3D tests structure should be instrumented to provide data on stress concentration factors (SCFs) at selected multiplanar joint intersections. The data could be gathered readily in the course of the structural collapse tests by expanding the logging equipment. The 3D tests provided an unprecedented opportunity to gather realistic SCF data at complex jacket type nodes with representative combinations of axial loads and moments in the bracing and chord.



Nodal joint nomenclature



Stress distribution in brace



Stress distribution in chord

Figure 1.1 Development of stress concentrations at the weld toe of nodal joints⁽¹⁴⁾

1.2 SCF STUDY SCOPE

The principal objective of this aspect of the Frames Project Phase III programme was:

- to benchmark industry practices for evaluating SCFs at multiplanar nodes using representative data from the 3D frame tests.

The work involved a number of distinct activities:

1. Development of a premise with procedures for undertaking the work.
2. Prediction of SCFs using parametric formulae and finite element analysis.
3. Selection of a node and weld toe locations for detailed examination.
4. Specification of instrumentation for recording SCFs and nominal stresses.
5. Data acquisition and data reduction.
6. Comparison of measured and predicted SCFs with supplementary analysis, as appropriate.
7. Reporting.

It was agreed that BG plc would undertake a significant part of the work by way of a contribution to the project. This report is therefore a bridging document between the main body of BOMEL reports describing the 3D test programme and the finite element analysis and SCF benchmarking undertaken and reported in a stand alone volume by BG⁽⁶⁾. The work proceeded on the basis of an initial specification prepared by BOMEL⁽⁶⁾ and an agreed workplan set out by BG⁽⁷⁾.

Section 2 outlines the basis for the joint selection and the extent of analysis performed by BG. The translation of the monitoring recommendations into the instrumentation scheme and reduction of test data, for which BOMEL was responsible, is detailed in Section 3. Section 4 then provides some initial comparisons which are developed further in the BG report⁽⁵⁾.

2. JOINT SELECTION

2.1 BASIS FOR JOINT SELECTION

The benchmarking of SCF predictions at multiplanar nodes was to be undertaken in the context of the series of collapse tests of the 3D frame. The bracing arrangements within the frame and the node and member referencing schemes are shown in Figure 2.1. Figure 2.2 shows the three axes for loading the structure. At the outset three ultimate strength tests were planned, one for each axis as shown; an additional cyclic test was to be performed on Line C for the 'Loadcase 1' configuration. Extensive component failures were anticipated in the vicinity of loading and elsewhere in the structure as the loads redistributed. Between tests it was planned to cutout and reinstate components where failure had occurred. This consideration was one of several factors influencing the node selection for SCF monitoring purposes. Considerations included:

- geometries and non-dimensional geometric parameters should be representative of jacket structures
- gaps between braces should be sufficient for meaningful SCFs to be recorded using strain gauges located in accordance with 'HSE' recommendations⁽⁸⁾
- multiplanar influences due to out-of-plane braces and loads should be significant so that the effects could be distinguished from scatter in planar data
- SCF instrumentation should be targeted at locations which were not expected to require repair or reinstatement following component failures in the ultimate strength tests; in this way SCF data for three different loading regimes (Loadcases 1, 2 and 3) could be gathered
- the chosen locations should experience different patterns of loading for the three loadcases
- the potential for comparison with previous component test data (eg. Lloyd's multiplanar acrylic nodes⁽⁹⁾ / Frames Project Phase I planar joint data⁽³⁾) should be considered.

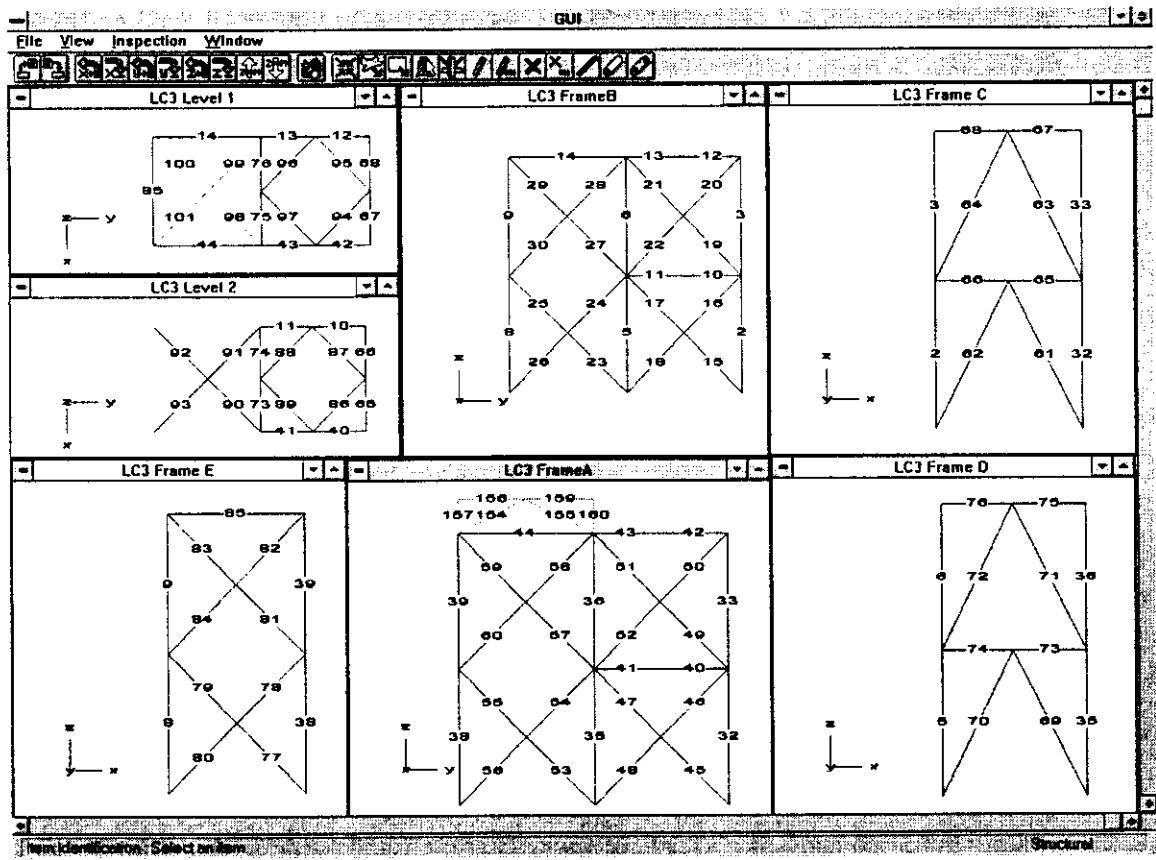


Figure 2.1(a) Member numbering scheme (Members 98-101 only in LC3, LC3CA and LC1CA tests)

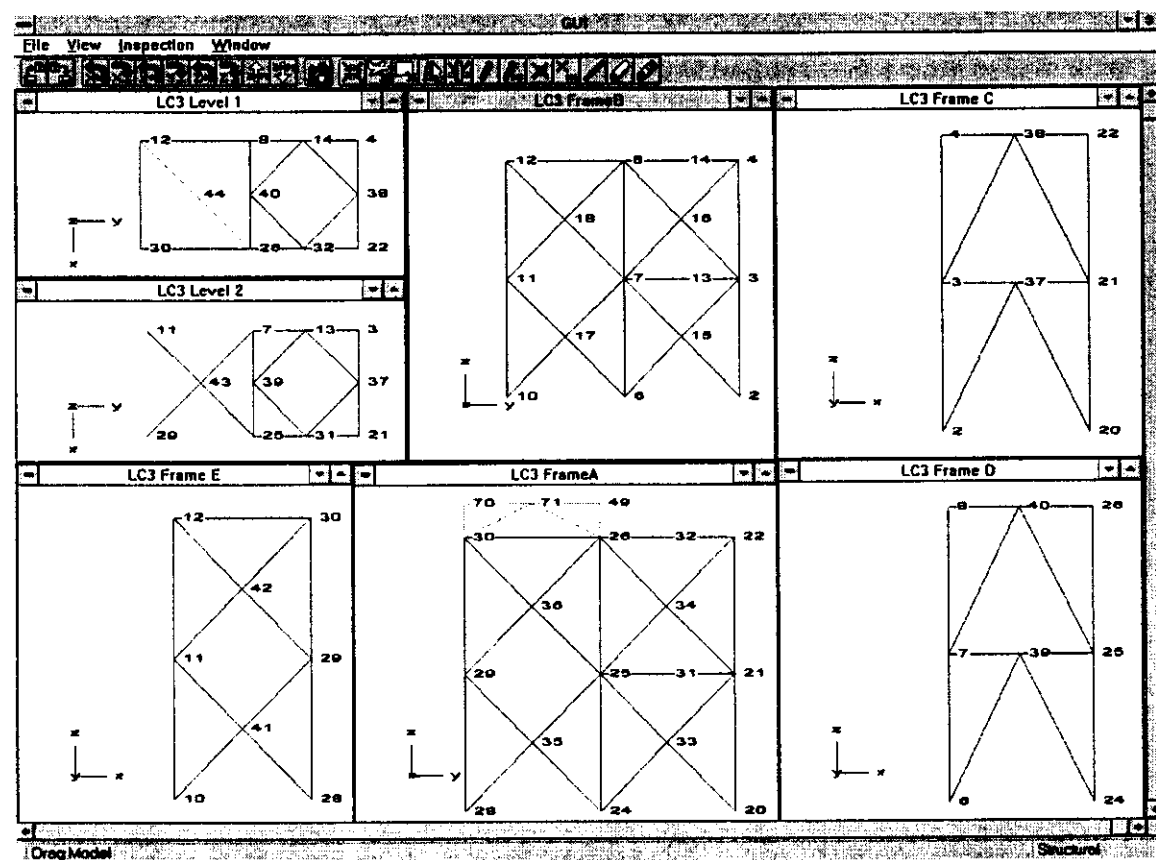


Figure 2.1(b) Node numbering scheme (Node 44 only present in LC3, LC3CA and LC1CA tests)

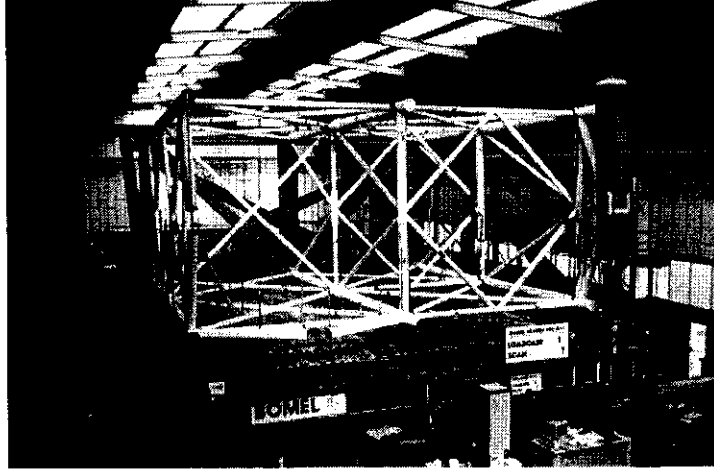


Figure 2.2(a) Loadcase 1 test configuration (LC1)

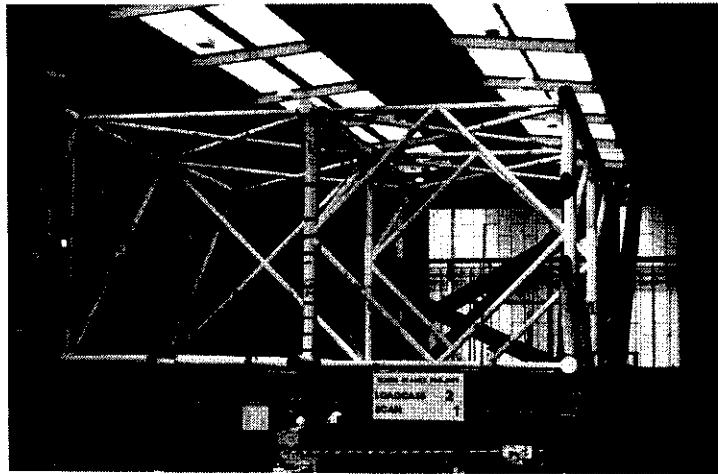


Figure 2.2(b) Loadcase 2 test configuration (LC2)

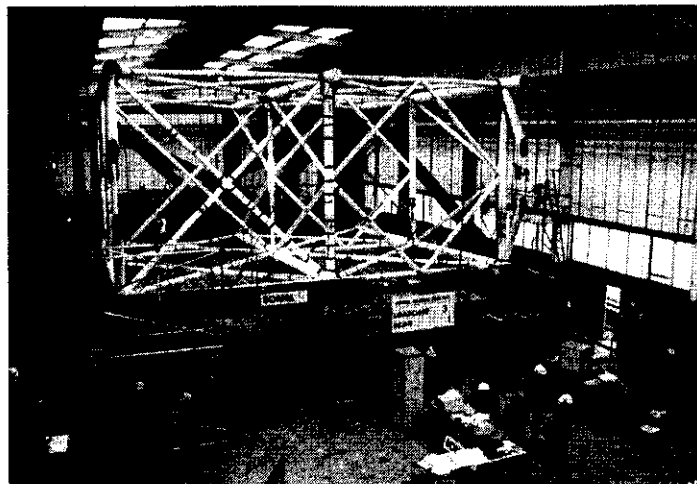


Figure 2.2(c) Loadcase 3 test configurations (LC3)

2.2 PRELIMINARY INVESTIGATIONS

During the early stages of the project when the prospect of monitoring SCFs was being considered, BOMEL prepared a briefing note for Participants⁽¹⁰⁾ which is included here in Appendix A. Three candidate nodes were identified (see Figure 2.1):

- Node 7 - eight brace multiplanar leg node - K (T) (N) KT
- Node 11 - five brace corner node - K (T) K
- Node 40 - four brace node K (K).

BG rescreened the options and concluded that these nodes offered the best potential. Cost precluded complete instrumentation and so further investigation was required to select one of the three candidate nodes and to identify key sites for instrumentation.

2.3 DETAILED INVESTIGATIONS

2.3.1 FE Analysis

Finite element (FE) models of all three nodes were developed by BG using ABAQUS 8-noded, thick shell reduced integration elements as shown in Figures 2.3 to 2.5. Analyses were performed for single brace loading of isolated nodes and the shell models were introduced to a 3D beam model of the test structure and reaction rig.

Stress concentration levels at all four crown and saddle positions to the chordside and braceside of each intersection were determined (eight locations total). Based on HSE recommendations⁽⁸⁾, principal stresses were calculated and extrapolated to the mid-surface intersections. Coacting axial and bending stresses in each brace were also determined. Uplift of the reaction rig was allowed for to provide direct comparison with the test. Modelling was elastic, enabling values to be factored for different load levels early in each test.

Comparative USFOS analyses were also undertaken to validate the global and local responses and to assess the 'elastic' limit.

2.3.2 Parametric SCF Assessment

For each node and loading configuration, SCFs were calculated at all eight sites using simple and multiplanar influence function approaches due to Efthymiou⁽¹¹⁾, Lloyd's Register⁽⁹⁾ and Kellogg⁽¹²⁾. The results are detailed in Reference 5 and Appendix B.

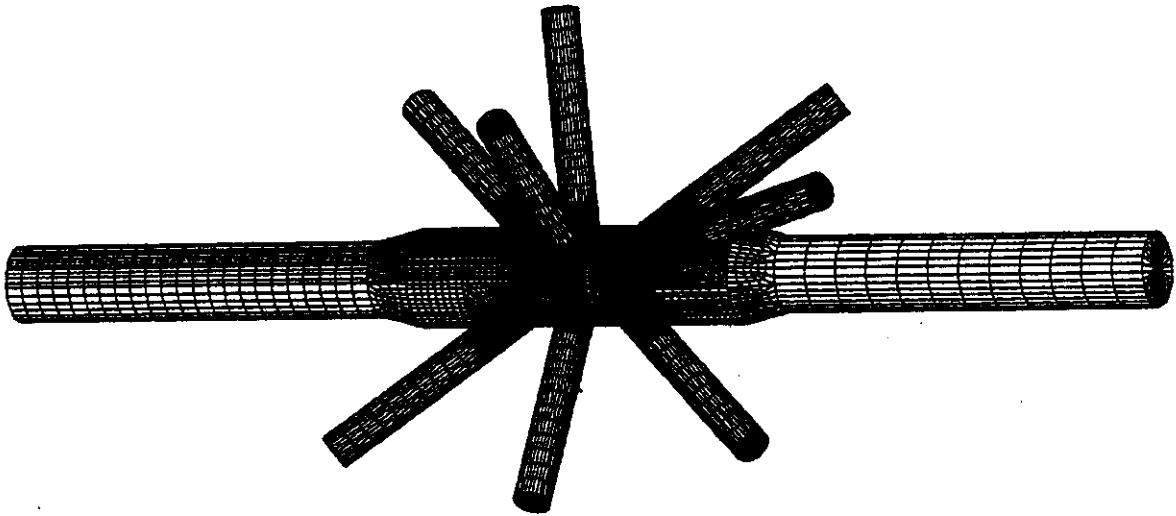


Figure 2.3(a) Node 7 - BG FE model - eight braces in three planes

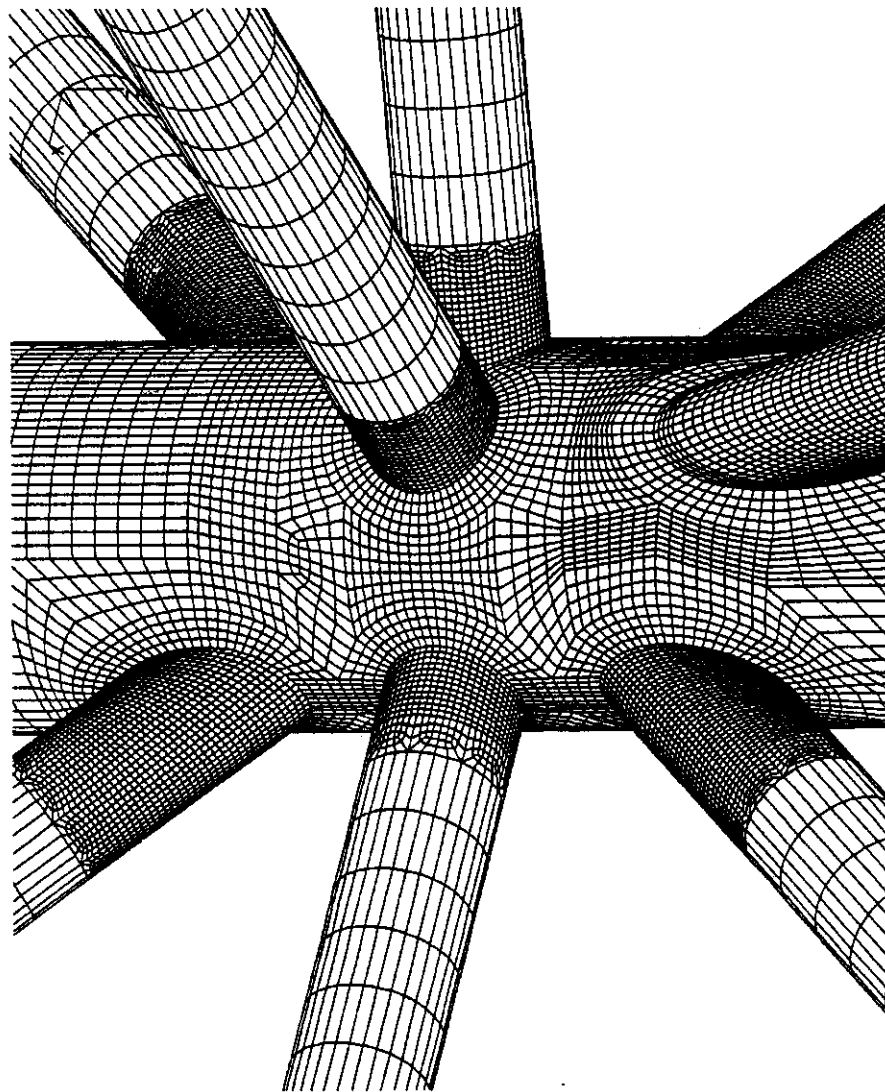


Figure 2.3(b) Node 7 - BG mesh - detail

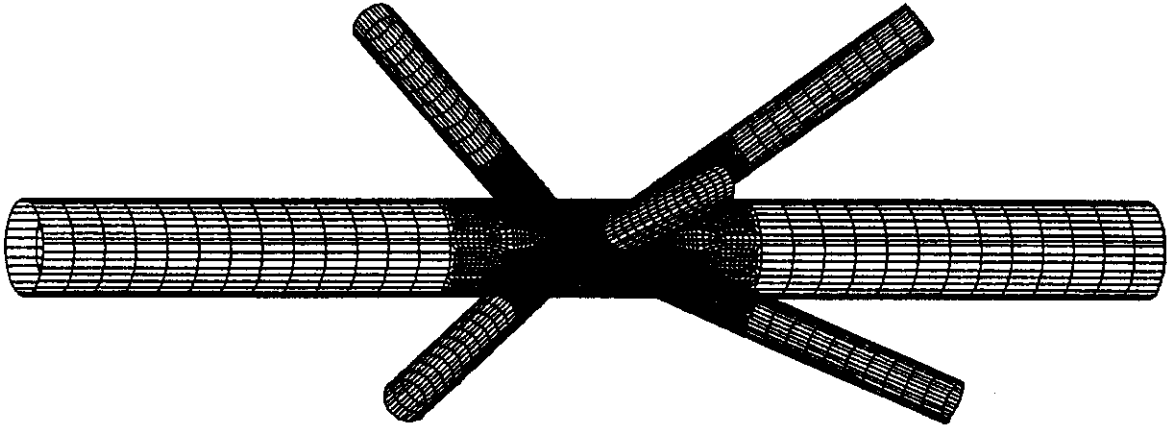


Figure 2.4 Node 11 - BG FE model

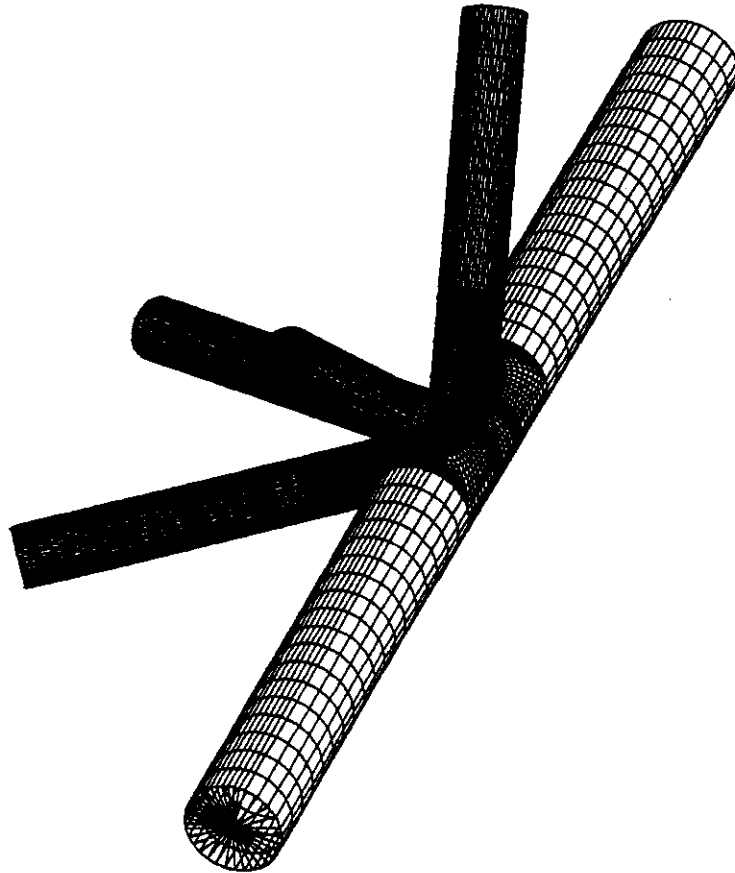


Figure 2.5 Node 40 - BG FE model

2.3.3 Evaluation

In order to compare the findings, BG devised a scoring system to reflect the stated selection criteria. It was considered to be important from a practical standpoint for SCF monitoring to focus on locations where the stress may be the highest for the intersection and would therefore govern in design. This followed particularly from the project emphasis on a demonstration to validate offshore practice rather than academic research. Furthermore it was important to use the test opportunity to resolve significant discrepancies between the calculation methods employed. The scoring system involved, for each of the eight locations around every intersection on all three nodes, identifying:

- (a) the number of approaches indicating the location gives the maximum stress from the intersection (ie. the hot spot)
- (b) the number of instances where FE and parametric methods differ
- (c) whether the stress level exceeds 50 N/mm² in order that the effects may be considered significant (1 - yes, 0 - no).

For each intersection the 'scores' for (a) and (b) were added and multiplied by (c). The cumulative totals for all intersections at each node and across the three primary loadcases were then determined. Some engineering judgement was also required to ensure a useful mix of brace/chord and crown/saddle positions was involved across different geometry classifications.

Careful study of the results in this way⁽⁵⁾ led to the recommendation that Node 7, the complex multibrace node at the top centre of the frame as viewed in Figure 2.2, be investigated.

'Other' factors influencing the selection of Node 7 included the fact that the joint experiences significant unbalanced loading. This is another common feature of real structures inadequately covered in laboratory research⁽³⁾. Table 2.1 summarises the axial and bending stresses determined by BG analytically. The varying stress pattern between each loadcase is clearly evident, as is the imbalance in certain cases for K brace pairs.

The planar joint definitions are:

- K - Braces 24 and 27
- T - Brace 91
- N - Braces 72 and 74
- KT - Braces 17, 11 and 22

It should be noted that the brace moments are given for the interface between beam and shell elements within each incoming brace member, not at the intersection, nevertheless the comparison is instructive.

Table 2.1 Node 7 - BG analytical comparison between nominal brace stresses in Loadcases 1, 2 and 3 (ABAQUS sign convention)

Brace	Loadcase 1 Applied Load 800kN Nominal brace stress (N/mm ²)			Loadcase 2 Applied Load 800kN Nominal brace stress (N/mm ²)			Loadcase 3 Applied Load 1750kN Nominal brace stress (N/mm ²)		
	Axial	IPB	OPB	Axial	IPB	OPB	Axial	IPB	OPB
11	-1.5	-5.3	-6.2	-6.5	6.2	4.2	-4.3	-13.3	0.8
17	21.0	-3.8	-0.1	-48.5	-0.7	6.2	51.7	-5.6	-3.3
22	-37.3	-0.9	-4.6	5.0	6.8	7.8	-46.3	-5.8	1.8
24	-78.4	7.4	0.4	31.2	-4.4	7.8	-34.3	3.9	-4.7
27	39.8	11.3	-12.8	-20.8	-4.8	24.7	33.7	2.2	4.3
72	-104.2	-2.7	-4.5	28.0	-7.6	-0.9	33.7	2.7	-2.0
74	25.5	-10.9	6.3	22.1	2.3	-24.7	-19.4	6.6	1.9
91	22.0	-5.9	-8.3	-64.4	-0.2	-20.3	0.1	5.0	4.5

Containing the SCF instrumentation within the budgets agreed, it was also possible for the coverage of SCF equations at Node 7 to be comprehensive as shown in Table 2.2. Figure 2.6 indicates the datum clock position on the brace footprints for reference.

Table 2.2 Node 7 - Summary of proposed gauge locations

Brace	CC0	CS90	CC180	CS270	BC0	BS90	BC180	BS270
11		x	x	x			x	x
17	x			x	x			
22		x				x		
24		x			x			
27		x			x			
72				x				x
74		x	x		x	x		
91	x			x	x			x
By Joint Type								
	CC	CS	BC	BS				
K	1	3	3	2				
T	1	1	1	1				
KT outer	1	3	1	1				
KT centre	1	2	1	1				
Key: CC - Chord crown 0°, 90°, 180°, 270° angular separation CS - Chord saddle BC - Brace crown BS - Brace saddle								

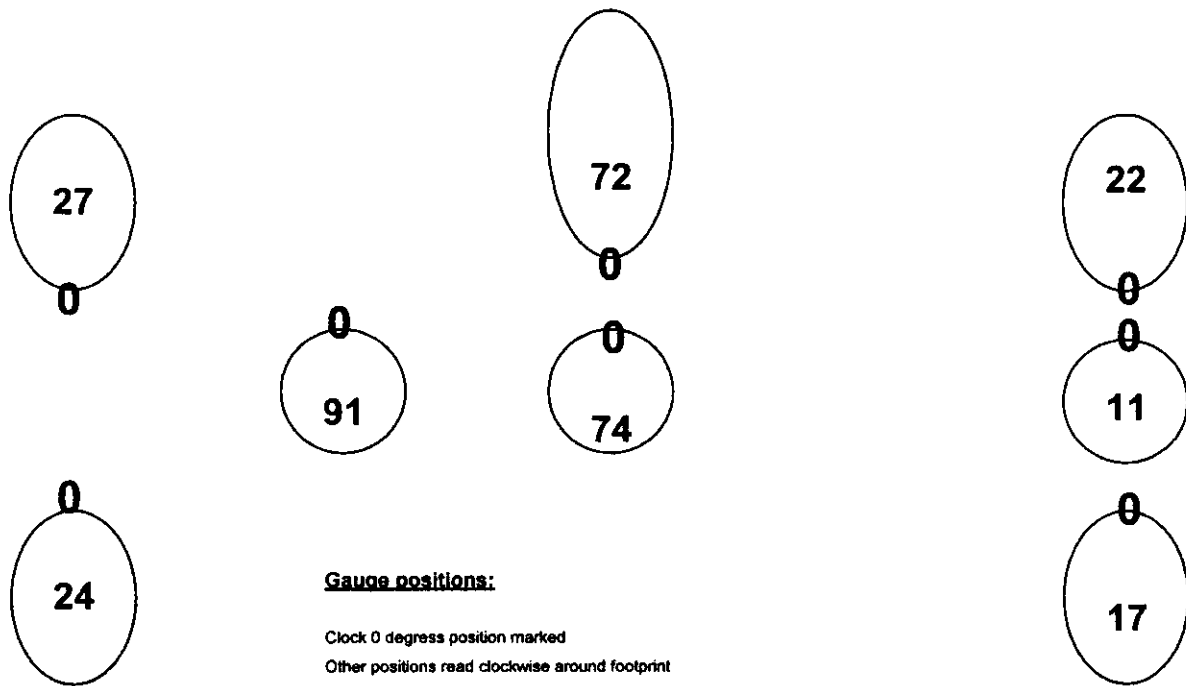


Figure 2.6 Node 7 developed - datum clock positions on the brace footprints

The node selection was endorsed by Project Participants and the instrumentation scheme was developed as described in Section 3.

2.3.4 Future Investigations

It is important to note that, although not all cases could be examined experimentally within the programme, the body of analytical results is in itself informative and valuable for future investigations. In addition, the SINTEF laboratory tests which supported the 3D frame test programme⁽¹⁵⁾ included SCF monitoring at planar and multiplanar K joints of a similar configuration to Node 40.

3. INSTRUMENTATION

3.1 GENERAL

The 3D structure was instrumented by AV Technology under contract to BOMEL Limited. The system comprised strain gauges and displacement transducers to deduce the member forces and global movements of the structure as it was loaded to failure in each test. All the instrumentation was connected to a central logging system providing output directly to a Microsoft Excel spreadsheet for data reduction and interpretation. Reference 13 provides a detailed description of all the 3D frame instrumentation. Key features relevant to the SCF monitoring system are described below.

3.2 SCF MONITORING INSTRUMENTATION

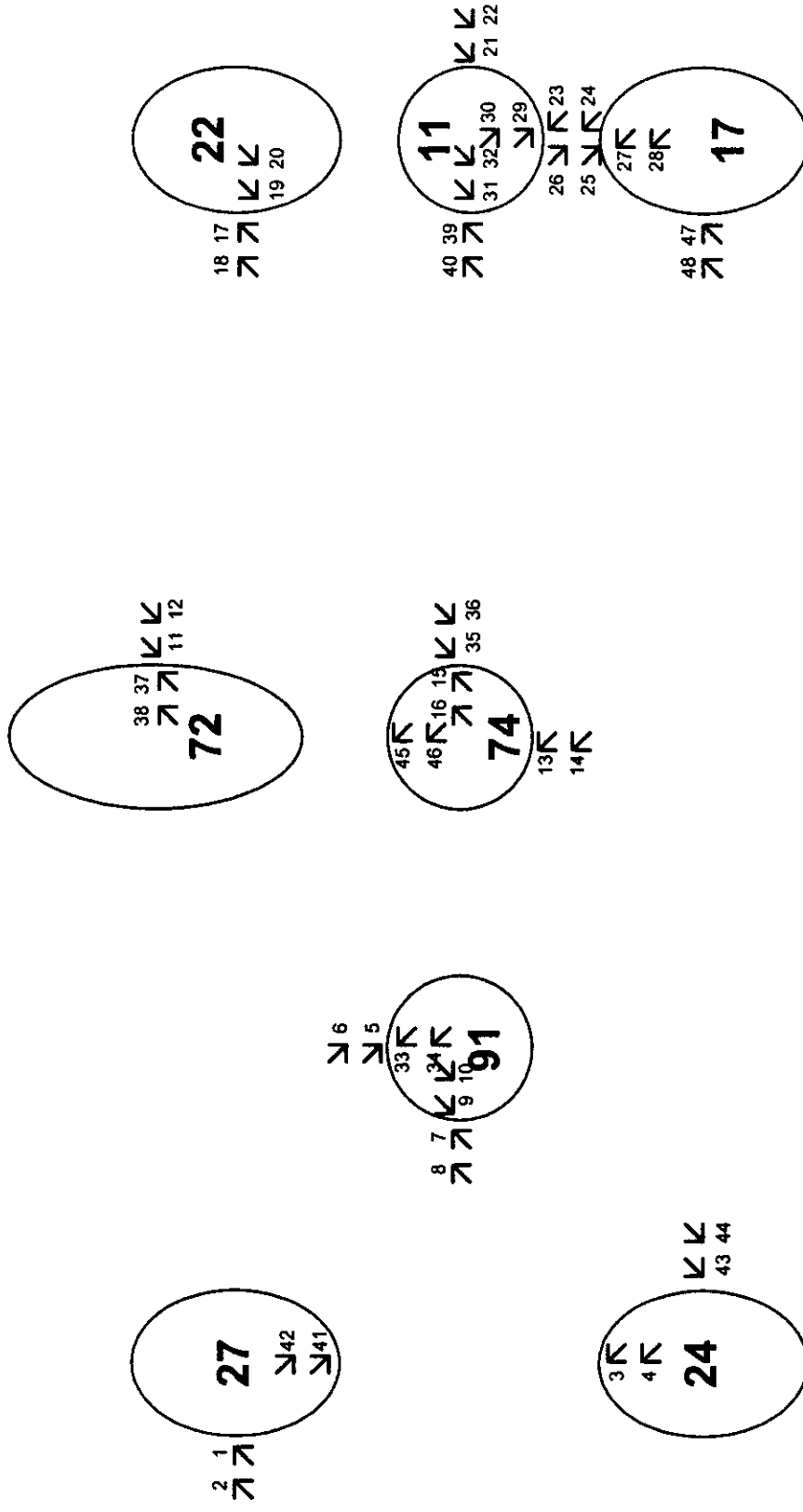
The general instrumentation was supplemented with additional gauges in the vicinity of Node 7 in order to capture comprehensive data on the SCFs.

Appendix C contains instrumentation layout drawings covering the 48 number 45° rosettes from which to determine weld toe principal stresses, and 56 additional linear strain gauges (ASGs) to determine nominal axial and bending stresses. In particular:

- Drawing C636\18\017D in Appendix C (also provided as Figure 3.1) shows the layout of 48 number 45° rosette type gauges from which to extrapolate stresses acting at the 24 nominated weld toe locations. Where the gauges are shown 'within the footprint' they are positioned on the braceside of the intersection. Tiny TML FRA-3-11-1L strain gauges were used in order that the rosettes could be affixed at the precise locations.
- Detail 6 on Drawing C636\15\013D shows the additional linear strain gauges (ASGs) positioned some three and six brace diameters from the brace chord intersections. The gauges were TML WFLA-6-11-1L pre-encapsulated pre-wired strain gauges. At each location four orthogonal gauges enable axial and bending stress components to be determined. Extrapolation from the ASGs and/or using data from other monitoring points along the member enabled moments at the intersections to be determined.

The rosette strain gauges were positioned in accordance with 'HSE' recommendations⁽⁸⁾ at the limits of the linear region shown in Figure 1.1 and defined in Figure 3.2. With nominal diameter / thickness properties for the chord and braces of 455.7 / 12.7mm and 168.3 / 4.5mm, the gauge positions indicated on Figure 3.1 were determined.

NODE 7 - SCF GAUGE POSITIONS



Key:



- 41 SCF gauge number
- A, B, C rosette gauge ID, clockwise from A
- A parallel to weld toe

Gauge positions:

- All brace side gauge pairs: 4mm and 12.7mm from weld toe
- Chord side gauge pairs at saddle location: 4mm and 19.9mm from weld toe
- Chord side gauge pairs at crown location: 4mm and 13.0mm from weld toe

Figure 3.1 Node 7 - SCF gauge positions



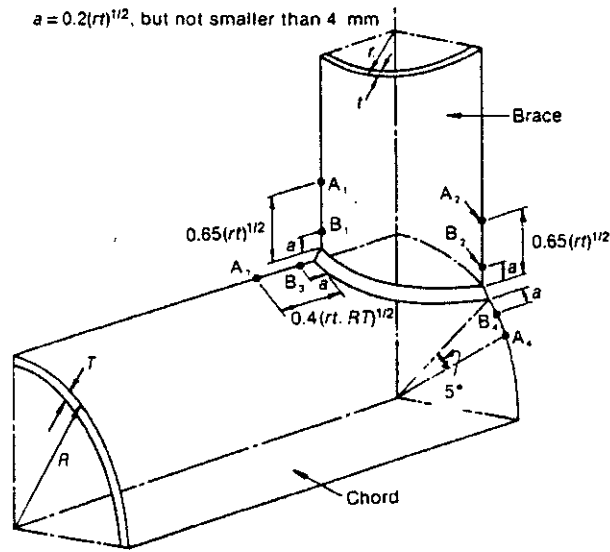


Figure 3.2 HSE⁽⁸⁾ definitions of regions of strain linearity

Together the above instrumentation systems enabled comprehensive data on nominal brace and weld toe stresses to be determined.

Figures 3.3 and 3.4 show opposite views of Node 7 once instrumentation was complete. Each gauge element was provided with dummy gauges to give complete compensation for thermal effects. The complexity and congestion of the instrumentation is evident.



Figure 3.3 SCF instrumentation of Node 7 - viewed from Frame C towards E

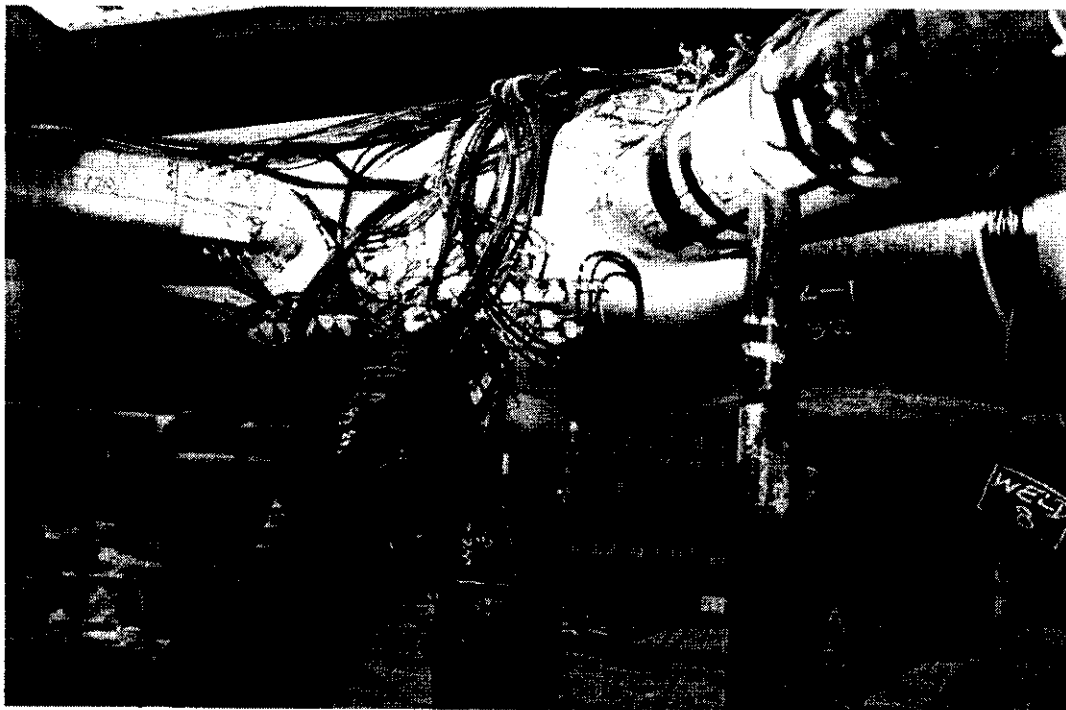


Figure 3.4 SCF instrumentation of Node 7 - viewed from Frame E towards C

Figure 3.5 shows a view up onto Node 7 on completion of the Loadcase 3 test. Some indication of local repairs can be seen in the singeing of the paint. These were effected after the Loadcase 1 test during which Brace 72 had buckled. Originally it had been planned to halt the test before Brace 72 was effected, however in the event it was decided to develop the full sequence of load redistribution. Reinstatement of Brace 72 meant that rosette gauges 11, 12, 37 and 38 associated with Brace 72, and 45 and 46 on Brace 74 had to be reinstalled. Similarly additional linear strain gauges on Brace 72 were replaced. All other gauges were adequately protected and performed completely satisfactorily in subsequent tests.



Figure 3.5 Node 7 after Loadcase 3 test

3.3 SIGN CONVENTION

A considerable complexity in generating 3D frame data and making analytical comparisons is the need for consistent sign conventions. For interpreting the SCF data some translation is required before comparisons between measured results and different analytical predictions can be made. Key elements of the different schemes are as follows:

- SCF rosettes - For consistency with rosettes elsewhere on the structure (but contrary in some instances to BG sketches) all SCF rosettes were oriented with Gauge Element 'A' parallel to the weld toe. Elements 'B' and 'C' were oriented through clockwise angles of 45° and 90° respectively. The configuration is shown in Figure 3.1.
- Linear strain gauges (ASGs) - For consistency with the instrumentation scheme throughout the structure, the four linear gauges at each measuring location were designated '1', '3', '5' and '7' where 1 and 5 are in the plane of bracing and 3 and 7 are out-of-plane. The axis convention is detailed in Reference 13 but Figure 3.6 shows the resulting positions for each brace at Node 7. The convention is that measured strains ϵ_1 - ϵ_5 and ϵ_3 - ϵ_7 give positive moments. The BG sketches for ASGs were based on analysis (with its own sign conventions) and gave an alternative numbering sequence. Table 3.1 presents the cross correlation between ASG reference numbers and the 1, 3, 5, 7 test designation.

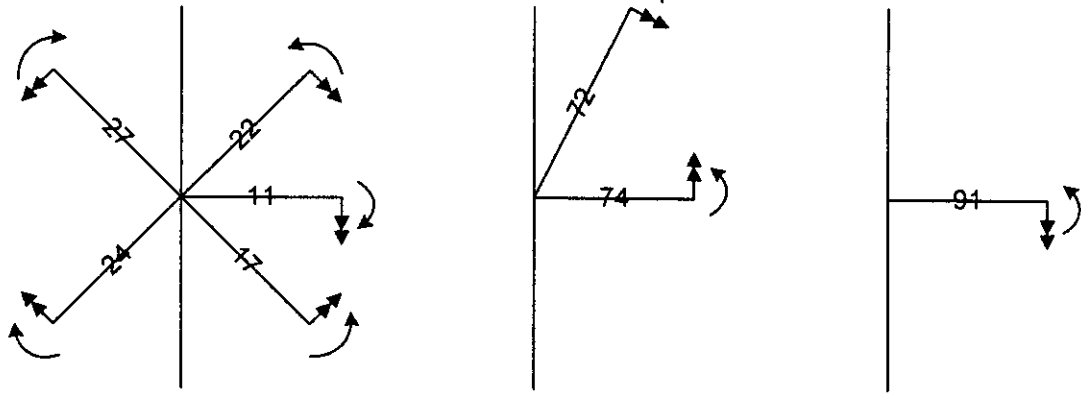
- Analysis - In the following sections comparison is made between analytical predictions and test results. BG ABAQUS and BOMEL SAFJAC analyses adopt different conventions. Figure 3.7 shows the positive orientation for in-plane and out-of-plane moments in BOMEL and BG analyses in comparison with the test convention. In all cases axial forces are considered positive in tension, and for clarity are not included. Table 3.2 confirm the conversion to translate each analysis into the test convention.

Table 3.1 Position of linear gauges on braces at Node 7

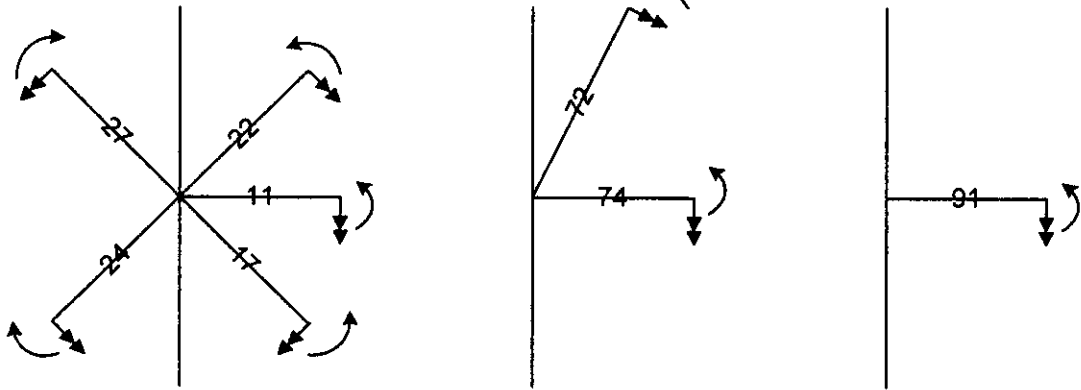
Brace	Gauges	Distance from chord face intersection (mm)	Strain gauge designation (ASG - uno)			
			In-plane 1	Out-of-plane 3	In-plane 5	Out-of-plane 7
1	ASG	505	55	54	53	56
	Strain gauge 11	1258	SG1	SG3	SG5	SG7
17	ASG	1010	57	58	59	60
	ASG	505	61	62	63	64
22	ASG	1010	41	44	43	42
	ASG	505	45	48	47	46
24	ASG	1010	11	12	9	10
	ASG	505	15	16	13	14
27	ASG	1010	3	2	1	4
	ASG	505	7	6	5	8
72	ASG	1010	27	26	25	28
	Load cell	1474	LC1	LC3	LC5	LC7
74	ASG	420	37	40	39	38
	Strain gauge 74	658	SG1	SG3	SG5	SG7
91	ASG	900	20	17	18	19
	ASG	505	24	21	22	23

Note: Reference Appendix C Drawing C636\15\013D and Figure 3.5.
Gauge: Load cell or strain gauge indicates data gathered from main instrumentation system
LC1 etc: In the context of this table refers to load cell strain measurements at positions 1, 3, 5, 7

SAFJAC



BG



TEST

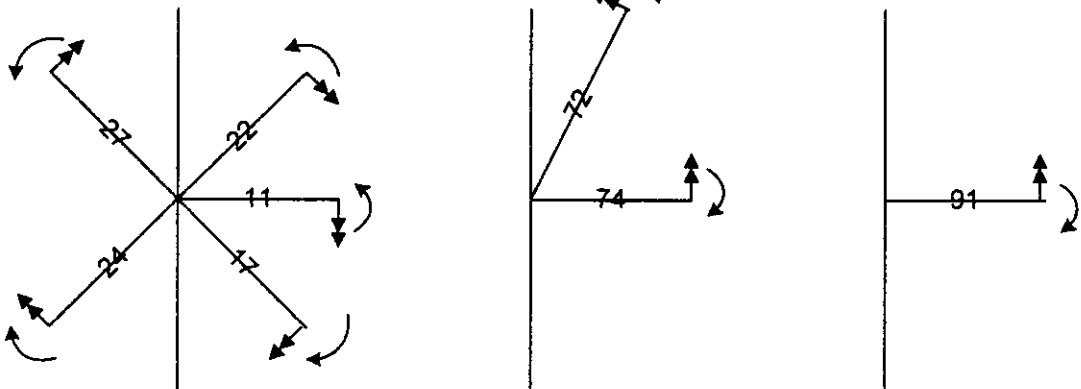


Figure 3.7 Comparison between analysis and test positive moment conventions.
Axial tension positive in all cases

Table 3.2 Conversion from analysis to test sign conventions

Brace	Analysis / Mode			
	BOMEL - SAFJAC		BG - ABAQUS	
	IPB	OPB	IPB	OPB
11	-1	1	1	1
17	-1	-1	-1	1
22	1	1	1	1
24	1	1	1	-1
27	-1	-1	-1	-1
72	-1	-1	-1	-1
74	-1	1	-1	-1
91	-1	-1	-1	-1

In the above it is also worthy of note that for the 'plan' brace 91, in-plane moments with respect to the X bracing are acting out-of-plane with respect to the chord at Node 7.

In the discussion of results which follows, all data are presented in accordance with the test conventions. The analytical results have been converted in accordance with the above.

3.4 SCF DATA REDUCTION

The convention for rosette strain gauging and SCF data reduction adopted is presented below.

In all instances at Node 7 the SCF gauges are positioned with Element 'A' parallel to the weld toe, Element 'B' oriented through clockwise angle of 45° and Element 'C' at 90° (ie. perpendicular to the weld toe). The raw strains (ϵ_a , ϵ_b and ϵ_c) are interpreted through Mohr's circle and translated into stresses, where the maximum (more positive) and minimum principal stresses σ_1 and σ_2 are given by:

$$\sigma_{1,2} = \frac{E}{2} \left[\frac{(\epsilon_a + \epsilon_c)}{(1 - \nu)} \pm \frac{\sqrt{2}}{(1 - \nu)} \sqrt{(\epsilon_b - \epsilon_a)^2 + (\epsilon_b - \epsilon_c)^2} \right]$$

where E = Young's modulus = 210×10^3 N/mm²

and ν = Poisson's Ratio = 0.3.

The clockwise rotation from the line of action of the principal stress to the axis perpendicular to the weld toe, shown in Figure 3.8, is calculated from θ , where:

$$\theta = 0.5 \tan^{-1} \left[\frac{2\epsilon_b - \epsilon_a - \epsilon_c}{\epsilon_c - \epsilon_a} \right]$$

However care is needed with respect to sign:

- Calculating θ_1 associated with the maximum (more positive) principal stress:

If $\epsilon_c > \epsilon_a$	then $\theta_1 = \theta$
If $\epsilon_c < \epsilon_a$ and $2\epsilon_b > \epsilon_a + \epsilon_c$	then $\theta_1 = \theta + 90^\circ$
If $\epsilon_c < \epsilon_a$ and $2\epsilon_b < \epsilon_a + \epsilon_c$	then $\theta_1 = \theta - 90^\circ$

- Calculating θ_2 for the minimum principal stress:

If $\theta_1 > 0$	$\theta_2 = \theta_1 - 90^\circ$
If $\theta_1 < 0$	$\theta_2 = \theta_1 + 90^\circ$

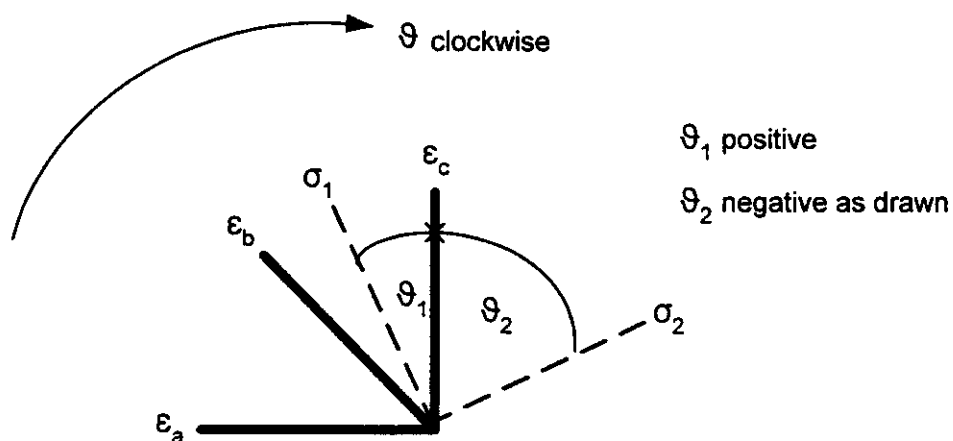


Figure 3.8 Sign convention for SCFs calculated in tests ($-90^\circ < \theta < 90^\circ$)

The extrapolation to the weld toe is based on results for the pairs of SCF gauges with due account for the distances from the weld toe detailed in Figure 3.1. Conventional practice⁽²⁾ is to extrapolate principal stresses taking the larger absolute principal stress at the gauge closer to the weld and the corresponding principal stress at the other gauge. However, this gives some ambiguity in the line of action of the weld toe stress. In simple loading cases, particularly in the

absence of chord load, weld toe stresses will be predominantly perpendicular to the weld toe. Whether strain components or the resulting principal values were extrapolated would make little difference to the results. In the more general case of the multiplanar node in the test structure, where there was significant modification to the stress field due to out-of-plane braces and the presence of chord loads, quite significant angular differences between principal stresses at the two gauge positions were found.

Extrapolation of principal stresses has no physical basis and therefore the more rigorous approach of extrapolating the strain components and then calculating the principal stress was adopted. The line of action of the principal stress was automatically defined. Comparisons show that the differences between the approaches were small, on average, nevertheless the work has highlighted concerns about the way hot spot determination is approached, particularly in FE analysis.

3.5 NOMINAL STRESS REDUCTION

In calculating bending stresses values were calculated at the interface between the brace footprint and the face of the chord. It is recognised that this differs from conventional analysis of jacket type structures where moments are generally determined at the intersection of centrelines. The approach is however in accordance with experimental investigations⁽²⁾ as it is conservative to determine SCFs based on the lower 'surface' moments and then apply these in design in conjunction with centreline moments. The distinction is less important when comparing absolute stress values nevertheless the need for consistency is recognised in the subsequent 'SCF' evaluations.

4. PRESENTATION OF RESULTS

4.1 SAMPLED RESULTS

Spreadsheet programs have been developed by BOMEL to draw in raw data pertinent to each of the 24 number SCF monitoring locations for all scans of the instrumentation system through any of the eight 3D frame tests. The eight tests involved various combinations of monotonic and cyclic loading applied in the three loading configurations shown in Figure 2.2. All the tests provide valuable SCF data as the pattern of brace loads at Node 7 varies with different failure scenarios at other locations in the structure. Nevertheless, as envisaged in the original SCF workscope, attention in this report focuses only on results for the three primary static collapse loadcases: LC1, 2 and 3.

These tests involved respectively 38, 49 and 73 scans of the instrumentation with different levels of applied load and different combinations of component forces as members failed. In order to provide comparison with 'elastic' analytical predictions the results are extracted for Scans early in each test. Figures 4.1 to 4.3 present global response plots for the LC1, 2 and 3 tests, further details are presented in the relevant test reports listed in the Foreword. The SCF data presented in this section relate to Scans 9, 11 and 9 in the three tests and it can be seen from the figures that in each case these are within the linear response region.

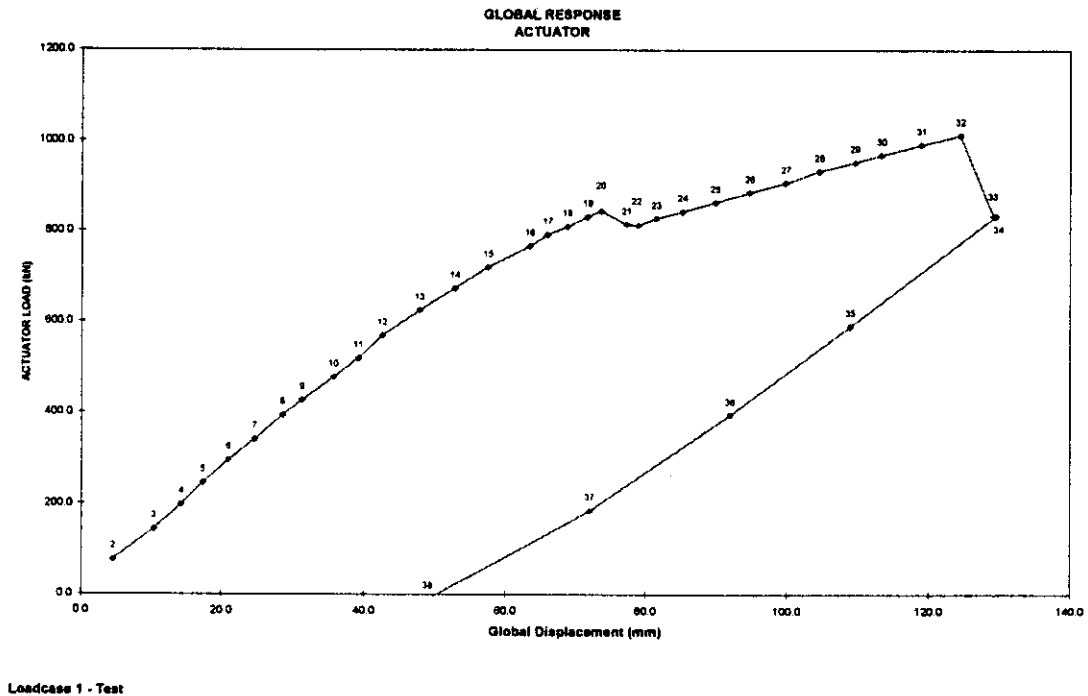
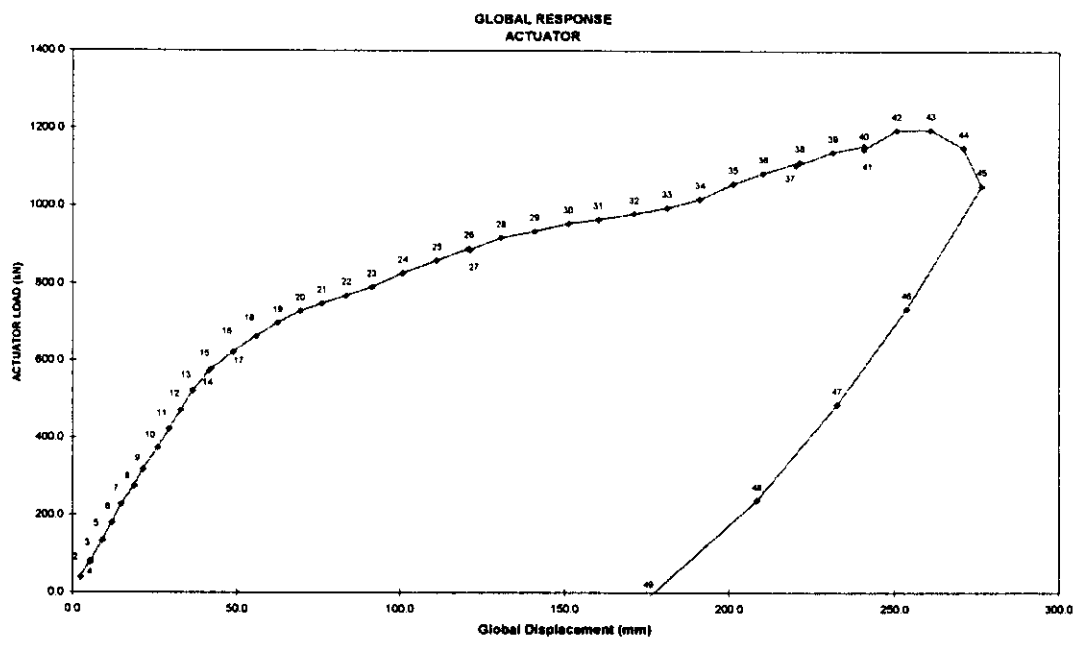
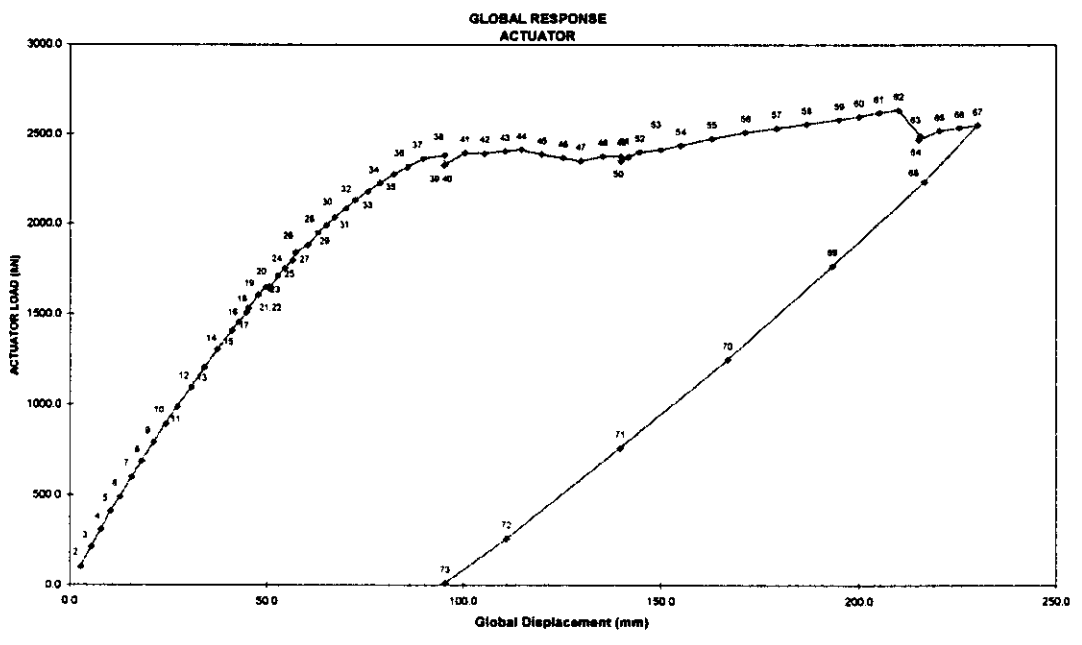


Figure 4.1 Loadcase 1 - Global response and numbered scan positions



Loadcase 2 - Test

Figure 4.2 Loadcase 2 - Global response and numbered scan positions



Loadcase 3 - Test

Figure 4.3 Loadcase 3 - Global response and numbered scan positions



Full results for all scans are presented on the project CD and can be provided to Participants at the draft report stage upon request. However in extracting the results the data have been reviewed to ensure that they are representative. In particular checks have been made to ensure:

- no gauge element is at the limit of its range or appears not to be functioning
- that the angle of principal stresses follows a consistent pattern at each location and that discrepancies between 'near' and 'far' rosette gauge output can be explained
- that nominal axial stress levels from linear strain gauges are consistent at different positions on the same member and that there is reasonable correlation with pre-calibrated load cells at distant points on a member
- that the sense and magnitude of moments seems reasonable when adjacent linear gauge sets on individual members are considered.

On this basis it was confirmed that the data presented in the following tables are representative. As with other parts of the investigation this scrutiny also indicated that the quality and accuracy of the data acquisition system was excellent.

Particular observations from this examination however did highlight some important aspects:

- Although maximum principal stresses generally act within a narrow zone perpendicular to the weld toe, for the plan braces - particularly when moments were high and axial forces low - the line of action was more oblique.
- If the moments are extrapolated from distant gauges towards the Node 7 intersection they do not generally coincide with values from the additional strain gauges (ASGs) at three and six diameters from the intersection. This indicates secondary influences due to local joint flexibility may be significant requiring care to ensure primary and secondary effects are separated.

Table 4.1 presents a reminder of the 24 locations for measuring weld toe stress concentrations as shown in Figure 3.1.

Tables 4.2 to 4.4 present results for all 24 locations at the nominated scans in each test. The raw data from the SCF rosettes are presented in the sequence A, B, C as discussed in Section 3.3. Similarly the linear strain gauge data for determining nominal stresses are presented in the sequence 1, 3, 5, 7 in accordance with the test convention. Maximum principal stresses are based on the extrapolation of strain components discussed in Section 3.4. The nominal axial and bending stresses are given consistent with the test convention in Section 3.3 (tension positive; bending 1-5 and 3-7 positive). In-plane or out-of-plane bending values are given corresponding to the SCF monitoring location (ie. IPB - crown; OPB - saddle). Where available, comparative



values from load cells are given together with an indication of the ratio of moments calculated at the centrelines or chord surface. Finally the nominal stresses pertinent to the SCF location are extracted; as before axial stress is positive for tension but bending stresses are re-signed to be positive if they are relatively tensile on the line of stress monitoring.

Table 4.1 Twenty-four locations for stress monitoring

Location 1: Member 27 saddle position (C) \ Strain Gauge Rosettes one and two (CS90)
Location 2: Member 24 crown position (B) \ Strain Gauge Rosettes three and four (BC0)
Location 3: Member 91 crown position (C) \ Strain Gauge Rosettes five and six (CC0)
Location 4: Member 91 saddle position (C) \ Strain Gauge Rosettes seven and eight (CS270)
Location 5: Member 91 saddle position (B) \ Strain Gauge Rosettes nine and ten (BS270)
Location 6: Member 72 saddle position (C) \ Strain Gauge Rosettes eleven and twelve (CS270)
Location 7: Member 74 crown position (C) \ Strain Gauge Rosettes thirteen and fourteen (CC180)
Location 8: Member 74 saddle position (B) \ Strain Gauge Rosettes fifteen and sixteen (BS90)
Location 9: Member 22 saddle position (C) \ Strain Gauge Rosettes seventeen and eighteen (CS90)
Location 10: Member 22 saddle position (B) \ Strain Gauge Rosettes nineteen and twenty (BS90)
Location 11: Member 11 saddle position (C) \ Strain Gauge Rosettes twenty one and twenty two (CS90)
Location 12: Member 11 crown position (C) \ Strain Gauge Rosettes twenty three and twenty four (CC180)
Location 13: Member 17 crown position (C) \ Strain Gauge Rosettes twenty five and twenty six (CC0)
Location 14: Member 17 crown position (B) \ Strain Gauge Rosettes twenty seven and twenty eight (BC0)
Location 15: Member 11 crown position (B) \ Strain Gauge Rosettes twenty nine and thirty (BC180)
Location 16: Member 11 saddle position (B) \ Strain Gauge Rosettes thirty one and thirty two (BS270)
Location 17: Member 91 crown position (B) \ Strain Gauge Rosettes thirty three and thirty four (BC0)
Location 18: Member 74 saddle position (C) \ Strain Gauge Rosettes thirty five and thirty six (CS90)
Location 19: Member 72 saddle position (B) \ Strain Gauge Rosettes thirty seven and thirty eight (BS270)
Location 20: Member 11 saddle position (C) \ Strain Gauge Rosettes thirty nine and forty (CS270)
Location 21: Member 27 crown position (B) \ Strain Gauge Rosettes forty one and forty two (BC0)
Location 22: Member 24 saddle position (C) \ Strain Gauge Rosettes forty three and forty four (CS90)
Location 23: Member 74 crown position (B) \ Strain Gauge Rosettes forty five and forty six (BC0)
Location 24: Member 17 saddle position (C) \ Strain Gauge Rosettes forty seven and forty eight (CS270)

Gauges and Interpretation	Brace 11 Intersection		Brace 17		Brace 22		Brace 24		Brace 27		Brace 72		Brace 74		Brace 81					
	CS90	CC180	BC180	BS270	CS270	CC0	BC0	CS270	CS90	BS90	BC0	CS90	BS90	BC0	CS270	BS270	CC0	CS270	BS270	
Raw data (microstrain)																				
Rosette near	-55	-10	-45	-82	-87	33	-23	-20	-35	-51	-133	-293	70	62	-74	-79	152	150	80	24
"	-125	-89	-39	-67	-81	-4	-4	-52	-135	-88	-307	-421	165	88	-39	107	273	209	171	137
"	-220	-124	-30	-84	-883	-10	59	-55	-90	-195	-386	-535	271	91	-87	-5	-312	373	355	63
Rosette far	-47	0	-28	-32	-106	27	-13	-30	-24	-46	-122	-191	14	56	-57	-105	112	86	71	45
"	-73	-79	-10	3	-85	-22	23	-61	36	-129	-205	-126	75	24	12	31	173	107	89	134
"	-136	-91	7	12	-108	-22	81	-71	-22	-156	-207	-121	154	3	-21	-103	159	191	197	82
Linear gauge near	-17	-17	-17	-17	-17	48	48	48	-67	-67	-224	-224	66	66	-338	-338	181	181	181	181
"	-25	-25	-25	-25	-25	15	15	15	-93	-93	-243	-243	164	164	-292	-292	57	57	57	57
"	8	8	8	8	8	14	14	14	-98	-98	-276	-276	178	178	-268	-268	-1	-1	-1	-1
"	14	14	14	14	14	35	35	35	-61	-61	-240	-240	81	81	-306	-306	141	141	141	141
Linear gauge far	4	4	4	4	4	60	60	60	-71	-71	-224	-224	84	84	-338	-338	188	188	188	188
"	-22	-22	-22	-22	-22	33	33	33	-106	-106	-256	-256	152	152	-274	-274	127	127	127	127
"	-22	-22	-22	-22	-22	24	24	24	-93	-93	-286	-286	100	100	-287	-287	8	8	8	8
"	17	17	17	17	17	58	58	58	-74	-74	-252	-252	82	82	-271	-271	56	56	56	56
Strain Gauge Rosettes																				
Extrapolated strain A	-58	-15	-53	-104	-108	36	-28	-17	-38	-53	-136	-340	98	64	-79	-67	170	180	82	15
Extrapolated strain B	-138	-93	-52	-99	-85	4	20	-50	-8	-137	-333	-557	206	104	-51	142	318	256	192	136
Extrapolated strain C	-241	-139	-47	-128	-108	-4	48	-51	-108	-213	-431	-726	324	113	-116	41	-528	457	395	54
Principal stress 1 (N/mm2)	-30	-13	-15	-31	-29	8	9	-6	-10	-27	-80	-129	81	31	-21	22	44	120	98	27
Principal stress 2 (N/mm2)	-60	-33	-16	-38	-36	1	3	-14	-34	-53	-110	-191	44	22	-37	-31	-152	71	45	-7
Angle Principal Stress 1 (Deg)	86	-83	-15	63	45	-75	7	-69	59	-89	-81	-86	-1	16	56	35	63	-12	-8	40
Angle Principal Stress 2 (Deg)	-4	7	75	-27	-45	15	-83	21	-31	1	9	4	89	-74	-34	-55	-27	78	82	-50
Angle of maximum principal stress (deg)	-4	7	75	-27	-45	-75	7	21	-31	1	9	4	-1	16	-34	-55	-27	-12	-8	40
Max Principal Stress (N/mm ²)	-80	-33	-16	-38	-36	8	9	-14	-34	-63	-110	-191	81	31	-37	-31	-152	120	98	27
Nominal stresses																				
Axial Strain near (Microstrain)	-5	-5	-5	-5	-5	28	28	28	-80	-80	-246	-246	123	123	-301	-301	94	94	94	94
Axial Strain far (Microstrain)	-6	-6	-6	-6	-6	44	44	44	-86	-86	-255	-255	104	104	0	0	95	95	95	95
Avg. axial stress (N/mm2)	-1	-1	-1	-1	-1	8	8	8	-17	-17	-53	-53	24	24	-69	-69	20	20	20	20
Comparative LC axial stress (N/mm2)	0	0	0	0	0	8	8	8	-20	-20	-53	-53	23	23	0	0	0	0	0	0
Bending Strain near (Microstrain)	-20	-13	-13	-20	-20	17	17	17	-16	-16	-1	26	-55	41	7	7	91	-42	-42	-91
Bending Strain far (Microstrain)	-19	-13	-13	-19	-19	18	18	18	-16	-16	-2	31	-8	35	-2	-2	90	-36	-36	-90
Bending stress at weld toe (N/mm2)	-4.2	-2.7	-2.7	-4.2	-4.2	3.3	3.3	3.3	-3.3	-3.3	-0.1	4.4	-21.6	10.0	3.4	3.4	19.4	-11.0	-11.0	-19.5
Bending stress at chord CL (N/mm2)	-4.2	-2.7	-2.7	-4.2	-4.2	3.2	3.2	3.2	-3.3	-3.3	0.0	3.7	-27.9	10.8	7.7	7.7	19.7	-12.3	-12.3	-19.7
SCF Evaluations																				
Axial Stress (N/mm ²)	-1.1	-1.1	-1.1	-1.1	-1.1	7.5	7.5	7.5	-17.4	-17.4	-62.5	-62.5	23.9	23.9	-69.2	-69.2	19.9	19.9	19.9	19.9
Relative bending Stress (N/mm ²)	-4.2	-2.7	-2.7	-4.2	-4.2	3.3	3.3	3.3	3.3	3.3	0.1	-4.4	21.6	10.0	-3.4	-3.4	19.4	11.0	11.0	19.5
Approx Axial SCF (Principal/axial)	54.5	30.4	14.2	34.7	262.7	1.1	1.3	-1.9	1.9	3.0	2.1	3.6	3.4	1.3	0.5	0.4	-7.7	6.0	4.9	1.4
Combined SCF (Principal/rel Bending)	11.3	8.9	4.1	-12.2	-92.7	0.8	0.9	-1.5	2.4	3.7	2.1	3.4	1.8	0.9	0.5	0.4	-3.9	3.9	3.2	0.7

Table 4.2 Loadcase 1 - Scan 9 - Node 7 SCF data



Gauges and Interpretation	Brace 11 Intersection			Brace 17			Brace 22			Brace 24			Brace 27			Brace 72			Brace 74			Brace 91				
	CS90	CC180	BC180	BS270	CS270	CC0	BC0	CS270	CS90	BS90	BC0	CS90	BC0	CS90	BC0	CS270	BS270	CC0	BS90	CS90	CC180	BC0	CS270	BS270		
Raw data (microstrain)																										
Rosette near																										
Position																										
A	-39	-9	-64	-155	-69	-114	-224	-53	6	-39	-8	6	-85	-73	13	22	193	230	149	42	-198	-117	-179	-241		
B	-155	-1	24	-279	-308	-166	-258	-194	-80	-98	17	-119	-174	67	88	114	302	361	-49	-204	-204	-98	-346	-398		
C	-233	-8	133	-415	-534	-258	-324	-384	-190	-164	-13	-131	-268	138	168	-86	408	481	83	-201	-132	-128	-553	-537		
Rosette far																										
A	-32	-27	-50	-87	-75	-112	-141	-43	13	-42	-11	-6	-41	-62	10	25	156	148	144	85	-137	-128	-161	-154		
B	-112	-27	50	-145	-203	-150	-69	-106	-75	-81	-23	10	-5	-102	40	68	15	140	290	-10	-55	-97	-253	-200		
C	-166	-43	158	-172	-308	-197	-36	-240	-140	-117	-85	68	25	-140	117	137	-70	142	357	91	41	-115	-300	-231		
Linear gauge near																										
1	21	21	21	21	21	-162	-162	-162	81	81	43	43	-21	-21	86	86	119	119	119	119	-60	-60	-60	-60		
3	13	13	13	13	13	-122	-122	-122	79	79	23	23	-120	-120	57	57	230	230	230	230	-181	-181	-181	-181		
5	-76	-76	-76	-76	-76	-178	-178	-178	0	0	78	78	-38	-38	17	17	75	75	75	75	-273	-273	-273	-273		
7	-51	-51	-51	-51	-51	-167	-167	-167	12	12	94	94	65	65	44	44	-41	-41	-41	-41	-187	-187	-187	-187		
Linear gauge far																										
1	-54	-54	-54	-54	-54	-156	-156	-156	73	73	46	46	-17	-17	65	65	127	127	127	127	-80	-80	-80	-80		
3	-11	-11	-11	-11	-11	-134	-134	-134	70	70	29	29	-104	-104	45	45	-44	-44	-44	-44	-182	-182	-182	-182		
5	-3	-3	-3	-3	-3	-167	-167	-167	13	13	73	73	-56	-56	16	16	81	81	81	81	-264	-264	-264	-264		
7	-48	-48	-48	-48	-48	-180	-180	-180	19	19	87	87	50	50	42	42	199	199	199	199	-188	-188	-188	-188		
Strain Gauge Rosettes																										
Extrapolated strain A	-41	-1	-71	-186	-67	-115	-263	-56	4	-38	-6	11	-105	-76	13	20	210	268	151	23	-226	-112	-184	-282		
Extrapolated strain B	-168	11	12	-340	-335	-174	-344	-216	-82	-106	27	43	-171	-193	74	97	160	377	379	-66	-273	-98	-370	-489		
Extrapolated strain C	-250	7	122	-527	-591	-285	-457	-420	-203	-185	5	88	-202	-300	143	182	-94	530	513	80	-312	-140	-617	-678		
Principal stress 1 (N/mm2)	-28	2	23	-78	-56	-48	-92	-42	-13	-22	4	21	-38	-38	34	43	47	141	130	35	-74	-33	-85	-112		
Principal stress 2 (N/mm2)	-61	0	-8	-135	-141	-74	-124	-101	-87	-85	38	-5	-80	-80	-2	-2	73	-5	7	-38	-88	-43	-155	-176		
Angle Principal Stress 1 (Deg)	-84	32	-4	87	-98	81	85	87	85	88	38	-5	-80	-80	-2	-2	73	-5	7	-38	-88	-43	-155	-176		
Angle Principal Stress 2 (Deg)	6	-58	86	-3	1	-9	-5	-3	-5	-2	-52	85	10	1	88	98	-17	85	-83	52	2	-32	-4	1		
Angle of maximum principal stress (deg)	6	32	-4	-3	1	-9	-5	-3	-5	-2	-52	85	10	1	88	98	-17	85	-83	52	2	-32	-4	1		
Max Principal Stress (N/mm ²)	-81	2	23	-135	-141	-74	-124	-101	-47	-45	-6	21	-64	-74	34	43	47	141	130	35	-88	-43	-155	-176		
Nominal stresses																										
Axial Strain near (Microstrain)	-23	-23	-23	-23	-23	-162	-162	-162	43	43	60	60	-28	-28	51	51	96	96	96	96	-175	-175	-175	-175		
Axial Strain far (Microstrain)	-29	-29	-29	-29	-29	-159	-159	-159	44	44	59	59	-32	-32	0	0	91	91	91	91	-178	-178	-178	-178		
Avg. axial stress (N/mm2)	-5	-5	-5	-5	-5	-34	-34	-34	9	9	12	12	-6	-6	10	10	20	20	20	20	-37	-37	-37	-37		
Comparative LC axial stress (N/mm2)	0	0	0	0	0	-34	-34	-34	9	9	11	11	-6	-6	0	0	0	0	0	0	-38	-38	-38	-38		
Bending Strain near (Microstrain)	32	49	49	32	32	8	8	32	34	34	-36	-18	9	-93	6	6	22	136	136	-22	3	3	108	106		
Bending Strain far (Microstrain)	19	26	26	19	19	5	5	23	26	26	-29	-13	20	-77	2	2	23	122	122	-23	3	3	92	92		
Bending stress at weld toe (N/mm2)	6.0	9.8	9.8	6.0	6.0	2.0	2.0	6.1	6.9	6.9	-7.7	-3.2	-0.3	-18.8	1.5	1.5	2.3	25.5	25.5	-2.2	0.2	0.2	19.5	19.5		
Bending stress at chord CL (N/mm2)	6.6	10.8	10.8	6.6	6.6	2.4	2.4	7.0	7.9	7.9	-8.4	-3.8	-1.5	-20.5	3.3	3.3	1.8	27.7	27.7	-1.8	0.2	0.2	21.0	21.0		
SCF Evaluations																										
Axial Stress (N/mm ²)	-5.5	-5.5	-5.5	-5.5	-5.5	-33.8	-33.8	-33.8	9.1	9.1	12.5	12.5	-6.3	-6.3	9.9	9.9	19.6	19.6	19.6	19.6	-37.1	-37.1	-37.1	-37.1		
Relative bending Stress (N/mm ²)	8.4	13.4	13.4	8.4	8.4	2.2	2.2	-8.8	-8.7	-8.7	8.8	4.9	0.6	-22.7	-2.3	-2.3	4.1	-33.7	-33.7	4.0	0.7	0.7	26.3	26.2		
Approx Axial SCF (Principal/Axial)	11.1	-0.4	-4.3	24.6	25.8	2.2	3.7	3.0	-5.1	-5.0	-0.4	1.7	8.6	11.8	3.4	4.4	2.4	7.2	6.6	1.8	2.4	1.2	4.2	4.7		
Combined SCF (Principal/rel Bending)	-20.7	0.3	2.9	9.7	10.2	2.4	3.9	2.4	-124.1	-120.5	-0.2	1.2	9.5	2.6	4.5	5.7	2.0	-10.0	-9.2	1.5	2.4	1.2	14.3	16.1		

Table 4.3 Loadcase 2 - Scan 11 - Node 7 SCF data



Gauges and Interpretation	Brace 11 Intersection			Brace 17			Brace 22			Brace 24			Brace 27			Brace 72			Brace 74			Brace 91			
	CS90	CC180	BC180	BS270	CS270	CC0	BC0	CS90	BS90	BC0	CS90	BC0	CS90	BC0	CS270	BS270	CC0	BS90	BC0	CS90	CC180	BC0	CS270	BS270	
Raw data (microstrain)																									
Rosette near																									
Position																									
A	-10	-58	-54	-4	9	100	134	65	-55	-83	-54	-120	97	43	26	31	-35	-36	-22	-4	12	-9	33	46	
B	-46	-51	-128	10	-19	226	248	119	-162	-227	-146	-184	146	114	54	12	12	-91	-83	82	16	29	66	75	
C	-76	-62	-190	-16	-4	337	347	231	-193	-216	-174	-245	214	143	86	77	-5	-111	-11	-38	16	18	86	86	
Rosette far																									
A	-7	-38	-28	2	13	93	73	54	-82	-70	-54	-70	33	35	22	28	-33	-30	-10	-18	16	-12	37	32	
B	-25	-16	-78	11	4	184	110	56	-106	-209	-83	-74	29	59	49	46	-11	-54	-111	72	7	25	57	44	
C	-35	-8	-126	-16	20	235	159	124	-76	-162	-71	-82	45	54	75	56	-29	-53	-56	-20	0	11	45	31	
Linear gauge near																									
1	-90	-90	-90	-90	-90	201	201	201	-148	-148	-111	-111	107	107	57	57	-50	-50	-50	-50	11	11	11	11	
3	-22	-22	-22	-22	-22	180	160	160	-131	-131	-109	-109	101	101	66	66	-44	-44	-44	-44	7	7	7	7	
5	48	48	48	48	48	153	153	153	-113	-113	-146	-146	125	125	58	58	-17	-17	-17	-17	28	28	28	28	
7	-16	-16	-16	-16	-16	183	183	183	-130	-130	-137	-137	123	123	45	45	-22	-22	-22	-22	40	40	40	40	
Linear gauge far																									
1	23	23	23	23	23	196	196	196	-148	-148	-113	-113	106	106	45	45	-54	-54	-54	-54	14	14	14	14	
3	-20	-20	-20	-20	-20	160	160	160	-132	-132	-112	-112	104	104	49	49	-27	-27	-27	-27	10	10	10	10	
5	-62	-62	-62	-62	-62	151	151	151	-117	-117	-142	-142	119	119	44	44	-20	-20	-20	-20	25	25	25	25	
7	-16	-16	-16	-16	-16	183	183	183	-139	-139	-139	-139	120	120	42	42	-40	-40	-40	-40	36	36	36	36	
Strain Gauge Rosettes																									
Extrapolated strain A	-10	-66	-67	-7	8	103	162	68	-55	-83	-54	-144	126	45	27	33	-36	-39	-25	2	11	-8	31	52	
Extrapolated strain B	-51	-66	-151	10	-24	245	311	135	-176	-235	-159	-249	200	128	56	-3	23	-109	-78	86	20	31	68	89	
Extrapolated strain C	-86	-66	-219	-16	-10	363	434	258	-222	-244	-189	-320	291	166	88	86	6	-138	0	-45	24	21	97	111	
Principal stress 1 (N/mm2)	-8	-21	-30	0	4	95	111	65	-27	-32	-25	-55	76	42	22	29	2	-18	7	11	6	7	25	29	
Principal stress 2 (N/mm2)	-21	-25	-55	-7	-4	50	67	33	-56	-66	-51	-84	49	21	12	7	-11	-35	-14	-24	4	-3	14	20	
Angle Principal Stress 1 (Deg)	-88	67	-87	51	-56	0	3	-8	-78	-69	-78	-84	-3	10	-2	-33	30	-79	-39	51	11	30	3	7	
Angle Principal Stress 2 (Deg)	2	-23	3	-39	34	-90	-87	82	12	21	12	6	87	-80	88	57	-60	11	51	-39	-79	-60	-87	-83	
Angle of maximum principal stress (deg)	2	-23	3	-39	34	0	3	-8	12	21	12	6	-3	10	-2	-33	-60	11	51	-39	-79	-60	-87	-83	
Max Principal Stress (N/mm ²)	-21	-26	-65	-7	-4	95	111	65	-66	-66	-61	-84	76	42	23	29	-11	-36	-14	-24	6	7	25	29	
Nominal stresses																									
Axial Strain near (Microstrain)	-20	-20	-20	-20	-20	174	174	174	-130	-130	-126	-126	114	114	56	56	-33	-33	-33	-33	21	21	21	21	
Axial Strain far (Microstrain)	-19	-19	-19	-19	-19	172	172	172	-134	-134	-127	-127	112	112	0	0	-35	-35	-35	-35	21	21	21	21	
Avg. axial stress (N/mm2)	-4	-4	-4	-4	-4	36	36	36	-28	-28	-26	-26	24	24	11	11	-7	-7	-7	-7	4	4	4	4	
Comparative LC axial stress (N/mm2)	0	0	0	0	0	36	36	36	-28	-28	-27	-27	25	25	0	0	0	0	0	0	4	4	4	4	
Bending Strain near (Microstrain)	-3	-69	-69	-3	-3	24	24	-12	-1	-1	14	17	-9	-11	10	10	-16	-11	-11	-11	-17	-17	-9	-9	
Bending Strain far (Microstrain)	-2	-43	-43	-2	-2	23	23	-11	4	4	14	15	-6	-8	4	4	-17	-7	-7	-7	-13	-13	-6	-6	
Bending stress at weld toe (N/mm2)	-0.9	-18.2	-18.2	-0.9	-0.9	5.4	5.4	-2.6	-1.2	-1.2	2.9	4.2	-2.4	-2.9	3.5	3.5	-3.1	-4.0	-4.0	-4.0	-4.5	-4.5	-2.6	-2.6	
Bending stress at chord CL (N/mm2)	-1.0	-19.9	-19.9	-1.0	-1.0	5.7	5.7	-2.6	-1.8	-1.8	2.9	4.6	-2.7	-3.2	6.4	6.4	-3.0	-4.9	-4.9	-4.9	-5.0	-5.0	-3.0	-3.0	
SCF Evaluations																									
Axial Stress (N/mm ²)	-4.1	-4.1	-4.1	-4.1	-4.1	36.4	36.4	36.4	-27.7	-27.7	-26.5	-26.5	23.8	23.8	10.6	10.6	-7.2	-7.2	-7.2	-7.2	4.5	4.5	4.5	4.5	
Relative bending Stress (N/mm ²)	-0.9	-18.2	-18.2	0.9	0.9	5.4	5.4	2.6	1.2	1.2	-2.9	-4.2	2.4	-2.9	-3.5	-3.5	-3.1	4.0	4.0	-3.1	-4.5	-4.5	-2.6	-2.6	
Approx Axial SCF (Principal/axial)	5.1	6.1	13.5	1.8	1.1	2.6	3.1	1.8	2.0	2.4	1.9	3.2	3.2	1.8	2.1	2.7	1.8	4.9	2.0	3.4	1.4	1.5	5.5	6.6	
Combined SCF (Principal/rel Bending)	4.2	1.1	2.5	2.2	1.4	2.3	2.7	1.7	2.1	2.5	1.7	2.7	2.9	2.0	3.1	4.0	1.1	11.1	4.5	2.3	-10.19	-10.75	13.5	16.0	

Table 4.4 Loadcase 3 - Scan 9 - Note 7 SCF data



4.2 COMPARISON OF RESULTS

Appendix D provides a series of plots comparing measured and predicted values.

4.2.1 Nominal Forces and Moments

The first three graphs in Appendix D compare the measured forces and moments for all eight braces at Node 7 with calculated values from BOMEL's SAFJAC benchmark analysis and BG's ABAQUS analysis including a shell model of Node 7 in the skeletal frame. The graphs are plotted to the same scale as a basis for comparison.

Load levels within the analysis have been converted pro-rata to the test level on the basis of elastic assumptions. The analysis output has also been factored to account for the different sign conventions as detailed in Table 3.2.

The sign of the axial forces is consistent in all cases although the magnitudes do differ slightly. At the scan levels selected the absolute stress levels are however small and it may be expected that differences due to different support conditions etc., may be relatively significant. Nevertheless the pattern of axial load is similar from all approaches.

In the case of moments the differences are somewhat greater and the direction of bending varies. There is no consistent polarity at specific locations confirming these are real differences rather than incorrect interpretation of sign conventions. However, the definition of moments is different in the three cases:

- test values are extrapolated to the face of chord
- SAFJAC values assume 'rigid' joints and are determined at centreline intersection
- BG model includes a shell representation of the node but moments are extracted in the member at the interface between shell and beam elements.

The comparison is therefore not pursued further at this stage but it does appear the braces in the test experienced relatively high moments due perhaps to secondary bending. Potential explanations are the joint flexibility and the fact that as-built out-of-straightness imperfections are neglected in the analysis.

4.2.2 Nominal and Principal Stresses

The central three graphs in Appendix D give a pictorial comparison of the nominal and corresponding principal stress levels acting at the 24 stress monitoring locations of interest. Again the scales are consistent for comparison. The considerable stress raising effects are evident. The relative contribution due to axial forces and moments from the corresponding and nearby braces is examined in Reference 5.



4.2.3 Measured and Predicted Principal Stresses

The final three figures in Appendix D provide a valid comparison between the principal stress levels at the 24 measurement locations for corresponding levels of applied load to the 3D structure. There is a slight discrepancy in that the BG analysis extrapolated principal stresses whereas the BOMEL test interpretation first extrapolated strain components. Nevertheless BOMEL investigations show the approaches agreed within 1%, on average, for the particular test cases in the figures.

Comparison is also made with parametric SCF predictions made by BG⁽⁶⁾ using Efthymiou's influence function method with or without multiplanar effects⁽¹¹⁾. It should be noted that the Efthymiou predictions were based on nominal data extracted from the BG analysis (Table 2.1) and there are some reservations regarding the position of the moments as noted above.

The findings are to be subject to detailed scrutiny and physical interpretation. Nevertheless an initial and very important observation is that the correlation between measured and FE values is quite reasonable.

Comparisons can be made relatively considering the ratio of measured to predicted values and averaging these. Results are aggregated for all 24 locations and three selected test scans:

- Test / FE : average = 1.12
- Test / Efthymiou planar prediction: average = 0.88
- Test / Efthymiou multiplanar prediction: average = 0.97

However in some cases the signs differ or large relative but small absolute differences distort the statistics. A more meaningful comparison is perhaps between average absolute principal stress levels:

- Test average = 58.8 N/mm²
- FE average = 44.2 N/mm²
- Efthymiou planar average = 49.3 N/mm²
- Efthymiou multiplanar average = 50.5 N/mm²

Again the generalisation is deceptive in that the planar and multiplanar Efthymiou predictions differ significantly in some instances apparently being reflected in the results in some cases (eg. Loadcase 2 Location 9) but not in others (eg. Loadcase 3 Location 9).

These basic results are developed and explained further in Reference 5.



5. REFERENCES

1. International Standards Organisation. 'Offshore structures for petroleum and natural gas industries - Part 2 Fixed steel structures', Committee Draft ISO/CD 13819-2, May 1999.
2. BOMEL Limited. 'Guide for the design and assessment of tubular joints'. BOMEL Reference C06060R, 1999.
3. 'Joint Industry Tubular Frames Project - Phase I', Nine volume report, SCI Reference SCI-RT-042, 1990.
4. BOMEL Limited. 'Joint Industry Tubular Frames Project - Phase II'. Nine volume report, BOMEL Reference C556R003.50 to 59, 1992.
5. BG plc. 'Frames Project - Multiplanar SCF investigations - final report', September 1999.
6. BOMEL Limited. 'Work specification for BG plc - Evaluation of multiplanar SCFs', BOMEL Reference C636\18\002S, Revision 0, August 1997.
7. BG plc. 'Workplan for BG plc evaluation of multiplanar SCFs', BG Reference BGT/TF3/001: Rev 1, December 1997.
8. Health & Safety Executive. 'Offshore Installations: Guidance on design, construction and certification', 4th Edition, 1990 (withdrawn 1999).
9. Lloyd's Register. 'Stress concentration factors for simple tubular joints - assessment of existing and development of new parametric formulae', OTH 91 354, HMSO, 1993.
10. BOMEL Limited. 'Briefing note on stress concentration factors for multiplanar joints within the Frames III test programme', BOMEL Reference C636\04\170U, Revision 0, April 1996.
11. Efthymiou, M. 'Development of SCF formulae and generalised influence functions for use in fatigue analysis', Offshore Tubular Joints Conference, Egham, Surrey, 1988.
12. American Petroleum Institute. 'Recommended practice for planning, designing and constructing fixed offshore platform - working stress design', API RP2A-WSD, 20th edition, July 1993.

13. BOMEL Limited. 'Test frame instrumentation', BOMEL Reference C636\25\017R, Revision 0, July 1999.
14. Health & Safety Executive. 'Fatigue background guidance document', OTH 92 390, HMSO.
15. SINTEF. 'Monotonic and cyclic testing of isolated K joints', SINTEF Reference STF22 F98704, BOMEL file C636\24, May 1999.

APPENDIX A

BRIEFING NOTE ON SCFs FOR MULTIPLANAR JOINTS WITHIN THE FRAMES III PROJECT TEST PROGRAMME

(BOMEL Reference C636\04\017U - 11 pages)

(Note: Brace referencing scheme superseded)



BRIEFING NOTE ON: STRESS CONCENTRATION FACTORS FOR MULTIPLANAR JOINTS WITHIN THE FRAMES III TEST PROGRAMME

1. INTRODUCTION

The purpose of this briefing note is to discuss the potential SCF data that could be obtained from the 3D Frames III test.

Some project funding has been allocated for the purchase and placement of strain gauges. These gauges will primarily be used to measure nominal stresses in members and joints, thus enabling both member loading and the onset of plasticity to be monitored. However, additional funds can be used to purchase further gauges, thereby enabling stresses to be measured near to tubular intersections, particularly on multiplanar connections where little SCF data has been published.

This briefing note reviews the nodal configurations on the Frames III test and following an appraisal of existing multiplanar SCF data gives recommendations on the nodes preferred for concentration of strain gauges.

2. NODAL JOINTS ON 3D FRAME III TEST

In addition to the brace inclination in-plane (θ), braces lie about the chord member and are described in terms of their out-of-plane angle (ϕ), see Figure 1. For each node, the joint configuration in each plane is identified with those in the 0° and 180° plane indicated in standard format while braces lying between 0° and 180° are indicated within parentheses. Figure 1 gives the general arrangement of the Frames III test. The 38 nodes comprising the Frames III test have been labelled on Figure 2 and are detailed in Table 1.

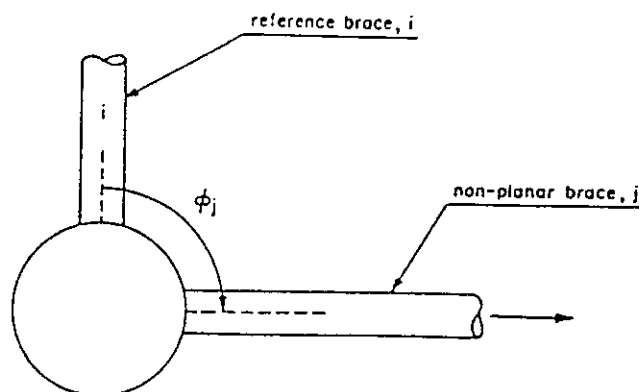


Figure 1 Definition of out-of-plane braces

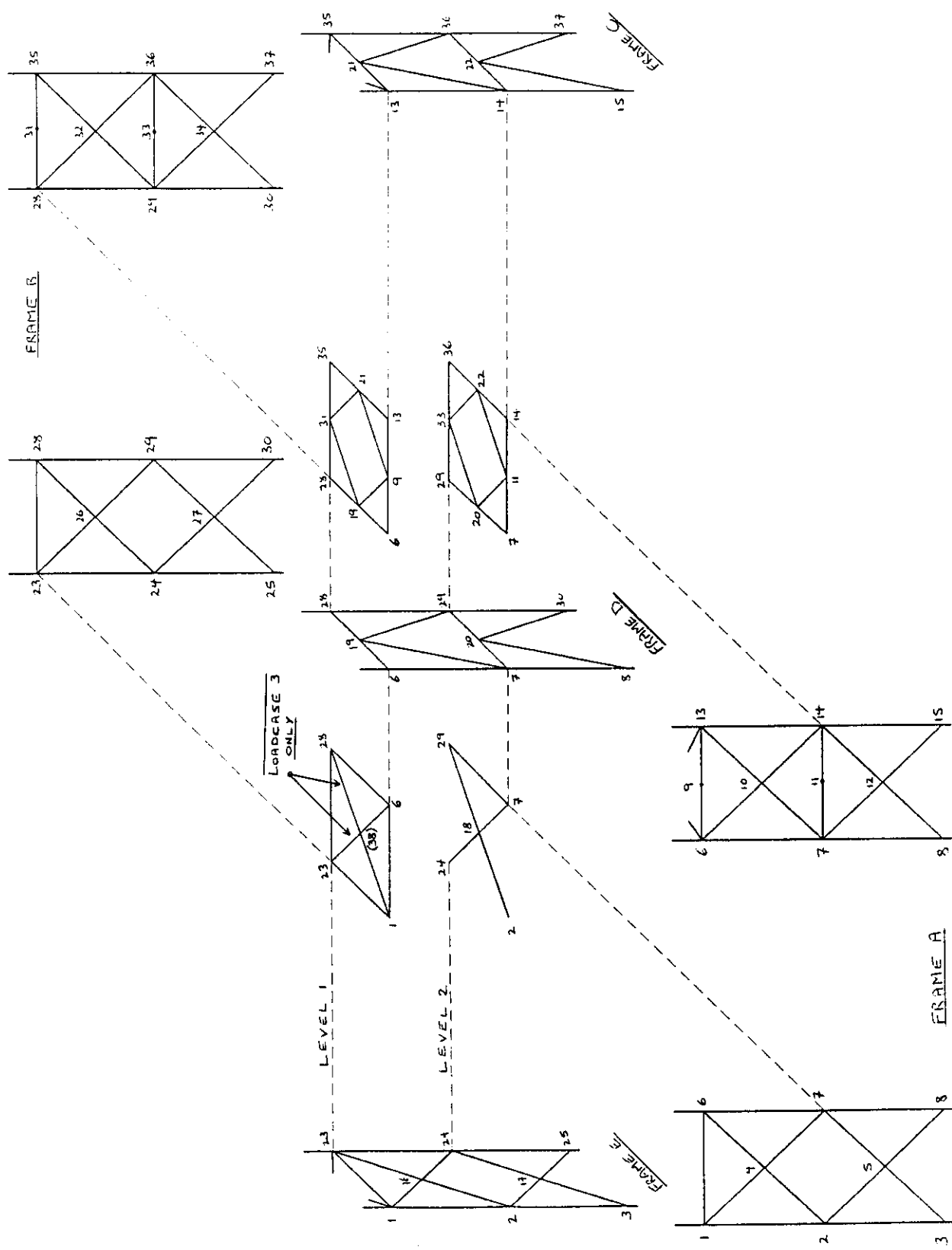


Figure 2 Frame III Configuration and Node Reference Numbers



Table 1 Classification of Frames III Nodal Joints

Node No.	Joint Classification	
	Loadcase 1 & 2	Loadcase 3
1	N (KT)	N (T) (KT)
2		K (T) (K)
3		Y (Y)
4		X
5		X
6	N (T) KT	N (T) (T) KT
7		K (T) (N) KT
8		Y (Y) Y
9		K
10		X
11		K
12		X
13		KT (N)
14		KT (N)
15		Y (Y)
16		X
17		X
18		X
19		K (K)
20		K (K)
21		K (K)
22		K (K)
23	N (KT)	N (T) (KT)
24		K (T) (K)
25		Y (Y)
26		X
27		X
28	N (T) N	N (T) (T) N
29		K (T) (N) KT
30		Y (Y) Y
31		K
32		X
33		K
34		X
35		N (N)
36		KT (N)
37		Y (Y)
38	-	X

Note:
T is a single perpendicular brace
Y is a single inclined brace
X is a cross brace where one of the members is classified as a chord member
K is two inclined braces
N is a perpendicular and an inclined brace
KT is two inclined braces with a single perpendicular central brace



The frequency of each type of node is given in Table 2 with symmetric configurations equated ie. KT(T) = T(KT).

Table 2 Nodal Configurations in the Frames III Test Specimen

Planes	Loadcase 1 & 2		Loadcase 3	
	Configuration	No of Nodes	Configuration	No of Nodes
Single plane	X	11	X	12
	K	4	K	4
Two planes	Y (Y)	4	Y (Y)	4
	K (K)	4	K (K)	4
	N (N)	1	N (N)	1
	KT (N)	5	KT (N)	3
Three planes	Y (Y) Y	2	Y (Y) Y	2
	N (T) N	1	N (T) N	0
	N (T) KT	1	N (T) KT	2
	K (T) (K)	2	K (T) (K)	2
Four planes	K (T) (N) KT	2	K (T) (N) KT	2
	N (T) (T) KT	0	N (T) (T) KT	1
	N (T) (T) N	0	N (T) (T) N	1
TOTAL		37	TOTAL	38

Following an appraisal of existing SCF data for multiplanar joints in Section 3, recommendations are given in Section 4 of the nodes for which strain gauging would appear most beneficial.

3. APPRAISAL OF EXISTING SCF DATA

BOMEL have recently completed a detailed review of test data and empirical formulae for both single and multiplanar tubular joints within the scope of Phase 4 of the Tubular Joints Group's activities - "Design and Reassessment of Tubular Joints for Offshore Structures. Chapter 4: Stress Concentration Factors and Local Joint Flexibility", C6060R08.01, Rev A, September 1993. This document highlights the lack of data on multiplanar joints, with only three test programmes reported using steel joints.

Tests by Dijkstra on T(T) joints showed that for the $\beta = 0.5$ configuration adopted the presence of the out-of-plane brace had little effect if unloaded, but significantly influenced the in-plane brace SCF once loading was applied.

Wimpey modelled a node for Occidental which consisted of an overlapped KT joint in-plane and an unloaded T brace out-of-plane. Therefore, the results of this node give little guidance on multiplanar effects, although it was noted that maximum stresses on this joint often occurred on the braceside away from the traditional hot-spot stress locations (ie. the saddle and crown).



Mitri, Scola et al contrasted T joints with T(T) joints, where the out-of-plane brace was inclined at 60°, 90° or 120° to the in-plane brace, for a range of β and γ value. Again for some configurations the maximum stress occurred between the saddle and crown positions.

The most systematic series of multiplanar SCF tests was performed by Lloyd's Register using small scale acrylic models. In this test series one K and two KT joint configurations were investigated with identical brace configurations in the 0°; 0° and 90°; 0° and 180° and 0°, 90° and 180° planes. The K Joints configuration is illustrated in Figure 3. Stresses in each brace were recorded following application of unit axial and out-of-plane bending load to each brace in turn. More complex load patterns were investigated on the assumption of superposition of the linear stresses. This assumption held for this test programme since only stresses perpendicular to the weld toe were considered even though, in general, the maximum principal stress is employed to determine joint fatigue life. A further restriction in this test series was that only the chord saddle was strain gauged, see Figure 3.

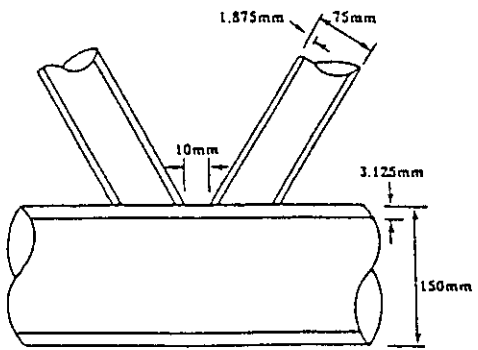
Other test programmes using either acrylic models, photoelastic models or more increasingly finite element analyses have been rather limited in their scope, with emphasis being placed on either perpendicular braces or on benchmarking an FE program to one specific nodal configuration under simple brace loading.

The most significant advance in the determination of SCFs in multiplanar joints came in 1988 with the publication by Efthymiou of influence function equations for axial load. Subsequently, Lloyd's Register have extended these to out-of-plane loading. Efthymiou validated his equations against the Lloyd's Register acrylic model tests but recognised the limitations in these test specimens, described above. For the nodes selected in the Frame III model, consideration should be given to correlating results to the Lloyd's Register tests and to avoiding over-complex nodes where braces may have little or no gap between them.

4. PREFERRED NODES IN FRAMES TEST

In Section 2 it was noted that of the 38 nodes on the Frames III model there were thirteen different nodal types, although each node type may vary in terms of chord and brace configuration. There appears little to be gained from strain gauging the single planar X and K joints for which a significant amount of data exists.

The first node proposed (No. 19) has two planes $\phi = 0^\circ$ (K) and $\phi = 90^\circ$ (K). This node is similar to the Lloyd's Register K configuration illustrated in Figure 2 with $\gamma \approx 24$, although the two planes differ in terms of the brace angle and gap. The second node (No. 24) has three planes $\phi = 0^\circ$ (K), $\phi = 45^\circ$ (T) and $\phi = 90^\circ$ (K). This node is also similar to the Lloyd's Register K joint configuration with all inclined braces identical having $\theta = 45^\circ$, although the γ value is lower at $\gamma = 14$. The other significant differences are the larger gap between in-plane braces and the T brace in the $\phi = 45^\circ$ plane. The third node (No. 29) has four planes $\phi = 0^\circ$ (K), $\phi = 45^\circ$ (T), $\phi = 90^\circ$ (T) and $\phi = 180^\circ$ (KT). This node is very complex with K, T and KT joints included and covers the effect of out-of-plane braces on planes with $\phi > 90^\circ$.



$\beta = 0.5$
 $\gamma = 24$
 $\tau = 0.6$
 $\theta = 45 \text{ deg}$

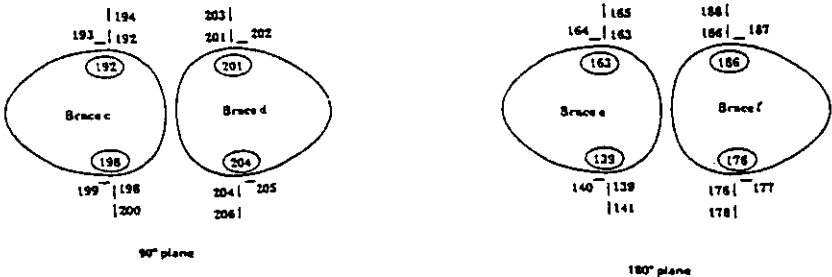
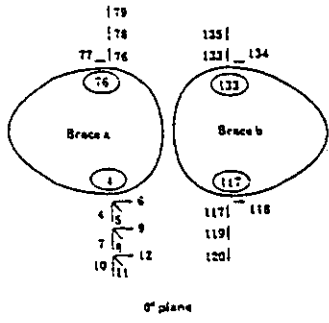
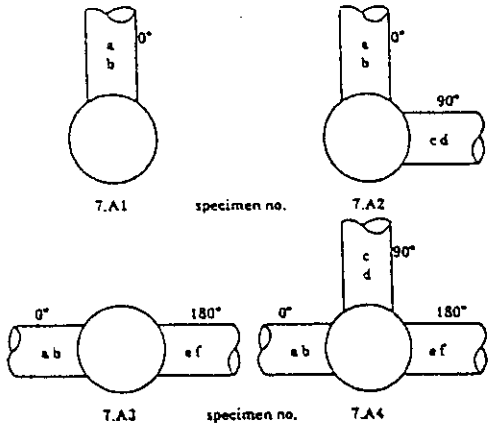


Figure 3 Multiplanar Acrylic K Joint Specimen Employed by Lloyd's Register



4.1 NODE 19 - K (K)

This node is located on Level 1 at the intersection of Level 1 and Frame D. The chord member has dimensions $D = 273\text{mm}$ and $T = 5.9\text{mm}$ (ie. $\gamma = 23.1$). This γ value is rather high for most UK offshore platforms but is more representative of GoM and Far Eastern structures, and also corresponds to the Lloyd's multiplanar test with $\gamma = 24$. On Level 1 (0°) the K joint is symmetrical with $d = 168\text{mm}$ ($\beta = 0.615$), $t = 4.5\text{mm}$ ($\tau = 0.76$), $\theta = 45^\circ$ and $g/D = 35.4/273 = 0.13$. In Frame D (90°) the K joint is symmetrical with $d = 168\text{mm}$ and $t = 4.5\text{mm}$ as for the other K joint. However the brace angle $\theta = 64^\circ$ and $g/D = 86.1/273 = 0.315$.

This joint is illustrated in Figure 4 on which it can be seen that the gap between out-of-plane braces is around 30mm. Overall, this joint is similar to the Lloyd's K joint specimen but will allow different brace angles and gaps to be assessed. The symmetry of the joint about the centre-line of the node will assist in the interpretation of results and the validation of the influence function approach. For these K joints, the recommended strain gauge locations for linear extrapolation to the individual braces is possible although due to the relatively small gap a nonlinear stress distribution is more likely.

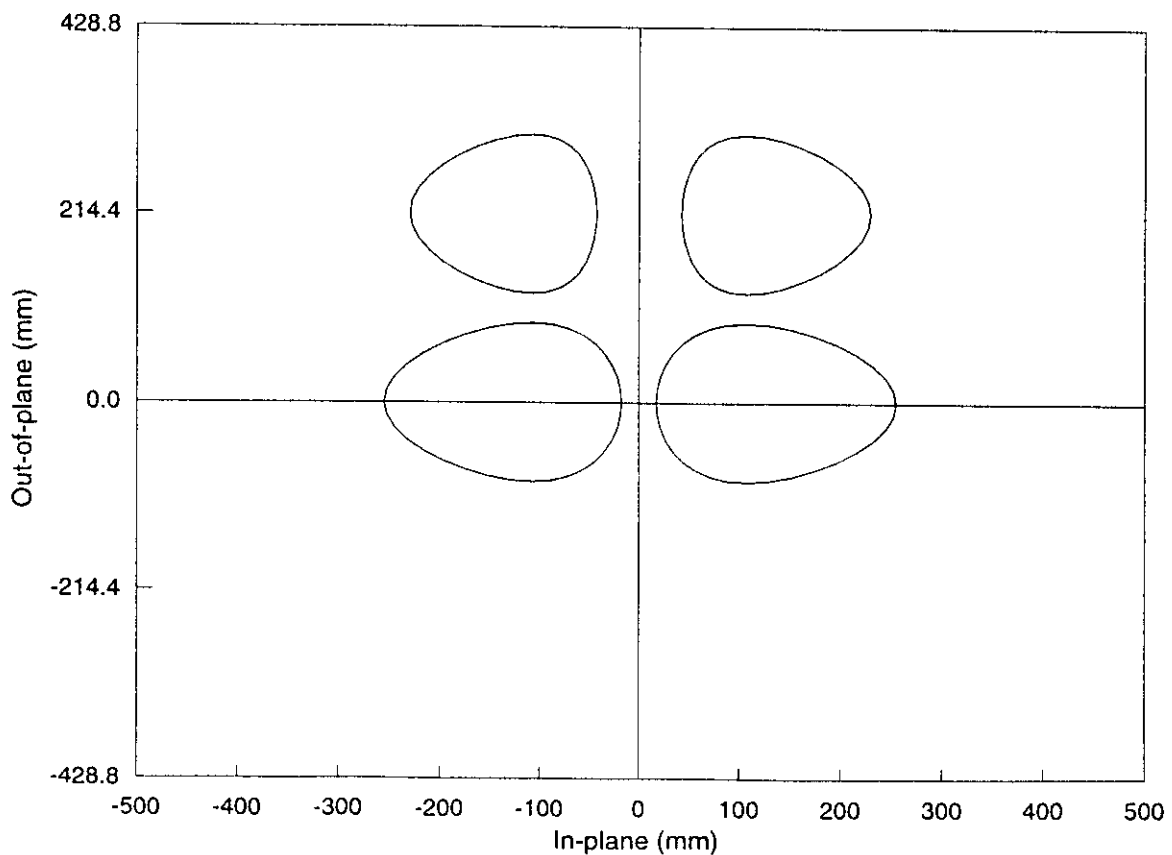


Figure 4 Node 19 : Brace Layout

4.2 NODE 24 - K (T) (K)

This node is located on Level 2 at the intersection of Frame B and Frame E. The chord member has dimensions $D = 355.7\text{mm}$ and $T = 12.7\text{mm}$ (ie. $\gamma = 14$, which is typical of North Sea offshore structures). In Frame B (0°) the K joint is symmetric with $d = 168\text{mm}$ ($\beta = 0.47$), $t = 8\text{mm}$ ($\tau = 0.63$), $\theta = 45^\circ$ and $g/D = 270/355.7 = 0.76$. In Frame E (90°) the K joint is identical to Frame B (0°). In Level 2, a T brace lies at $\phi = 45^\circ$ to Frame B with dimensions $d = 139.7\text{mm}$ ($\beta = 0.39$), $t = 5.4\text{mm}$ ($\tau = 0.425$).

The relationships between these five braces is illustrated in Figure 5. It can be seen that the gap between the K braces is relatively large at 270mm ($10.6''$), and consequently the influence between these braces will be less than for a smaller gap. This gap has been specified to allow the T brace to be clear of the other brace members. The symmetry of the node in both directions and the relatively large gap between braces ($>100\text{mm}$) will allow comprehensive strain gauging and the potential to fully interpret the SCF results. Braces in three planes can be investigated with the highly loaded T brace having an equal influence on all four inclined braces.

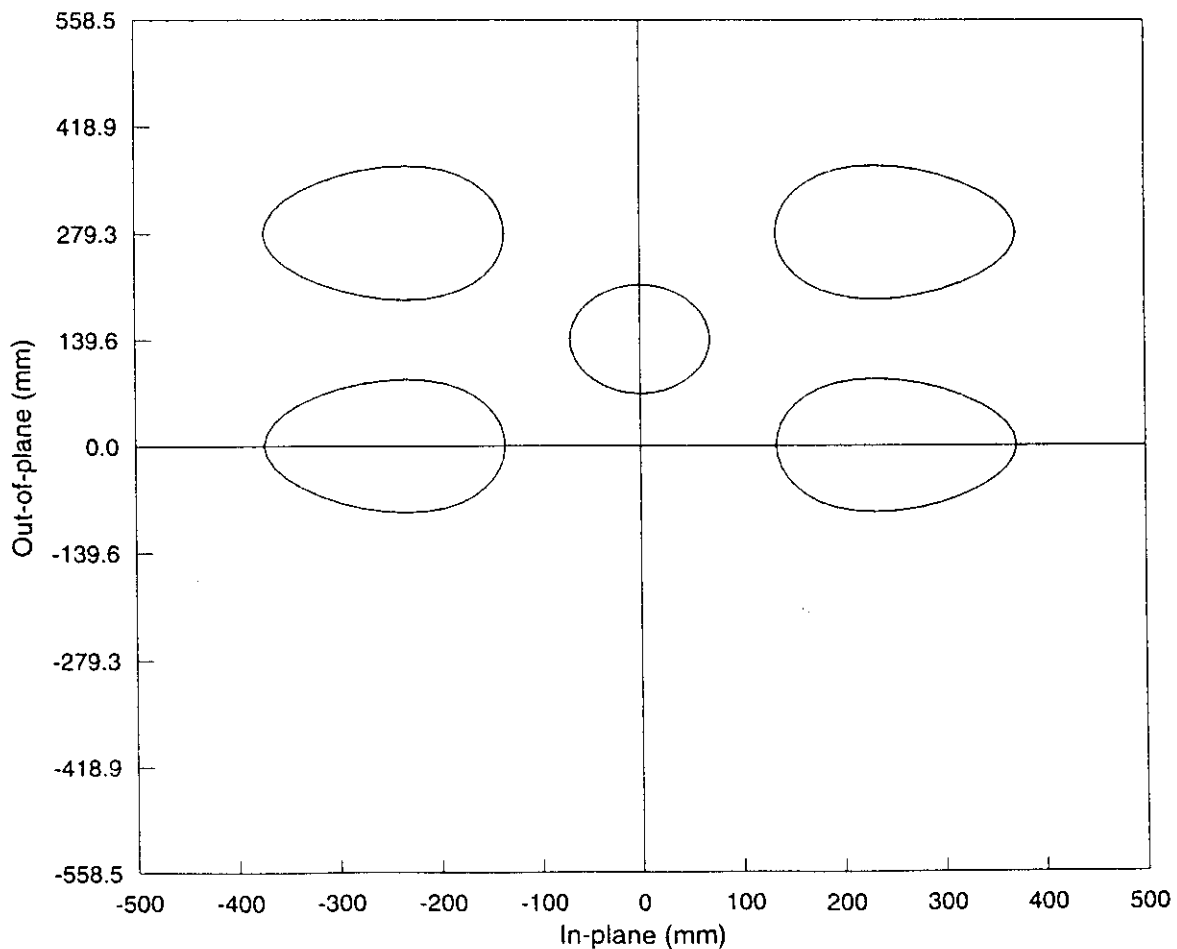


Figure 5 Node 2 : Brace Layout



4.3 NODE 29 - K (T) (N) KT

This node is located on Level 2 at the intersection of Frame B and Frame D. The chord member has dimensions $D = 457\text{mm}$ and $T = 12.7\text{mm}$ ($\gamma = 18$). In Frame B (0°) the K joint has $d = 168\text{mm}$ ($\beta = 0.37$), $t = 8\text{mm}$ ($\tau = 0.63$), $\theta = 45^\circ$ and $g/D = 219.4/457 = 0.48$. In Frame B (180°) the KT joint also has $d = 168\text{mm}$ ($\beta = 0.37$) and $t = 8\text{mm}$ ($\tau = 0.63$) for all braces. The brace angles are $\theta = 45^\circ/90^\circ/45^\circ$ with $g_1/D = g_2/D = 25.7/457 = 0.156$, ie. the gap between the weld toes of the outer braces is the same as that for the K joint in the $\phi = 0^\circ$ plane. On Level 2 (45°) the T joint has $d = 139.7\text{mm}$ ($\beta = 0.31$) and $t = 5.4\text{mm}$ ($\tau = 0.425$), while the T joint on Level 2 in Frame D has $d = 168\text{mm}$ ($\beta = 0.37$) and $t = 8\text{mm}$ ($\tau = 0.63$) in accordance with the braces in the 0° and 180° planes.

This joint is illustrated in Figure 6 on which it can be seen that the out-of-plane gap is around 40mm between the braces in the 0° , 45° and 90° planes. Strain gauges at the saddle would need to be placed around 4-5mm and 20mm from the chord saddle for linear extrapolation and thus the gap is just large enough for extrapolation in line with the recommended method. However, it should be noted that there is likely to be a nonlinear stress distribution in this region due to the complex stress interaction between braces. This node will provide a substantial amount of data but the cost will be both financial in terms of strain gauging and possibly technical with individual influence effects between braces significantly more difficult to determine than the other two nodes presented.

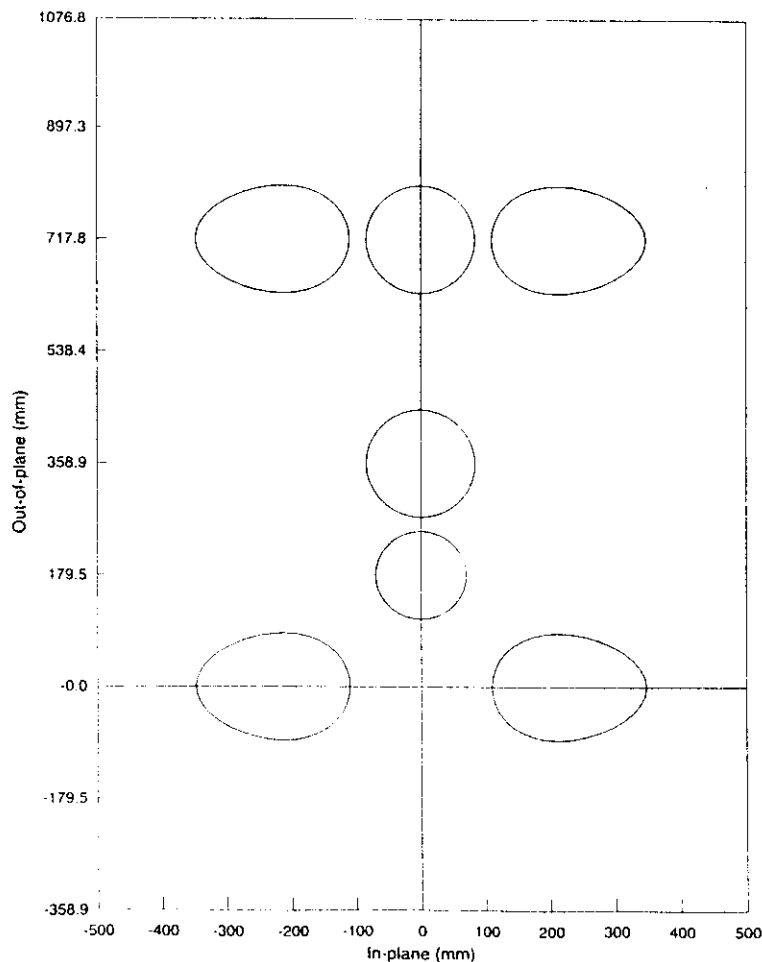


Figure 6 Node 6 : Brace Layout



5. STRAIN GAUGE PLACEMENT

As noted in Section 3, the location of the maximum SCF, even under relative simple loading conditions, can occur well away from the saddle and crown locations where strain gauges tend to be concentrated. For all three loadcases in the Frames III test there will be components of axial load and both out-of-plane and in-plane bending on each brace. Therefore the location of maximum stress will probably vary for each loadcase and will be difficult to predict with accuracy. Since the strain gauges are very sensitive it would not be feasible to move the gauges between loadcases.

At this stage it is envisaged that strain gauges would need to be placed around the full brace/chord intersection on both the chord and brace, for all joints on the node. The complexity of the loading would require gauges every 22.5° around the intersection, with three-gauge rosettes employed to allow maximum principal stresses to be determined.

Therefore, for each brace the following gauges may be required:

	16	locations around brace/chord intersection
x	6	gauges per location (3-gauge rosettes)
x	2	members (chord and brace)
+	(8x2)	nominal stress gauges away from the intersection
	<u>208</u>	

In addition the chord member may require 8x2 nominal stress gauges either side of the node, ie. 32 gauges.

Therefore, for the three preferred nodes described in Section 4 the strain gauge requirement would be:

- Node 19 864 gauges
- Node 24 1072 gauges
- Node 29 1488 gauges

(NB. Further analysis of these nodes may lead to some reduction in these requirements).



6. SUMMARY AND CONCLUSIONS

In this briefing note the complex multiplanar joints on the Frames III test specimens have been assessed in terms of potential for recording stress concentration factors. It has been noted that little data exist, from steel joints in particular, on SCFs for multiplanar joints. Although, with the publication by Efthymiou of influence function equations, the design and reassessment of complex multiplanar joints is becoming increasingly used to justify extended fatigue design lives.

Three nodes have been identified that will allow: detailed investigation of multiplanar joint under complex loading, comparisons with existing data from multiplanar joints, validation of the Efthymiou influence function approach, consideration of the validity of superposition of maximum principal stresses, and quantification of the difference between single and multiplanar design approaches. The complexity of the joints and applied loading means that in excess of 200 strain gauges may be required on each brace leading to a cost of between £30,000 and £60,000 per node, subject to finalising the cost of gauge purchase, placement and interpretation.

Comment on this briefing note is sought from the sponsors.

APPENDIX B

BG COMPARISON OF WELD TOE STRESS PREDICTIONS - LOADCASES 1, 2 AND 3

(BOMEL References Incoming Document file C636\18:
11354 and 12127 for Node 7 - 5 pages
9266 for Node 40 - 3 pages
9314 for Node 11 - 3 pages)

(Note: The 'Total SCFs' presented compare the weld toe stresses with nominal axial and in-plane plus out-of-plane bending stresses in the associated brace. In general, in-plane bending stresses are not considered to influence saddle nor do out-of-plane bending stresses affect crown SCFs. The 'Total SCFs' should therefore be viewed with caution. The assessment of final results is more discerning in this respect)

Joint 7, Load Case 1																			
Brace	Location	FE	TOTAL Alpha Kelllogg		TOTAL		TOTAL		+- %	Erthymou		TOTAL		+- %	Lloyd's		TOTAL		+- %
			SCF	planar	SCF	m-planar	SCF	planar		SCF	m-planar	SCF	planar		SCF	m-planar	SCF	planar	
27	CC 0	118	3.1	97	2.5	97	2.5	-18	118	3.1	154	4.0	31	127	3.3	120	3.1	1	
	CS 90	96	2.5	99	2.6	99	2.6	3	130	3.4	92	2.4	-4	125	3.3	89	1.8	-29	
	CC 180	54	1.4	56	1.5	56	1.5	3	84	2.2	120	3.1	122	95	2.5	86	2.3	62	
	CS 270	59	1.5	53	1.4	53	1.4	-10	72	1.9	41	1.1	-31	72	1.9	52	1.3	-12	
	BC 0	120	3.1	101	2.6	101	2.6	-16	139	3.6	149	3.9	24	120	3.1	114	3.0	-6	
	BS 90	116	3.0	104	2.7	104	2.7	-10	144	3.8	93	2.4	-20	136	3.5	177	4.6	53	
	BC 180	24	0.6	57	1.5	57	1.5	136	78	2.0	88	2.3	266	78	2.0	72	1.9	200	
	BS 270	42	1.1	54	1.4	54	1.4	29	73	1.9	30	0.8	-30	65	1.7	107	2.8	166	
24	CC 0	-166	2.4	-163	2.3	-163	2.3	-2	-206	2.9	-175	2.5	5	-222	3.1	-215	3.0	29	
	CS 90	-217	3.1	-149	2.1	-149	2.1	-31	-242	3.4	-232	3.3	7	-229	3.3	-259	3.7	19	
	CC 180	-95	1.3	-137	1.9	-137	1.9	44	-183	2.6	-152	2.2	60	-201	2.8	-194	2.7	104	
	CS 270	-189	2.7	-151	2.1	-151	2.1	-20	-244	3.5	-236	3.4	25	-231	3.3	-226	3.2	19	
	BC 0	-177	2.5	-170	2.4	-170	2.4	-4	-235	3.3	-223	3.2	26	-204	2.9	-197	2.8	11	
	BS 90	-229	3.2	-155	2.2	-155	2.2	-82	-260	3.7	-257	3.8	12	-236	3.4	-279	4.0	22	
	BC 180	-43	0.9	-141	2.0	-141	2.0	124	-195	2.8	-183	2.8	191	-176	2.5	-170	2.4	189	
	BS 270	-196	2.6	-157	2.2	-157	2.2	-29	-262	3.7	-263	3.7	34	-240	3.4	-262	4.0	44	
91	CC 0	60	7.7	70	9.0	70	9.0	17	69	6.9	43	5.5	-29	82	10.6	82	10.6	37	
	CS 90	91	11.7	44	5.7	44	5.7	-61	99	12.8	99	12.8	6	120	15.4	119	15.4	31	
	CC 180	17	2.2	49	6.3	49	6.3	167	47	6.0	20	2.6	18	59	7.6	59	7.6	248	
	CS 270	132	17.0	74	9.6	74	9.6	-44	164	21.1	164	21.1	24	166	24.0	166	24.0	41	
	BC 0	36	4.9	61	7.9	61	7.9	61	76	9.6	66	8.5	73	65	8.4	65	8.4	71	
	BS 90	40	5.2	33	4.3	33	4.3	-17	126	16.3	126	16.2	216	109	14.1	109	14.1	173	
	BC 180	14	1.6	38	4.9	38	4.9	172	46	5.9	35	4.5	149	36	4.9	36	4.8	188	
	BS 270	109	14.0	66	8.5	66	8.5	-46	206	26.6	206	26.5	69	179	23.1	179	23.1	64	
72	CC 0	-125	1.1	-127	1.1	-127	1.1	2	-206	1.9	-203	1.8	62	-271	2.4	-268	2.4	116	
	CS 90	-65	0.6	-114	1.0	-114	1.0	34	-156	1.4	-156	1.4	65	-100	0.9	-67	0.6	-21	
	CC 180	-105	0.9	-117	1.1	-117	1.1	12	-203	1.8	-197	1.8	67	-266	2.4	-264	2.4	161	
	CS 270	-76	0.7	-130	1.2	-130	1.2	71	-172	1.5	-159	1.4	109	-109	1.0	30	-0.3	-140	
	BC 0	-156	1.4	-186	1.7	-186	1.7	19	-265	2.4	-242	2.2	65	-340	3.1	-331	3.0	112	
	BS 90	-76	0.7	-172	1.5	-172	1.5	127	-196	1.8	-224	2.0	196	-170	1.5	-185	1.7	144	
	BC 180	-120	1.1	-176	1.6	-176	1.6	47	-251	2.3	-227	2.0	69	-332	3.0	-323	2.9	169	
	BS 270	-73	0.7	-190	1.7	-190	1.7	160	-214	1.9	-226	2.0	209	-186	1.7	-201	1.8	176	
74	CC 0	124	5.9	69	4.2	69	4.2	-22	136	6.5	190	9.1	69	105	5.0	100	4.6	-19	
	CS 90	141	6.7	60	3.8	60	3.8	-37	139	6.6	351	16.6	149	170	6.1	206	9.9	46	
	CC 180	-54	-2.6	49	2.4	56	2.8	-207	94	4.5	148	7.1	-374	62	3.0	56	2.8	-207	
	CS 270	91	4.4	58	2.8	66	3.2	-27	91	4.3	303	14.5	233	122	5.8	160	7.6	76	
	BC 0	115	5.5	79	3.8	86	4.1	-25	153	7.3	202	9.7	76	91	4.4	85	4.1	-26	
	BS 90	123	5.9	70	3.3	77	3.7	-37	154	7.4	193	9.2	67	105	5.0	186	6.9	51	
	BC 180	-33	-1.6	36	1.7	43	2.1	-232	96	4.6	145	6.9	-639	41	2.0	34	1.6	-204	
	BS 270	45	2.2	45	2.2	52	2.5	16	95	4.5	133	6.4	196	55	2.6	135	6.5	201	
22	CC 0	-66	2.1	-73	1.7	-73	1.7	-17	-100	2.3	-62	2.2	6	-127	3.0	-122	2.9	39	
	CS 90	-67	2.0	-63	1.5	-63	1.5	-27	-106	2.5	-32	0.7	-64	-93	2.2	-96	2.2	10	
	CC 180	-46	1.1	-70	1.6	-70	1.6	46	-97	2.3	-69	2.1	66	-125	2.9	-120	2.6	190	
	CS 270	-66	2.3	-60	1.9	-60	1.9	-19	-132	3.1	-192	4.5	66	-115	2.7	-147	3.4	66	
	BC 0	-67	2.0	-76	1.8	-76	1.8	-13	-126	2.9	-101	2.4	16	-127	3.0	-122	2.9	46	
	BS 90	-100	2.3	-65	1.5	-65	1.5	-66	-127	3.0	-29	0.7	-71	-95	2.2	-116	2.7	16	
	BC 180	-28	0.7	-73	1.7	-73	1.7	169	-121	2.8	-66	2.2	244	-123	2.9	-119	2.6	325	
	BS 270	-66	2.1	-63	1.9	-63	1.9	-6	-159	3.7	-226	5.3	166	-120	2.8	-141	3.3	61	
11	CC 0	23	-1.8	5	-0.4	-49	3.7	-111	6	-0.5	13	-1.0	-43	6	-0.5	6	-0.5	-74	
	CS 90	-54	4.2	-15	1.2	-69	5.3	26	-34	2.6	-47	3.7	-12	-34	2.6	-104	6.0	62	
	CC 180	-55	4.2	-14	1.0	-68	5.2	23	-15	1.1	-6	0.6	-66	-15	1.1	-15	1.1	-73	
	CS 270	-44	3.4	7	-0.6	-47	3.6	7	13	-1.0	-25	1.9	-44	13	-1.0	-44	3.4	-6	
	BC 0	25	-1.9	7	-0.5	-38	2.9	-263	6	-0.6	16	-1.3	-34	6	-0.6	6	-0.6	-66	
	BS 90	-43	3.3	-15	1.2	-61	4.7	41	-33	2.5	-69	5.3	69	-33	2.5	-33	2.5	-23	
	BC 180	-34	2.6	-14	1.1	-59	4.5	79	-16	1.2	-6	0.6	-77	-16	1.2	-16	1.2	-63	
	BS 270	-33	2.5	9	-0.7	-36	2.8	16	14	-1.1	-41	3.1	23	14	-1.1	14	-1.1	-144	
17	CC 0	30	1.8	47	2.8	47	2.8	67	65	3.8	63	3.7	111	79	4.6	74	4.3	145	
	CS 90	45	2.6	40	2.3	40	2.3	-11	59	3.4	33	1.9	-26	50	2.9	-42	-2.4	-192	
	CC 180	10	0.6	33	2.0	33	2.0	233	53	3.1	52	3.0	417	66	4.0	63	3.7	626	
	CS 270	-17	-1.0	40	2.4	40	2.4	-336	60	3.5	40	2.3	-336	60	2.9	-16	-0.9	-6	
	BC 0	46	2.7	49	2.9	49	2.9	7	66	5.2	60	3.5	39	79	4.6	75	4.4	63	
	BS 90	29	1.7	42	2.4	42	2.4	43	78	4.5	37	2.1	26	51	3.0	72	4.2	149	
	BC 180	6	0.4	34	2.0	34	2.0	473	68	4.0	39	2.3	666	65	3.8	61	3.6	613	
	BS 270	-31	-1.8	42	2.5	42	2.5	-236	76	4.6	46	2.7	-246	51	3.0	73	4.3	-336	

BOMEL ENGINEERING CONSULTANTS

23 NOV 1998

Inc. Doc. No. 12127

To HRS



Joint 7, Load Case 2

Brace	Location	FE	TOTAL SCF	Alpha Kellogg planar	TOTAL SCF	m-planar	TOTAL SCF	± %	Ertymidou planar	TOTAL SCF	m-planar	TOTAL SCF	± %	Lloyd's planar	TOTAL SCF	m-planar	TOTAL SCF	± %	
27	CC 0	-81	91.1	-48	54.5	-99	111.3	22	-80	67.7	-70	76.3	-13	-65	72.7	-61	68.6	-26	
	CS 90	-108	121.5	-84	94.9	-135	151.6	28	-109	122.3	-212	238.4	98	-103	115.7	-196	220.0	81	
	CC 180	-38	42.7	-31	34.9	-41	91.6	114	-46	51.2	-66	62.8	47	-61	57.3	-47	53.1	24	
	CS 270	-61	68.8	5	-5.5	-46	51.3	-38	3	-3.4	-65	95.2	38	0	-0.0	-68	109.7	60	
	BC 0	-71	78.8	-61	57.1	-103	114.1	46	-70	78.2	-74	83.4	4	-61	68.6	-68	64.8	-18	
	BS 90	-124	139.5	-90	100.8	-142	159.8	18	-126	141.6	-146	162.9	17	-120	136.3	-142	159.9	15	
	BS 270	-48	78.5	7	-7.8	-46	51.2	-33	13	-14.3	13	14.7	-119	15	-17.2	-7	7.4	-60	
24	CC 0	46	1.3	68	2.0	68	2.0	47	85	2.5	78	2.2	64	91	2.6	87	2.5	90	
	CS 90	32	0.9	74	2.1	74	2.1	130	109	3.1	11	0.3	-46	103	3.0	6	0.2	-80	
	CC 180	46	1.3	62	1.5	62	1.5	12	71	2.1	62	1.8	35	79	2.3	75	2.2	63	
	CS 270	49	1.4	46	1.3	46	1.3	-7	73	2.1	-44	-1.3	-180	71	2.0	-53	-1.5	-206	
	BC 0	62	1.8	71	2.0	71	2.0	14	67	2.8	92	2.7	48	84	2.4	81	2.3	51	
	BS 90	29	0.8	77	2.2	77	2.2	168	120	3.5	110	3.2	279	111	3.2	133	3.8	368	
	BS 270	19	0.5	53	1.5	53	1.5	181	74	2.1	68	2.0	280	68	2.0	95	1.9	241	
91	CC 0	-73	8.9	-174	2.0	-174	2.0	138	-180	2.0	-108	1.3	48	-207	2.4	-207	2.4	189	
	CS 90	-156	1.8	-211	2.5	-211	2.5	36	-464	5.5	-464	5.5	187	-629	6.2	-288	3.4	66	
	CC 180	-61	1.1	-175	2.1	-175	2.1	62	-170	2.0	-109	1.3	18	-208	2.4	-448	5.3	282	
	CS 270	-278	3.3	-138	1.6	-138	1.6	60	-307	3.6	10	-367	4.3	10	-367	4.3	-126	1.5	-65
	BC 0	-85	1.0	-145	1.7	-145	1.7	71	-178	2.1	-153	1.8	81	-180	1.8	-447	5.3	458	
	BS 90	-353	4.2	-185	2.2	-185	2.2	48	-684	6.9	-684	6.9	66	-806	8.0	-235	2.3	-33	
	BS 270	-88	1.0	-146	1.7	-146	1.7	69	-179	2.1	-154	1.8	79	-181	1.8	-423	5.0	382	
72	CC 0	50	2.8	19	1.0	65	3.3	30	54	2.8	18	0.9	-84	65	3.3	65	3.3	28	
	CS 90	53	2.7	35	1.8	80	4.1	81	48	2.5	81	3.1	16	34	1.8	142	7.3	188	
	CC 180	80	3.1	47	2.4	92	4.7	84	71	3.6	34	1.8	-43	78	4.0	78	4.0	30	
	CS 270	75	3.9	31	1.8	77	4.0	2	47	2.4	28	1.4	-63	32	1.7	94	4.8	28	
	BC 0	39	2.0	34	1.7	102	5.2	160	57	2.9	78	4.0	88	78	3.9	76	3.9	84	
	BS 90	40	2.1	50	2.8	118	6.1	188	61	3.1	84	4.3	111	64	2.8	54	2.8	34	
	BS 270	58	2.9	64	3.3	131	6.8	184	68	3.1	119	6.1	113	98	5.1	98	5.1	77	
74	CC 0	21	-66.8	56	-178.7	104	-331.8	368	54	-170.7	-19	60.9	-181	64	-203.8	64	-203.2	204	
	CS 90	182	-679.3	15	-48.3	64	-308.1	-65	38	-122.2	109	-346.5	-46	58	-185.1	146	-464.3	-30	
	CC 180	-64	171.9	64	-203.4	113	-368.3	-368	63	-169.2	-10	32.4	-81	73	-332.7	73	-332.3	-236	
	CS 270	73	-322.4	104	-331.9	153	-488.8	169	226	-718.7	300	-864.2	311	244	-778.2	331	-1053.3	383	
	BC 0	51	-162.3	45	-144.0	88	-273.1	68	55	-178.4	8	-29.3	-42	48	-147.1	48	-146.8	-10	
	BS 90	157	-466.7	2	-6.0	42	-134.1	-73	50	-180.5	101	-322.9	-36	41	-130.0	41	-129.3	-74	
	BS 270	32	-101.9	54	-172.9	95	-302.0	198	67	-214.2	21	-68.1	-39	57	-181.4	57	-181.1	78	
22	CC 0	39	2.0	22	1.1	22	1.1	-44	24	1.2	77	3.9	97	27	1.4	26	1.3	-33	
	CS 90	-111	-6.8	-5	-0.2	-6	-0.2	-66	-8	-0.4	-91	-4.8	-18	-7	-0.3	-103	-6.2	-7	
	CC 180	-18	-0.9	-3	-0.1	-3	-0.1	-46	4	0.2	56	2.9	-412	8	0.4	7	0.3	-137	
	CS 270	3	0.2	24	1.2	24	1.2	682	36	1.8	-84	-4.3	-3887	31	1.6	-27	-1.4	-1008	
	BC 0	22	1.1	23	1.2	23	1.2	8	37	1.9	40	2.0	80	30	1.5	29	1.5	31	
	BS 90	-105	-5.3	-6	-0.3	-5	-0.3	-66	-9	-0.5	-53	-2.7	-48	-10	-0.5	-6	-0.2	-66	
	BS 270	-10	-0.5	-3	-0.2	-3	-0.2	-67	0	0.0	3	0.2	-134	5	0.2	4	0.2	-137	
11	CC 0	-22	-6.7	-29	-7.4	-107	-27.8	388	-31	-8.1	30	7.7	-327	-31	-8.1	-31	-8.1	42	
	CS 90	-61	-18.7	-10	-2.6	-88	-22.7	48	-26	-7.2	-234	-61.1	283	-28	-7.2	-143	-36.7	134	
	CC 180	38	8.8	-4	-1.8	-65	-21.7	-322	-7	-1.8	55	14.0	43	-7	-1.8	-7	-1.8	-118	
	CS 270	-234	-60.2	-25	-6.4	-103	-28.5	-66	-80	-15.3	-169	-43.5	-28	-60	-15.3	-190	-48.9	-19	
	BC 0	-36	-8.3	-27	-8.9	-62	-22.8	188	-31	-7.9	14	3.7	-140	-31	-7.9	-31	-7.9	-14	
	BS 90	-49	-12.6	-6	-1.7	-72	-18.4	48	-24	-6.3	-236	-60.7	382	-24	-6.3	-24	-6.3	-60	
	BS 270	17	4.4	-3	-0.6	-68	-17.4	-488	-2	-0.5	43	11.1	183	-2	-0.5	-2	-0.5	-112	
17	CC 0	-61	1.9	-61	2.1	-65	2.2	17	-118	2.7	-65	1.6	-16	-158	3.7	-158	3.8	85	
	CS 90	-115	2.7	-62	1.9	-65	2.0	-36	-156	3.6	-217	5.0	68	-140	3.3	-138	3.2	38	
	CC 180	-74	1.7	-64	2.2	-68	2.3	32	-121	2.8	-71	1.8	-6	-180	3.7	-158	3.7	114	
	CS 270	-217	5.0	-104	2.4	-108	2.5	-80	-191	4.4	-230	5.3	6	-170	3.9	-216	5.0	-1	
	BC 0	-102	2.4	-65	2.2	-69	2.3	-3	-137	3.2	-112	2.6	18	-186	3.6	-155	3.6	62	
	BS 90	-108	2.5	-64	2.0	-68	2.1	-19	-170	3.8	-198	4.8	60	-146	3.4	-150	3.3	38	
	BS 270	-44	1.0	-68	2.3	-102	2.4	131	-141	3.3	-116	2.7	188	-159	3.7	-158	3.7	288	

BG Technology

Phone: 01509 282845
 FAX: 01509 283080
 email:
 marc.nunn@bgtech.co.uk

BOMEL ENGINEERING CONSULTANTS

07 SEP 1998

Inc. Doc. No. 11354

To HRS/KRM

Facsimile

To: Keith McDonald/Helen Bolt
 @Fax: 01628 777877
 From: Marc Nunn
 Date: Monday, September 7, 1998 @ 2:40
 Re: Frames Project
 Pages: 2, including this

With reference to your fax sent today, here is the information you require for the joint that was instrumented (joint 7). The brace numbers are consistent with the numbering system used in the benchmarking exercise.

Load Case 1 :

Applied load to loading beam = 800kN

brace	Axial	Stress (MPa)	
		OPB	IPB
27	39.8	-12.8	11.3
24	-78.4	0.4	7.4
91	22.0	-8.3	-5.9
72	-104.2	-4.5	-2.7
74	25.5	6.3	-10.9
22	-37.3	-4.6	-0.9
11	-1.5	-6.2	-5.3
17	21.0	-0.1	-3.8

Load Case 2 :

Applied load to loading beam = 800kN

brace	Axial	Stress (MPa)	
		OPB	IPB
27	-20.8	24.7	-4.8
24	31.2	7.8	-4.4
91	-64.4	-20.3	-0.2
72	28.0	-0.9	-7.6
74	22.1	-24.7	2.3
22	5.0	7.8	6.8
11	-6.5	4.2	6.2
17	-48.5	6.2	-0.7

Load Case 3 :

Applied load to loading beam = 1750kN

brace	Axial	Stress (MPa)	
		OPB	IPB
27	33.7	4.3	2.2
24	-34.3	-4.7	3.9
91	0.1	4.5	5.0
72	33.7	-2.0	2.7
74	-19.4	1.9	6.6
22	-46.3	1.8	-5.8
11	-4.3	0.8	-13.3
17	51.7	-3.3	-5.6

I am currently working on a report of the analysis work that we have performed to date. I have also been working under the assumption that we would be doing a small amount of re-analysis work to use the actual member stresses as inputs to the finite element model and parametric equations in order to accurately assess each of the methods of SCF prediction.

Interestingly, I have recently discovered an interesting thing about the Efthymiou equations. It appears that Mike Efthymiou, when producing his equations, attempted to take into account hot spot stresses at the 45° positions by including these results in the 90° positions. This has never been documented anywhere, however (and I only found out about this through discussions with one of Mike's ex-colleagues). As a result of this, I would expect the Efthymiou equations to over-predict the SCF in some instances.

If you need further information, please get in touch.

Regards,



Marc Nunn
Senior Engineer

Inc Doc. 9314

Joint 11, Load Case 1											
Brace	Location	FE	Alpha Kellogg		+/- %		Eftymiou		m-planar		+/- %
			planar	m-planar			planar	m-planar			
25	CC 0	-42	16	16	-139	23	0	0	-101	29	-168
	CS 90	-41	4	4	-111	16	2	2	-105	12	-17
	CC 180	-19	23	23	-222	32	9	9	-149	34	-279
	CS 270	22	35	35	60	59	43	43	93	52	158
	BC 0	-0	18	18	-6061	27	20	20	-6930	24	-8038
	BS 90	-63	4	4	-106	15	17	17	-127	11	-117
	BC 180	10	25	25	155	38	31	31	211	31	212
	BS 270	-24	39	39	-264	67	65	65	-372	62	-357
30	CC 0	24	13	54	124	18	-4	-4	-118	18	-27
	CS 90	39	14	54	39	24	12	12	-69	21	-51
	CC 180	13	5	46	254	7	-15	-15	-212	11	-12
	CS 270	26	5	46	75	11	4	4	-85	9	-88
	BC 0	26	14	59	127	21	17	17	-35	17	-35
	BS 90	44	15	60	35	26	31	31	-29	24	-48
	BC 180	7	6	50	617	9	5	5	-32	8	21
	BS 270	24	5	50	107	12	21	21	-11	10	-60
79	CC 0	105	129	129	23	174	151	151	44	204	87
	CS 90	150	125	125	-16	187	167	167	11	156	124
	CC 180	68	111	111	68	150	127	127	92	190	183
	CS 270	85	114	114	35	172	156	156	84	142	65
	BC 0	159	141	141	-11	191	182	182	15	190	176
	BS 90	131	137	137	5	200	192	192	47	171	74
	BC 180	45	121	121	169	162	154	154	242	170	248
	BS 270	83	125	125	51	181	179	179	116	153	153
84	CC 0	-129	-99	-99	-23	-132	-154	-154	19	-154	14
	CS 90	-80	-103	-103	15	-132	-136	-136	62	-116	6
	CC 180	-56	-74	-74	31	-98	-120	-120	114	-134	126
	CS 270	-75	-69	-69	-9	-98	-92	-92	23	-72	-75
	BC 0	-172	-109	-109	-37	-141	-142	-142	-17	-147	-22
	BS 90	-133	-114	-114	-15	-140	-130	-130	-2	-128	39
	BC 180	-31	-80	-80	158	-101	-102	-102	229	-119	241
	BS 270	-102	-75	-75	-26	-102	-78	-78	-24	-73	27
92	CC 0	-42	-50	-50	18	-54	-28	-28	-33	-71	69
	CS 90	-107	-60	-60	-44	-126	-126	-126	17	-142	32
	CC 180	-59	-60	-60	1	-65	-39	-39	-34	-82	39
	CS 270	-95	-48	-48	-48	-101	-101	-101	6	-116	22
	BC 0	-21	-41	-41	97	-56	-46	-46	119	-46	121
	BS 90	-101	-53	-53	-47	-161	-4	-4	60	-138	37
	BC 180	-30	-53	-53	76	-71	-61	-61	103	-60	101
	BS 270	-86	-41	-41	-52	-132	-132	-132	54	-112	30

Joint 11, Load Case 2												
Brace	Location	FE		Alpha Kellogg		Efrhymiou		m-planar		Lloyd's		+/- %
				planar	m-planar	planar	m-planar	planar	m-planar	planar	m-planar	
25	CC 0	285	294	301	6	394	457	456	434	456	434	52
	CS 90	310	273	280	-10	387	363	301	220	301	220	-29
	CC 180	141	216	223	58	288	352	394	372	394	372	184
	CS 270	250	237	243	-3	315	318	254	110	254	110	-56
	BC 0	421	323	331	-21	420	418	436	397	436	397	-6
	BS 90	285	289	307	8	388	323	327	495	327	495	74
	BC 180	79	234	242	206	295	293	349	310	349	310	293
	BS 270	252	258	265	5	327	270	267	435	267	435	73
30	CC 0	-478	-407	-407	-15	-550	-482	-642	-620	-642	-620	30
	CS 90	-421	-358	-358	-15	-546	-482	-453	-340	-453	-340	-19
	CC 180	-240	-344	-344	43	-465	-397	-591	-569	-591	-569	137
	CS 270	-328	-393	-393	20	-595	-524	-498	-347	-498	-347	6
	BC 0	-494	-447	-447	-10	-608	-580	-596	-557	-596	-557	13
	BS 90	-432	-391	-391	-10	-677	-583	-489	-658	-489	-658	52
	BC 180	-211	-375	-375	78	-507	-479	-525	-486	-525	-486	130
	BS 270	-348	-431	-431	24	-636	-614	-546	-715	-546	-715	108
79	CC 0	-262	-135	-239	-9	-185	-117	-200	-189	-200	-189	-24
	CS 90	-157	-110	-214	36	-209	-142	-179	-121	-179	-121	-23
	CC 180	-161	-98	-202	26	-138	-67	-170	-170	-170	-170	6
	CS 270	-226	-123	-227	1	-227	-147	-166	-92	-166	-92	-59
	BC 0	-211	-149	-262	24	-220	-193	-183	-183	-183	-183	-14
	BS 90	-226	-120	-234	4	-225	-214	-189	-202	-189	-202	-10
	BC 180	-55	-108	-220	299	-161	-134	-142	-141	-142	-141	156
	BS 270	-279	-135	-248	-11	-247	-219	-220	-224	-220	-224	-20
64	CC 0	114	25	215	89	33	97	25	24	25	24	-79
	CS 90	131	63	253	94	65	96	81	158	81	158	19
	CC 180	33	-13	177	445	-18	46	-6	-6	-6	-6	-119
	CS 270	65	-52	139	112	-50	-57	-68	-113	-68	-113	-273
	BC 0	147	28	236	61	38	39	30	29	30	29	-80
	BS 90	189	72	260	48	73	46	101	105	101	105	-45
	BC 180	10	-15	193	1807	-22	-22	-12	-13	-12	-13	-232
	BS 270	121	-59	149	23	-57	-135	-88	-84	-88	-84	-169
92	CC 0	246	-50	-50	-120	199	103	250	250	250	250	2
	CS 90	303	-60	-60	-120	346	346	392	392	392	392	29
	CC 180	119	-60	-60	-150	157	60	207	207	207	207	74
	CS 270	254	-49	-49	-119	333	333	379	379	379	379	49
	BC 0	220	-41	-41	-119	221	182	187	187	187	187	-15
	BS 90	347	-53	-53	-115	447	447	382	382	382	382	10
	BC 180	143	-53	-53	-137	162	123	133	133	133	133	-7
	BS 270	284	-41	-41	-114	433	433	369	369	369	369	30

Joint 11, Load Case 3												
Brace	Location	FE	Alpha Kellogg planar	m-planar	+/- %	Eifhymiou planar	m-planar	+/- %	Lloyd's planar	m-planar	+/- %	
25	CC 0	-91	-62	-62	-32	-85	-52	-42	-98	-98	7	
	CS 90	-60	-41	-41	-31	-88	-61	2	-74	-31	-49	
	CC 180	-27	-62	-62	130	-86	-54	98	-98	-98	263	
	CS 270	-49	-83	-83	68	-147	-118	135	-128	-110	123	
	BC 0	-95	-67	-67	-29	-102	-91	-4	-86	-86	-10	
	BS 90	-80	-44	-44	-45	-93	-92	15	-79	-79	-2	
	BC 180	-13	-68	-68	442	-103	-92	631	-86	-86	586	
	BS 270	-42	-91	-91	118	-162	-157	275	-147	-147	252	
30	CC 0	-40	-13	-13	-68	-16	13	-132	-18	-18	-55	
	CS 90	-22	-4	-4	-83	-10	-13	-40	-8	-47	119	
	CC 180	13	-7	-7	-153	-10	21	55	-13	-13	-201	
	CS 270	-16	-16	-16	1	-28	-25	56	-24	-42	159	
	BC 0	-26	-14	-14	-46	-21	-23	-12	-17	-17	-35	
	BS 90	-18	-4	-4	-79	-10	-44	153	-8	-8	-56	
	BC 180	15	-8	-8	-151	-12	-14	-193	-11	-11	-171	
	BS 270	-19	-18	-18	-6	-31	-59	205	-29	-29	48	
79	CC 0	-44	-42	-42	-6	47	21	-147	53	53	-221	
	CS 90	-45	-38	-38	-16	70	40	-188	61	30	-165	
	CC 180	-9	-42	-42	351	46	21	-319	53	53	-667	
	CS 270	-14	-47	-47	240	58	31	-326	50	-6	-59	
	BC 0	-51	-46	-46	-9	56	48	-195	47	47	-193	
	BS 90	-23	-41	-41	83	77	73	-423	69	69	-404	
	BC 180	-5	-46	-46	828	55	48	-1056	47	47	-1034	
	BS 270	23	-51	-51	-319	62	62	167	55	55	134	
84	CC 0	-15	-15	-15	2	-21	10	-167	-24	-24	57	
	CS 90	-28	-4	-4	-84	-17	6	-121	-11	-11	-202	
	CC 180	-10	-14	-14	37	-19	12	-222	-22	-22	123	
	CS 270	-8	-25	-25	193	-38	-20	143	-37	-34	308	
	BC 0	-6	-17	-17	160	-25	-22	274	-21	-21	250	
	BS 90	-33	-4	-4	-87	-18	-30	-7	-10	-10	-70	
	BC 180	-6	-15	-15	163	-23	-20	250	-19	-19	238	
	BS 270	-5	-27	-27	408	-41	-61	1034	-43	-43	699	
92	CC 0	41	85	85	109	92	39	-5	117	117	187	
	CS 90	113	67	67	-41	136	136	20	156	156	38	
	CC 180	35	72	72	106	79	25	-29	103	103	192	
	CS 270	149	90	90	-40	189	189	27	213	213	43	
	BC 0	42	75	75	78	101	80	89	86	86	103	
	BS 90	103	55	55	-47	179	179	74	152	152	47	
	BC 180	34	60	60	80	82	61	80	68	68	101	
	BS 270	140	81	81	-42	243	243	74	208	208	49	

Joint 40, Load Case 1		FE	Alpha Kellogg	Efthymiou	Lloyd's	m-planar	+/- %	planar	+/- %	m-planar	+/- %
Brace	Location		planar	planar	planar	m-planar					
71	CC 0	-375	-317	-428	-674	-428	-15	-674	14	-674	80
	CS 90	-312	-269	-383	-291	-379	-14	-291	22	-360	15
	CC 180	-138	-220	-335	-566	-335	59	-566	142	-566	308
	CS 270	-278	-268	-380	-289	-379	-4	-289	36	-327	17
	BC 0	-368	-280	-382	-492	-382	-24	-492	3	-492	33
	BS 90	-337	-236	-329	-250	-326	-30	-250	-3	-250	-26
	BC 180	-58	-192	-275	-408	-275	231	-408	375	-408	605
	BS 270	-269	-235	-327	-249	-326	-13	-249	21	-249	-8
	Min	-375	-317	-428	-674	-428	-15	-674	14	-674	80
72	CC 0	382	318	428	677	430	-17	677	13	677	77
	CS 90	287	269	382	290	385	-6	290	34	339	18
	CC 180	145	222	338	571	339	54	571	134	571	294
	CS 270	312	271	386	294	388	-13	294	24	378	21
	BC 0	370	281	383	494	383	-24	494	3	484	34
	BS 90	281	237	328	249	331	-16	249	18	249	-11
	BC 180	57	194	278	412	277	238	412	384	412	618
	BS 270	339	238	332	252	334	-30	252	-1	252	-25
	Max	382	318	429	677	430	-17	677	13	677	77
96	CC 0	231	231	251	400	251	21	400	8	400	73
	CS 90	143	176	188	137	215	57	137	50	167	10
	CC 180	90	150	185	324	185	120	324	107	324	262
	CS 270	198	205	248	185	218	27	185	10	331	67
	BC 0	245	205	228	310	228	0	310	-7	310	26
	BS 90	153	154	155	92	173	28	92	13	92	-40
	BC 180	49	130	135	250	135	250	250	175	250	407
	BS 270	256	180	208	140	189	-13	140	-26	140	-45
	Max	256	231	251	400	251	9	400	-2	400	57
97	CC 0	-237	-232	-251	-401	-251	19	-401	6	-401	69
	CS 90	-201	-208	-255	-202	-226	28	-202	13	-321	60
	CC 180	-96	-150	-185	-325	-185	107	-325	92	-325	237
	CS 270	-144	-173	-182	-131	-214	55	-131	49	-153	6
	BC 0	-248	-205	-229	-310	-229	0	-310	-8	-310	25
	BS 90	-261	-184	-214	-145	-196	-13	-145	-25	-145	-44
	BC 180	-51	-130	-135	-250	-135	245	-250	188	-250	395
	BS 270	-158	-152	-150	-87	-170	24	-87	7	-87	-45
	Min	-261	-332	-255	-401	-251	8	-401	-4	-401	64

inc. doc. 0266

Joint 40, Load Case 2		Alpha Kellogg		Efhymiou		m-planar		Lloyd's		m-planar		+/- %	
Brace	Location	FE	planar	m-planar	planar	m-planar	planar	planar	planar	m-planar	planar	planar	+/- %
71	CC 0	93	91	91	121	119	188	188	188	188	188	188	27
	CS 90	94	78	78	118	117	94	94	94	115	115	115	25
	CC 180	45	56	56	87	85	149	149	149	149	149	149	89
	CS 270	81	68	68	90	85	71	64	64	71	71	71	4
	BC 0	48	80	80	109	107	138	138	138	138	138	138	123
	BS 90	40	68	68	102	102	79	79	79	79	79	79	157
	BC 180	15	48	48	70	69	108	108	108	108	108	108	363
	BS 270	36	60	60	77	73	57	57	57	57	57	57	100
	Max	94	91	91	121	119	188	188	188	188	188	188	27
	CC 0	-93	-89	-89	-119	-119	-186	-186	-186	-186	-186	-186	28
	CS 90	-85	-66	-66	-120	-120	-96	-96	-96	-96	-96	-96	41
	CC 180	-41	-54	-54	-85	-85	-146	-146	-146	-146	-146	-146	109
CS 270	-61	-76	-76	-85	-83	-75	-60	-60	-60	-60	-60	37	
BC 0	-48	-79	-79	-107	-107	-136	-136	-136	-136	-136	-136	122	
BS 90	-40	-58	-58	-69	-69	-80	-80	-80	-80	-80	-80	156	
BC 180	-14	-47	-47	-72	-71	-105	-105	-105	-105	-105	-105	394	
BS 270	-33	-68	-68	-120	-120	-64	-54	-54	-54	-54	-54	116	
Min	-93	-89	-89	-120	-120	-186	-186	-186	-186	-186	-186	29	
CC 0	-57	-54	-54	-58	-58	-92	-92	-92	-92	-92	-92	2	
CS 90	-40	-38	-38	-34	-47	-41	-23	-23	-23	-23	-23	19	
CC 180	-11	-32	-32	-41	-40	-72	-72	-72	-72	-72	-72	263	
CS 270	-43	-50	-50	-65	-51	-49	-53	-53	-53	-53	-53	20	
BC 0	-66	-48	-48	-54	-54	-71	-71	-71	-71	-71	-71	-19	
BS 90	-38	-31	-31	-28	-28	-36	-14	-14	-14	-14	-14	-5	
BC 180	-5	-28	-28	-29	-28	-28	-55	-55	-55	-55	-55	469	
BS 270	-14	-45	-45	-55	-46	-38	-38	-38	-38	-38	-38	229	
Min	-66	-54	-54	-65	-58	-92	-92	-92	-92	-92	-92	-12	
CC 0	74	59	59	62	61	98	98	98	98	98	98	-18	
CS 90	46	37	37	65	50	53	53	53	53	53	53	7	
CC 180	11	30	30	39	38	71	71	71	71	71	71	250	
CS 270	37	51	51	36	47	26	25	25	25	25	25	26	
BC 0	75	52	52	59	58	76	76	76	76	76	76	-23	
BS 90	58	33	33	55	45	38	38	38	38	38	38	-22	
BC 180	-2	26	26	26	25	54	54	54	54	54	54	-1400	
BS 270	37	45	45	30	37	16	16	16	16	16	16	-1	
Max	75	59	59	65	61	98	98	98	98	98	98	-19	

Joint 40, Load Case 3		FE	Alpha Kellogg	m-planar	+/- %	Eftymiou	m-planar	+/- %	Lloyd's	m-planar	+/- %
Brace	Location	planar	planar	planar		planar	planar		planar	planar	
71	CC 0	98	98	98	-0	134	125	28	213	213	117
	CS 90	39	73	73	91	82	73	90	51	60	55
	CC 180	46	76	76	66	113	105	130	189	189	312
	CS 270	79	100	100	26	165	152	91	137	184	107
	BC 0	81	86	86	6	118	111	36	155	155	90
	BS 90	58	64	64	10	70	63	8	50	50	-15
	BC 180	30	67	67	119	94	87	187	136	136	349
	BS 270	68	89	89	29	143	133	94	112	112	63
	Max	98	100	100	2	165	152	55	213	213	117
72	CC 0	-91	-93	-93	3	-127	-127	39	-201	-201	121
	CS 90	-69	-88	-88	27	-94	-82	18	-66	-76	10
	CC 180	-38	-69	-69	81	-104	-103	171	-174	-174	357
	CS 270	-20	-74	-74	275	-136	-138	599	-110	-108	444
	BC 0	-76	-82	-82	9	-113	-113	50	-147	-147	94
	BS 90	-56	-77	-77	37	-80	-68	21	-60	-60	6
	BC 180	-19	-60	-60	223	-86	-86	364	-125	-125	574
	BS 270	-21	-65	-65	211	-118	-118	465	-91	-91	336
	Min	-91	-93	-93	3	-136	-138	52	-201	-201	121
96	CC 0	87	110	110	27	122	119	37	197	197	127
	CS 90	98	97	97	-1	110	92	-8	83	95	-3
	CC 180	35	87	87	148	103	100	186	178	178	410
	CS 270	9	100	100	1063	116	117	1263	89	53	513
	BC 0	72	97	97	35	108	105	46	154	154	114
	BS 90	67	85	85	28	91	78	17	58	58	-13
	BC 180	17	76	76	356	80	78	368	135	135	714
	BS 270	-36	88	88	-345	97	101	-383	62	62	-274
	Max	98	110	110	13	122	119	22	197	197	101
97	CC 0	-82	-108	-108	31	-119	-118	44	-191	-191	133
	CS 90	-69	-117	-117	70	-66	-94	38	-41	-23	-66
	CC 180	-34	-84	-84	148	-100	-99	193	-173	-173	410
	CS 270	-84	-75	-75	-10	-153	-129	55	-126	-133	59
	BC 0	-75	-95	-95	26	-105	-104	39	-150	-150	99
	BS 90	-37	-103	-103	180	-53	-67	82	-24	-24	-35
	BC 180	-12	-73	-73	501	-78	-77	534	-131	-131	976
	BS 270	15	-65	-65	-550	-130	-116	-898	-93	-93	-739
	Min	-84	-117	-117	40	-153	-129	55	-181	-191	129

APPENDIX C

INSTRUMENTATION LAYOUT DETAILS

Load cell details - C636\11\011D

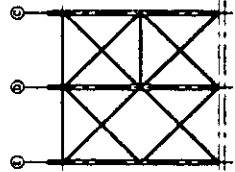
Strain gauging details - sheet 1 of 2 - C636\15\012D

Strain gauging details - sheet 2 of 2 - C636\15\013D

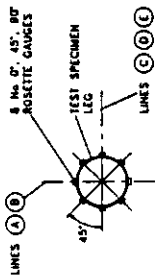
Node 7 SCF gauge positions - C636\18\017D

NOTES

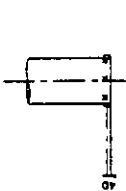
1. FOR GENERAL NOTES SEE DWG. C636/15/0020
2. FOR LOCATION OF DETAILS 1 TO 4 SEE DWG. C636/15/0120
3. DETAILS 3, 4 AND 5 - GAUGES CLOSEST TO INTERSECTION DENOTED 'NEAR'. OTHER SETS DENOTED 'FAR'.
4. _____ 2 DENOTES DETAIL 2
5. ASG 37-38 DENOTES LOGGER REFERENCE OF ADDITIONAL STRAIN GAUGES.



ELEVATION ON LINE B
KEY ELEVATION

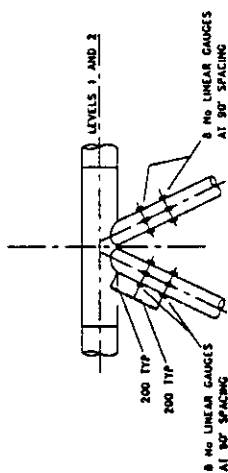


GAUGE ARRANGEMENT

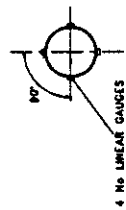


1820-9 L 6350 FABRICATED BY BEAM TO LONGING INC.
ELEVATION

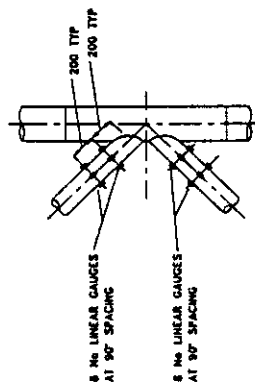
DETAIL 1



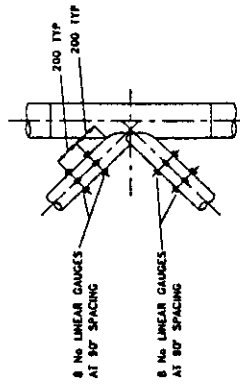
DETAIL 1



DETAIL 2

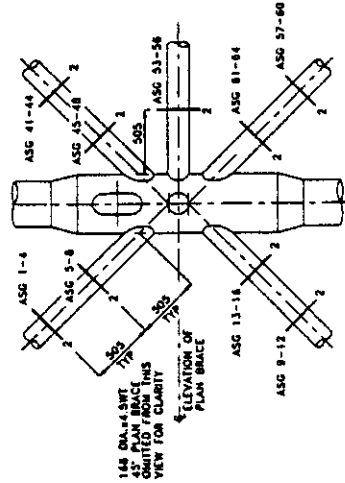


DETAIL 2



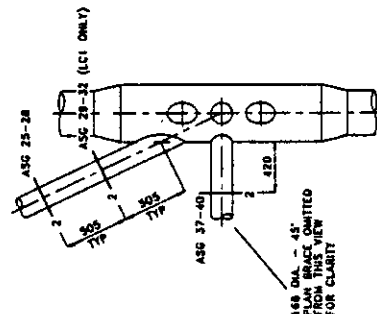
DETAIL 3

DETAILS 3, 4 AND 5 - NEAR AND FAR GAUGES INSTALLED FOR LOADCASES LC1 AND LC1C
FAR GAUGES ONLY INSTALLED FOR LOADCASES LC3CA AND LC1CA



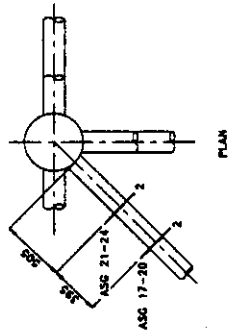
ELEVATION ON LINE B

DETAIL 4



ELEVATION ON LINE D

DETAIL 5



ELEVATION ON LINE E

DETAIL 6

ITEM	QTY	DESCRIPTION	UNIT	PRICE	TOTAL
1	1	AS BUILT - INCLUDING DETAIL 5	TAG	JACO	HMB
2	1	AS BUILT	TAG	JACO	HMB
3	1	SPECIFICATION	TAG	JACO	HMB
4	1	AS BUILT	TAG	JACO	HMB
5	1	SPECIFICATION	TAG	JACO	HMB
6	1	AS BUILT	TAG	JACO	HMB
7	1	SPECIFICATION	TAG	JACO	HMB
8	1	AS BUILT	TAG	JACO	HMB
9	1	SPECIFICATION	TAG	JACO	HMB
10	1	AS BUILT	TAG	JACO	HMB
11	1	SPECIFICATION	TAG	JACO	HMB
12	1	AS BUILT	TAG	JACO	HMB
13	1	SPECIFICATION	TAG	JACO	HMB
14	1	AS BUILT	TAG	JACO	HMB
15	1	SPECIFICATION	TAG	JACO	HMB
16	1	AS BUILT	TAG	JACO	HMB
17	1	SPECIFICATION	TAG	JACO	HMB
18	1	AS BUILT	TAG	JACO	HMB
19	1	SPECIFICATION	TAG	JACO	HMB
20	1	AS BUILT	TAG	JACO	HMB
21	1	SPECIFICATION	TAG	JACO	HMB
22	1	AS BUILT	TAG	JACO	HMB
23	1	SPECIFICATION	TAG	JACO	HMB
24	1	AS BUILT	TAG	JACO	HMB
25	1	SPECIFICATION	TAG	JACO	HMB
26	1	AS BUILT	TAG	JACO	HMB
27	1	SPECIFICATION	TAG	JACO	HMB
28	1	AS BUILT	TAG	JACO	HMB
29	1	SPECIFICATION	TAG	JACO	HMB
30	1	AS BUILT	TAG	JACO	HMB
31	1	SPECIFICATION	TAG	JACO	HMB
32	1	AS BUILT	TAG	JACO	HMB
33	1	SPECIFICATION	TAG	JACO	HMB
34	1	AS BUILT	TAG	JACO	HMB
35	1	SPECIFICATION	TAG	JACO	HMB
36	1	AS BUILT	TAG	JACO	HMB
37	1	SPECIFICATION	TAG	JACO	HMB
38	1	AS BUILT	TAG	JACO	HMB
39	1	SPECIFICATION	TAG	JACO	HMB
40	1	AS BUILT	TAG	JACO	HMB
41	1	SPECIFICATION	TAG	JACO	HMB
42	1	AS BUILT	TAG	JACO	HMB
43	1	SPECIFICATION	TAG	JACO	HMB
44	1	AS BUILT	TAG	JACO	HMB
45	1	SPECIFICATION	TAG	JACO	HMB
46	1	AS BUILT	TAG	JACO	HMB
47	1	SPECIFICATION	TAG	JACO	HMB
48	1	AS BUILT	TAG	JACO	HMB
49	1	SPECIFICATION	TAG	JACO	HMB
50	1	AS BUILT	TAG	JACO	HMB
51	1	SPECIFICATION	TAG	JACO	HMB
52	1	AS BUILT	TAG	JACO	HMB
53	1	SPECIFICATION	TAG	JACO	HMB
54	1	AS BUILT	TAG	JACO	HMB
55	1	SPECIFICATION	TAG	JACO	HMB
56	1	AS BUILT	TAG	JACO	HMB
57	1	SPECIFICATION	TAG	JACO	HMB
58	1	AS BUILT	TAG	JACO	HMB
59	1	SPECIFICATION	TAG	JACO	HMB
60	1	AS BUILT	TAG	JACO	HMB
61	1	SPECIFICATION	TAG	JACO	HMB
62	1	AS BUILT	TAG	JACO	HMB
63	1	SPECIFICATION	TAG	JACO	HMB
64	1	AS BUILT	TAG	JACO	HMB
65	1	SPECIFICATION	TAG	JACO	HMB
66	1	AS BUILT	TAG	JACO	HMB
67	1	SPECIFICATION	TAG	JACO	HMB
68	1	AS BUILT	TAG	JACO	HMB
69	1	SPECIFICATION	TAG	JACO	HMB
70	1	AS BUILT	TAG	JACO	HMB
71	1	SPECIFICATION	TAG	JACO	HMB
72	1	AS BUILT	TAG	JACO	HMB
73	1	SPECIFICATION	TAG	JACO	HMB
74	1	AS BUILT	TAG	JACO	HMB
75	1	SPECIFICATION	TAG	JACO	HMB
76	1	AS BUILT	TAG	JACO	HMB
77	1	SPECIFICATION	TAG	JACO	HMB
78	1	AS BUILT	TAG	JACO	HMB
79	1	SPECIFICATION	TAG	JACO	HMB
80	1	AS BUILT	TAG	JACO	HMB
81	1	SPECIFICATION	TAG	JACO	HMB
82	1	AS BUILT	TAG	JACO	HMB
83	1	SPECIFICATION	TAG	JACO	HMB
84	1	AS BUILT	TAG	JACO	HMB
85	1	SPECIFICATION	TAG	JACO	HMB
86	1	AS BUILT	TAG	JACO	HMB
87	1	SPECIFICATION	TAG	JACO	HMB
88	1	AS BUILT	TAG	JACO	HMB
89	1	SPECIFICATION	TAG	JACO	HMB
90	1	AS BUILT	TAG	JACO	HMB
91	1	SPECIFICATION	TAG	JACO	HMB
92	1	AS BUILT	TAG	JACO	HMB
93	1	SPECIFICATION	TAG	JACO	HMB
94	1	AS BUILT	TAG	JACO	HMB
95	1	SPECIFICATION	TAG	JACO	HMB
96	1	AS BUILT	TAG	JACO	HMB
97	1	SPECIFICATION	TAG	JACO	HMB
98	1	AS BUILT	TAG	JACO	HMB
99	1	SPECIFICATION	TAG	JACO	HMB
100	1	AS BUILT	TAG	JACO	HMB

ELEVATION ON LINE F

ELEVATION ON LINE G

ELEVATION ON LINE H

ELEVATION ON LINE I

ELEVATION ON LINE J

ELEVATION ON LINE K

ELEVATION ON LINE L

ELEVATION ON LINE M

ELEVATION ON LINE N

ELEVATION ON LINE O

ELEVATION ON LINE P

ELEVATION ON LINE Q

ELEVATION ON LINE R

ELEVATION ON LINE S

ELEVATION ON LINE T

ELEVATION ON LINE U

ELEVATION ON LINE V

ELEVATION ON LINE W

ELEVATION ON LINE X

ELEVATION ON LINE Y

ELEVATION ON LINE Z

ELEVATION ON LINE AA

ELEVATION ON LINE AB

ELEVATION ON LINE AC

ELEVATION ON LINE AD

ELEVATION ON LINE AE

ELEVATION ON LINE AF

ELEVATION ON LINE AG

ELEVATION ON LINE AH

ELEVATION ON LINE AI

ELEVATION ON LINE AJ

ELEVATION ON LINE AK

ELEVATION ON LINE AL

ELEVATION ON LINE AM

ELEVATION ON LINE AN

ELEVATION ON LINE AO

ELEVATION ON LINE AP

ELEVATION ON LINE AQ

ELEVATION ON LINE AR

ELEVATION ON LINE AS

ELEVATION ON LINE AT

ELEVATION ON LINE AU

ELEVATION ON LINE AV

ELEVATION ON LINE AW

ELEVATION ON LINE AX

ELEVATION ON LINE AY

ELEVATION ON LINE AZ

ELEVATION ON LINE BA

ELEVATION ON LINE BB

ELEVATION ON LINE BC

ELEVATION ON LINE BD

ELEVATION ON LINE BE

ELEVATION ON LINE BF

ELEVATION ON LINE BG

ELEVATION ON LINE BH

ELEVATION ON LINE BI

ELEVATION ON LINE BJ

ELEVATION ON LINE BK

ELEVATION ON LINE BL

ELEVATION ON LINE BM

ELEVATION ON LINE BN

ELEVATION ON LINE BO

ELEVATION ON LINE BP

ELEVATION ON LINE BQ

ELEVATION ON LINE BR

ELEVATION ON LINE BS

ELEVATION ON LINE BT

ELEVATION ON LINE BU

ELEVATION ON LINE BV

ELEVATION ON LINE BW

ELEVATION ON LINE BX

ELEVATION ON LINE BY

ELEVATION ON LINE BZ

ELEVATION ON LINE CA

ELEVATION ON LINE CB

ELEVATION ON LINE CC

ELEVATION ON LINE CD

ELEVATION ON LINE CE

ELEVATION ON LINE CF

ELEVATION ON LINE CG

ELEVATION ON LINE CH

ELEVATION ON LINE CI

ELEVATION ON LINE CJ

ELEVATION ON LINE CK

ELEVATION ON LINE CL

ELEVATION ON LINE CM

ELEVATION ON LINE CN

ELEVATION ON LINE CO

ELEVATION ON LINE CP

ELEVATION ON LINE CQ

ELEVATION ON LINE CR

ELEVATION ON LINE CS

ELEVATION ON LINE CT

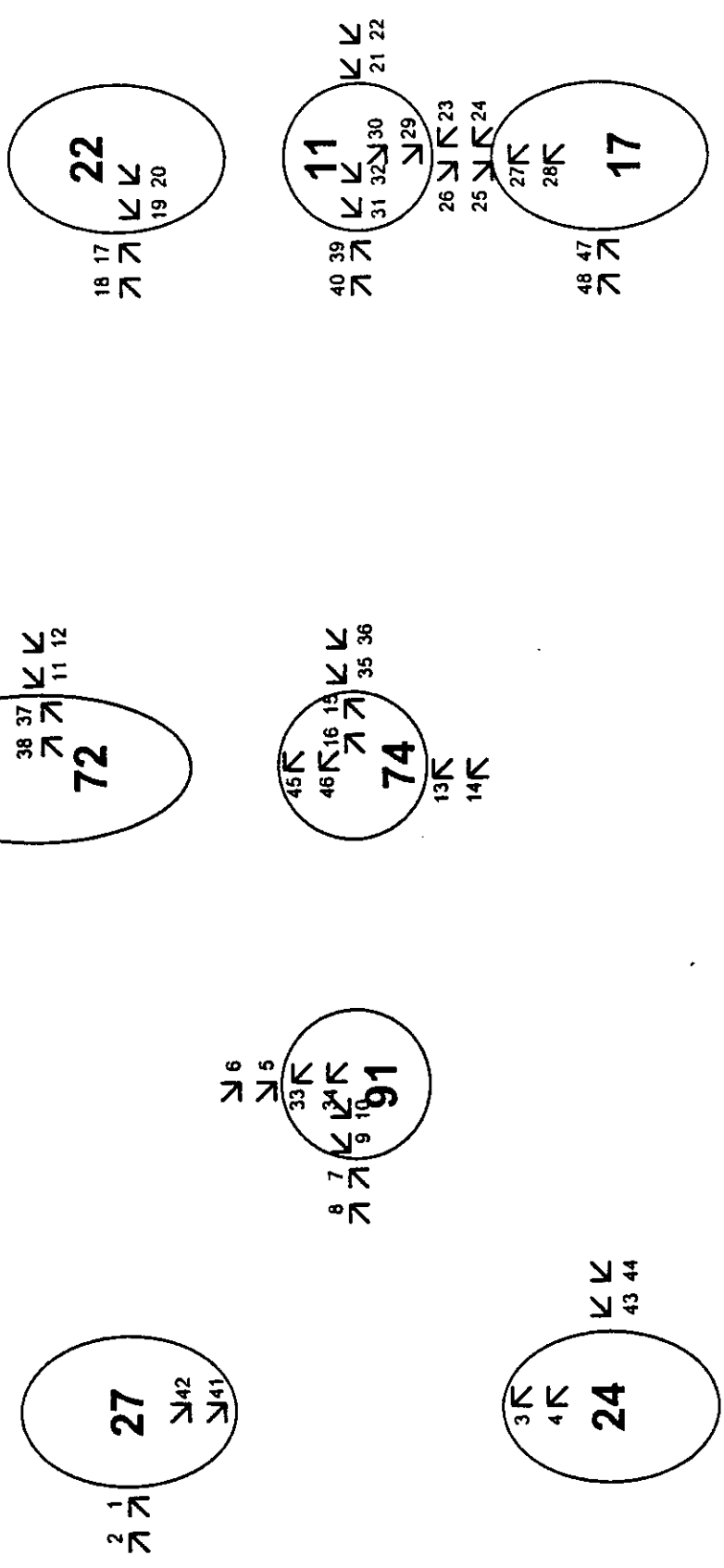
ELEVATION ON LINE CU

ELEVATION ON LINE CV

ELEVATION ON LINE CW

ELEVATION ON LINE CX

NODE 7 - SCF GAUGE POSITIONS



Key:



- 41 SCF gauge number
- A, B, C rosette gauge ID, clockwise from A
- A parallel to weld toe

Gauge positions:

- All brace side gauge pairs: 4mm and 12.7mm from weld toe
- Chord side gauge pairs at saddle location: 4mm and 19.9mm from weld toe
- Chord side gauge pairs at crown location: 4mm and 13.0mm from weld toe

APPENDIX D

COMPARISON OF RESULTS

Comparison of test and predicted nominal stresses - C636\43\027W (3 pages)

Comparison between nominal and principal stresses in tests - C636\43\028W (3 pages)

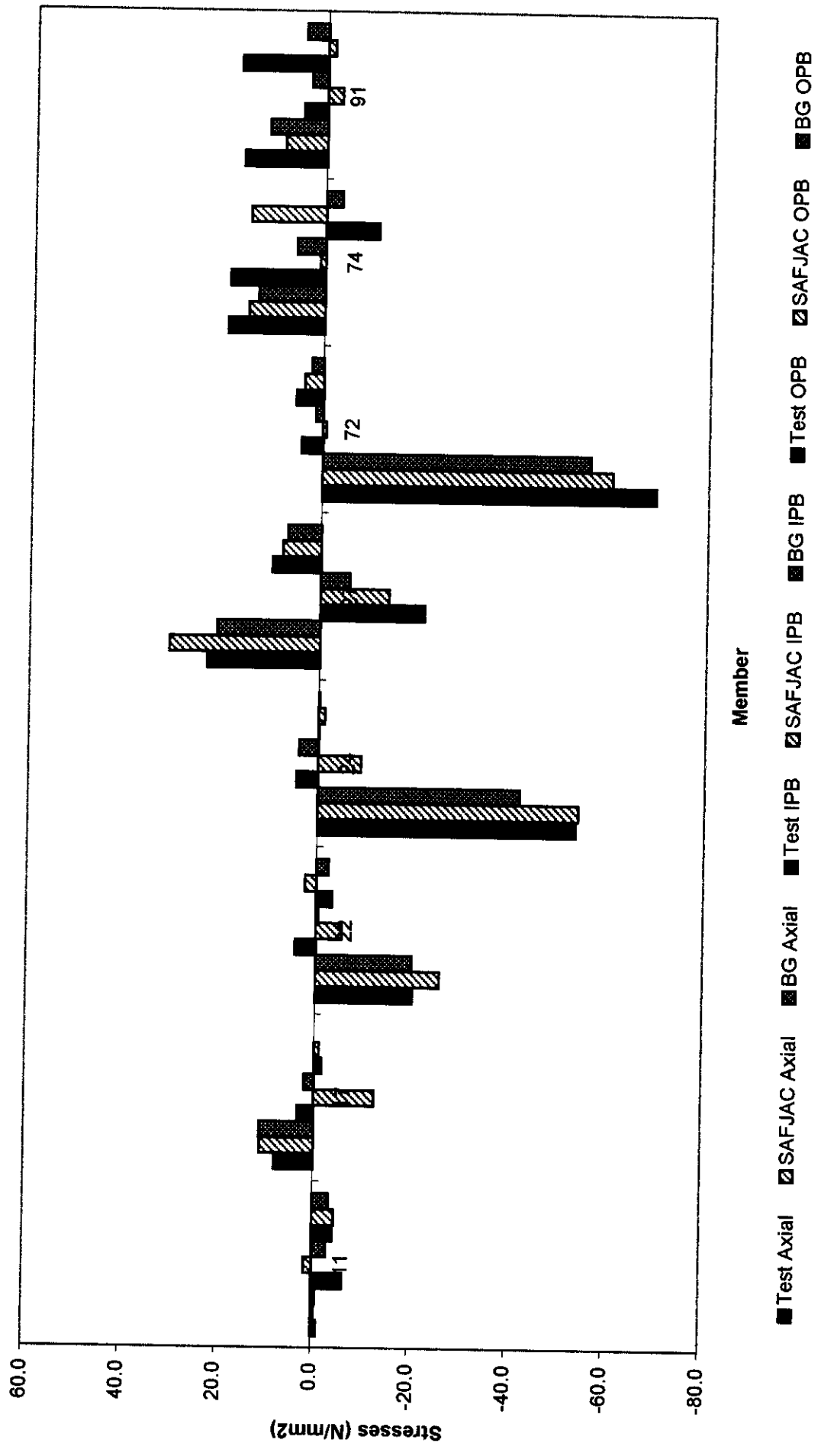
Comparison between measured and predicted principal stresses - C636\43\029W (3 pages)

Comparison for Loadcase 1 at Scan 9

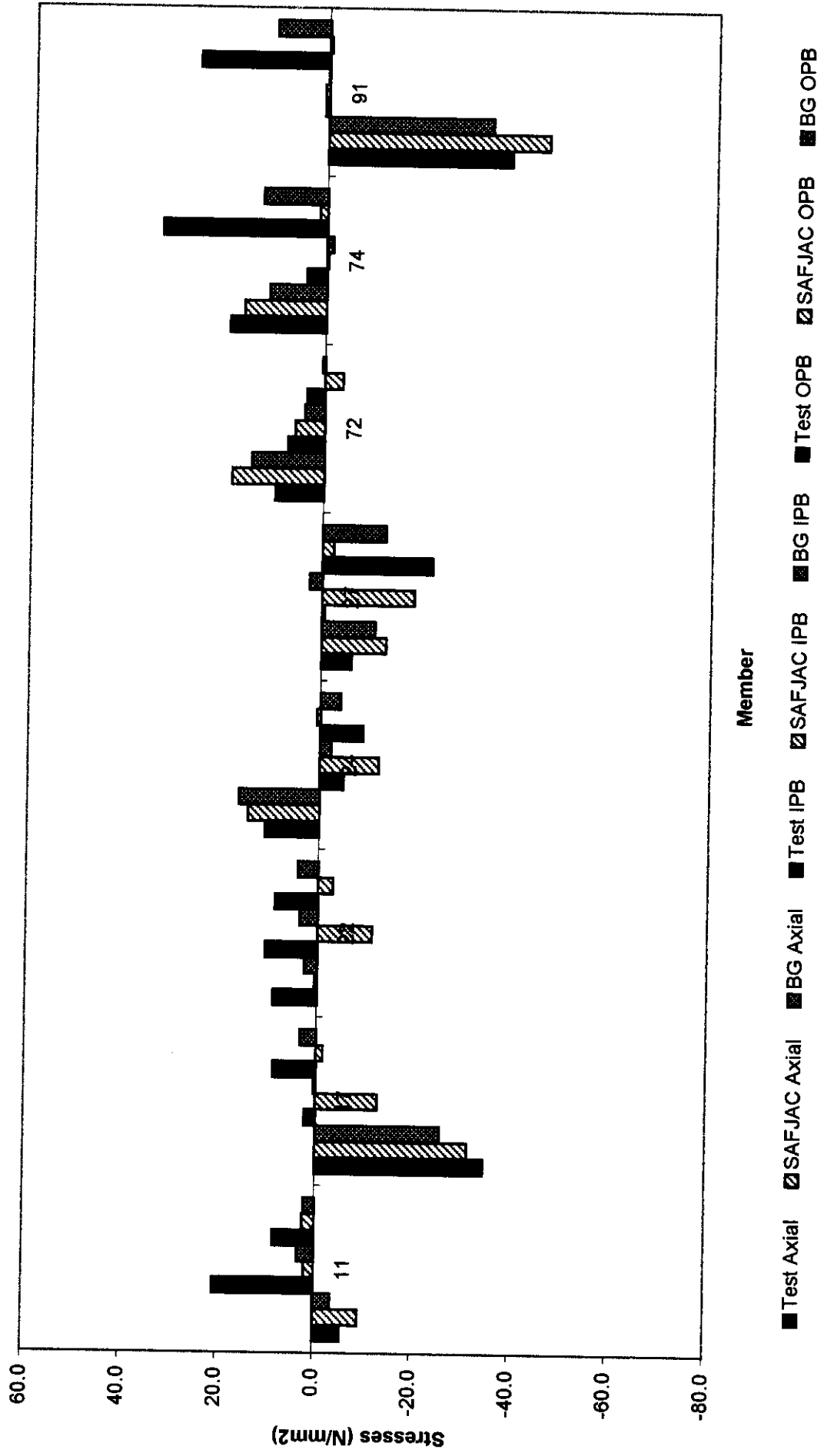
Comparison for Loadcase 2 at Scan 11

Comparison for Loadcase 3 at Scan 9

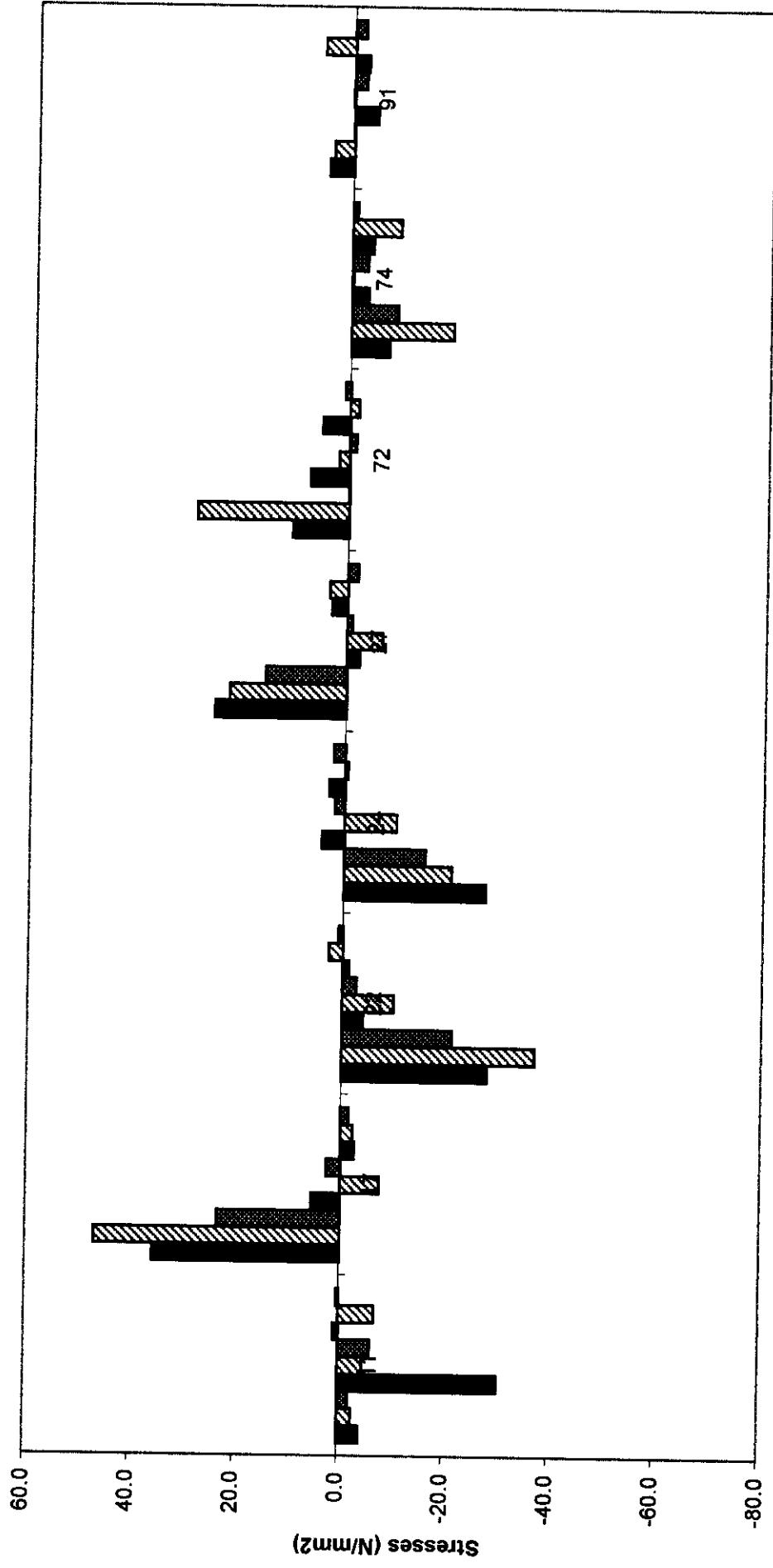
Comparison of test and predicted stresses - Loadcase 1 - Applied Load ~400kN



Comparison of test and predicted stresses - Loadcase 2 - Applied Load ~400kN



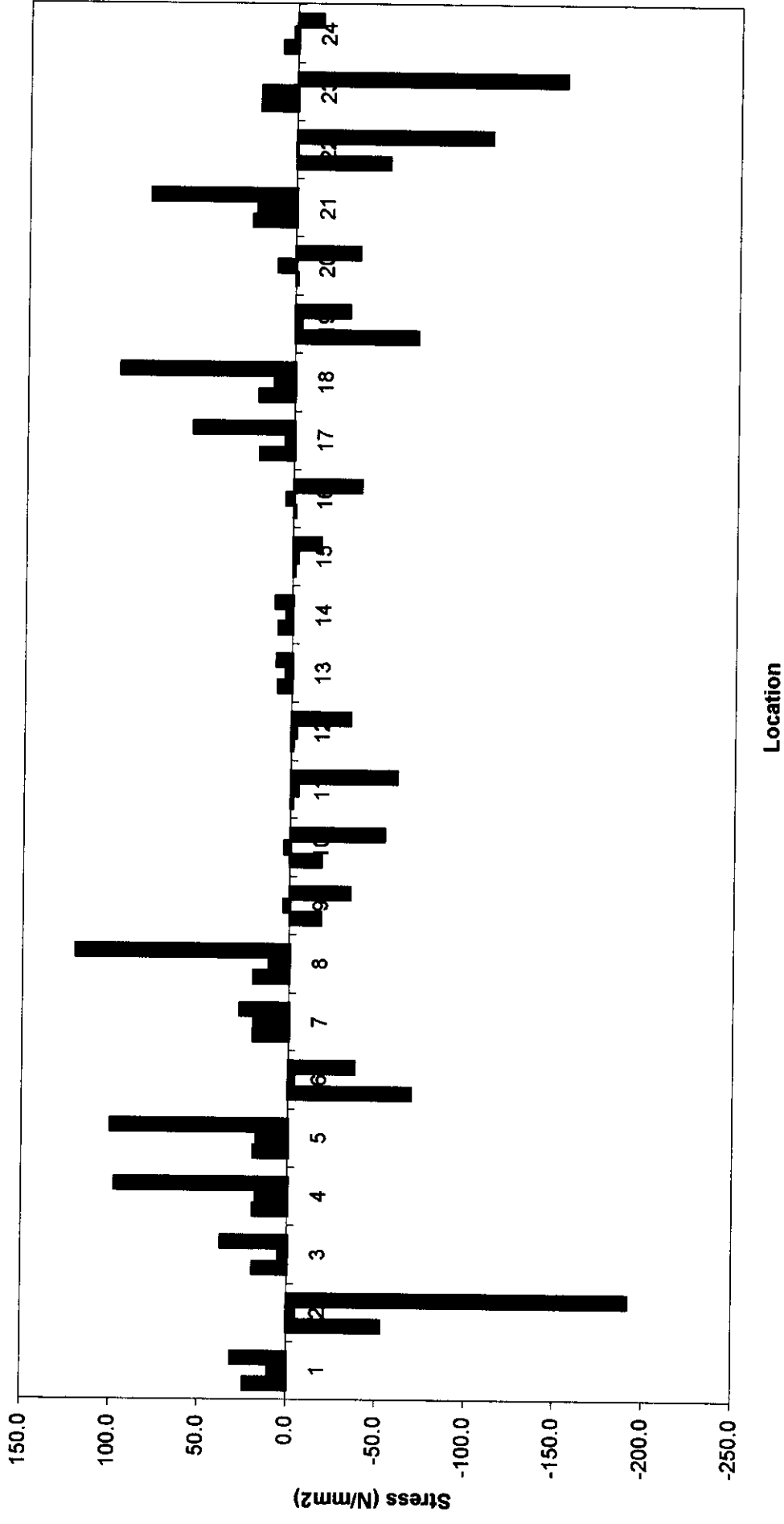
Comparison of test and predicted stresses - Loadcase 3 - Applied Load ~800kN



Member

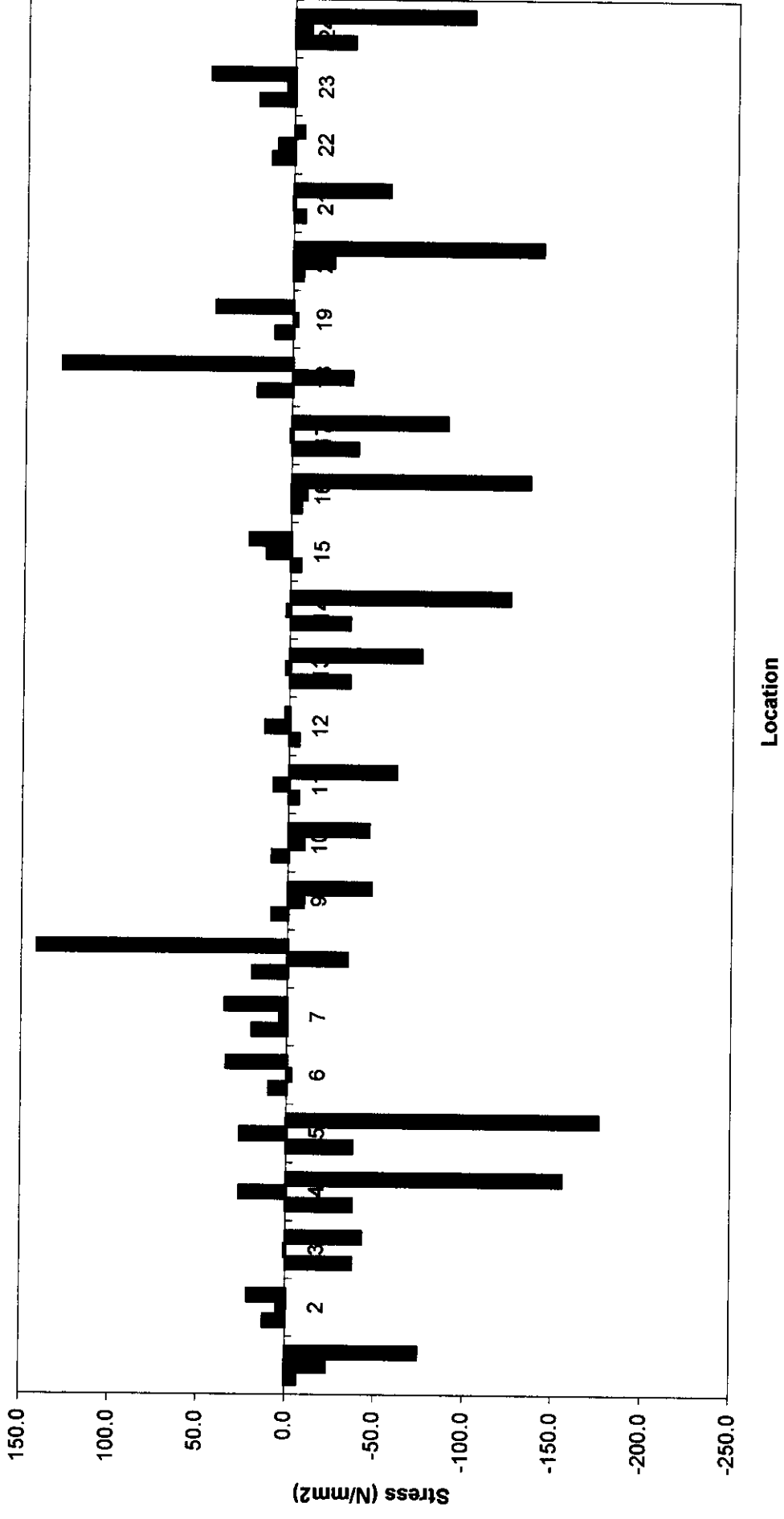
- Test Axial
- ▨ SAFJAC Axial
- BG Axial
- Test IPB
- ▨ SAFJAC IPB
- BG IPB
- Test OPB
- ▨ SAFJAC OPB
- BG OPB

Comparison between nominal and principal stresses - Loadcase 1 ~400kN

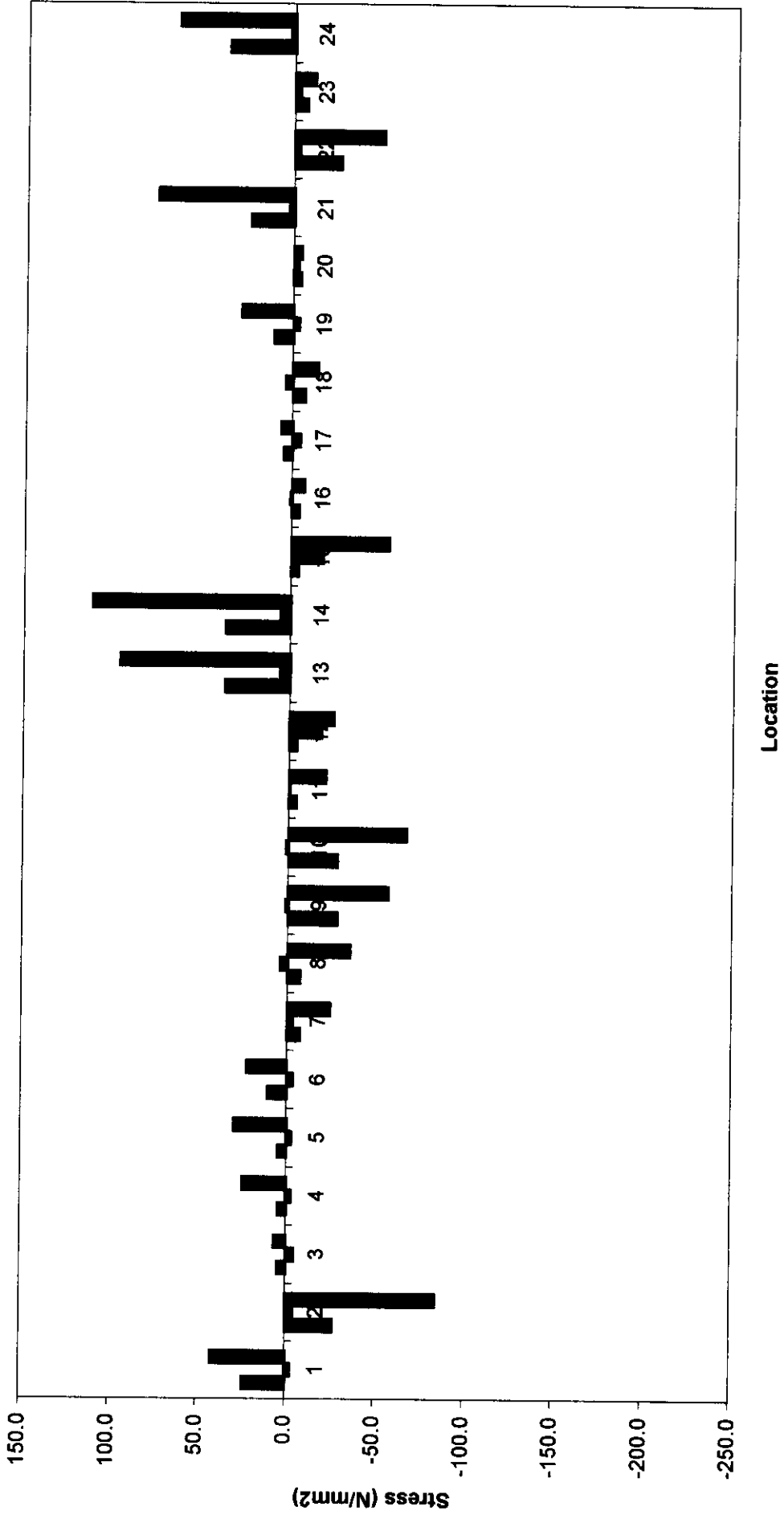


Legend: ■ Nominal axial stress, ■ Nominal bending stress, ■ Maximum principal stress at weld

Comparison between nominal and principal stresses - Loadcase 2 ~400kN

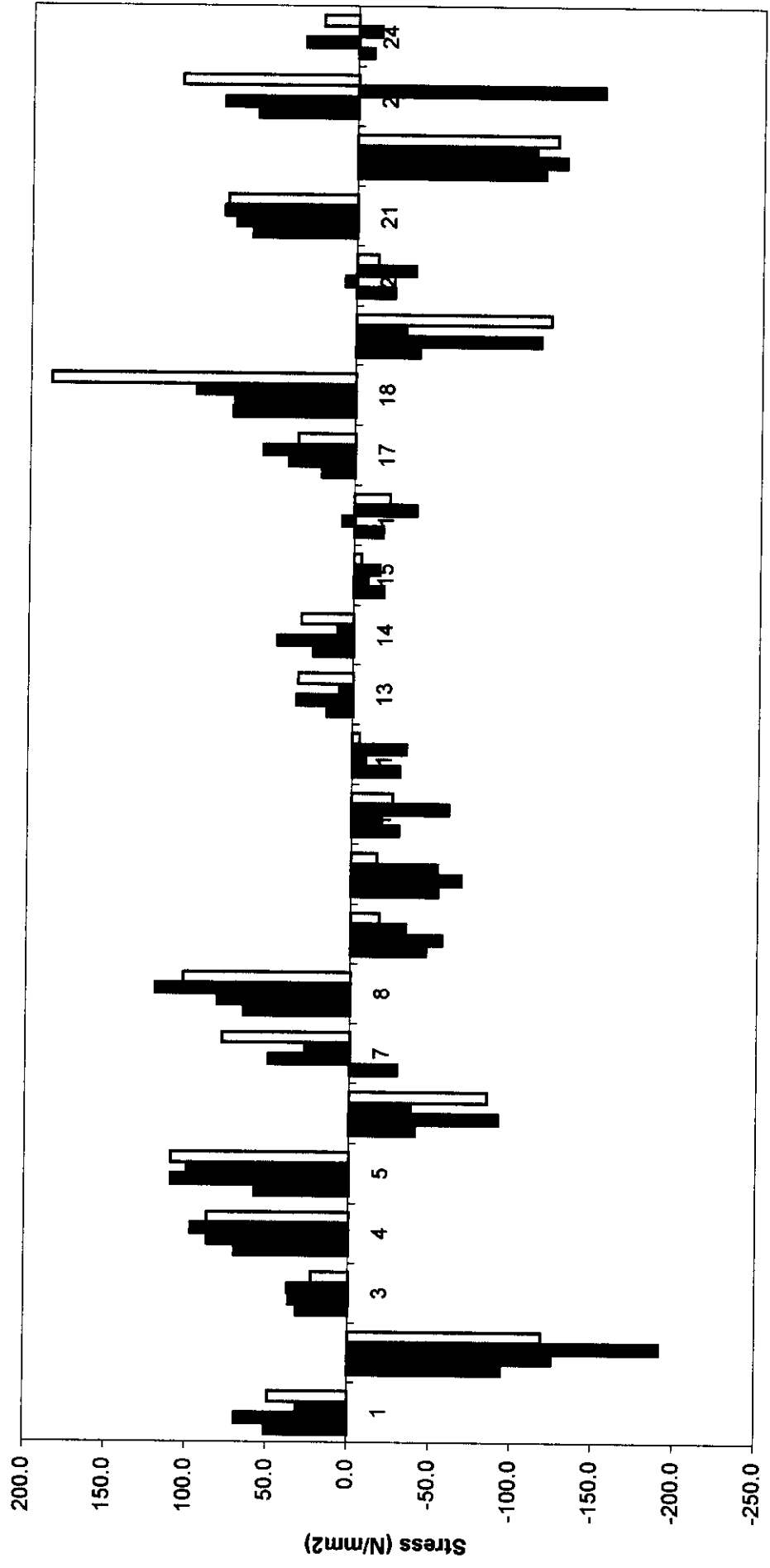


Comparison between nominal and principal stresses - Loadcase 3 ~800kN

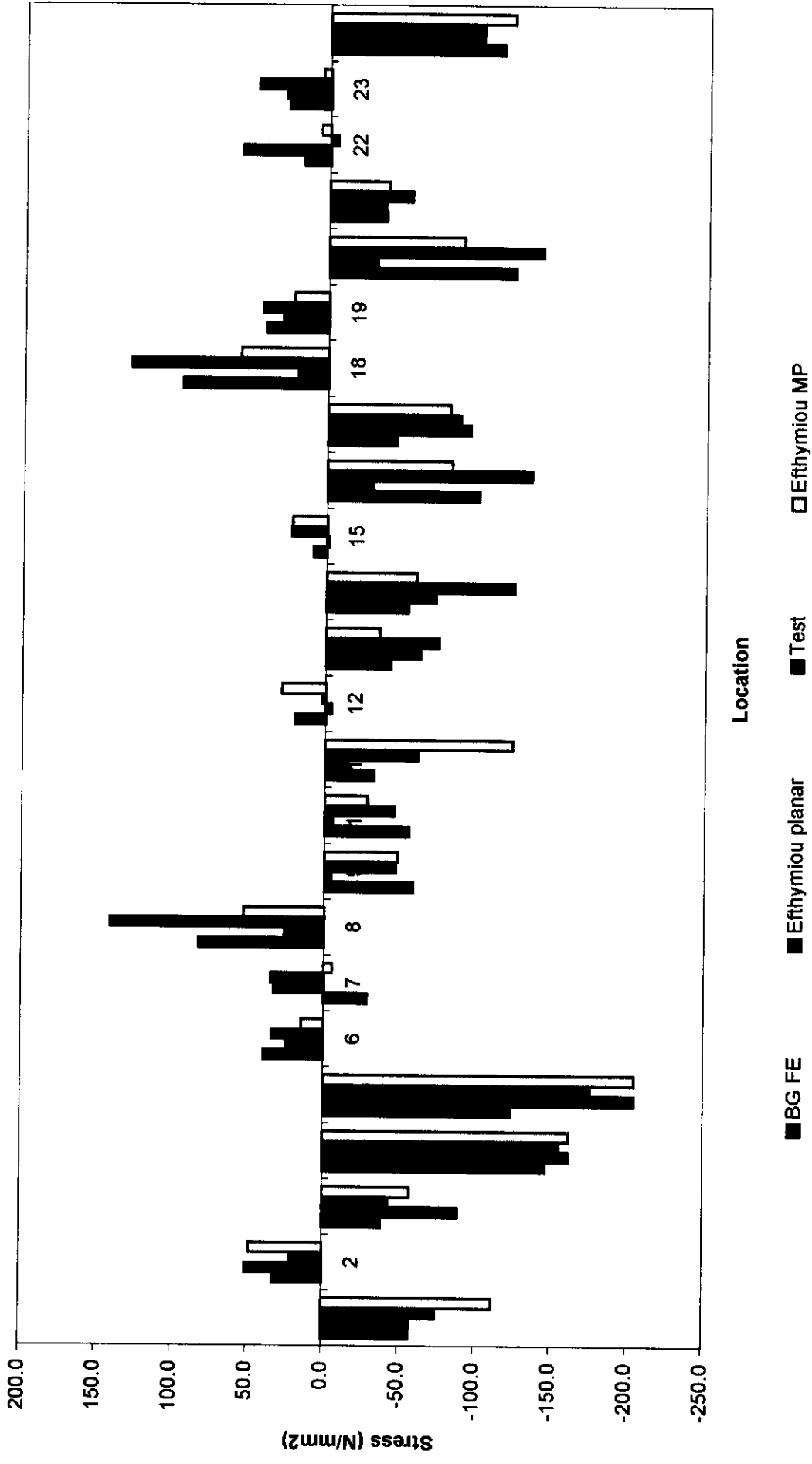


Nominal axial stress
 Nominal bending stress
 Maximum principal stress at weld

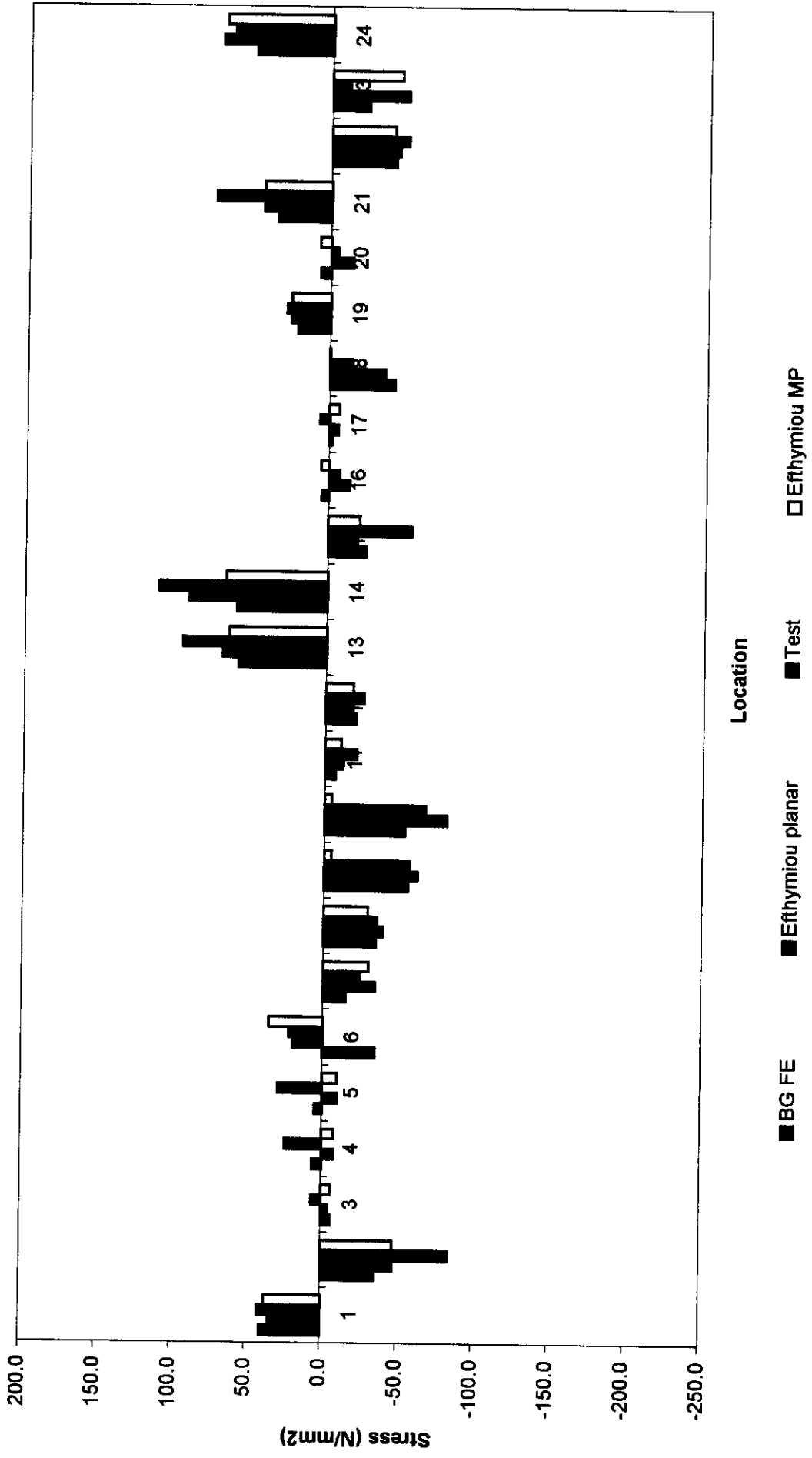
Comparison between measured and predicted principal stresses - Loadcase 1 ~400kN



Comparison between measured and predicted principal stresses - Loadcase 2 ~400kN



Comparison between measured and predicted principal stresses - Loadcase 3 ~800kN





APPENDIX E

DETAILED RESULTS

(Supplied to BG plc only at draft report stage - available to other Participants on request)

Force comparisons - C636\43\027W.xls sheet Sheet 1 + plots (4 pages)

Nominal and extrapolated comparisons - C636\43\028W.xls sheet Data + plots (4 pages)

Comparison between principal stresses - C636\43\029W.xls sheet Data + plots (4 pages)

Loadcase 1 SCF data - C636\43\012W-a-1.xls

- Brace stress summary (2 pages)

- Locations 1 to 24 (48 pages)

Loadcase 2 SCF data - C636\43\012W-a-2.xls

- Brace stress summary (2 pages)

- Location 1 to 24 (48 pages)

Loadcase 3 SCF data - C636\43\012W-a-3.xls

- Brace stress summary (2 pages)

- Location 1 to 24 (76 pages)